

Planning the Future Electricity Mix:
Designing the Use of Artificial Neural
Networks to Investigate Energy Potentials
of Renewable Generation Technologies,
Electric Vehicles, Their Use Cases

Michael Craig Allison

A thesis submitted in partial fulfilment of the
requirements of Teesside University for the degree of
Doctor of Philosophy

August 2022

Abstract

The world is currently in the midst of a fourth major energy transition which is intended to reduce dependency on fossil fuels. This transition is motivated by the desire to move towards a more sustainable energy paradigm which is less harmful to the environment, and which will also increase the energy security of countries. Increasing levels of renewable technologies such as photovoltaic (PV) systems into the fuel mix of the global electricity generation sector and the electrification of the transport sector are essential to support the move to a sustainable energy paradigm.

Whilst electrifying the transport sector and increasing the penetration levels of PV can support the move to a sustainable energy paradigm, they also pose a major challenge for electricity network operators and their aging and overworked systems. These challenges are heightened for operators in the global south where electricity demand is predicted to increase exponentially this century due to ambitious economic and social development programs. One of the major challenges facing operators is predicting how these changes will affect patterns and peaking characteristics of load profiles especially as the rate and scale of change is unknown.

This research presents a new scalable computational method which is proven to be capable of synthetically generating load profiles of electricity networks which will inevitably become significantly more complex in the near future. A systematic design approach that can be used to ensure that an optimal model can be found for any unique load forecasting scenario is also presented and forms the basis of investigation of select future energy use cases.

Many countries in the global south are currently engaged in programmes that aim to exploit high indigenous renewable energy potential to meet forecasted increasing demand for electricity. A case study of Yangon City, Myanmar was used to investigate the suitability of using PV in these endeavours and to examine the diurnal variation in PV output and the effects of this variable output on local load demand profiles over the course of a year. The results of the study demonstrated a strong correlation between PV output and local load demand, meaning that there would be little grid support needed from non-renewable generation and storage technologies to accommodate increasing PV levels.

The output from PV systems at times need to be curtailed to prevent network conditions such as voltage rise. This curtailment negatively affects the financial viability of PV systems. A case study of three countries at different stages of economic development was carried out to investigate the efficacy of different low-cost smart grid solutions in reducing or even preventing PV curtailment. Results showed that updating grid codes alone can prevent curtailment in some locations. They also showed that combining different smart grid solutions for locations in the global south could reduce curtailment at all PV penetration levels.

List of Contents

Abstract.....	i
List of Contents.....	iii
List of Figures.....	viii
List of Tables.....	xii
List of Abbreviations.....	xiv
Introduction.....	1
1.1 Background.....	1
1.2 Research Aims and Objectives.....	4
1.3 Original Contribution.....	4
1.4 Overview of the Thesis.....	5
Literature review: The Future of the Energy Mix.....	7
2.1 Historical Energy Mix.....	7
2.2 Energy Sources.....	9
2.2.1 Fossil Fuels.....	10
2.2.2 Low Carbon Fuels.....	14
2.2.3 Link with Economic Growth.....	28
2.2.4 Present Day Energy Mix.....	29
2.3 The Environment and Climate Change.....	31
2.3.1 Environmental Kuznets Curve.....	34
2.3.2 Traditional Thinking.....	35
2.3.3 Factors in the Decrease of Pollution.....	36
2.3.4 Developed and Developing Countries.....	37
2.3.5 Environmental Sustainability.....	37
2.4 Energy Equality.....	38
2.5 Energy Security.....	39
2.6 Energy Diversity.....	41

2.7 Transportation sector.....	42
2.7.1 Green House Gas Emissions	42
2.7.2 Air Quality	43
2.7.3 Noise.....	43
2.7.4 Electrification of the Transport Sector.....	43
2.7.5 Electric Vehicle Stock Levels.....	44
2.8 Electricity.....	45
2.8.1 Electricity Networks.....	46
2.8.2 Diversity and Electricity	46
2.8.3 Access to Electricity	47
2.8.4 Ageing Networks.....	47
2.8.5 EVs and the grid.....	48
2.8.6 Generation	48
2.8.7 Demand Side Management.....	49
2.9 Energy Trilemma	50
2.9.1 De-carbonisation	51
2.9.2 Energy Transition.....	52
2.9.3 International Policies and Treaties	52
2.9.4 Increasing Demand for Energy.....	54
2.10 The Role of Renewables in the Transition to a Sustainable Future.....	55
2.10.1 Penetration Levels	56
2.10.2 Progress in Realising the Energy Transition.....	57
2.10.3 Continuing Progress.....	58
2.11 The Impact of COVID on Energy	58
2.12 Predicting Future Energy Use.....	59
2.12.1 Load Profiles	60
2.12.2 Load Forecasting	61
2.12.3 Load Forecasting for Future Electrical Power Systems	63
2.12.4 Load Forecasting Methods and Techniques.....	64

Renewable Energy Technologies and Their Potential in the Global South	67
3.1 Electricity situation in the Global South	68
3.1.1. China	68
3.1.2. Association of Southeast Asian Nations (ASEAN)	73
3.2. Case Study Country—Myanmar	74
3.2.1. Background.....	74
3.2.2. Climate Conditions in Myanmar.....	77
3.2.3. Myanmar’s Electricity Fuel Mix.....	77
3.2.4. Solar Photovoltaic (PV) Potential in Myanmar	77
3.2.5. Future Energy Outlook	78
3.3. Methodology for Assessing Photovoltaic Energy Potential and its Impact on Electricity Demand Profiles.....	78
3.3.1. Case Study Location	78
3.3.2. PV Generation Modelling	79
3.3.3 PV Generation Forecasting.....	80
3.3.4. Electricity Demand Forecasting.....	80
3.3.5. Load Matching	82
3.3.6 Scenarios Considered.....	83
3.4. PV Generation Potential Analysis.....	83
3.5. Solar Supply and Load Matching	89
3.6. Implications On Future Electricity Mix Planning	92
Forecasting: An Important Tool for Electricity Planning	94
4.1 Proposed Future Load Profile Generation (Forecasting) Framework	94
4.2 Choice of Artificial Intelligence Model	96
4.3 Viability of Future Load Profile Generation Based on Public Data using ANN.....	97
4.3.1 Data Description.....	98
4.3.2 PV Generation	98
4.3.3 PV and EV Penetration Scenarios.....	99
4.3.4 Creation of Composite Future Load Profiles.....	99

4.3.5 ANN Design and Training.....	100
4.3.6 Prediction Performance Metrics	101
4.3.7 Validation and Viability of ANN use	101
4.4 Knowledge gap in the design of ANN load forecasting methods	104
Development of a Systematic Artificial Neural Network (ANN) Design Approach for Load Forecasting using Matlab	106
5.1 Matlab Parameter Testing	106
5.1.1 Performance Indicators	107
5.1.2 Default Matlab ANN Network Architecture Testing	107
5.1.3 Network Architecture Testing	122
5.1.4 Transfer Function Testing	131
5.1.5 Discussion of Results	136
5.2 Systematic ANN Design Approach developed for load forecasting using MATLAB..	138
5.2.1 Use of the Systematic Design Approach	139
Investigating Energy Potential for Future Electricity Mix Planning	141
6.1 Background	141
6.2 Case Study.....	143
6.2.1 Countries and Locations Considered.....	143
6.2.2 Climate Conditions of Locations Under Investigation.....	143
6.2.2 Distribution Networks Considered	144
6.2.3 PV Generation Simulation	146
6.2.4 PV Penetration Scenarios for Assessment.....	147
6.2.5 Smart Grid Solutions Investigated	148
6.3 Performance Assessment.....	153
6.4 Net Load Profiles	156
6.4.1 Newcastle Case	158
6.4.2 Mumbai Case.....	159
6.4.3 Yangon Case	160
6.5 PV Energy Yield Estimation Algorithms	162

6.6 Results and Discussions.....	164
6.6.1 Base Case Scenario	164
6.6.2 Case Scenario with Demand Side Management	170
6.6.3 Case with Demand Side Management and Active Voltage Control	174
6.7 Conclusions.....	182
Conclusions	183
7.1 Transition to a Sustainable Energy Future	183
7.2 Load Forecasting.....	185
7.3 Renewable Energy Potential.....	186
7.4 Systematic ANN Design Approach	188
7.5 Maximising PV Energy Output Potential	189
7.6 Recommendations for Future Work.....	191
References	193

List of Figures

Figure 1 - Outline of Modelling Requirements for Energy Policymaking	2
Figure 2 - Historical Global Primary Energy Mix (Data Source: 26)	8
Figure 3 - Historical Fossil Fuel Dominance of Global Fuel Mix.....	10
Figure 4 - Recent Coal Consumption by Region	13
Figure 5 - Energy Consumption by Sector in the US in 2020.....	29
Figure 6 - Global Primary Energy Mix 2019.....	30
Figure 7 - Electricity Fuel Mix 2019.....	30
Figure 8 - Global Greenhouse Gas Emissions by Sector 2016.....	31
Figure 9 - Historical Global CO ₂ Emissions	33
Figure 10 - Environmental Kuznets Curve.....	36
Figure 11 - Energy Trilemma Venn Diagram	50
Figure 12 - Energy Trilemma Triangle.....	51
Figure 13 - Typical Seasonal Weekday Load Profiles for The England and Wales Transmission Network.....	61
Figure 14 - Historical Global Energy Consumption [274].....	68
Figure 15 - Electricity Consumption in China (1965 - 2018) [274].....	70
Figure 16 - Historical Global Electricity Consumption by Region [274]	71
Figure 17 – Electrification Rate in Myanmar [293].....	76
Figure 18 – Averaged Synthetic Daily Load Profiles for Residential Properties in Urban Yangon City	81
Figure 19 – Energy Injected into the Grid in the Month of June.....	84
Figure 20 – Energy Injected into the Grid in the Month of February.....	84
Figure 21 - Average Monthly Performance Ratio.....	86
Figure 22 – System Loss Diagram of Simulated PV System in Yangon City	87
Figure 23 – Normalised Monthly Production.....	88
Figure 24 – Averaged Daily PV Output Profiles.....	89
Figure 25 – Load Matching in 2020.....	90
Figure 26 – Load Matching in 2025.....	91
Figure 27 – Load Matching in 2030.....	91
Figure 28 – Solar Supply Rate and Load Matching for First 10 Years of Operation.....	92
Figure 29 – Proposed Net Residential Load Profile Generation Framework.....	95
Figure 30 – Seasonal Variation in PV Output Profiles of the Typical PV system.....	99
Figure 31 – ANN Architecture for Future Load Profile Prediction Model	100
Figure 32 – Training Results for 10% PV and 10% EV Penetration in Spring.....	102
Figure 33 – Training Results for 50% PV and 70% EV Penetration in Winter.....	102

<i>Figure 34- Testing Results for 20% PV and 30% EV Penetration in Autumn</i>	104
<i>Figure 35 – Error of Backpropagation Training Functions that use Jacobian Derivatives in Neuron Testing</i>	109
<i>Figure 36 – Error of Backpropagation Training Functions that use Gradient Derivatives in Neuron Testing</i>	109
<i>Figure 37 – Error of Supervised Weight/Bias Training Functions in Neuron Testing</i>	110
<i>Figure 38 - Error of Backpropagation Training Functions that use Jacobian Derivatives in Layer Testing</i>	113
<i>Figure 39 - Error of Backpropagation Training Functions that use Gradient Derivatives in Layer Testing</i>	113
<i>Figure 40 - Error of Supervised Weight/Bias Training Functions in Layer Testing</i>	114
<i>Figure 41 – Performance of Top 5 Training Functions During Neuron Testing of the Fitnet Network</i>	121
<i>Figure 42 - Performance of Top 5 Training Functions During Layer Testing of the Fitnet Network</i>	121
<i>Figure 43 - Network Architecture Initial Testing</i>	124
<i>Figure 44 - Top 3 Network Architectures from Initial Testing</i>	125
<i>Figure 45 – Average Training Time of Network Architectures During Neuron Testing</i>	126
<i>Figure 46 - Average Error of Network Architectures During Neuron Testing</i>	127
<i>Figure 47 - Average R-Value of Network Architectures During Neuron Testing</i>	127
<i>Figure 48 - Average Training Time of Network Architectures During Layer Testing</i>	129
<i>Figure 49 - Average Error of Network Architectures During Layer Testing</i>	130
<i>Figure 50 - Average R-Value of Network Architectures During Layer Testing</i>	130
<i>Figure 51- Average Error During Hidden Layer Transfer Function Testing</i>	133
<i>Figure 52 - Average of Top 5 During Hidden Layer Transfer Function Testing</i>	133
<i>Figure 53 - Average Error During Output Layer Transfer Function Testing</i>	135
<i>Figure 54 - Average of Top 3 During Output Layer Transfer Function Testing</i>	135
<i>Figure 55 – Flowchart: Proposed Systematic Design Approach</i>	139
<i>Figure 56 - Case Study Locations</i>	144
<i>Figure 57 - Typical UK Distribution Network [372]</i>	145
<i>Figure 58 - Typical South-East Asian Distribution Network</i>	146
<i>Figure 59 - Average Monthly Output of PV Systems</i>	147
<i>Figure 60 (a) Before Load Shifting and (b) After Load Scheduling</i>	149
<i>Figure 61 - Smart Grid Architecture (adapted from [374]) with an Indicative ADSM Controller</i>	149
<i>Figure 62 - Typical Load Profiles of Flexible Loads (a) Washing Machine, (b) Dishwasher and (c) Electric Water Heating for A Single Domestic Dwelling</i>	151

<i>Figure 63 - One Phase of Primary Substation Transformer</i>	152
<i>Figure 64 – Maximising OV Energy Capture by DSM and AVC</i>	154
<i>Figure 65 – Load Shifting DSM Scheme Considered</i>	155
<i>Figure 66 – AVC Operation Scheme Considered</i>	156
<i>Figure 67 – Net Residential Load Profile Generation Framework</i>	157
<i>Figure 68 – ANN Based Net Load Profile Generation for Newcastle</i>	159
<i>Figure 69 - ANN Generated Synthetic Residential Load Profiles for Mumbai</i>	160
<i>Figure 70 - Averaged Synthetic Daily Load Profiles for Urban Yangon City</i>	161
<i>Figure 71 (a) Bus Voltages and (b) Bus 17 Voltage at 90% PV Penetration for the Newcastle Case During Peak Summer Day</i>	165
<i>Figure 72 (a) Bus 17 Voltage and (b) Duration of Voltage Limit Violation at 100% PV Penetration for the Newcastle Case During Peak Summer Day</i>	165
<i>Figure 73 (a) Bus Voltages and (b) Bus 17 Voltage at 40% PV Penetration for The Mumbai Case During the Peak Summer Day</i>	166
<i>Figure 74 - All Bus Voltage for 50-100% PV Penetration Levels for the Mumbai Case During the Peak Summer Day</i>	167
<i>Figure 75 (a) Bus 17 Voltage and (b) Duration of Bus 17 Voltage Limit Violation at 50% PV Penetration for the Mumbai Case During the Peak Summer Day</i>	167
<i>Figure 76 (a) Bus 17 Voltage and (b) Duration of Bus 17 Voltage Limit Violation at 100% PV Penetration for the Mumbai Case During the Peak Summer Day</i>	168
<i>Figure 77 - Annual Energy Curtailment for the Base Case in Mumbai</i>	168
<i>Figure 78 (a) Bus Voltage and (b) Bus 17 Voltage at 40% PV Penetration for The Yangon Case During Peak Summer Day</i>	169
<i>Figure 79 - Bus 17 Voltages for the Newcastle Case at 100% PV Penetration During Summer (a) Base Case and (b) With 50% Housing Participation in DSM Program</i>	171
<i>Figure 80 - Bus 17 Voltages for the Newcastle Case at 100% PV Penetration During Summer (a) Base Case and (b) With 50% Housing Participation in DSM Program</i>	171
<i>Figure 81 - Bus 17 Voltages for the Mumbai Case at 70% PV Penetration During Summer (a) Base Case and (b) With 50% of Housing Participation in DSM Program</i>	172
<i>Figure 82 - Annual Energy Curtailment for the Mumbai Case with 15% Housing Participation in DSM</i>	172
<i>Figure 83 - Annual Energy Curtailment for the Mumbai Case with 50% Housing Participation in DSM</i>	173
<i>Figure 84 - Bus 17 Voltages for the Yangon Case at 40% PV Penetration During Summer (a) Base Case and (b) With 50% of Housing Participation in DSM Program</i>	174
<i>Figure 85 (a) Bus Voltages and (b) Bus 17 Voltage at 100% PV Penetration for the Newcastle Case During Peak Summer with 15% Housing Participation in DSM and AVC</i>	175

<i>Figure 86 (a) Bus Voltages and (b) Bus 17 Voltage at 70% PV Penetration for the Mumbai Case During Peak Summer with 15% Housing Participation DSM and AVC.....</i>	<i>175</i>
<i>Figure 87 (a) Bus Voltages and (b) Bus 17 Voltage at 80% PV Penetration for the Mumbai Case During Peak Summer with 15% Housing Participation DSM and AVC.....</i>	<i>176</i>
<i>Figure 88 (a) Bus Voltages and (b) Bus 17 Voltage at 90% PV Penetration for the Mumbai Case During Peak Summer with 15% Housing Participation DSM and AVC.....</i>	<i>176</i>
<i>Figure 89 (a) Bus Voltages and (b) Bus 17 Voltage at 100% PV Penetration for the Mumbai Case During Peak Summer with 15% Housing Participation DSM and AVC.....</i>	<i>177</i>
<i>Figure 90 - Duration of Bus 17 Voltage Violation for the Mumbai case at 100% PV Penetration During Peak Summer (a) Base, Case, (b) 15% Housing Participation DSM and (c) 15% Housing Participation DSM and AVC.....</i>	<i>177</i>
<i>Figure 91 - Annual Energy Curtailment for the Mumbai Case with 15% Housing Participation DSM and AVC.....</i>	<i>178</i>
<i>Figure 92 (a) Bus Voltages and (b) Bus 17 Voltage at 50% PV Penetration for the Yangon Case During Peak Summer with 15% Housing Participation DSM and AVC.....</i>	<i>180</i>
<i>Figure 93 (a) Bus Voltages and (b) Bus 17 Voltage at 60% PV Penetration for the Yangon Case During Peak Summer with 15% Housing Participation DSM and AVC.....</i>	<i>181</i>

List of Tables

<i>Table 1 - Coal Reserves by Region</i>	11
<i>Table 2 - Hydropower’s Historical Share of the RES Mix</i>	18
<i>Table 3 - Global Wind Installations by Region (Data [109])</i>	24
<i>Table 4 - Employment in Renewables Sector in 2016</i>	28
<i>Table 5 - Number of Electric PLGs on the Roads in 2015 [120]</i>	44
<i>Table 6 - Percentage of Global Electricity Consumption by Region [274]</i>	71
<i>Table 7 – Top 10 Consumers of Electricity Per Capita [290, 291]</i>	75
<i>Table 8 – Climate Conditions in Yangon City</i>	78
<i>Table 9 – Photovoltaic Installation Details</i>	79
<i>Table 10 – Daily Average Energy Injected into Grid</i>	83
<i>Table 11 – Artificial Intelligence Model Testing Results</i>	96
<i>Table 12 – Training Performance of ANN and MLR for All Four Seasons Combined and The Full Range of EV and PV Penetration Scenarios</i>	103
<i>Table 13 – Testing Performance of ANN and MLR for 20% PV Penetration and 30% EV Penetration in Autumn</i>	104
<i>Table 14 - Matlab NNTool-Box Training Functions</i>	107
<i>Table 15 – Error of Different Training Functions in a Single Layer Network</i>	111
<i>Table 16 – Coefficient of Correlation of Different Training Functions in a Single Layer Network</i>	112
<i>Table 17 – Percentage Change in Error Brought About by Adding Layers to Backpropagation Training Functions that use Jacobian Derivatives</i>	114
<i>Table 18 - Percentage Change in Error Brought About by Adding Layers to Backpropagation Training Functions that use Gradient Derivatives</i>	115
<i>Table 19 - Percentage Change in Error Brought About by Adding Layers to Supervised Weight/Bias Training Functions</i>	115
<i>Table 20 - Error of Different Training Functions in Multiple Layer Networks</i>	116
<i>Table 21 - Coefficient of Correlation of Different Training Functions in Multiple Layer Networks</i>	117
<i>Table 22 – Average Results of the Neuron Testing</i>	118
<i>Table 23 - Average Results of the Layer Testing</i>	119
<i>Table 24 – Training Function Matrix</i>	120
<i>Table 25 – Comparison of Results from Fitnet Testing</i>	120
<i>Table 26 - Matlab Network Topologies</i>	122
<i>Table 27 – Average Error of Top 3 In Network Architecture Initial Testing</i>	124
<i>Table 28 - Average R-Value of Top 3 In Network Architecture Initial Testing</i>	124

<i>Table 29 – Average Error of Network Architectures During Neuron Testing</i>	127
<i>Table 30 - Average Error of Network Architectures During Layer Testing</i>	130
<i>Table 31 - Matlab Neural Network Toolbox Transfer Functions</i>	131
<i>Table 32 - Average Error During Hidden Layer Transfer Function Testing</i>	133
<i>Table 33 – Top 5 Functions in Hidden Layer Transfer Function Testing</i>	134
<i>Table 34 - Average Error During Output Layer Transfer Function Testing</i>	135
<i>Table 35 - Top 5 Functions in Output Layer Transfer Function Testing</i>	136
<i>Table 36 - PV System Loses</i>	147
<i>Table 37 - Details of Flexible Loads Chosen for DSM</i>	150
<i>Table 38 – PV Penetration Level vs Buses with Voltage Limit Violation for The Mumbai Case During the Peak Summer Day</i>	166
<i>Table 39 - PV Penetration Level vs Buses with Voltages Greater Than 1.1 p.u. for The Yangon Case During the Peak Summer Day</i>	170
<i>Table 40 - Comparison of Voltage Levels for Bus 17 in the Yangon Network When PV Penetration was 40%</i>	174
<i>Table 41 - Summary of Aggregate Annual PV Energy Curtailment in the LV Network for the Mumbai Case</i>	178
<i>Table 42 - Prevented Financial Loss at Different PV Penetration Levels for the Mumbai Case</i>	179
<i>Table 43 - Comparison of Threshold Voltage Violations for the Base Case and AVC Scenarios of Yangon for Penetration Levels of 50 – 100%</i>	181

List of Abbreviations

ACE	ASEAN Centre for Energy
ADMD	After Diversity Maximum Demand
ADSM	Active Demand Side Management
AI	Artificial Intelligence
ANN	Artificial Neural Network
ARIMA	AutoRegressive Integrated Moving Average
ASEAN	The Association of Southeast Asian Nations
ARMAX	Auto-Regressive Moving-Average with eXogenous input
AVC	Active Voltage Control
bcm	billion cubic metres
BEVs	Battery Electric Vehicles
BP	British Petroleum
BTFGDs	Backpropagation Training Functions that use Gradient Derivatives
BTFJDs	Backpropagation Training Functions that use Jacobian Derivatives
CER	Chinese Economic Reform
CH ₄	Methane
CIS	Commonwealth of Independent States
CO ₂	Carbon Dioxide
dB	decibel
DG	Distributed Generation
DSM	Demand Side Management
EDC	Emerging and Developing Country
EJ	ExaJoule (10 ¹⁸ Joule),
EESI	Environmental and Energy Study Institute
EKC	Environmental Kuznets Curve
EU	European Union
EVs	Electric Vehicles
FFN	Feed Forward Network
GDP	Gross Domestic Product

GHGs	Greenhouse Gasses
GIS	Geographic Information System
GUI	Graphical User Interface
GW	gigawatt (10^9 watt)
HGVs	Heavy Duty Vehicles
HVAC	Heating, Ventilation and Air-Conditioning
IAEA	International Atomic Energy Agency
ICEVs	Internal Combustion Engine Vehicles
IEA	International Energy Agency
IEC	International Electrotechnical Commission
IPCC	International Panel on Climate Change
IREA	International Renewable Energy Agency
KG	Köppen-Geiger
km	kilometre (10^3 metre)
kV	KiloVolt (10^3 volt)
kW	Kilowatt (10^3 watt)
kWh	Kilowatt-hour (10^3 watt-hour)
kWp	Kilowatt peak
LCoE	Levelized Cost of Energy
LMS	Least Mean Square
LCL	Low Carbon London
LTFs	Long-Term Forecasts
LV	Low Voltage
m	metre
ML	Machine Learning
MLR	Multiple Linear Regression
MTFs	Medium-Term Forecasts
Mtoe	Million tonnes of oil equivalent
MVA	MegaVolt-Amperes (10^6 volt-amperes)
MW	Megawatt (10^6 watt)

MWh	Megawatt-hour (10^6 watt-hour)
NARX	Nonlinear Autoregressive Neural Network
NEP	National Electrification Plan
N ₂ O	Nitrous Oxide
NN	Neural Network
NNTool-Box	Neural Network Toolbox
NREL	National Renewable Energy Laboratory
NREPP	National Renewable Energies Policy and Planning–Draft
OECD	Organisation for Economic Co-operation and Development
OLTC	On-Load Tap-Changing transformers
PDSM	Passive Demand Side Management
PEV	Plug-In Electric Vehicles
PHEV	Plug-In Hybrid Electric Vehicles
PLGs	Private Light Vehicles
PR	Performance Ratio
PSPs	Pumped Storage Plants
p.u.	Per Unit
RE	Renewable Energy
RER	Renewable Energy Resources
RES	Renewable Energy Sources
RL	Reinforcement Learning
SL	Supervised Learning
SO ₂	Sulphur dioxide
STFs	Short-Term Forecasts
SVM	Support-Vector Machines
SWBTFs	Supervised Weight/Bias Training Functions
ToU	Time of Use
TW	Terawatt (10^{12} watt)
TWh	Terawatt-hour (10^{12} watt-hour)
UK	United Kingdom

UKREC	UK Energy Research Centre
UL	Unsupervised Learning
UN	United Nations
UNCSD	United Nations Conference on Sustainable Development
UNFCCC	United Nations Framework Convention on Climate Change
USTFs	Ultra-Short-Term Forecasts
US	United States
US-EIA	United States Energy Information Administration
UsWBTFs	Unsupervised Weight/Bias Training Functions
VES	Variable Energy Sources
WEC	World Energy Council
WHO	World Health Organisation

Chapter 1

Introduction

This PhD research considers the evolution of the energy mix due to climate change mitigation low carbon targets into more electrical energy-based solution with greener technologies like renewable generation and electrical vehicles. Planning of the future electricity mix needs development of new tools and techniques. Artificial intelligence is one of the technologies looked at very favourable at the current time as a technology that has a lot of potential in reducing human effort. This work explores designing the use of one artificial intelligence technology namely Artificial Neural Networks (ANN) in the planning of the future electricity mix from an energy, sustainability, technical design and deployment, and economic points of view.

1.1 Background

The decarbonisation of the energy network has created higher demand for electricity over oil and coal. Some of the electrical power network assets such as transformers and switchgear assets were installed as early as the 1950s and are still in use today [1]. For example, the UK's National Infrastructure Delivery Plan 2016–2021 identifies that “much of the existing infrastructure which has served us well is now old” and that “major investment is required to accommodate new generation and replace ageing assets”. However, there is also a greater focus now on lowering the cost of delivering electricity. The performance-based electricity distribution model Revenue = Incentives+ Innovation+ Outputs (RIIO) model of the UK which has been in operation from 2015 [2] is representative of this drive. In the continuing drive to reduce cost, given the high cost of assets, especially at the transmission and sub-transmission voltage levels, it is safe to assume that even in the near- or medium-term, power networks will be mostly composed of present-day assets.

There will be high volumes of customer-side renewable generation due to the decarbonisation targets. However, the exact penetration levels, renewable generation type and their share in the demand mix is presently uncertain. A decentralised power supply becomes problematic for the traditional operating mode of the electricity network where net load on the network is largely foreseeable, power supply is controlled and there is a uni-directional electricity flow from large generators to consumers [3]. Power networks are currently moving into the smart grid paradigm. The inherent cost attached to smart grids technologies means that the global economic inequality will be reflected in their deployment.

Developing nations with lower economic reserves to spare are often constrained in terms of the level and nature of changes they could make to their power networks. However, owing to energy supply deficits, load growth, dependency on fossil fuel imports etc. developing nations are in greater need of cheaper low carbon generation. This can only be realised through efficient and sustainable energy policies. Figure 1 is representative of the modelling requirements within the energy policy nexus. A multitude of scenarios of with variations in underlying technical processes, energy behaviour and associated economics needs investigation for effective policymaking.

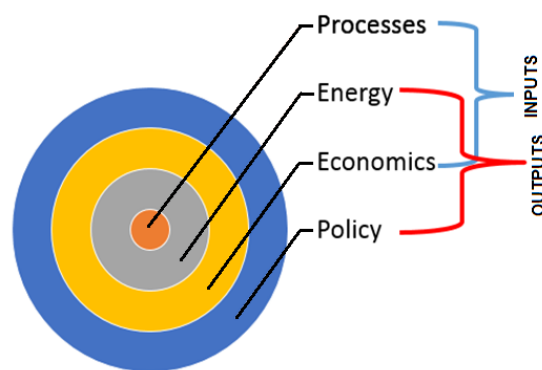


Figure 1 - Outline of Modelling Requirements for Energy Policymaking

As energy flow becomes inevitably more complex with larger integration of renewable generation, electric vehicles and energy storage in modern power networks, power system planning methods are becoming more complicated compared to how they were with conventional, mostly thermal, generation. It was evident from a survey of recent literature on power system planning that there is a significant focus recently on largescale renewable integration, specifically with regards to generation expansion planning focusing on national energy policies [4]. Majority of literature tends to concentrate on optimisation of transmission and distribution planning, ultimately underpinned by load flow analysis [5]. As an emerging area there is a high level of attention given to energy storage from the point of view of technical constraints, given the uncertainty around their economics [6]. There is also focus on the drivers and challenges of renewable penetration such as carbon tax [7] and resource uncertainty and variability [8]. Resource planning [9] and mitigating strategies such as demand side management (DSM) and On-Load Tap-Changing transformers (OLTC) for voltage rise mitigation [8] is investigated in this context.

Authors of [10] reviewed power system planning challenges for India with increasing penetration of renewables given the ambitious installed capacity targets. The current energy

policies are summarised, and it is recommended that India learn from international experiences and adopt best practices from developed countries. The need for DSM and advanced forecasting methods is also emphasised along with other recommend actions to facilitate higher renewable penetration. In [11] a method combining probabilistic duck curve and probabilistic ramp curve to efficiently compensate the imbalance between the high PV generation time and peak time of load was demonstrated for a use case of China. The authors of [12] emphasise that load forecasting is often the first step in power system planning. Plug-in electric vehicles (PEVs) and the Korean government PEV targets are focussed on. A stochastic method for forecasting PEV load profiles is introduced focusing on the PEV expansion target, statistics of existing vehicles and consumer numbered connected to substations. Ref. [13] focuses on the voltage rise problem with increased renewable penetration for ageing power networks and introduces an algorithm for carrying out decision-making on asset upgrades or network reinforcement by addition of components and modification of topology. The trade-off between power line upgrades and placements and operation of on-load tap-changing transformers (OLTC) in the network was investigated from the point of view of technical constraints. In [14] authors identify that increasing renewable penetration is confidential with increasing need for flexibility within power systems. Market design is identified as the structural tool that can facilitate flexibility. Potential market reforms are outlined with a focus on DSM. The impact of the difference in nature and requirements of different regional networks and availability of flexible loads are acknowledged. It is recommended that future research focus on planning and operation of power system factoring the difference into account. In [15], a multi-region power system planning approach named REPLAN is proposed for Nigeria. The focus was on improved energy exporting and importing arrangement between regions and overall energy cost reduction by forecasting inter-regional transmission capacity and pathways for developing regional generation. Although the study emphasised the need to investigate local (regional) network models, it was aimed at long-term power system planning and not on diurnal power system operation.

It was evident from the literature surveyed and cited above that there is a strong focus on energy policies. However, the focus is mostly at the higher-level vision-type policies, often at the national level, setting the energy targets rather than the policies or grid codes at the operational level, which translate the envisioned benefits to reality. Revenue from energy is the basis of renewable energy economics. Policy makers will not be able to capture the full picture for facilitating higher penetration of renewable like PV based on research that just focus on maximum hosting capacity, the implications of technical measures / constraints to PV energy and PV system owners also need to be understood. In this context, the main aim

of this work is to support scenario-based impact assessments for power system planning by means of ANN and thus aid sustainable energy policymaking, especially for developing countries.

1.2 Research Aims and Objectives

As mentioned above, the main aim of this work is to support scenario-based impact assessments for planning the future electricity mix which would have high shares of renewable generation technologies and electric transport by utilising the artificial intelligence technology ANN and thus aid sustainable energy policymaking, especially for developing countries. The objectives have been defined as:

1. To conduct a detailed literature review on the current energy mix evolving into a more electricity-based situation based on climate change mitigation low carbon targets to understand the planning needs for future energy mixes, especially for developing countries.
2. To review the tools for electricity planning with a specific focus on energy use forecasting and the use of ANNs in the field, in order to outline how to properly design ANN based forecasting tools.
3. To investigate different parameters, algorithms, structures, types attached to ANNs to identify candidate architectures, their testing, optimal configurations and finally their validation.
4. To develop a Systematic Artificial Neural Network (ANN) Design Approach for load forecasting using MATLAB.
5. To analyse the effectiveness of ANN forecasters in investigating the energy potentials of renewables and electric vehicles (EVs) for future electricity mix planning based on select use case scenarios in both the developed and developing world.

1.3 Original Contribution

The following original contributions resulted as part of the research work done during the course of the PhD:

1. Development of a computational procedure for PV and EV penetration scenario-based future load profile generation based on public data and its testing for a case study in Middlesbrough, UK.
2. Assessment of the PV potential for a selected location in Myanmar to determine the impacts on current and future electricity demand profiles in order to aid system planning.

3. Development of a systematic approach for designing ANN load forecasting that could be employed by global south countries to generate accurate and realistic synthetic PV output and load profiles which can be used by system operators and planners to forecast future load profiles.
4. Introduction of a net prosumer load forecasting framework and demonstration of its application for select use cases.
5. Analysis of the effectiveness of ANN forecasters in investigating the energy potentials of renewables and EVs for future electricity mix planning based on select use case scenarios in both the developed and developing world.

These contributions are supported by the following publications:

Publications

1. Allison, M., Akakabota, E. and Pillai, G., 2018, February. Future load profiles under scenarios of increasing renewable generation and electric transport. In *2018 5th International Conference on Renewable Energy: Generation and Applications (ICREGA)* (pp. 296-300). IEEE.
2. Akakabota, E., Pillai, G. and Allison, M., 2019, September. Supporting LV distribution network voltage using PV inverters under high EV penetration. In *2019 54th International Universities Power Engineering Conference (UPEC)* (pp. 1-6). IEEE.
3. Allison, M. and Pillai, G., 2018, November. Photovoltaic Energy Potential and its Impact on Electricity Demand Profiles. In *International Conference on Science and Technology for Sustainable Development*, Yangon, Myanmar.
4. Allison, M. and Pillai, G., 2020. Planning the Future Electricity Mix for Countries in the Global South: Renewable Energy Potentials and Designing the Use of Artificial Neural Networks to Investigate Their Use Cases. *Designs (MDPI)*, *4*(3), p.20.
5. Pillai, G., Allison, M., Tun, T.P., Chandrakumar Jyothi, K. and Kollonoor Babu, E., 2021. Facilitating higher photovoltaic penetration in residential distribution networks using demand side management and active voltage control. *Engineering Reports (Wiley)*, p.e12410.

1.4 Overview of the Thesis

The rest of the thesis is presented as follows: **Chapter 2** is a literature review on the energy and energy use. It covers areas such as the role of energy in human activities as well as historical, present day and future use, sources of energy and the impact of energy use to the environment. **Chapter 3** investigates the potential of renewable energy to meet the

forecasted energy demands of developing countries in the global south. **Chapter 4** explores the importance of load forecasting in electricity planning operations. **Chapter 5** details the findings of work carried out to investigate the degree to which different design features of Artificial Neural Networks (ANNs) can affect forecasting performance. Chapter 5 also presents a systematic approach that can be used to increase the performance of ANNs used in forecasting problems. **Chapter 6** investigates the ability of smart grid strategies to promote the use of PV systems by minimising energy curtailment. **Chapter 7** gives the main conclusions of this work and suggests how the work could be carried on in the future.

Chapter 2

Literature review: The Future of the Energy Mix

The utilization of energy has played a fundamental role in human development throughout history [16]. Access to energy in modern societies is crucial to the economic and social development of countries [16-19]. Energy affects all aspects of human life and improves the quality of life of individuals [16, 17, 20-22] and is critical for eradicating poverty [20]. Increasing energy consumption usually leads to improved lifestyles [16]. The role of energy in human development has seen its demand grow exponentially. Demand is predicted to continue to grow by 45% between 2015 and 2030 and by over 300% by the end of the century [18]. Meeting this demand is one of the most important global issues today [23]. The fuels that have traditionally been used to meet energy demand cause serious environmental and health problems [17]. This has led to the realisation that both energy and energy sustainability are necessary for humans and the planet [22]. Indeed, the global sustainable energy agenda has become the primary challenge for many developed and developing countries [19]. This chapter looks reviews the state of play in terms of the different aspects contributing to and affecting the energy mix as well as its future global outlook.

2.1 Historical Energy Mix

Pre-industrial society energy needs were met by wood and waterpower [24]. Since this time the world has witnessed a number of significant structural changes known as energy transitions [24]. These energy transitions do not see the total elimination of an energy source but significant levels of use of additional sources [24]. The first major energy transition dates to the industrial revolution(s) of the mid-19th century when due to wood supply shortages other (lower cost) energy sources were explored [25]. Along with the creation of the coal-powered steam engine this led to large scale use of coal, followed by oil and gas [24].

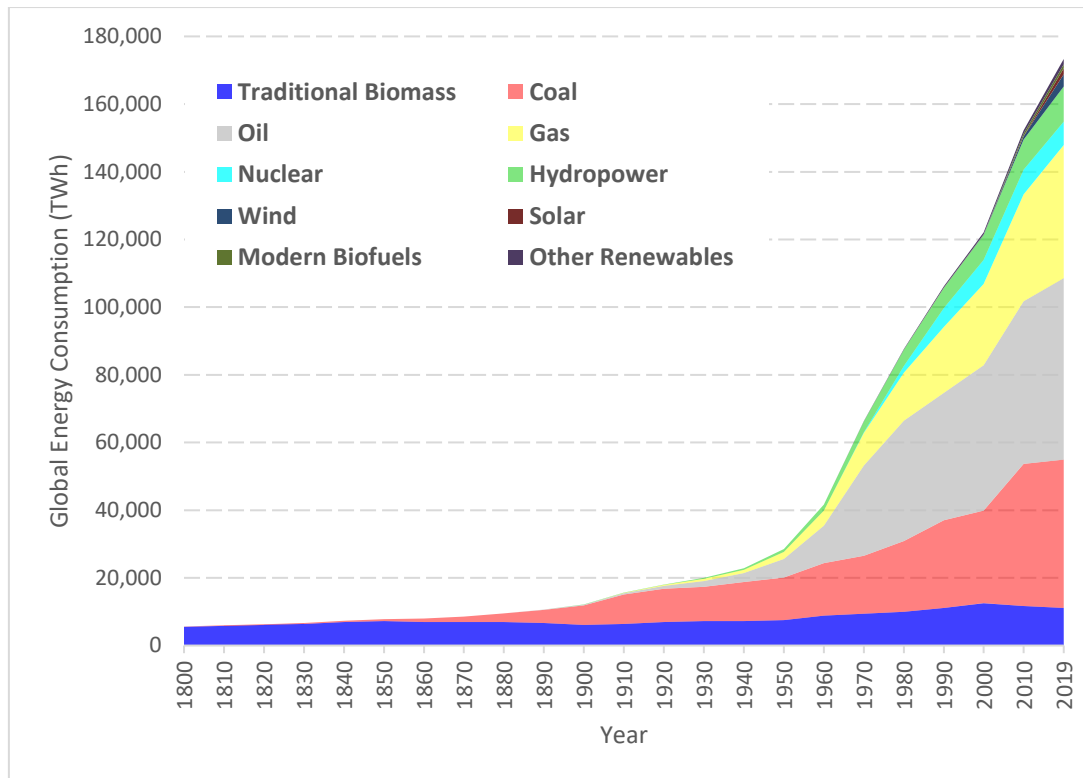


Figure 2 - Historical Global Primary Energy Mix (Data Source: 26)

The turn of the century saw the rise of hydropower [26]. The invention of the diesel engine in the 1910's heralded the second major transition due to its use of oil [27]. The transition to oil was intensified by World War II [24]. The 1960's witnessed the introduction of nuclear energy into the mix [26]. A Third major transition took place in the 1970's driven by natural gas due to its superior performance over coal and oil and because of its cleaner burning characteristics when compared to other fossil fuels [28-29].

The fourth major transition began in the 1980's when increasing levels of modern renewables such as solar/PV and wind were introduced to the mix [24, 26]. Along with technological advances this transition has been motivated by a desire to decrease reliance of fossil fuels [24, 30-31].

An energy supply system is defined as "the chain of systems and activities required to ensure supply of energy and include supply sector, energy transforming sector and energy consuming sector" [32]. The utilisation of energy is crucial to economic and social development and increasing energy consumption typically leads to improved lifestyles [33]. Therefore, access to adequate and secure energy supply is a necessity in contemporary society [34]. The importance of energy to human development has seen its consumption

grow exponentially since the first industrial revolution of the mid-19th century. This growth is predicted to continue well into the near future with energy demand expected to be 300% higher by the end of the century compared to 2015 levels [18].

Energy demand has historically been met by fossil fuels (coal, oil, and natural gas). Fossil fuels are a finite and diminishing resource which is increasingly leaving countries vulnerable to disruptions of supply, infrastructure failure and higher price fluctuations [35].

Fossil fuels also emit high levels of greenhouse gasses (GHGs) such as carbon dioxide (CO₂) which is the most significant long-lived cause of climate change [36]. These factors have forced policy makers around the globe to conclude that energy and energy sustainability are both necessary for people and the planet [22]. Indeed, the global sustainable energy agenda has become the primary challenge for many countries and organisations around the world [19].

The transportation sector is a vital part of today's society [37]. It is a key driver of economic and social development which has seen its demand grow over recent decades [38]. Traditionally the production of energy has often been associated with negative environmental costs such as the emission of airborne pollutants and GHGs [39]. Global transportation is almost completely dependent on oil to meet its energy needs which makes the sector one of the major emitters of airborne pollutants and GHGs [37]. Reducing the dependence on oil to meet the increasing demand is a major challenge for the transportation sector (particularly light-duty road transportation) [40-41]. Electric vehicles (EVs) are around three times more efficient than Internal Combustion Engine Vehicles which are powered by oil [42]. EVs also move the point of GHG emissions from the tail pipe to the electricity generation sector where they can be more efficiently and cost-effectively reduced. This has seen national policies implemented around the globe aimed at paving the way for the electrification of the transportation sector [37, 39-40, 42].

2.2 Energy Sources

Primary energy sources are energy sources that can be used directly as they are found in the natural environment without the need of any human engineered conversion process. Primary energy sources can be categorized as fossil, fissile (commonly referred to as nuclear) and renewable [16]. Oil, coal and natural gas are the most widely used fossil fuels, nuclear fuels include uranium and thorium [43]. Renewable energy sources come from

natural sources what are constantly replenished such as hydropower, wind, solar/PV, geothermal and modern biofuels [43].

2.2.1 Fossil Fuels

As show in *Figure 3* fossil Fuels have been the dominant energy source since the industrial revolution [44-46], and they are still heavily relied upon in today’s energy systems and currently meet around 80% of global demand [16, 19, 47-48]. Although in North America, Europe and other OECD countries fossil fuel use has been declining over recent decades [45]. Fossil fuels are used in the electricity generation, transportation, and industry sectors as well as in household consumption [49]. The use of fossil fuels has helped accelerate the development of both global economy and human civilisation [17, 50].

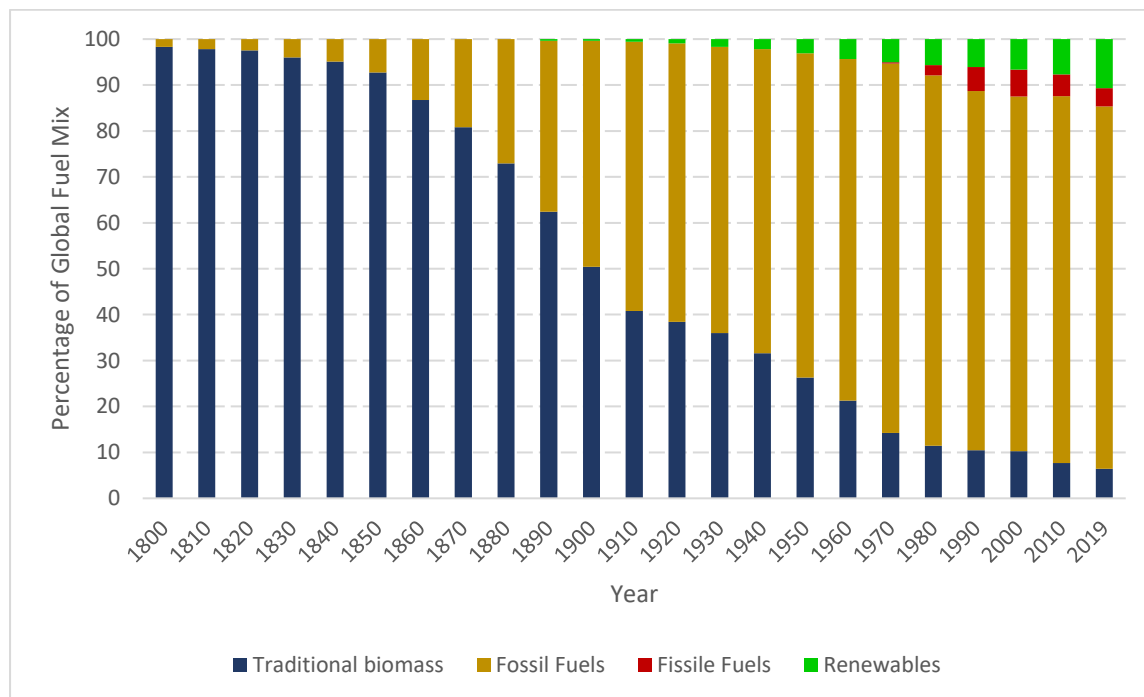


Figure 3 - Historical Fossil Fuel Dominance of Global Fuel Mix

Whilst the use of fossil fuels has helped accelerate economic and social development it has also caused major damaged to the environment and human health [17, 48]. Two-thirds of global greenhouse emissions come from the burning of fossil fuels [17, 51]. CO₂ emissions vary between different fossil fuels [52]. Fossil fuels as a whole were responsible for 9.9 billion metric tonnes of global CO₂ emissions in 2014 [45]. Coal was the highest contributor to this figure (45%) followed by oil (35%) and natural gas (20%) [45].

The International Energy Agency (IEA) have stated that current trends in fossil fuel demand are patently economically, environmentally and socially unsustainable [53]. The international community are collectively working towards limiting the use of fossil fuels with the aim of transitioning to a sustainable low-carbon future [50]. This has included countries supporting the development of low-carbon technologies, often through subsidies, which is forecasted to change the value of high-carbon fossil fuels [50].

Reserves

Fossil fuel sources are finite [49] and accurately determining their reserves is not a straightforward task [54]. Whilst reserves are diminishing ever faster [16], commercially recoverable reserves of fossil fuels are still relatively plentiful [44, 54]. However, reserve levels are not the main concern for fossil fuels. Due to environmental concerns sustainable energy consumption has become a global priority [16, 44]. Organisation such as the IEA state that in order to meet the target of restricting the increase in global temperature to 2°C by 2050 33% of oil reserves, 50% of natural gas reserves and 80% of coal reserves must be unused up to this time [54].

Coal

Coal has the largest reserves (1,055 billion tonnes as of 2018) of fossil fuels and the longest time to exhaustion (153 years at current levels of production) [45, 55-56]. Coal is more abundant and widely distributed compared to oil and natural gas [16]. However, five countries hold three quarters of the world's reserves: United states (23.7%), Russian Federation (15.2%), Australia (14%), China (13.2%) and India (9.6%) [55]. *Table 1* shows global coal reserves and how they are distributed by region.

Table 1 - Coal Reserves by Region

Region	Million Tonnes	Global Share
North America	258,012	24.5%
South & Central America	14,016	1.3%
Europe	134,593	12.8%
CIS	188,853	17.9%
Middle East & Africa	14,420	1.4%
Asia Pacific	444,888	42.2%
World	1,054,782	100.0%

Whilst coal powered the industrial revolution and has aided economic development around the world it is also the largest emitter of CO₂ amongst fossil fuels [45]. Globally consumption of coal has declined at an average of 0.9% since 2013 [52]. This decline has been driven by a shift towards renewable sources and less harmful natural gas in developed countries [45, 52, 57]. In the UK, the birthplace of the industrial revolution, the use of coal has been rapidly declining in recent times and could be phased out by as early as 2025 [52]. Large decreases in coal use have also occurred in Canada and across the European Union [52].

However, the decrease in coal use in developed nations could soon be outpaced by the increase in developing countries, particularly those where energy poverty is prevalent [45, 52, 57]. Regions such as South & Central America and Asia Pacific have seen use increase around 3% per year [52], where coal is used for generating electricity [45]. The Asia Pacific region is the major consumers of coal, and their share of the global total has increased from 64.5% (2,261million tonnes of oil equivalent (Mtoe)) in 2008 to 75.3% (3,772Mtoe) in 2018 [55]. *Figure 4* shows the change in coal consumption between 2008 and 2018.

In terms of individual countries whilst the consumption of coal is decreasing in the United States, it was still used to meet one third of the country's electricity needs in 2016 (3,780m MWh out of 11,067m MWh) [58] and as of 2018 it was still the third largest consumer of coal at 8.4% of the global total [55]. India's consumption of coal has grown at a rate of 4.8% annually in recent years [52] and is currently the second largest consumer of coal accounting for 12% of the global total [55]. If the country's consumption continues at current rates it will double in less than two decades leading to an increase of an extra billion tonnes of CO₂ emissions annually [52]. China has consistently been the heaviest consumer of coal in recent times and as of 2018 accounted for over half of global consumption at 50.5% [55]. Turkey also depends heavily on coal to meet its increasing energy demands with 37.3% of the country's electricity in 2018 obtained through burning coal [59]. Other developing nations in the Asia Pacific such as Indonesia and Vietnam have also seen increased coal consumption in recent years [57].

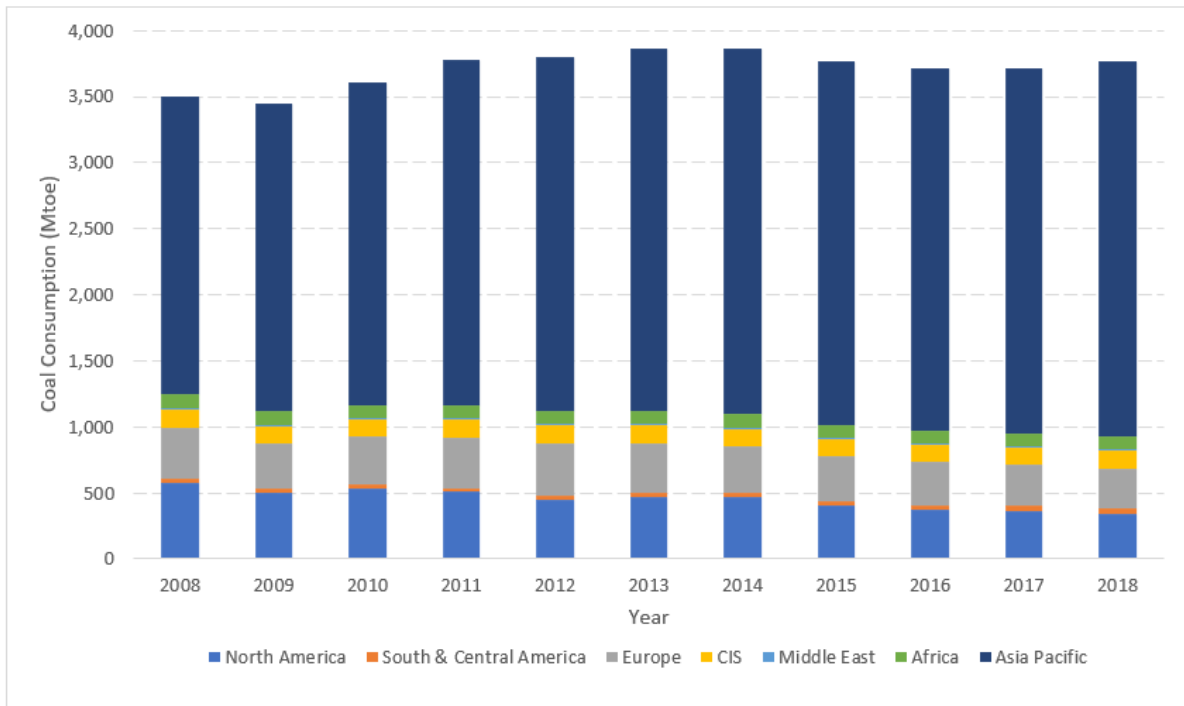


Figure 4 - Recent Coal Consumption by Region

Crude Oil

As with coal, oil is believed to have aided economic development around the world which is why it is often referred to as 'black gold' or 'industrial blood' [17]. Once it has been refined, oil is used in several sectors including industry and building, however, it is primarily used in the transportation sector [60]. Despite the increase in penetration levels of electric vehicles 90% of global transport energy demand is still met by oil-refined liquids today [17]. In recent decades the ownership of private vehicles has been steadily increasing because of increased income levels, particularly in developing nations [60]. These factors combined have seen the consumption of oil grow at an average of 1.4% globally since 2012 [52].

The growth in consumption has been led by countries in the developing world such as China and India where increases in consumption has been around 5% per year since 2012 [52, 57]. In China 19% of present primary energy demand is met by oil which mostly comes from imported sources (70%) [60]. Whilst in the US and EU the increase has been below the global average at 1.3% and 0.4% annually respectively [52]. Other OECD countries have also witnessed below global average increases [57].

British Petroleum (BP) and the Energy Agency (EA) both predict that oil consumption will peak around 2030 and be a significant part of the global energy mix up to 2040 [60].

Natural Gas

Natural gas is a naturally occurring mixture of saturated hydrocarbons and inorganic gas mixture that consists primarily of methane [16]. It emits lower levels of pollutants such as CO₂ when compared to other fossil fuels such as coal or oil [16, 29, 61]. Due to its cleaner burning characteristics it is viewed as a more attractive fuel than other fossil fuels [29]. However, it is still a major source of the increase of global CO₂ emissions [52].

In 2017 the EU's member states consumed 466.8bcm of natural gas which met 24% of the union's primary energy demand [62]. Whilst the consumption of coal and gas has been declining since the 1970's the consumption of natural gas has been growing [26, 52]. Consumption of natural gas increased by 5.3% in 2018 and 2% (78 billion cubic metres (bcm)) in 2019 [57]. The 2% increase in 2019 is below the 10-year average and is a result of decreased energy demands caused by COVID restrictions that were in place during most of the year [57].

The growth in consumption has been witnessed in every region and in many countries around the world [52]. In 2019 demand in the US grew by 27bcm, mostly at the expense of coal used in electricity generation [57]. In China consumption has increased by 8.4% per year since 2012 [52], and by 24bcm in 2019 (280bcm in 2018 to 304bcm in 2019) [57, 60]. The increased demand in both countries is arbitrated to their respective environmental protection policies [52].

Analysists predict the growth in consumption of natural gas will continue for the foreseeable future [29]. The growth is expected to occur in developed nations such as the US [29] and developing nations around the world [61].

2.2.2 Low Carbon Fuels

Nuclear and renewable energy sources are collectively known as low carbon fuels. They are called low carbon fuels because unlike fossil fuels their use does not produce carbon dioxide emissions [63]. They are considered to be cost-effective and environmentally friendly energy sources by today's policymakers [64].

Nuclear

Nuclear energy is obtained by releasing the binding energy in the nucleus of atoms through either fusion, decay or fission reactions [65]. Fusion is the process of two or more small nuclei fusing together to form one larger nucleus [66]. The energy available from fusion is almost limitless but its application is still largely theoretical [66]. Decay is the process of converting the heat released during the decay of radioactive material into electricity [66]. Decay is only used in niche application such as powering space probes [66]. Fission releases the energy, in the form of heat, of nuclei by splitting an atom into smaller atoms [65-67]. Nuclear fission is primarily used to generate electricity in nuclear power plants [65, 67].

The first commercial nuclear power plant began operation in the late 1950's in the US [58, 66]. Nuclear energy became a popular option in the late 1960's [16]. Today there are nuclear power plants operating in over 50 countries [66]. In 2019 nuclear energy met 3.95% of primary energy demand [26]. In the US nuclear energy currently meets 20% of the country's electricity demand and it is expected to be a significant part of its electricity fuel mix for the foreseeable future [58, 67].

Nuclear power plants provide continuous reliable and cost-effective energy over the plant's lifespans, which can be more than 80 years [68]. Nuclear energy also generates much lower levels of CO₂ than fossil fuels (a few grams per kWh generated) [56]. These attractive features have led to many developing countries today considering adding nuclear to their energy mixes [16]. 2016 saw the largest increase in global nuclear capacity for a quarter century with over 9GWe coming online [64]. Studies have predicted that nuclear energy could meet a quarter of global electricity demand by 2050 [64].

Organisations such as the IEA and the International Atomic Energy Agency (IAEA) have stated the importance of nuclear energy in achieving sustainable energy mixes [63]. However, nuclear energy is a highly controversial subject due to several disadvantages [16, 68].

The disadvantages of nuclear energy include the need for well-trained and competent operational staff and large investment and operational costs [16, 68]. The long-lived radioactive waste created by nuclear power plants remains hazardous for hundreds of thousands of years and its disposal costs the industry around £2.5 billion per year [68]. The hazardous nature of the radioactive waste also means that potential accidents at nuclear

power plants are a major security concern due to the likelihood of causing serious damage to human life and the environment. To date the world has witnessed 33 accidents at nuclear power facilities, the most famous of which being at the No. 4 reactor in the Chernobyl Nuclear Power Plant in 1986 which still poses risks to both human life and the environment today [68]. The accident at the Fukushima Daiichi Nuclear Power Plant in 2011 also showed that nuclear facilities are particularly vulnerable to natural events such as tsunami and earthquake [68]

The disadvantages associated with nuclear energy means it has many, often strong, opponents who say it is expensive, high risk and environmentally unfriendly [68]. The opposition to nuclear energy has seen interest in the technology decline in recent years in many developed economies [16, 58].

Renewables

Renewable Energy Sources (RES) come from natural, sustainable sources which are constantly replenished such as the sun [36, 69]. The world is reducing its dependence on non-renewable energy sources [47, 64]. This has led to RES currently being the fastest growing energy source around the world and seen its penetration in the global energy mix grow rapidly since the end of the 2000s [16, 19, 35, 57]. In 2019 the consumption of RES increased by 3.2 exajoule (EJ), led by China (0.8 EJ), the US (0.3 EJ) and Japan (0.2 EJ) [57].

Biomass

Biomass is non-living fossil and biodegradable organic material [17]. The Environmental and Energy Study Institute (EESI) define it as 'living or recently dead organisms and any by-products of those organisms, plant or animal' [70]. The EESI carry on saying that biomass excludes coal and oil [70]. Before the first industrial revolution it was the main source of global energy. It is still the fourth largest source of global primary energy today accounting for 10% of energy consumption in industrialized countries and as much as 35% in developing countries [17]. 38% of the global population (2.7 billion people) still rely on biomass for cooking, mainly in Asia and Sub-Sahara Africa [64]. Around 224×10^9 tons of dry biomass can be produced globally per year due to photosynthesis [17]. Biomass can also be used to produce energy for transportation known as biofuels by fermenting corn or sugarcane [48]. Biofuels are in wide use in both Brazil and the US [48].

Hydropower

Humans have harnessed the kinetic energy of water since ancient times to power mechanical devices such as watermills, sawmills and domestic lifts [71-72]. Hydropower is the harnessing of the kinetic energy in water of rivers and lakes to generate electricity [71, 73]. As the water is not used up or reduced in the process and is constantly replenished by the earth's water cycle hydropower is a renewable energy source [71]. As hydropower relies on the water in rivers and lakes resources around the globe vary substantially [73].

Hydropower is the most mature and well-established RES and has provided electricity for over a century [74]. The first machine to generate electricity through hydropower was built by William Armstrong in Northumberland, England in 1878 and was used to power a single lamp [75]. The first electricity generated by hydropower the US came shortly after in 1880 where it was used to power 16 brush-arc lamps at the Wolverine Chair Factory in Grand Rapids, Michigan [72]. The Schoelkopf Power Station became the first commercial hydropower station when it began using water from the Niagara River three years later to power streetlights in nearby New York [75]. The first commercial hydropower station Europe began operation in Italy in 1885 and by the early 1890's hydropower had become well established in both Europe and North America [73].

To increase electrification of rural communities the US Army core of Engineers began building hydropower plants across mainland US in the 1920's with their most famous project, the Hoover Dam, being completed in 1937 [76]. Since that time thousands of hydropower plants were built across North America and Europe [76].

Like all RES hydropower is a low carbon energy source [74, 77]. Unlike other RES hydropower can be quickly dispatched and its output can be quickly adjusted at minimal cost [76, 77]. It is also well suited to frequency control [74, 77]. They are also seen as a way of improving transportation and of promoting economic development [73].

Hydropower plants can also be used as Pumped Storage Plants (PSPs) [74, 77]. PSPs act as a battery by using excess electricity in grids to pump water uphill at times of low demand where it is stored until times of high demand or times of low water levels when it is released back to the lower reservoir which turns the plants turbine and generates electricity [71]. Unlike small scale storage devices such as batteries which are used for short term storage (daily or shorter) PSPs can store energy for weeks and even months [78]. The use of PSPs

is extensive in developing countries such as Brazil and Chile [77]. PSPs are seen as attractive as they can enhance the flexibility of electrical systems by balancing systems caused by daily and seasonal variations and the increased penetration of intermittent RESs [74, 77-78].

Hydropower does have some negatives as well. Hydropower projects require large areas of land and often requires altering the elevation of groundwater [73]. This leads to inevitable change and damage to the local ecosystem [73]. The changes to the local area around hydropower projects has also caused millions of people to be resettled and has led to the loss of livelihoods [73, 76]. They are expensive to build [74]. Unlike other RES such as wind and solar/PV hydropower plants take a long time to design and construct [77]. As the water used in hydropower is often used for other purposes such as irrigation the operation of hydropower stations can be constrained [77]. They are subject to seasonal changes which can see their potential output lowered in dry seasons and excess potential unutilised in rainy seasons [73]. Projected climate change is likely to lead to water shortages in the future which has raised doubts about the reliability of hydropower in the near future [73, 76].

Only around 22% of the global hydropower potential has been exploited to date [76]. However, due to the negative aspects discussed here most developed countries stopped the building of new hydropower projects decades ago [74]. Instead in regions such as Europe and North America the focus has been on refurbishment of some plants and the removal of others [74, 76]. Up to 2018 the UK, France, Switzerland, Portugal, Sweden and Spain removed 3,450 hydropower plants and between 2006 and 2014 a further 546 plants were removed in the US at enormous financial cost [76].

Excluding traditional biomass hydropower has been the largest RES since its first use in the latter part of the 19th century [76]. However, due to the decommissioning of plants and the increasing penetration levels of other renewables such as wind and solar/PV its share of the RES mix has been declining for some decades now (as shown in *Table 2*) [16]. At the start of the new millennium hydropower accounted for 91.1% of the RES mix [26]. This figure fell by 14.4% in 2010 and a further and a further 20.3% between 2010 and 2019.

Table 2 - Hydropower's Historical Share of the RES Mix

Year	Hydropower	Other RES
1890	100.0	0.0

1900	100.0	0.0
1910	100.0	0.0
1920	100.0	0.0
1930	100.0	0.0
1940	100.0	0.0
1950	100.0	0.0
1960	100.0	0.0
1970	97.9	2.1
1980	97.2	2.8
1990	93.4	6.6
2000	91.1	8.9
2010	76.7	23.3
2019	56.4	43.6

Whilst the use of hydropower has been declining globally since the 1970's it has continued to grow in developing countries [76]. In countries that have an abundance of hydro resources such as Brazil hydropower is an increasingly important part of the fuel mix [77]. China which also has extensive hydro resources has been the largest generator of hydropower since 2004 when it exceeded 100,000MW [73]. The installed capacity exceeded 200,000MW in 2010 and 300,000MW in 2015 [73]. China's theoretical hydropower reserves of approximately six trillion kWh per year accounts for 15% of the world's supply. [73] The large hydropower power potential in China is expected to see the resource play an important role in the country's electricity generation industry [73]. Developing countries continue to build ever larger projects along the Mekong, Amazon and Congo River basins which have overlooked the ecological damage in favour of increasing access to electricity [76].

Solar/Photovoltaic

Radiation from the sun (solar radiation) that reaches the Earth's surface drives a series of environmental processes that are critical to life [79]. The energy in the solar radiation that reaches the Earth's surface is about 1,000 times greater than the global annual consumption of fossil fuels [80]. This energy is continuously replenished and will continue to do so for as long as the sun continues to shine [81]. The heat energy in solar radiation is utilised for the desalination of seawater and water heating and cooling [17]. Whilst the light energy in solar radiation is converted into electricity using solar/photovoltaic (PV) systems [82].

Levelised Cost of Electricity (LCoE) calculates the average net present cost of each unit of electricity generated by a plant or system over its lifetime [58, 83]. The cost of manufacturing

PV systems has been consistently decreasing recently whilst at the same time efficiency has been increasing [76, 84]. This led to the LCoE of large-scale PV installations drop 73% between 2010 and 2017 [85]. The decrease in the LCoE of PV generation has seen it reach parity with traditional fossil fuel plants, and leading energy companies, consultancies and non-governmental organisations all forecast that this parity will continue into the near future [84].

The parity of PV to fossil fuels has seen support in the technology grow in policy makers around the globe who see it as a cost-effective way of empowering the energy transition [17, 86-87]. This support has seen PV systems installed in a wide range of sizes in recent years, from residential, prosumer, systems of 10kW and less to utility size installations between 1 and 10 MW [58]. These installations have combined to see global PV capacity increase significantly in the past decades [86, 88].

Global installed PV capacity reached 100 GW in 2012 [89]. In 2017 new installations of PV surpassed that of fossil fuel and nuclear installations combined [85]. The majority of these new installations were at the distribution level where generous feed-in tariffs encouraged homeowners to install small PV systems on their roof-tops in countries such as Germany, the UK and Japan [46, 89]. 272 GW of electricity generating capacity was connected globally in 2018 and 47 GW of capacity was decommissioned [89]. Of the 272 GW of new capacity 39% (107 GW) was PV [89]. The new capacity saw PV meet 2.6% of global electricity demand in 2018 [88]. By the end of 2019 this figure passed 3% [46], and global PV capacity reached 586 GW [90]. China had the largest installed capacity (205 GW) followed by Japan (61.8 GW), the USA (60.5 GW), Germany (49 GW), India (34.8 GW) and Italy (20.9 GW) [90]. The 49 GW of PV capacity in Germany is more than 30% of the country's thermal electricity generating plant capacity and the 20.9 GW in Italy is more than 20% of their thermal plant capacity [89].

The recent increases in PV capacity all exceeded forecasts and this trend is expected to continue as the transition to a sustainable future accelerates [46]. It is predicted that PV capacity could reach as high as 1.4 TW by 2024 [89]. Along with wind energy PV is forecasted to increase more than other energy source beyond this date and up to 2050 [91]. By which time wind and PV combined is expected to meet between one-third and two-thirds of total global electricity demand [84]. According to "A European long-term strategic vision for a prosperous, modern, competitive and climate neutral economy" in order for the EU to

meet 2050 decarbonisation targets in the power sector the member states would require a combined PV capacity of between 441 GW and 825 GW installed by that time [89].

Figures from the IEA show that \$1.85 trillion was invested in the global energy sector in 2018 [89]. 42% (\$775 billion) of this figure was invested in the electricity generation sector [89]. RES received the highest share of this investment (\$304 billion) followed by network infrastructure upgrade (\$293 billion), fossil fuel power (\$127 billion), nuclear power (\$47 billion) and energy storage (\$4 billion) [89]. A further \$25 billion of the investment in the global energy sector went towards RES for transport and heating [89]. Developing countries invested more than developed countries on RES in 2018, continuing a trend begun in 2014 [89].

PV attracted the largest share of the investment in RES every year between 2000 and 2018 [89]. In 2018 PV attracted 42.5% (\$140 billion) of the total investment in RES [89]. This investment was spread evenly between developed (\$65 billion) and developing economies (\$75 billion). \$2.1 billion of the global investment in PV was spent on research and development projects which were mostly supported by the EU and the Chinese government [88].

The investment in PV saw manufacturing levels increase 40% on average each year between 2004 and 2018 [89]. In 2018 around 120 GW of PV was manufactured across the world in Europe, Japan, China, and other Asian countries such as Taiwan, India, Malaysia, Thailand, the Philippines and Vietnam. [89]. The increase in manufacturing levels has moved the PV industry closer to the mass-producing industry that is required meet the predicted rise in demand.

Curtailment of Solar/PV Output

Whilst PV is pivotal in meeting decarbonisation targets increasing penetration levels also pose significant challenges to network operators [92-94]. This is particularly true at the low voltage distribution level where the existing infrastructure is ill suited to high penetration levels of renewables such as PV [95]. For example, at times of high PV generation and low customer demand (e.g. UK summer), reverse power flow will likely cause network voltage to rise beyond limits mandated by grid codes [94]. This will result in a curtailment of PV generation, unless appropriate control means are used.

Curtailement is defined as the “reduction in the output of a generator from what it could otherwise produce given available resources, typically on an involuntary basis” [96]. Curtailement is primarily induced by network operators for two purposes: a temporal mismatch between supply and demand (oversupply), and to avoid overvoltage [96-97]. Curtailement has been a standard practice since the start of the electric power industry [96]. However, as PV penetration levels increase so does the risk of oversupply and voltage violations and therefore curtailement of PV [98-99].

A recent study found that in 2018 around 6.5 million MWh of PV electricity was curtailed in Chile, China, Germany and the U.S. [100]. As penetration levels of PV continue to increase so do the instances of curtailement. For example, in California curtailement of PV has doubled between 2018 and 2019 [100]. The curtailement of PV is expected to continue to increase significantly in the near future, with one recent study projecting curtailement could reach 30-60% of potential output [99].

When the output of a conventional fuel-based generators is curtailed the unused fuel can be burned at a later time [100]. However, the curtailement of PV output is often considered a loss, as effectively free energy is wasted and unused [101]. Curtailement of PV also represents missed chances to reduce CO₂ emissions of electricity networks [102]. These factors reduce the economic viability of PV projects and could deter future PV deployment by undermining investor confidence [96, 98-100, 103]. Therefore, current thinking is that curtailement of PV output should be a last resort in order to maximize the potential of the technology [97, 101].

A popular measure for reducing PV curtailement in literature is increasing energy storage [92, 104]. However, increasing energy storage would require a significant capital investment from network operators [100]. Instead, operators and planners are seeking strategies to manage networks that minimize curtailement whilst also minimising network upgrades [100, 105]. One strategy that has been proposed is to discretely size PV systems that minimise investment whilst avoiding excess generation [101]. However, this approach limits the potential capital return of any PV project [98-99].

Wind Energy

The original source of the energy in wind comes from the sun [106]. Uneven heating of the earth’s surface by the sun causes pressure differences that in turn causes wind [106-107]

Wind is present everywhere around the globe but at different densities in different locations [106, 108]. According to the WEC around 27% of the Earth's land area has annual wind speed of more than 5m/s at 10m above ground level [17]. Harnessing the energy in wind is a free, clean (carbon neutral) and unlimited source of energy [109]. Global wind energy resources are larger than the anthropological primary energy demand [110], with around 10 million MW of wind energy continually available [107]. Wind energy, along with PV, is the fastest developing RES [111].

The power of the wind has been harnessed since the earliest history of human civilization [84]. Firstly, for transportation by propelling sailing vessels and latter for mechanical applications such as windmills which were used for grinding grain or pumping water [84, 106, 109]. Interest in wind energy faded due its intermittent nature and because of the invention of steam power in the 18th century followed by latter technologies which harnessed the energy in fossil fuels [106, 109].

Windmills convert the kinetic energy of wind into mechanical energy [106]. Wind turbines convert the wind's kinetic energy into electrical energy [106-107]. The first wind turbine was built in Denmark in 1890, by 1910 the country was home to several hundred wind turbines which each had a capacity of between 5 and 25 kW [109]. Commercial wind turbines were introduced to the US in the mid 1920's where they were used on farms to charge storage batteries which were in turn used to power small electrical appliances such as radios and lights [109]. Up until the 1970s wind turbines where primarily used to supply electricity to communities who lacked access to national electricity networks [84]. The Arab oil crisis of the 1970's intensified the interest in wind turbines and saw governments around the world examine the potential of the technology to meet significant portions of their electricity needs [84, 106].

The utilization of any energy sources is highly dependent on its cost [112]. The cost effectiveness off wind turbines is dependent on their size and power rating [107]. The size and power ratings of individual wind turbines has increased since interest in their application was intensified in the 1970's [107, 112]. By 1980 the typical wind turbine had a rotor diameter of 15m and a power rating of 50 kW [112]. In 1990 the typical figures increased to 40m and 500 kW and increased further to 80m and 2 MW in 2000 [107]. Today typical turbines have diameters of 190m and power ratings of 10 MW [112].

Technological improvements during this time have also seen the efficiency of wind turbines increase annually [106-107]. They have also increased the lifespan of today's turbines to between 20 and 25 years [113]. The increased power ratings and efficiency have seen the cost of wind-energy decrease to a fraction of its 1970's level [84]. This reduction in cost has seen wind energy become a cost competitive technology in most markets [84, 112-114]. Indeed, BloombergNEF, IEA and BP have all stated that wind has achieved price parity with natural gas and that they anticipate this to continue into the coming decades [84]. This in turn has seen wind energy playing an increasingly important role in the global primary energy mix especially for the generation of electricity [84, 112].

Due to the differences in wind densities in different locations it has been found that to better utilise wind resources it is often more advantageous to install several wind turbines at the same site [106]. As well as capturing more wind energy from high density locations this also reduces operational costs by concentrating repair and maintenance equipment and labour [106]. The arrays of wind turbines on a site can range from a small number to several hundreds and are known as wind farms [108]. Larger wind farms have capacities of comparable to traditional power stations [112].

Individual wind turbines and wind farms can be constructed both onshore and offshore. However, the majority are currently installed onshore (95.2% as of 2020) (see *Table 3*) [115]. This is because whilst there is more wind resource at higher speeds and less turbulence at sea offshore wind is significantly more expensive to construct and operate [106, 113].

Table 3 - Global Wind Installations by Region (Data [109])

Region	Year	On-Shore Installations (MW)		Off-Shore Installations (MW)		Combined (MW)	
		New	Total	New	Total	New	Total
Americas	2019	13,437	148,081	0	30	13,437	148,111
	2020	21,750	169,758	12	42	21,762	169,800
Africa & Middle East	2019	830	6,454	0	0	830	6,454
	2020	823	7,277	0	0	823	7,277
Asia-Pacific	2019	28,626	283,780	2,616	7,301	31,242	291,081
	2020	52,546	336,286	3,120	10,414	55,666	346,700
Europe	2019	11,741	182,651	3,627	21,901	15,368	204,552
	2020	11,813	194,075	2,936	24,837	14,749	218,912
World	2019	54,634	620,966	6,243	29,232	60,877	650,198
	2020	86,932	707,396	6,068	35,293	93,000	742,689

Despite the differences in costs there has been a significant increase in offshore wind energy since the start of the millennium [111, 113]. One reason is the maturity of offshore wind energy has seen the gap between the cost to onshore narrow [114]. The other reason is the limit of onshore wind potential due to the lack of land space with sufficient wind resources and public opposition [106, 111, 113].

The concept of offshore wind turbines was developed in the 1930's by the German inventor Hermann Honnef [106]. In the 1970's wind farms off the coast of Massachusetts were proposed but never built [106]. It wasn't until 1991 that the first offshore wind turbine was installed 350m off the coast of Sweden [106, 111]. The following year the first offshore wind farm was construction near the town of Vindeby in Denmark [106]. The 1990's witnessed rapid growth in the European wind industry with experimental projects built up to 4km off coasts [111, 114].

Europe is the largest consumer of offshore wind energy while the UK, Germany, Denmark, the Netherlands and Sweden are all major consumers [111, 114]. The UK is the global leader in terms of offshore installed capacity with 10.2 GW as of 2020 [111, 115]. The UK government has set an ambitious target of almost quadrupling this figure to 40GW by 2030 [115]. In 2020 the UK installed 483 MW of new offshore wind and Germany installed 237 MW but the world leader, for the third year in a row, was China who installed 3 GW of new capacity in 2020 [115]. These new installations have seen China overtake Germany for second spot in terms of capacity [114-115]

In 2016 figures from the Global Wind Energy Council (GWEC) showed the global cumulative capacity of both onshore and offshore wind energy grew by 54.6 GW to 486.74 GW [110]. By region the Asia-Pacific led the way of new installations with 203.6 GW followed by Europe with 166.3 GW [110]. Further figures from GWEC show that by 2020 the cumulative total had reached 742.7 GW after experiencing a year-on year growth of 53% [109]. The growth in capacity of wind in recent decades show the resource meet 1% of the global electricity demand for the first time in 2007 [132], and 5% for the first time in 2019 [26]. Several countries have surpassed the global average and meet 10-20% of their electricity demand from wind [84]. On the 3rd of November 2013 Denmark became the first country to produce more electricity through wind energy than was consumed at the national level, which has now become a regular occurrence in the country [112]. The growth in capacity is expected to increase by a factor of 10 by 2050 [84]. Therefore, wind is expected to play a

significant role in the global energy mixes of the present and near future [91, 107, 112]. With some experts predicting it will meet 25-33% of global electricity demand by 2050 [84].

The life cycle harmful emissions of wind energy are extremely low [84]. In scenarios created by the Global Wind Organisation it was predicted that wind energy saved 1.2 billion tons of CO₂ emissions in 2020, and that this figure could rise to 2.6 billion tons per year by 2030. [110]. Therefore, wind is predicted to be a major contributor to the growing sustainable energy of the world in the future [84].

Penetration levels of renewables varies by region and country [20]. The acceptance of renewables is high in developed nations and is rising in developing nations [47] especially in the Asia Pacific region [20]. In 2018 the highest concentration of RES was in Asia (43.54%), followed by Europe (22.82%) and North America (15.59%) [119]. In terms of per capita consumption Iceland, Denmark, Germany, Sweden, and Finland lead the way [36]. In the EU one-third of energy demand is met by RES, in China it is one-fourth, and in the US, India and Japan it is one-sixth [19]. In Asia wind and solar/PV are both significant contributors to the rise in RES in the region, with 600GW of the two sources having been installed since 2010 [19].

RES and Electricity Generation

The penetration of RES has increased in several sectors such as heating, transport and cooling [36]. They are predominantly recommended for electricity generation [86-87]. In the member states of OECD and EU the proportion of RES in the electricity fuel mix has increased significantly in recent years [19]. In 2019 the share of RES in the global electricity fuel mix increased 1.1% from the previous year reaching 10.4%, surpassing nuclear for the first time [57]. RES, in particular solar/PV, wind and hydropower, is expected to increasingly meet electricity demand in both developed and developing nations [36, 116].

Benefits of the Use of RES Technologies in Generating Electricity

To keep global warming to below 2°C a report in 2017 published by the International Renewable Energy Agency (IRENA) argued that global CO₂ emissions would need to be reduced to 9.5 Gt by 2050 [63]. RES do not emit CO₂ or other GHGs in their day-to-day operations [35, 44, 117]. Therefore, they are seen as a vital component in the fight to limit global warming [63]. However, several studies have reported that RES will only be able to have a positive impact on the fight against global warming once a minimum threshold of

penetration levels has been reached [64]. The authors of [118] calculated that RES need to supply 8.39% of global energy demand before any impact on CO₂ emissions could be observed. Whilst the report by IRENA stated that RES needs to supply 80% of global electricity demand by 2050 to ensure global warming targets are met [63].

RES are also seen as a way of increasing energy security by reducing the dependency on foreign energy sources [16]. The technological advancement and lowering costs of RES in recent decades has seen them increasing be seen as a way to improve energy equality [19, 35].

The ability of RES to address all three dimensions of the energy trilemma highlights their potential to play a major role in the transition to a sustainable energy paradigm [35-36, 44, 86]. This has seen interest in RES is growing internationally [44] and especially in Asia [19]. They play a key role in defining energy policies around the globe [86] in areas such as the EU, UK, US and Asian countries such as China, India and Japan [19].

Penetration Levels of RES

Penetration levels of renewables varies by region and country [20]. The acceptance of renewables is high in developed nations and is rising in developing nations [47] especially in the Asia Pacific region [20]. In 2018 the highest concentration of RES was in Asia (43.54%), followed by Europe (22.82%) and North America (15.59%) [119]. In terms of per capita consumption Iceland, Denmark, Germany, Sweden, and Finland lead the way [36]. In the EU one-third of energy demand is met by RES, in China it is one-fourth, and in the US, India and Japan it is one-sixth [19]. In Asia wind and solar/PV are both significant contributors to the rise in RES in the region, with 600GW of the two sources having been installed since 2010 [19].

The penetration of RES is increasing significantly in member states of OECD and EU [19]. In 2019 RES accounted for 80% of new generation in OECD countries, in non-OECD countries it accounted for 35% of growth [36]. If the adoption of RES in the EU continues to grow at the same rate of the last decade, they will supply more energy than coal by 2021 in the region [52]. The EU want the increase of RES to continue and have set the target of 27% RES by 2030 [120]. The IEA has predicted that renewable energy sources could increase their share in the electricity fuel mix to 12.4% in 2023 [50] and 39% in 2050 [36].

The expenditure on RES grew 63.3% (\$177 billion to \$289 billion) globally from 2008 to 2018 [36]. In developed countries expenditure rose 12.6% (\$120.9 billion to \$136.1 billion), whilst in developing countries the rise was 102% (\$30.5 billion to \$61.6 billion) [36].

Employment

In 2016 the global renewables sector employed 9.8 million people (see *Table 4*) [20]. Solar/PV was the largest employer with 31.6% of the renewables total, followed by modern biofuels, hydropower, wind, solid biomass and other technologies which includes biogas, small hydropower, geothermal and concentrated solar power [121]. China was the largest employer in the renewables sector (40.3% of global total), followed by the European Union (12.3%) and Brazil (10.8%) [20].

Table 4 - Employment in Renewables Sector in 2016

Technology Sector	Employees (millions)	Share of Renewables
Solar/PV	3.1	31.6
Modern Biofuels	1.72	17.6
Hydropower	1.52	15.5
Wind	1.16	11.8
Solid Biomass, Heating & Cooling	1.55	15.8
Other Technologies	0.75	7.7
Total	9.8	100

2.2.3 Link with Economic Growth

It has long been known that electricity consumption and energy consumption in general are key drivers for both economic and socio-economic growth [17, 36, 107, 122-123]. It has also been found that there is an intimate and symbiotic relationship between energy and economic growth [122]. This relationship means that whilst economies grow so does energy demand [117]. Today this means the energy sector accounts for nearly 10% of global GDP [123]. Due to the diminishing reserves of fossil fuels and their negative impacts on the environment discussed earlier, alternative (environmentally friendly) energy sources have been investigated to determine their potential to replace environmentally damaging fossil fuels [47, 124].

The relationship between renewable energy consumption and economic growth has been examined in several recent studies. These studies have examined individual countries such

as the United States [125], Germany [126], India [127] and Indonesia [128]. Other studies have examined different regions such as Asia [129-131], Africa [132-134], the European Union [135-136] and the Commonwealth of Independent States [137]. Some have examined Groups such as the Organisation for Economic Co-operation and Development (OECD) [138-140]. Whilst others concentrated on low and middle-income countries around the globe [141].

These studies and others found a strong symbiotic relationship between the consumption of renewable energy and economic growth, particularly in emerging economies [126]. The findings in [126] showed that a 1% increase in the consumption of renewable energy led to economic growth of 0.219%. Whilst the findings in [36] found that an increase of 1% in per capita income results in a 3.5% increase in the consumption of renewable energy.

2.2.4 Present Day Energy Mix

By sector electricity generation and transportation are the major consumers of energy globally. Figures from the United States Energy Information Administration (US-EIA) show that in 2020 they combined to consume 64% of the energy in the United States (US), followed by industry, commercial, and residential (see Figure 5) [142]. Electricity generation and transport are also the main contributors to CO₂ emissions globally through their heavy reliance on fossil fuels [45].

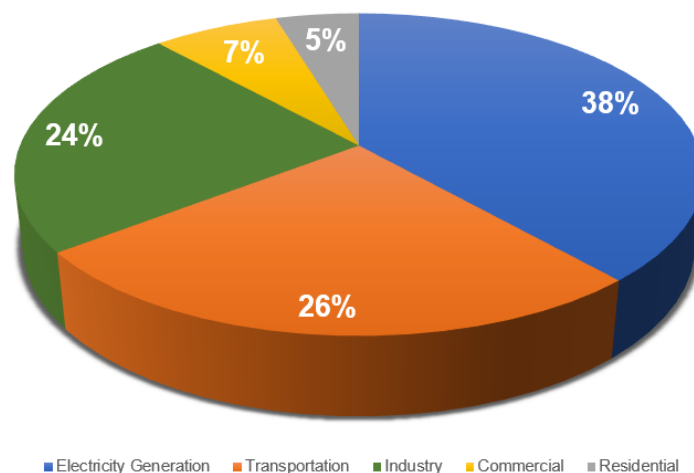


Figure 5 - Energy Consumption by Sector in the US in 2020

In 2019 fossil fuels continued to dominate the global primary energy mix meeting 84.4% of demand [26]. The other 15.6% being met through low carbon sources (see Figure 6). The ratio between high carbon and low carbon sources in the electricity fuel mix was better during the year with fossil fuels meeting 63.3% of demand and low carbon source meeting the other 36.7% (see Figure 7). Despite the penetration levels of low carbon energy sources, in particular renewables, continuing to increase year on year the world burns more fossil fuels each as energy demands increase. In The 10 years up to 2019 energy production from fossil fuels increase from 116,214 TWh to 136,761 TWh [26]

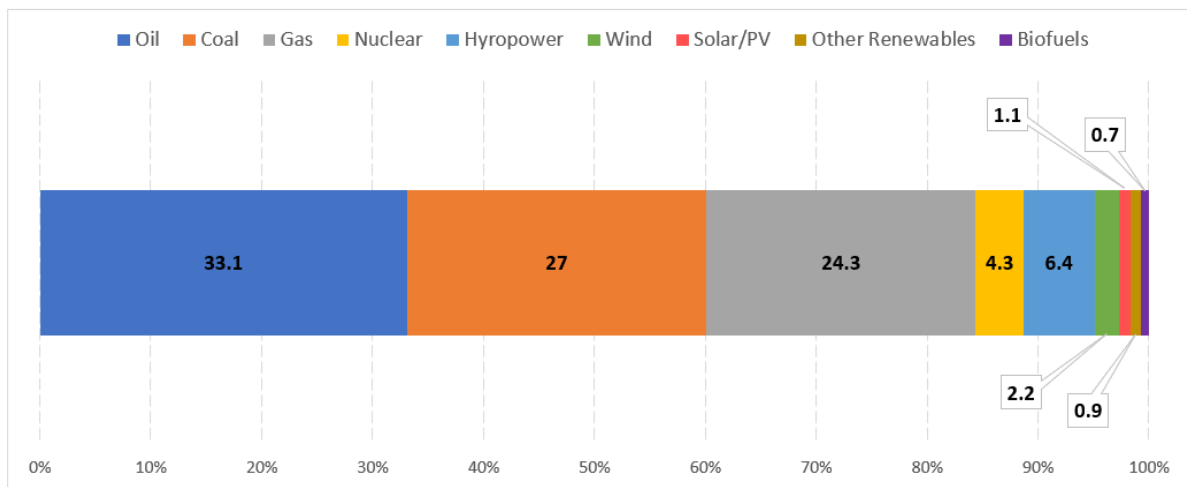


Figure 6 - Global Primary Energy Mix 2019

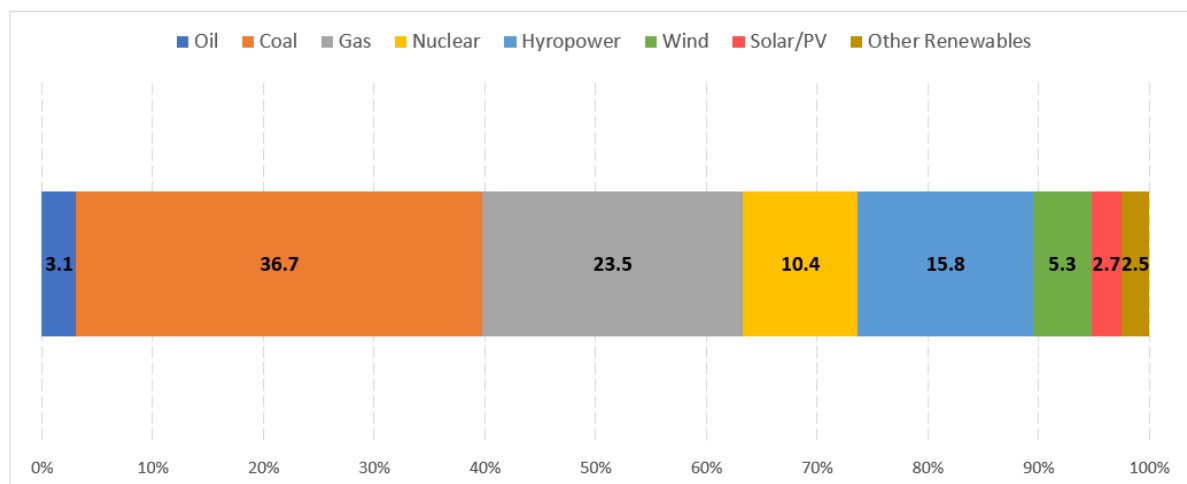


Figure 7 - Electricity Fuel Mix 2019

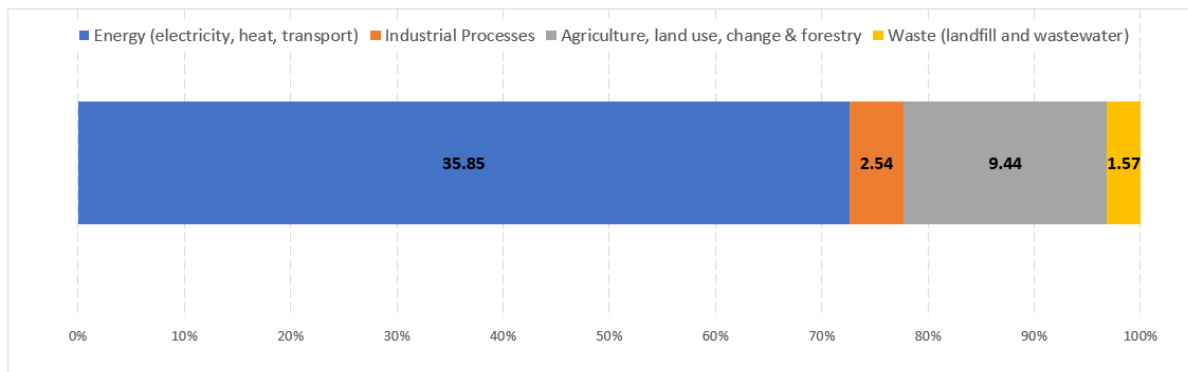


Figure 8 - Global Greenhouse Gas Emissions by Sector 2016

2.3 The Environment and Climate Change

The increasing consumption of fossil fuels is unsustainable [16]. Whilst energy consumption from fossil fuels leads to economic and social growth it also leads to environmental degradation most notably in the form of significantly increased greenhouse gas emissions which leads to climate change [47, 124].

Climate change is defined as “the variability of the climate system that includes the atmosphere, the biogeochemical cycles (carbon cycle, nitrogen cycle and hydrological cycle), the land surface, ice and the biotic and abiotic components of the planet earth” [143]. A major impact of climate change is global warming which is the increase of the mean global temperature [143].

The International Panel on Climate Change (IPCC) state that global mean temperatures have risen by 0.85°C (with a range of 0.65-1.06°C) since the second industrial revolution of the 1820s [45, 52, 144]. This increase in temperature is evidenced in a recent report from the IPCC that showed that seventeen of the eighteen warmest years occurred in the 21st century [145]. Whilst this temperature rise may appear small it has increased extreme weather events and climate disasters [45, 143, 146]. Global warming has seen sea levels rise causing the flooding of coastal areas and the disruption of global rainfall and water supply [17, 146]. This is reflected in the damage caused to the northern range of the Great Barrier Reef in Australia which has lost half its coral cover since 2014 due to extreme weather events [52].

Extreme weather and climate disasters are also responsible for the loss of human life and the disruption of societies and cause severe financial burden, for example in the 2017 it is

estimated they cost the United States \$306 billion [52]. Climate change can also alter insect and plant phenology and affect global food production levels [143]. The impacts of climate change are potentially long-term [17]. Indeed, if global warming is not stopped some of the main landmasses and islands around the world will become uninhabitable. [147]

Human activities such as the burning of wood have affected the environment throughout history by causing deforestation and creating air pollution [16]. However, the impacts of human activity on the environment have increased massively since the industrial revolutions of the eighteenth and nineteenth centuries [16]. The exponential growth in the consumption of fossil fuels since the first industrial revolution has led to large amounts greenhouse gasses being released into the atmosphere [16-17].

The emissions of greenhouse gases (GHG) such as carbon dioxide (CO₂), methane (CH₄), and nitrous oxide (N₂O) are the main proponents of climate change and global warming [143]. Greenhouse gasses collect in the atmosphere where they stay for centuries absorbing sunlight and trapping heat [148]. CO₂ forms the largest component of harmful GHG emissions and therefore is the most responsible for climate change [52, 59].

Figure 9 shows historical global CO₂ emissions. Prior to the first industrial revolution CO₂ emissions, also referred to as carbon emissions, were very low [26]. Up to the middle of the 20th century the growth in emissions was still relatively low. In 1950 global CO₂ emissions were just below 6 billion tonnes [26]. Between 1950 and 2000 emissions grew at an average of 2.9% per year.

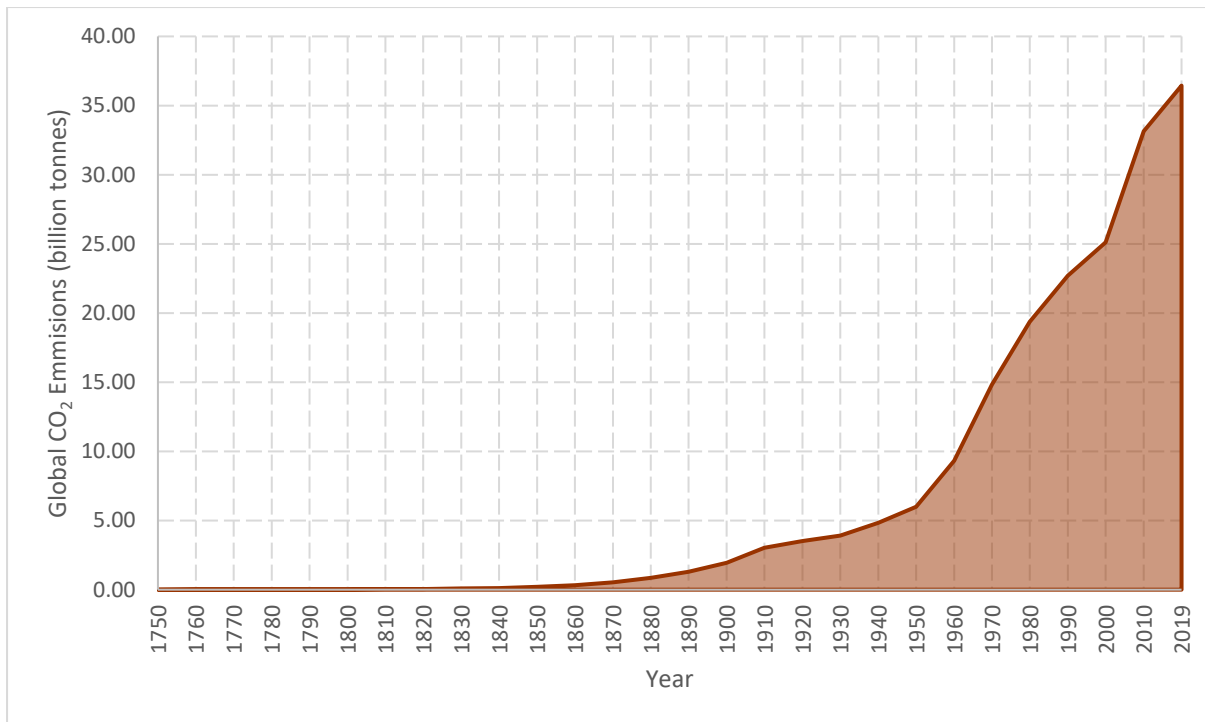


Figure 9 - Historical Global CO₂ Emissions

Between 2008 and 2018 the growth in CO₂ emissions continued to grow but at a slower rate, 1.1% per year on average [57]. In 2019 the growth slowed to 0.5% [57]. Global emissions passed 364 billion tonnes by the end of the year with the US alone emitting about the same amount as the entire world did in 1950 and China twice as much [26]. China, the US and India together have been responsible for 85% of the increase in emissions since 2018 [59].

The negative effects of CO₂ emissions on the environment are largely irreversible for 1,000 years after the emissions stop [146]. Research has shown that there is a limit to the amount of GHG such as CO₂ that the earth's atmosphere can absorb before the effects of global warming are irreversible [45]. In 2018 the IPCC stated that we are close to passing this point and that the world needs to reach net zero emissions by 2040 to prevent this point being reached [45].

The scientific community and policy makers around the world agree that climate change is one of the most pressing global issues of the 21st century [16, 47, 54, 59, 64]. Restricting global temperature rise to 2°C compared to pre-industrialization levels is seen as key to combating climate change [45, 54, 63]. To this end, 196 parties signed a legally binding international treaty known as the Paris Agreement in Paris, France on the 12th of December

2015. The goal of the treaty is to limit global warming to below 2°C (preferably 1.5°C) compared to pre-industrial levels [89].

In order to restrict global warming to 2°C a number of governments of developed and developing countries have set targets to reduce their CO₂ emissions [36, 26]. As a result, several policies and initiatives have been developed at national and international level with the common aim of mitigating climate change [54]. Key to these policies and initiatives is reducing the dependence on fossil fuels [47]. As whilst emissions from fossil fuels appear to be slowing, they have not yet reached their peak [26]. One area where emissions are rising the highest is the global south where emissions have risen steadily since the 1980's due to the urbanisation and economic development programs instigated by countries in the region [45]. This was seen in a study of the urbanisation of India between 1901 and 2011 which found that whilst the urbanisation promoted economic growth it also increased CO₂ emissions [64].

As energy is the main contributor to greenhouse gas emissions and climate change, clean and affordable energy is seen as an important tool in combating climate change and meeting sustainable goals [20]. Indeed, the decarbonisation of the global energy system and the electrification of final use of energy is seen as the single most important component in limiting global warming and meeting the aims of the Paris Agreement [89, 149]. A model developed by the IEA found that the decarbonation needs to be achieved well before 2050 [89]. The decarbonisation of energy systems will involve the transition to more environmentally sustainable systems that use clean energy sources [81, 150].

2.3.1 Environmental Kuznets Curve

The Environmental Kuznets Curve (EKC) hypothesizes that there is an inverted U-Shaped relationship between of economic growth and environmental degradation [151-152]. This means that the early stages of economic growth contributes to environmental degradation. However, as growth continues degradation declines, and when a certain point of development is achieved the trend reverses and further economic development leads to environmental improvement. Some authors have used the theory to claim that “there is clear evidence that, although economic growth usually leads to environmental degradation in the early stages of the process, in the end the best—and probably the only—way to attain a decent environment in most countries is to become rich” [153].

The theory is based on the premise that the economic development of pre-industrial economies requires increasing levels of energy [51]. It also assumes that environmental protection will be seen as a conflicting goal to growth in the early stages of economic development [124, 152]. The recent industrialisation of China is often used as to demonstrate this as during the early stages of its economic growth the country relied almost exclusively on environmentally damaging fossil fuels to meet its rapidly increasing energy demands. China also demonstrates that as an economy reaches a certain stage it will focus more and more on trying to achieve sustainable energy paradigms.

2.3.2 Traditional Thinking

The approach taken by China to achieve economic development was the same approach that has been taken by numerous countries since the 1st industrial revolution. It is the traditional thinking associated with this approach that assumes that economic development and environmental protection are conflicting goals [152]. Traditional thinking also assumes that there is a scale effect to economic growth and environmental damage [152]. This assumes there is a scale effect between the two factors that means a 1% increase in economic growth causes a 1% increase in environmentally damaging emissions if there is no change in the technologies and industries driving an economy. However, different industries have different pollution concentrations [152]. Over the course of an economies development the industries driving growth will change. In the early stages of development heavy industry which is a severe polluter replaces low polluting agriculture. In the later stages of development heavy industry is replaced by less intensive light manufacturing and service sectors [152]. It is this shift in industries which creates the Kuznets Curve and gives it a quadratic appearance, as can be seen in *Figure 10*.

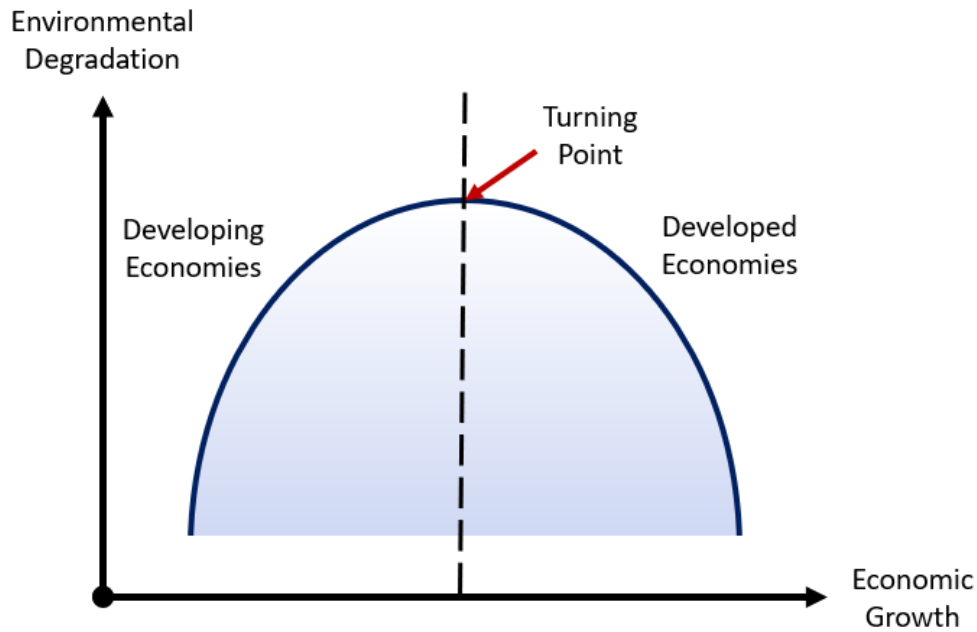


Figure 10 - Environmental Kuznets Curve

2.3.3 Factors in the Decrease of Pollution

Along with the change in industries driving economies there are several other factors which decrease pollution levels of economies. These include improvements in technologies that increase productivity and reduce emissions of processes [152]. Improvements in technology also lead to more efficient use of natural resources and recovery of some resources through recycling. Increasing income levels of populations also make them more willing to pay for a cleaner environment [51]. However, the most significant means of reducing pollution is the substitution of fossil fuels with RES technologies in fuel mixes [51].

The effectiveness of RES in reducing pollution levels was demonstrated by the authors of [154]. The authors examined the factors that reduced pollution levels of seventeen OCED countries. The findings confirmed the most significant factor was the increasing penetration levels of RES in their respective fuel mixes of the countries studied. The findings also confirmed the validity of the EKC hypothesis by showing that the more developed an economy became the less harmful pollutants it emitted. The findings of [155] also confirmed the effectiveness of increasing RES penetration levels in reducing damaging pollutants.

2.3.4 Developed and Developing Countries

Energy demand is higher for developing economies compared to developed economies [47]. According to the IEA by 2040 developing nations will account for 64% of energy demand with Asia expected to see the largest increase in demand [19]. This was shown in the findings of [156] which examined 90 countries at different stages of economic development. The study found that energy demands were higher for developing countries especially those in the early stages of development. The study also found that high income countries such as the USA and UK had reached the turning point of the EKC and were actively seeking ways of significantly reducing their damaging effects on the environment. Heightened environmental awareness in both policy makers and the public of developing countries has seen an increase in the support of the use of RES in the early stages of development of many developing nations around the globe in the aim of transitioning towards a more sustainable future [51].

2.3.5 Environmental Sustainability

According to the World Energy Council (WEC) environmental sustainability is the transition of “energy systems towards mitigating and avoiding potential environmental harm and climate change impacts” [157-159]. The environmental sustainability dimension of the energy trilemma focuses on decarbonisation to combat climate change through increasing productivity and efficiency of generation, transmission and distribution of energy [21, 24, 160-161].

The United Nations Framework Convention on Climate Change (UNFCCC) states that countries have a common but differentiated responsibility towards environmental sustainability [161]. The UNFCCC goes on to say that developed countries should take the lead on environmental sustainability [161]. This is generally the case and means that the most environmentally sustainable energy systems are found in the developed nations of Europe [21]. However, various institutions are increasingly expecting developing nations to mitigate climate change more actively [161]. Indeed, climate change considerations are increasingly important criteria for international development banks in their dealings with developing countries [161]. Today most countries in the developed and developing world see the transition to environmentally sustainable energy systems as a top priority in their policy making [123].

The energy mix of a nation is crucial to it achieving environmental sustainability [162]. Diversifying fuel mixes is seen as key to achieving long-term sustainable energy paradigms and de-carbonising economies [62, 162]. The two most often talked about strategies for creating long-term sustainable energy systems are the electrification of the transport sector and the increase in penetration levels of clean RES into fuel mixes [89]. Of the RES currently widely available PV has been highlighted as playing a significant role in these two strategies due to the maturity of the technology, its modular design and its continual decreasing cost [163].

2.4 Energy Equality

Energy equality concerns the access to electricity, heat, or other modern energy services for both domestic and commercial use at affordable prices [24, 161, 164]. WEC defines energy equality as “a country’s ability to provide universal access to reliable, affordable, and abundant energy for domestic and commercial use” [21]. It is estimated that 1.4 billion people (20% of the global population) lack access to reliable electricity and 2.7 billion depend on biomass for cooking [161]. The people living in these conditions are said to be living in energy poverty. Due to population increases energy poverty is on the rise. The ranks of people living in energy poverty is predicted to increase by several hundred million in the coming years, mostly in the global south [24].

Due to the importance of energy equality in enabling social and economic prosperity irradiating energy poverty is a top priority for many developing countries in the global south, particularly those in Southeast Asia. This has led to several governments in Southeast Asia to enact ambitious national electrification programs [165]. Southeast Asia has large concentrations of populations and economic activities along its extensive coastlines and has a strong reliance on the region’s natural resources such as agriculture and forestry [166]. Therefore, it is at high risk from the effects of climate change [166]. As a result of this, policymakers in the region are focused on finding a sustainable energy model that allows the region to irradiate energy poverty without compromising energy security or damaging the environment [165, 166]. Policy makers in Africa, where accesses to electricity is also low, are also focused on finding sustainable energy models and see investment in RES as a way to achieve this as well as create employment [162].

The COVID-19 pandemic which was first identified in Wuhan, China, in December 2019 highlighted the importance of energy equality. Energy services have been pivotal in the

response to the pandemic by powering healthcare facilities, supplying clean water for hygiene and enabling communication services whilst people were following social distancing rules [164].

2.5 Energy Security

The concept of energy security used to be concerned with the balance between supply and demand [23]. The modern concept of energy security has evolved to include environmental and social concerns and is incorporated into national security policies [23]. Today's energy security paradigm must consider several geopolitical dimensions such as international trade, political stability and foreign affairs [18, 23, 35].

The WEC defines energy security in today's world as "a nation's capacity to meet current and future energy demand reliably, withstand and bounce back swiftly from system shocks with minimal disruption to supplies" [21]. Whilst the United Nations Development Program defines energy security as "the constant availability of energy in sufficient and affordable quantities without any adverse economic and environmental impacts" [162].

Energy security incorporates the efficiency of the management of both domestic and foreign energy sources, the quality of supply and the reliability and resilience of energy systems [21, 24]. It covers short-term facets such as the ability of energy systems to respond swiftly changes in the balance between supply and demand, and long-term facets such as the investment to supply energy in a socioeconomic and sustainable way [167]. Achieving a secure supply of energy is a prerequisite of modern economies functionality and critical to technological revolution [35]. In regions with low access to energy such as Africa energy security is seen as one of the most important strategies to alleviating poverty [162].

Different countries and organisations have very different positions on energy security dependant on domestic energy resources and reliance on imported sources of energy [21]. Countries which depend heavily on imports due to limited natural resources are thought of as suffering energy security vulnerability [35]. This is true of many of the countries in the EU which as a whole is one of the largest energy importers around the globe [18, 62]. 90% of the crude oil and 66% of the natural gas consumed in the EU come from external sources [35]. Most of the natural gas consumed by EU member states, particularly those countries in the Baltic region and eastern Europe, comes from one source, Russia which supplies 39% of the EUs demand [35, 39, 168].

The dependence on a single supplier leaves the member states of the EU vulnerable to disruptions of supply, infrastructure failure and higher price fluctuations [18, 35]. These vulnerabilities were highlighted in by a number of disputes between Russian and Ukrainian gas companies between 2009 and 2014 and the Ukrainian civil war and Russian annexation of Crimea in 2014 [62, 168]. These events resulted in cuts to the gas supply to Ukraine in June 2014 which restricted the supply to the EU countries [18, 168].

These events have seen energy security receive increasing attention and become one of the primacies of the EUs energy policy [18, 35, 168]. These policies are intended to reduce member states dependence of energy from politically un-stable regions [39].

Approximately two-thirds of the crude oil consumed in the US comes from foreign sources with 68% coming from countries in the middle east [56]. Almost all the natural gas imported into the US (98%) comes from one source, Canada [39]. These figures have seen numerous US political figures call for an end to the dependence on foreign oil and gas since the Arab oil embargo of 1973 [29]. Today reducing this dependence is seen as key to achieving energy security [56]. Achieving energy security is in turn understood as vital in growing the country's economy and meeting its defence needs [56].

As an energy exporting country, the Russian concept of energy security is different to most other countries around the globe [169]. Due to its vast domestic fossil fuel resources one quarter of Russia's GDP comes from energy exports [169]. Therefore, Russia's energy security policies concentrate more on the security of demand which has been hit by sanctions from EU countries since the annexation of Crimea in 2014 [169]. The depletion of fossil fuel reserves is another concern for Russia and its economy [18].

The energy mix of a nation is an important aspect of its energy security [162]. Reducing the dependence on external energy suppliers by diversifying energy mixes is seen by policy makers in developed and developing countries as essential to achieving energy security [23, 62, 168, 170]. For example, EU leaders have implemented a number of policies such as the European Energy Security Strategy of 2014 which aim to diversify the fuel mixes of member states in order to reduce their dependence on Russian natural gas supplies [62, 171].

Concentrations of fossil fuels are limited to a small number of locations around the globe [16]. This fact along with depleting reserves can create military tensions and even conflicts [16, 35]. This in turn can adversely influence the energy market due to concerns over the reliability of supply [56]. This forces many countries to stockpile fossil fuels to ensure continuity of supply such as Japan who stockpile a 90-day supply of oil and a 50-day supply of natural gas respectively [35].

The potential of military conflicts and political instability significantly increase the price of fossil fuels at times [64]. A recent example of this was the conflict between Europe's two biggest natural gas suppliers, Russia and Ukraine, in 2014 discussed earlier [169]. This led to a significant increase in energy costs across Europe for a considerable length of time. The fear of these price rises and their potential to remain persistently high as well as the reliability of supply means that many governments now view reliance on fossil fuels as a serious risk to their energy security [64, 172-173].

The COVID-19 pandemic which caused a reduction in demand for oil highlighted the susceptibility of global fossil fuel markets to price shocks [162]. This fall in demand led to a massive fall in oil prices and a collapse in the market which saw oil record negative prices for the first time in history on the 20th of April 2020 [162, 174]. The susceptibility of these markets has led to several countries with high indigenous fossil fuel resources such as Canada and Russia view diversification as a way of improving energy security [21, 162].

2.6 Energy Diversity

All energy sources are subject to market forces which can result in large price rises and even interruption of supply [175]. Even if the risks associated with any one source of energy are low the consequences of the risks associated with interruption of supply are extremely high [162]. Energy diversification is the introduction of different energy sources into a mix and increasing the share of energy from each source to avoid the dependence of any single source [162, 170]. This is seen as a way of reducing the risk of interruption of supply as diverse energy systems are more likely to continue in the presence of the failure of any singular energy source [170].

Countries with rich fossil fuels reserves such as Russia view diversification as a major risk to their energy security [169]. However, they are aware that they need to adapt to the structural changes that will occur in the energy sector [169]. Whilst countries that are heavily reliant on

energy imports are looking to diversify their energy mixes that will increase energy security without damaging the environment [23]. The strategy employed by the EU to achieve this goal is the replacement of imported fossil fuels with indigenous RES technologies which they state will allow them to increase energy security of member countries and help them meet de-carbonisation targets [18, 35].

2.7 Transportation sector

2.7.1 Green House Gas Emissions

The transport sector is one of the major consumers of primary energy in the world today. In the EU it consumes over a third of the country-members primary energy [176]. Current research points to the importance of the role the transport sector needs to play in mitigating climate change [177]. The sector is the second largest CO₂ emitter in the world, behind electricity generation [120]. And it is the only major sector where global GHG emissions are continually rising year on year in developed regions such as the EU [176-177]. GHG emissions increased by nearly 20% between 1990 and 2014 in the sector [176]. In 2014 the sector accounted for 21% of total GHG emissions around the world [178]. In 2017 emissions by the sector were close to 26% of the global total [145].

Road transport is the main driver of increasing GHG emissions in the sector. The number of private light vehicles (PLGs) is rising rapidly which has seen road transport emissions increase by 71% between 1990 and 2016 [178]. In 2016 PLGs and other transport on the road, Heavy Duty Vehicles (HGVs), accounted for 95% of all the GHG emissions in the transport sector [145].

Global trends in population increase, urbanisation and motorisation all indicate that the number of PLGs on the world's roads will continue to rise sharply well into the middle of the century [176]. Therefore, it is reasonable to assume that unless major changes occur in the sector its global emissions will continue to rise at an ever-increasing rate. Indeed, if emissions in the transport sector follow current trends then they are predicted to grow 38% between 2014 and 2040 when the sector will emit 10,317 million tons of CO₂ [178].

2.7.2 Air Quality

As well as contributing to climate change the emissions from road going internal combustion engines vehicles (ICEVs) detrimentally effect health by reducing air quality in the localised vicinity. Stringent tailpipe emission limits on new vehicles have been enforced to try to combat this issue but exposure to tailpipe emissions such as particulate matter and nitrogen oxides (NO_x) is still a major health hazard in urbanised areas [120]. In the European region alone the air pollution in urbanised areas is linked to 100,000 deaths per year with a significant fraction of these deaths attributable to the air pollution created by ICEVs [120].

2.7.3 Noise

Noise is increasingly seen as another as a major health risk of ICEVs. According to the World Health Organisation (WHO) traffic noise in urban areas of Europe affects the health of nearly one third of local populations [120]. They go on to say that in the EU around 40million people in urban areas and 25 million people outside of metropolitan areas are exposed to street level noise of 50 decibel (dB) at night due mainly to road transport [120].

2.7.4 Electrification of the Transport Sector

Due to the forecasted rise of GHG emissions in the transport sector policy makers around the globe have prioritised its transition to a low-carbon model [176]. Electrification is regarded as the best strategy for decarbonising the transport sector [179]. As road vehicles are the main cause of GHG emissions in the sector policy makers around the globe such as the EU have focused their attention in recent times on electrifying road transport, in particular PLGs [145]. The EU has set the goal of road transportation being 100% CO₂-free by 2050 with the vehicle fleet being mostly electric with only a minor portion being powered by other fuels [120].

Replacing ICEV stock with state-of-the-art electric vehicles (EVs) is seen as an efficient way of reducing GHG emissions in the sector [120]. As well as reducing GHG emissions the electrification of PLGs will improve energy efficiency and reduce localised air pollution [145]. The electrification of PLGs and HGVs can also reduce noise pollution in urban environments especially when they are driven at slow to medium speeds [120]. Countries such as China also view EVs as a way of improving energy security by reducing the dependence of foreign oil supplies [180].

The use of the batteries in electric vehicles when they are connected to a smart grid could also create a more harmonised system by acting as temporary energy storage/source for fluctuating renewable energy sources such as wind and PV [120].

2.7.5 Electric Vehicle Stock Levels

The numbers of EVs on the roads today are relatively small compared to ICEVs [145]. Current EV stock levels are currently primarily made up of two different technologies, Battery Electric Vehicles (BEVs) and Plug-In Hybrid Electric Vehicles (PHEVs) [120]. In 2015 there were approximately 1.25million EVs on the roads with the vast majority registered in Europe and other major economies around the world [120]. The largest share of vehicles was in the US (33.3%) and China (23.1%) with Japan a distant third (10.8%) (see *Table 5*).

Table 5 - Number of Electric PLGs on the Roads in 2015 [120]

Country	BEVs	PHEVs	Combined
Austria	5,000	1,500	6,500
Belgium	3,900	4,700	8,600
Denmark	7,600	500	8,100
Finland	600	1,500	2,100
France	44,000	10,600	54,600
Germany	25,500	10,800	36,300
Ireland	1,000	200	1,200
Italy	4,200	500	4,700
Netherlands	9,400	78,200	87,600
Portugal	1,300	800	2,100
Spain	3,600	1,100	4,700
Sweden	4,800	9,800	14,600
Switzerland	6,300	2,700	9,000
Turkey	200	0	200
UK	20,000	27,000	47,000
Norway	70,700	12,100	82,800
USA	214,600	191,900	406,500
Canada	7,900	7,700	15,600
China	199,800	81,800	281,600
South Korea	8,800	1,500	10,300
Japan	76,900	55,200	132,100
Australia	2,500	1,300	3,800

In 2016 the different EV technologies made up only 1% of road transport vehicles [145]. Between 2016 and 2017 the registration of BEVs increased by 51% and registration of PHEVs increased by 35% [145]. Whilst currently low EV stock levels are increasing worldwide as manufactures introduce more models to the market [120, 145].

Governments are also introducing policies aimed at increasing EV levels. These policies include the funding of vehicle purchase schemes and public charging infrastructure installation and levy taxes related to CO₂ emissions [145]. India has initiated a policy which has the commitment to end the sale of ICEVs by 2030 and China is working on a policy to end the sale of ICEVs by 2050 [177]. Several developing countries are looking to follow the lead of India and China and are embracing the future of electric transportation [177]. The increase in EV penetration will significantly contribute towards climate change mitigation and increase energy security by reducing dependence on foreign supplies of oil [120, 177]. It will also aid realise the four freedoms of the EU – goods, capital, services and people [120].

2.8 Electricity

Electricity is the most important form of energy in the modern world [47]. It is essential for nearly every activity of industry, commerce, and individuals [16, 33, 181-182]. It is one of cornerstones of economic and social development [182]. Therefore, reliable and secure access to the resource around the clock is essential for economic and social development [19, 34, 181-183].

Due to its role in facilitating economic and social development electricity generation and distribution is especially important to developing countries [183]. Due to this Governments in many developing countries have created polices aimed at increasing access to electricity of their populations. An example being the National Electrification Plan which was introduced in 2014 by the government of Myanmar in South-East Asia which aims to provide access to the country's entire population by 2030 [184].

The importance of electricity in contemporary society and the increase of access to electricity is seeing demand of the resource constantly increase [185, 144]. Between 2000 and 2017 global demand increased by an average of 3% per year [19]. The electrification of the transport sector will further accelerate demand for electricity and change the nature of

demand patterns. Bloomberg New Energy Finance estimate access programs, electrification of the transport sector along with population growth will grow from 25,000 terawatt-hours in 2017 to over 38,000 terawatt-hours by 2050 [84].

Meeting the increasing electricity demands is a main goal of countries around the globe [16, 183]. However, increased awareness of climate change has seen the focus shift towards meeting future demand in a sustainable way [36, 150, 181, 186]. Key to achieving a move to a more sustainable electricity generation paradigm is the replacement of fossil fuels with environmentally friendly renewable energies sources (RES) [17]. Increasing RES penetration levels is seen as a way of not only facilitating the transition to a sustainable low carbon economy but also increase energy security by reducing dependence on fossil fuels [187]. The reducing costs of RES technologies and the abundance of RES potential such as PV in many developing nations has seen policy makers in such countries increasingly view RES as a suitable way of increasing energy equality to their citizens [182].

2.8.1 Electricity Networks

To ensure all sections of a society has a continuous source of electricity countries all around the world have built complex systems known commonly as electricity networks, power networks or grids [181]. The main purpose of these networks historically has been to meet the yearly peak electricity demand in a reliable way [188] and provide around the clock supply [34]. However, in the aim of abating the impacts of climate change the decarbonisation of these networks is seen as playing a major role in the transition to a more sustainable paradigm [36, 188].

Many of the top electricity consuming countries around the globe have been engaged in transitioning to more sustainable electricity networks that can still support economic and social development for several decades now [186]. The main focus of these countries has been the reduction of fossil fuels and diversifying their electricity generation fuel mix [54, 73].

2.8.2 Diversity and Electricity

The diversity of the fuel mix to generate electricity is particularly seen as a way of measuring the effectiveness of energy policies [35]. Diversifying the electricity mix is seen as a major route to achieving energy security, equality and sustainability [35]. There has been progress

in diversifying the electricity fuel mix since the middle of the 20th century, however the growth of diversity needs to increase if global sustainability is to be achieved [76].

Reducing the levels of environmentally damaging fossil fuels in the electricity fuel mix is the major driver for diversification for most policy makers [33, 189]. However, countries without indigenous supplies of fossil fuels also view diversification as a strategy to increase energy security [21]. Key to this strategy is maximising the use of domestic RES [23]. The US for example views increasing RES as key to diversifying their electricity fuel mix and increasing energy security [56].

2.8.3 Access to Electricity

Reports from the IEA showed that in 2010 there were 1267m people around the globe without access to electricity, with the figure growing to 1285m in 2012 [19]. The majority of these people live in developing countries in Latin America, Africa and Asia where population growth is outpacing access to electricity [19]. In 2020 there were still 770 million people without access to electricity [109]. As the global population continues to increase it is expected that this figure will rise by several hundred million in the coming years, again in developing countries [24]. The ratio of people without access to electricity in developed and developing countries highlights the social inequality involved [24]. For example, the per capita energy usage in the US is times higher than that of India, where hundreds of millions currently do not have access to electricity [52].

2.8.4 Ageing Networks

The electricity grid is described as “the largest interconnected machine on Earth, so massively complex and inextricably linked to human involvement and endeavour that it has alternately (and appropriately) been called an ecosystem” by the U.S. Department of Energy [53]. It has been hailed as the greatest engineering achievement of the twentieth century by the National Academy of Engineering [190].

Electricity grids have served us well for a long time. They have evolved to become ever more complex systems that are now true marvels of engineering [53]. However, the majority of the infrastructure that built these grids have been in use since the early part of the 20th century. The aged equipment has begun to struggle to meet the demands placed by the ever-increasing demand and is rapidly running up against their limitations [53, 179]. This has

caused policy makers to become concerned about the ability of the aging networks to continue to reliably serve the 21st century they helped fashion [16]. Network operators need to contend with the issues of overtaxing demand and aged equipment whilst meeting challenging targets for de-carbonising of their systems [179].

2.8.5 EVs and the grid

Whilst the electrification of the transportation sector has been successful in reducing the tailpipe emissions of vehicles it has increased the load on the worlds ageing electricity networks [38, 177, 189]. Whilst this increase in load is relatively small today it is expected to increase significantly in the near future as the penetration levels of EVs increase [38]. In the UK the transport sector consumes 36% of the country's energy with 75% of the transport sector energy in the UK is consumed by PLGs (41,199 tons of oil the equivalent) [179]. Transferring this load to the already over worked National Grid in the UK would require an extra 479.2TWh generation capacity [179]. Worldwide the electrification of the transport sector would require a twofold increase in present electricity generation output [179].

Accommodating the forecasted increase in charging of EVs at the distribution level of networks is a major challenge for network operators [37, 179]. The increased load caused by the charging of EVs can negatively impact voltage stability, harmonics and reduce the reliability of networks [38]. To try to mitigate these issues accurate information on charging patterns and load profiles needs to be used to allow 'intelligent' charging to occur [37]. Accommodating the increase of EV charging will require additional infrastructure and generation capability [179]. To meet de-carbonisation targets in both the transport and electricity generation sectors the fuel mix of this extra generation needs to be carefully considered [33, 38, 177].

2.8.6 Generation

The fundamental principles of electricity generation were discovered by the British scientist Michael Faraday in the 1820s and early 1830s [191]. Faraday found that the motion of a loop of copper wire between the poles of magnet was all that was needed to generate electricity. Since the early days of the first industrial revolution the burning of fossil fuels has been used to turn the turbine of generators which use Faraday's principles to generate electricity. This model of electricity generation is still widely used today and meets the large majority of current day demand [191].

Traditionally these electricity generating plants, or power plants, have been located far from areas where the electricity is consumed [182]. The employment of these large 'centralised' power plants requires an extensive transmission and distribution infrastructure [182]. The evolution of electricity grids has seen a move away from this centralised generating model to a distributed generating model [182]. Distributed Generation (DG) is defined as electricity produced close to the load source and seeks to introduce new technologies that significantly reduce the cost of producing energy [192]. DG decentralises electricity generation and facilities generation closer to the point of consumption [182].

DG has several advantages over the traditional centralised model. It reduces transmission costs and helps reduce technical losses and installation time [182]. It attracts private investment and increases energy stability and grid optimisation [182]. DG also increase diversity by increasing use of RES and even allows consumers to generate their own electricity whereby they become known as prosumers [182]. Moving to a DG model with increase levels of RES has emerged as the preferred choice in the sector to de-carbonisation and reducing GHG emissions [147, 193].

Whilst there are several benefits to the DG model there also some significant challenges that need to be assessed in accommodating large amounts of RES. There is an uncertainty and variability in the production output of RES [147, 193]. Escalating penetration levels of RES also have technical impacts on electricity grids such as voltage rise and reverse power flow [194]. The inverters used by RES can also cause power quality issues such as harmonics and flickers [147]. So, to facilitate the move to a DG paradigm and increase in RES penetration levels on grids these issues need to be investigated and accurate information on how RES will affect networks is essential for proper operation and planning.

2.8.7 Demand Side Management

Demand Side Management (DSM) is a smart grid solution used in the DG model to control customer loads to achieve a better match between the available supply and the demand [195]. It is commonly used to reduce peak load demand and prevent the need to increase generation capacity [196].

2.9 Energy Trilemma

Whilst sustainable energy normally focuses on environmental protection it covers a complex and multidimensional range of interrelated areas across different disciplines [20, 47]. Sustainable energy is energy that can be used to improve the quality of life of present generations in an economic, ecological and social way so as not to compromise the ability of future generations to meet their own needs [20, 47, 197].

The WEC state that achieving energy sustainability involves “managing three core dimensions: environmental sustainability, energy security and energy equality of energy systems throughout the transition process” [21, 24]. The WEC collectively name these three elements as the “energy trilemma” [53, 123]. The term energy trilemma has emerged recently as a means of describing the complexity of meeting the economic, social and environmental challenges in order to achieve energy sustainability [24, 53-54]. Balancing the trilemma enables individual countries to achieve prosperity and competitiveness [21].

Graphically the energy trilemma can be represented by a Venn diagram made up of three sets (dimensions) as shown in *Figure 11*. The overlapping area of the three sets characterises energy sustainability [53]. The other areas illustrate the interdependence and trade-offs between the environmental, security and equality dimensions [53].

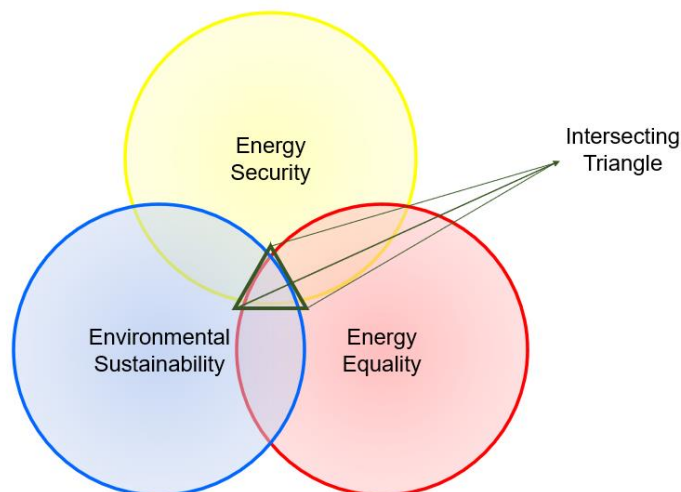


Figure 11 - Energy Trilemma Venn Diagram

It is more commonly presented as a triangle whose three points represent the core dimensions of the energy trilemma (see *Figure 12*).

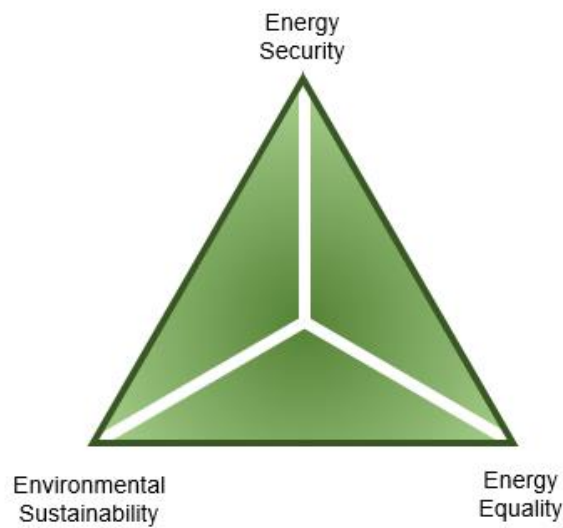


Figure 12 - Energy Trilemma Triangle

The three dimensions of the energy trilemma are often thought to be competing demands which therefore leads to trade-offs needing to be made when formulating sustainable energy policies [53, 159-161]. For example, in the mid-1980s countries such as England, Wales, Norway and Chile restructured their respective energy markets to increase energy security and energy equality without considering environmental sustainability equally [198]. In more recent times the priority of many developing countries has been to alleviate energy poverty, with little consideration given to energy security or environmental sustainability [160-161]. Today developed countries are mostly concerned with increasing the environmental sustainability of their systems as policy makers try to combat climate change [24, 198]. These decisions were all made because it was thought at the time that policymakers could only choose one or two of the energy trilemmas dimensions to focus on [159].

An opposing approach to the world energy trilemma recognises that progress can be made in all three dimensions of the trilemma once deep-seated obstacles are overcome [159]. Overcoming these obstacles allow strong energy systems to be created which are environmentally sustainable, secure and equitable [160].

2.9.1 De-carbonisation

Solving the energy trilemma involves creating healthy systems which are environmentally sustainable, equitable and secure. Key to achieving this is the rapid transition to a

decentralised and de-carbonised future [199]. As electricity generation is the largest consumer of primary energy the sector was identified by the IPCC in 2014 as critical to this transition [200-202].

2.9.2 Energy Transition

The transition to a de-carbonised future is the fourth major energy transition and is considered to have begun in the 1980's when modern renewables such as solar/PV and wind were first introduced to the energy fuel mix [24, 26]. These RES were introduced at the time to investigate their potential to decrease reliance on fossil fuels and to find a cleaner energy source [24, 30-31].

Realising this fourth energy transition will create a sustainable energy paradigm in which energy can be used to improve the quality of life of the present generations in an economic, ecological and social way so as not to compromise the ability of future generations to meet their own needs [20, 47, 197]. The transition to a sustainable energy paradigm is central in combating climate change and greenhouse gas emissions [22, 24, 47]. Achieving sustainability in the energy sector requires a transition in the use of energy for electricity, transport and heating & cooling [22, 117, 197].

2.9.3 International Policies and Treaties

In recent decades there have been several major international treaties brought forward which are aimed at facilitating the transition to a sustainable energy paradigm. These treaties have been signed by the majority of the world's governments in both developed and developing countries. In the treaties all signatories agreed to set individual goals and targets to meet the overriding goal of mitigating climate change.

On the 11th of December 1997 one-hundred and ninety-three countries signed up to the Kyoto Protocol [150, 203]. The protocol is an international treaty that committed the signatories to de-carbonise energy systems to reduce their GHG emissions (relative to 1990 levels) which came into force on the 16th of February 2005 [150]. Each country agreed to adopt policies to meet individual targets for reductions and to report on progress periodically [150, 203].

The World Energy Assessment published in September 2000 by the UN investigated the relationship between energy, the environment, health and other social issues [20]. The report found a strong link between energy, the environment and social development. The report also highlighted the importance of the role of energy in the economic prosperity of developing countries [20]. The findings of this report were discussed at United Nations Conference on Sustainable Development (UNCSD) in Rio, Brazil in June 2012. The conference was attended by 192 UN members and several private organisations. The conference culminated with the writing of a non-binding document called "The Future We Want" which laid out 17 objectives for sustainable development [20]. Of the 17 objectives laid out two were identified as having the potential to impact the whole of humanity most significantly. These were Goal 7 "Ensure access to affordable, reliable, sustainable and modern energy for all" and Goal 13 "Take urgent action to combat climate change and its impacts" [20].

In 2015 the UN updated the goals laid out in the Future We Want and set out new targets to be met by 2030 [20]. In September the governments of one-hundred and ninety-three developed and developing countries signed up to meeting these targets known as the Sustainable Development Goals (SDGs) [19, 24, 117]. The SDGs were 17 interlinked global goals which were designed by the United Nations General Assembly to "achieve a better and more sustainable future for all" [19]. Goal 13 – Climate Action was widely regarded by the signatories as the most important of the goals [24]. The SDGs again were not enforceable [24].

At the 2015 United Nations Framework Conference on Climate Change (UNFCCC) in Paris, France 195 countries agreed to take actions aimed at reducing CO₂ emissions to zero by 2050 in order to prevent "dangerous anthropogenic interference with the climate system" [110, 146, 149]. The main goal of these actions was to keep global warming to below 2°C (compared to pre-industrial levels) [145]. The participants also expressed their intention to take actions to limit temperature even further to 1.5°C [120].

Policy makers such as those in the EU are strongly committed to meeting the targets of these different policies as they have stated their belief that ensuring an efficient, sustainable and secure supply of energy is one of the most important tasks of our time [35]. To successfully transition to a sustainable future the EU agreed to reduce their GHG emissions 20% by 2020 [63]. They further committed to reducing emissions by at least 60% by 2040

and 80% by 2050 [63, 120]. The EU are strongly committed to meeting these targets and have adopted comprehensive strategies to reduce GHG emissions [117]. The EUs 2030 climate and energy framework stated that all economy sectors would need to participate in the effort to meet these targets but highlighted the electricity generation sector as having to play a key role [90].

2.9.4 Increasing Demand for Energy

The global demand for energy began to increase sharply in the 19th century when it was used to fuel the industrial revolution. This rise has continued in recent decade when demand increased 53% between 1995 (8,588.9 million tonnes) and 2015 (13,147.3 million tonnes) [19]. Demand is forecasted to continue to rise into the near future. In one scenario studied by the IEA the findings estimated that global energy demand would continue to increase 75% between 2008 and 2035 [110].

One of the main drivers of the forecasted energy demand is the rapid increase in the global population [46, 204]. By 2050 the global population is projected to reach 9.8 billion an increase of 2.2 billion from 2017 [84]. The IEA estimates this will increase energy demand by 1.6% annually [110]. The developing and transitioning nations of the global south are predicted to see the largest increase in population and are therefore expected to witness the greatest increase in energy demand (60-65% of the global total) [110]. This is currently being seen in India where the growing population is driving the increase in energy demand [47]. Energy equality and economic development programs will also increase energy demand in the global south into the near future [204].

The forecasted increase in energy demands highlights the complexity involved in solving the energy trilemma. The increased demand will need to be met to achieve energy security and equality [204]. Lessons learnt from countries such as China who used fossil fuels to power their economic development have shown that achieving energy security and equality can be done at the expense of environmental sustainability [21]. Only if all three dimensions of the energy trilemma are addressed will the transition to a sustainable de-carbonised future be realised [160].

2.10 The Role of Renewables in the Transition to a Sustainable Future

To realise their sustainability targets the EU identified the need to transition away from fossil-based economies [145]. In 2011 the European Commission acknowledged the potential of RES and smart grid technologies to enable the member states to transition away from fossil-fuels and to meet GHG emissions targets through the de-carbonisation of their electricity networks by 2050 [149, 201]. In December 2011 the EU Commission published 'A Clean Planet for All' which laid out their plans for de-carbonisation by 2050 [89]. The plan stated that to meet the de-carbonisation target RES penetration levels would need to be greater than 60% by 2050 [89]. To promote the increased penetration of RES in their electricity fuel mix the EU have introduced several policies such as the European Directive 2001/77/C [205].

Other policy makers and energy experts around the world agree with the EU with regards to the importance of RES in meeting decarbonising targets [16, 36, 111, 199, 206]. Increasing decarbonisation through the electrification of the transport sector by the mass employment of EVs has also gained interest from many policy makers around the globe in recent years [38]. To fully utilise the potential of EVs to reduce GHG emissions many countries have set high RES penetration targets in their respective electricity fuel mixes [90,207].

Environmental protection is the most commonly talked about aspect of energy sustainability and considered the most important part. However, there is growing understanding that to successfully transition to a sustainable future the other two dimensions of the energy trilemma, security and equality, also need to be addressed at the same time [161]. Recent research has shown that RES also have the potential to significantly improve both security and equality whilst playing a primary role in environmental sustainability efforts [24, 160, 198, 208]. At the same time as reducing carbon emissions replacing fossil fuels with RES will also improve security by reducing the dependence on imported sources [24, 149, 201]. RES can further increase security as they are not subjected to the same volatility in price increases of fossil fuels [50, 76, 162].

The UN stated in the 'Future We Want' publication of 2000 that to achieve energy equality there would need to be a substantial increase in the share of RES in the global fuel mix by 2030 [159]. PV is regarded by many as the best candidate RES to realise energy equality [159, 208]. The maturity level of the technology has realised consistent and significant reduction in generation costs over recent decades [36]. And the generation costs of PV are

now comparable to traditional fossil fuel sources [36, 116, 209]. PV has lower maintenance requirements and costs compared to traditional fuels and other RES such as wind. The modular nature of PV allows the technology to be effectively employed in small- and large-scale projects and has short installation times. Due to all these factors PV is seen as a good option in reducing energy inequality, especially in the global south where inequality is most prevalent and PV resources are high [145, 208].

Due to the potential of PV to empower the transition to a de-carbonised future and improve all three dimensions of the energy trilemma governments all around the world have introduced initiatives such as tax reductions and grants to encourage growth of PV generation [36]. These initiatives have been initiated by developed countries such as the US, UK and the member states of the EU and numerous developing countries in Africa, Asia and Latin America [36].

2.10.1 Penetration Levels

The amount of attention given to RES by policy makers has seen investment increase in the sector. In 2017 RES accounted for two thirds of the total investment in global spending of electricity generation [145]. This investment has seen their share in the global electricity fuel mix increase at a steady rate in recent times. The share of RES in the global mix grew by 2% between 2019 and 2020 [210]. Overall RES grew from 26% to 28% in this time with PV and wind increasing from 8% to 9% [210]. Despite issues in the supply chain and construction phase caused by the Covid-19 crisis RES generation has continued to grow at a rate of 5% [210].

The European region has seen one of the largest increases in the deployment of RES. Between 2004 and 2016 the share of RES in Europe grew on average by 6% per year which saw its share double in that period [145]. The US has also witnessed a significant increase in the share of RES in recent times where it reached 17% in 2017 [211]. At the beginning of 2020 the penetration of RES in India reached 23.41% in terms of installed capacity [116].

Of the individual RES wind and PV have seen the most dramatic growth in installed capacity in recent years [145, 212]. Wind energy presently contributes over 10% of the electricity produced in eight countries [211]. In 2000 there was almost zero PV global capacity, yet in only 16 years global capacity surpassed 100GW [145]. In 2017 PV meet more than 7% of the demand for electricity in Greece and Italy and 3.7% of the overall demand in the EU

[145]. PV capacity is forecasted to double between 2019 and the end of 2022 [211]. The increase in PV has been driven in part by individuals and small to medium sized business who have installed small PV systems at their properties to help meet their electricity demands and to sell unused electricity to network operators [210]. In 2019 these prosumers made up one-fifth of all RES capacity deployed worldwide [210].

The penetration levels of RES are expected to continue to grow up to 2050 and beyond as countries work towards meeting the targets they signed up in international treaties such as the Kyoto Protocol and the UNFCCC [58]. Wind and PV are forecasted to continue to make up the biggest share of RES up to this time [208].

As stated previously the cost of PV generation has reached parity with conventional fossil fuels. There is an abundance of PV resources spread evenly around the world. The maturity of PV and technological advancements have increased the working life of crystalline-silicon systems to 25-30 years and increased efficiencies [145, 213]. PV systems are also easy to install due their modular nature and require little to no expert maintenance making them ideal for remote isolated communities [214]. They are also viewed as a way of optimising electricity consumption in areas already connected to networks, even in countries such as Sweden which has low PV resources [214]. The public view PV more favourably than other RES technologies such as wind which has perceived issues with regards to noise and appearance [215].

Due to these reasons in the Near-term PV is set to see the fastest increase in growth of the RES technologies [210]. The IEA forecasts that by 2050 solar/PV will make up 22% of the global electricity fuel mix [213]. Many developing and transitioning countries in the global south have high indigenous PV resources. For example, the National Institute of Wind Energy has stated that India a PV potential of 750 GW, two and half times greater than the country's wind potential [116]. In 2018 the Ministry of New and Renewable Energy of India enacted a policy to exploit 100 GW of this potential by the end of 2022 [116].

2.10.2 Progress in Realising the Energy Transition

Many European countries have made great strides in realising the transition to a sustainable energy paradigm [21]. The UK has reduced CO₂ emissions by 31.5% since 2000 and levels now match those of 1888 [21]. This has been accomplished by tactics such as the reduction of coal in the fuel mix to 5% by replacing it with offshore wind [21]. This tactic saw the UK be

one of only 19 countries to significantly decrease CO₂ emissions whilst global emissions rose [52]. Despite these achievements if the UK is to continue to meet its obligations and decarbonisation targets it will need to employ new strategies such as the wide scale deployment of EVs [21].

Developing and transitioning countries are also actively engaged in the energy transition [208]. The majority of these countries have focussed their attention on RES and have implemented legal frameworks and tax incentives to encourage the integration of RES on to their networks [208]. This has led to the investment in RES by these nations being greater than that of the developing world since 2015 [216]. In 2019 developing and transitioning economies invested \$152 billion in RES compared to the developing economies investment of \$130 billion [208]. This investment has seen an improvement in environmental sustainability of Asian countries such as China and Cambodia [21]. However, as Asia is currently the largest importer of fossil fuels more work still needs to be done especially as many countries in the region seek to increase energy equality [21].

2.10.3 Continuing Progress

Policy makers now face the challenge of continuing this progress in the energy transition [208]. To this end many governments are continually drafting new energy policies which continue to support measures already in place and introduce new ones [21]. This will require significant investment which can be problematic for developing nations who are also working to meet increasing energy demands [207]. Due to the significant role played by RES in progress made to date most of this investment is expected to go to the most well-established RES technologies [160].

2.11 The Impact of COVID on Energy

The coronavirus disease 2019, known commonly as COVID-19, is an infectious disease caused by the recently discovered SARS-CoV-2 that mainly affects the respiratory system [217]. It was first identified in Wuhan, China on the 31st of December 2019 [218]. Since that time it has become a pandemic which has spread right across the world and has caused an excess of five million deaths [217]. The measures taken to combat the pandemic have affected every aspect of human life [35].

COVID lockdown measures have curtailed industrial and commercial activities in most countries around the world [210]. In countries such as the United Kingdom, France, Italy, Spain and India who have all implemented full lockdown measures electricity demand has significantly reduced (at least 15%) [210]. Whilst lockdown measures reduced demand also highlighted the critical role electricity plays in key aspects of human life such as health by powering vital medical equipment and allowing businesses to continue to operate by enabling teleworking and videoconferencing equipment to operate [35].

Lockdown measure led to a global decrease in the demand of fossil fuel-based energy sources such as natural gas (5% in 2020) and coal which witnessed the largest drop in demand since World War II (8%) [210]. Oil was also exposed to a collapse in demand for transportation fuels where COVID lockdown measures led to global road transport levels falling to 50% of 2019 levels, and air travel levels declining more than 90% in some European countries [210]. The combined decrease in demand for electricity and transport led to global demand for oil decreasing by 57% in 2020 [210].

The magnitude and speed of the decline in demand for these fossil fuels far exceeded the market flexibility of supply. The financial and macroeconomic consequences of which could undermine industry's ability to ramp up production levels to pre-COVID levels and cause further financial strain and could become a significant energy security concern creating uncertainty about the outlook [210]. Whilst demand for fossil fuels has been hit by the lockdown measures the penetration of RES has accelerated faster than pre-pandemic forecasts [210].

Renewable energy sources such as wind and PV proved to be the most resilient fuel source to the global pandemic and saw an increase in use of around 1.5% in 2020 compared to 2019 figures [210]. This was in part due to new wind (approximately 60GW) and PV (excess of 100GW) installations which were completed in this time and because renewables are usually dispatched before other sources of electricity [210]. The manufacture of PV modules has also started to ramp back as countries such as China, who manufacture 70% of global total, restart operations as lockdown measures ease [210].

2.12 Predicting Future Energy Use

The topics discussed in this literature review highlight the complexities facing policy makers and network operators as they aim to implement the transition to a sustainable energy

future. Accurate information is critical to this endeavour to allow proper allocation of funds and resources [160]. Accurate predictions of the future energy demand and its patterns are one of the most vital components of this information [16].

2.12.1 Load Profiles

Load (electricity demand) profiles show the variation in electricity demand over time. They are normally recorded at the system level or the customer category level (residential, commercial etc.) They are an indispensable tool for companies and organizations in the power sector and are used in the decision-making process in areas such as volume of generation and maintenance scheduling. Load varies greatly throughout the course of a day due to customer activities and other factors such as customer class [185, 219-220]. Load profiles are essential for power transmission and distribution companies in order to make important decisions on the volume of generation, power purchase agreements, operation and maintenance scheduling, development of network infrastructure etc [221-222]. Traditionally load profiles are created using historical data [223] and are used in many countries to balance load demand [224].

The most significant factor to affect demand is the weather, in particular the temperature [181, 185, 220, 225-229]. As well as affecting the intraday patterns in electricity demand, temperature also greatly influences seasonal demand [227, 229, 230]. Higher and lower temperatures both lead to increases in demand [227]. This is particularly true in residential areas [228]. Higher temperatures in the summer season increase demand for air-conditioning, whereas lower temperatures in winter increase the demand due to heating requirements [231]. The demand for these two services typically occurs at different times of the day which changes the pattern of demand throughout the year. Variations in seasonal demand are particularly pronounced in countries with temperate climates as the UK where demand is significantly dependant on seasonality (as shown in *Figure 13*) [185, 232].

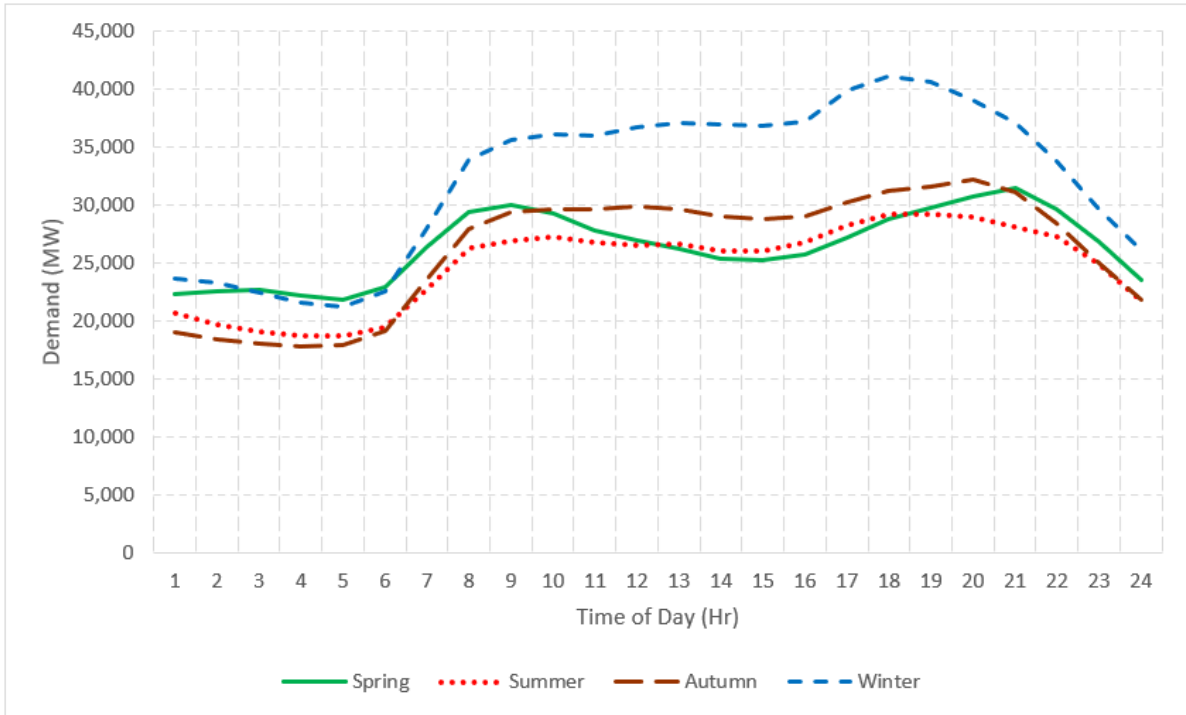


Figure 13 - Typical Seasonal Weekday Load Profiles for The England and Wales Transmission Network

Load profiles are graphical representations of these variations of demand over a day [233]. Profiles can represent transmission networks, distribution networks or individual customer classes on a network (residential, commercial and industrial) [233]. Load profiles are complex signals due to the stochastic and non-linear behaviour of customers and the other factors which influence demand such as weather patterns [181, 226].

Electricity is unlike material products [219, 230, 232, 234]. It cannot be stored in large quantities yet and therefore must be generated as soon as it is demanded [185, 219, 230-231, 234]. This means the variability in demand is a significant issue for the various organisations in the electricity sector [229], and that demand needs to be accurately estimated in advance to balance supply and demand at all times [219].

2.12.2 Load Forecasting

Forecasting is the predication of future events and conditions [235]. Load forecasting is the technique used to estimate electricity demand in advance [219, 236]. Load forecasting has been used in the electricity industry for over a century [237]. It is the key task in any planning operation in the electricity industry as it determines the required resources needed to operate networks that efficiently and securely meet customer demands [230]. It has been

widely studied from the points of view of the different organisations involved in the industry [157]. Today it is a critical task for network operators [183, 225] and compulsory for the proper functioning of the industry [219]. Accurate load forecasts lead to significant savings in operation and planning and maintenance, and this has meant that research into forecasting has become a major field in power engineering [238].

As well as being used to balance supply and demand, load forecasting plays a crucial role in a wide range of planning and operational activities of the different organisations involved in the electricity sector such as generation companies, network operators and financial institutions [220, 226, 230-231]. It is used in designing expansions to networks to ensure they can adequately and securely meet future demand [181, 225, 230] and reduce unexpected losses and costs [225, 235]. It is also used in the decision-making process on contract evaluation, purchasing and generation of electricity, load switching, voltage control and infrastructure development [220, 239-240]. It also minimises blackouts and losses [232]. Load forecasting is also important for a country's economic development, security and daily life of its population [228, 234].

Accurate load forecasts allow stakeholders in the electricity industry to make optimal decisions to increase economic benefits [226-227]. Increasing the accuracy of forecast by as little as 1% can considerably reduce costs [225, 230, 240]. According to a conservative estimate increasing forecast accuracy by 1% would reduce costs by up to \$1.6 million a year of a 10 GW utility in 2018 [181]. Therefore, increasing the accuracy of load forecasting techniques and developing new methods has become an important goal for researchers [226, 241].

Time Horizons

Load forecasting can be carried out to perform prediction from minutes to years ahead [241]. Forecasts are classified in terms of the time horizons they are predicting [230]. There is no current precise standard for classifying these time horizons [234]. Some authors divide forecasts into three time horizons: short-term, medium-term and long term [157, 183, 225, 232, 236-237], whilst some authors use a fourth horizon known as ultra-short term [234-235].

Ultra-short-term forecasts (USTFs) range from a minute up to one hour ahead [234-235]. USTFs are used for real time control of networks [234, 241].

Short term forecasts (STFs) range is from one hour to one week ahead [219, 230, 234, 241]. They are important for the management, security and planning operations of networks [239]. STFs are used for day-to-day operations such as the scheduling of generation [181, 227, 234]. They can also be used to make decisions about load flow in order to prevent overloading and improve reliability [219, 220]. STFs are especially crucial in regions where several countries have heavily inter-connected networks such as in the EU [226]. STFs can achieve an accuracy of around 1-3% [220].

Medium term forecasts (MTFs) range is from one week up to one year ahead [219, 234]. MTFs are important for planning maintenance operations of a network [122, 225, 235]. They are used for planning fuel purchases and maintenance scheduling [157, 183, 219, 234]. There is less need for accuracy in MTFs compared to other time horizons such as STFs [235].

Long term forecasts (LTFs) generally cover the horizon of one year to 20 years ahead [230, 232, 234-235]. LTFs are extremely important for the economic [225, 183] and planning [122, 157, 183, 243] operations of a network. They are used to strategic planning, construction of new generation and the expansion and of networks [181, 183, 219, 230]. Accurate long-term forecasting is difficult to carry out as the long-time horizons contain significant uncertainties in the factors that drive demand [181, 183, 220].

The authors of [234] carried out a review of academic research (in English only) on electrical load forecasting and found 276 papers (journal and conference) on the Web of Science online database. Their analysis of this body of works found that where the time horizon was relevant or emphasized the majority of the papers focused on short term and ultra-short-term prediction. Indeed, short term forecasting has been a very popular area of study over recent decades and several different methods have been presented suitable for the short-term time horizon [240]. Despite the volume of research on load forecasting more accurate models are still required particularly for the longer time horizons where uncertainties make it difficult to match the accuracy of STFs [158, 226].

2.12.3 Load Forecasting for Future Electrical Power Systems

Load forecasting is becoming ever more important due to the restructuring of the electricity industry [219]. There is a growing global tendency to deregulate the electricity sector which has seen networks unbundled into several different sectors (generation, transmission and

distribution) [181, 219, 230]. Load forecasting is vitally important in this deregulated economy as there is an increased demand on planning management and operations by all the participants in the industry [219-220, 234]. Accurate long-term forecasting in particular is more important in deregulated economies [220].

Demand is also continually increasing and changing in pattern due to the use of new technologies such as the charging of electric vehicles [230, 234]. This has made demand patterns more complex and unrecognisable compared to historic patterns [230]. Generation patterns are also changing due to the increase in the penetration levels of renewable energy sources onto networks (particularly at the distribution level) [181]. Load forecasting is crucial in ensuring that the electricity from these intermittent sources can be effectively utilised [158, 225, 240, 244].

2.12.4 Load Forecasting Methods and Techniques

As electricity demand varies continuously over time it is considered to be a non-stationary time series [230, 235, 245]. It is also well established that demand is nonlinear which makes it difficult to describe using an explicit mathematical formula [200]. Therefore, traditionally load forecasting was carried out using different time series methods such as the Box–Jenkins or autoregressive integrated moving average (ARIMA) approach which were all based on the understanding that demand is a time series signal with known seasonal, weekly and daily patterns [185, 228, 231, 245]. This allowed future demand to be modelled as a function of historical load and other exogenous factors [16, 181, 219, 227, 230, 235, 246].

Due to the continuing changes to networks and demand patterns around the globe traditional load forecasting methods based on historical data are becoming obsolete as they cannot be used to accurately interpret the uncertainties in future demand [158, 181, 231, 247-248]. As a result, over recent decades several different approaches to load forecasting have been proposed [183, 220, 225-226, 231].

Due to its simplicity linear regression has been used in load forecasting [144]. However, the method can produce biased results as it does not address the issue of multicollinearity (the occurrence of high intercorrelations among two or more independent variables in a model) amongst the explanatory variables [144]. Several classical statistical techniques have also been applied to load forecasting, including regression models, semi-parametric models and

Kalman filtering [225, 236]. These techniques perform well under normal conditions [236]. However, they struggle to model networks with high penetration levels of renewable sources which can cause abrupt changes in generation to occur [225, 236]. The accuracy of statistical techniques also reduces as the time horizons being forecasted increase [225].

Artificial Intelligence

Computational techniques known collectively as machine learning (ML) or artificial intelligence (AI) techniques have increasingly been utilised in load forecasting [226, 236-237, 239-241]. AI techniques have proven powerful tools well suited to dealing with complex non-linear problems [225, 241]. This allows them to overcome the deficiencies of traditional methods and generate more accurate forecasts [181, 239].

AI techniques that have been applied to load forecasting in research literature include:

- support-vector machines (SVM) [181, 220, 227, 230, 237],
- expert systems [225, 230, 235, 237],
- genetic algorithms [236]
- random forests [181],
- regression trees [227],
- fuzzy logic [185, 220, 230, 235, 237],
- ant colony [230],
- self-organising maps [185],
- wavelet transform [185],
- chaotic artificial bee colony algorithm [185],
- artificial neural networks (ANN) [158, 181, 185, 220, 227, 230, 235-237, 241].

Artificial Neural Networks (ANN)

ANNs have proven their ability to learn the complex nonlinear function mapping without the need of explicit mathematical formulation [157, 200, 237, 239, 249]. ANNs are used in a wide variety of tasks in different fields including finance, industry, science, and engineering [250-253]. Previous research has also shown that amongst the different AI techniques ANNs produce the highest levels of accuracy in load forecasting problems [227, 237, 245-246]. These factors have made ANNs the most studied and applied AI technique to load forecasting [183, 220, 225, 227, 234, 239, 254]. They have been widely applied to load forecasting of modern-day networks such as smart grid applications [158] and networks with RES generation such as solar/PV [246].

Research literature shows that ANNs are easily applied to STF and USTF time horizons [236, 239, 254-255]. However, due to the large uncertainties involved ANN models have not typically been applied to LTF [245, 254].

ANNs can be created using a variety of programming languages such as C or FORTRAN [200]. Using programming languages requires knowledge of computer programming and the particulars of the specific language being used. Their use also makes designing an ANN model more complex and more time consuming [200]. The use of specialist ANN design software disembarasses users from elaborate programming [256]. This speeds up the design process and allows users to concentrate on optimising the performance of their ANN model [200].

Chapter 3

Renewable Energy Technologies and Their Potential in the Global South

Ample and reliable electricity supply is vital to modern life [257]. Demand for electricity has been rising sharply globally for decades [258]. This increase has been driven by developing nations in the global south, such as those in Southeast Asia who have increased their share of global consumption dramatically in the past few decades [259–262]. This is due to the understanding of the importance of electricity as a tool for economic growth [258, 263-265] and as many developing nations increase access levels to the resource through national electrification programs as a tool for social development [259].

At the same time governments and the public alike have realized that current electricity networks are environmentally, economically and socially unsustainable due to their heavy reliance on fossil fuels such as coal [266-267]. This has led to an increase in the interest in exploiting rich local renewable energy resources (RER). Several studies have demonstrated the potential of solar photovoltaic (PV) in Southeast Asia [268–270]. However, the variable nature of the output of renewable energy sources such as PV installations makes managing electrical power networks more challenging.

This chapter assesses the potential of PV to play a significant role in meeting the increasing energy demands of developing nations in the global south through the use of a case study of Yangon City, Myanmar. Load matching is used to investigate the diurnal variation and degradation of a typical PV system over the course of its lifetime and to determine the impacts on current and future electricity demand profiles. The use of load matching and degradation also allows a thorough study of the correlation between PV and electricity demand of developing nations in the global south to be carried out. This will aid system planning by determining the impacts of increasing penetration levels of RES such as PV on local electricity networks and understanding what grid support such as storage technologies will be needed to accommodate increasing PV levels.

3.1 Electricity situation in the Global South

3.1.1. China

The second industrial revolution (1870–1914) was triggered in part by the introduction of public electricity [258]. Since its introduction the demand for electricity across the world has constantly grown as shown in *Figure 14* [271-272]. Electricity is now considered to be indispensable in modern day life [263, 273], which has led to a steady growth in demand over recent decades [258].

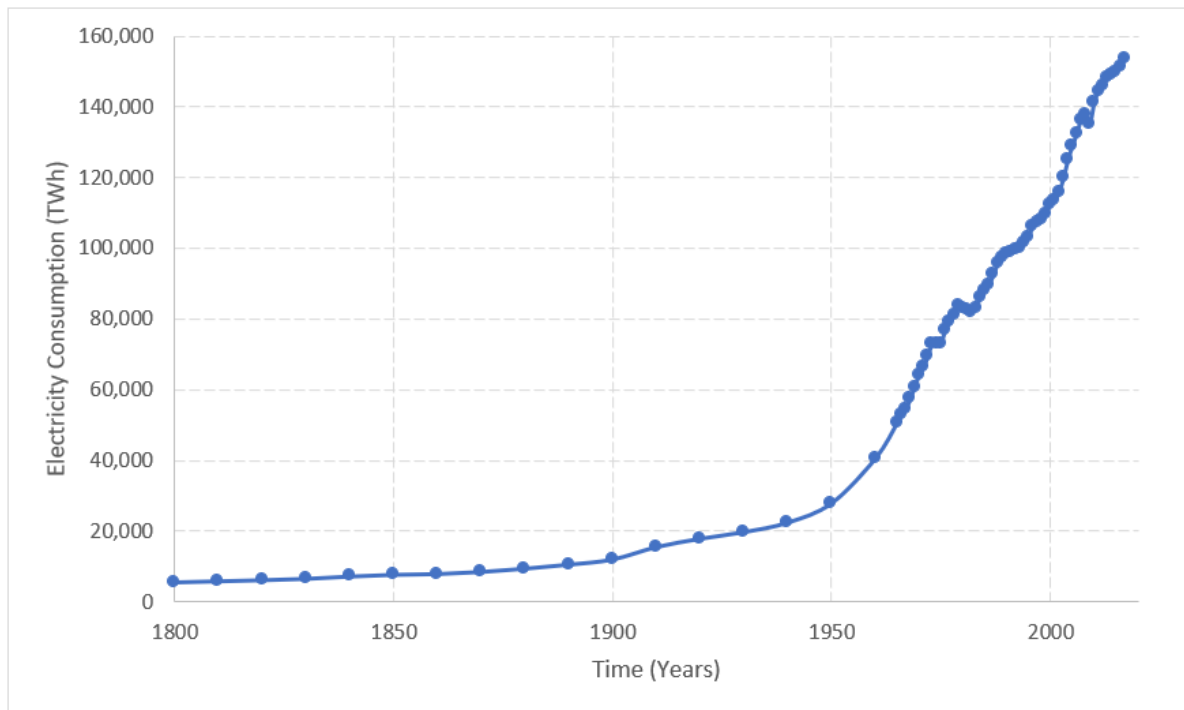


Figure 14 - Historical Global Energy Consumption [274]

In 1978, Kraft and Kraft discussed the relationship between electricity consumption and economic growth using data from 1947 to 1974 [275]. Since this time there has been a significant volume of research on the connection between the two factors [276]. Today it is widely believed that electricity consumption is the engine of modern economic growth [258, 263–265], especially in developing countries [263].

China can be used as a case study of the connection between electricity consumption and economic growth. Since the Chinese Economic Reform (CER) in 1978 the country has experienced rapid economic growth and development with an average GDP growth rate of 9.8% [258]. This figure is far higher than the rest of the world and has made China the second largest economy after the United States (US) since 2020 [258].

Prior to the CER China ran an administered labour system in which almost all urban jobs were with state-owned enterprises in which roles were allocated by a bureaucracy [277-278]. Under this system, labour mobility was not permitted which meant that workers were allocated life-long jobs [277]. The CER saw China move away from this centrally planned socialist system to a market orientated system in which labour turnover and mobility was permitted [277-278] which in turn led to a massive growth in China's domestic urban workforce market [279-280].

The new mobility of the (increased) workforce allowed China to change from an agricultural society to a more industrial-focused one. It also led to urbanization of the country as large portions of the population left rural areas seeking newly attainable work. The industrialization and urbanization of the country along with agricultural modernization are considered to have triggered the economic development of China and were all supported by an increase in electricity consumption [258].

There is a documented link between economic growth and residential electricity consumption as seen in China where there has been a five-fold increase in electricity consumption in residential buildings between 2000 and 2015 [267]. Before its economic reform, China was the third largest consumer of electricity globally [258]. Since the reform, China has become the principal driver of the increase in global electricity consumption with an average national increase in demand over the past few decades of 9.3% [265, 281]. This has seen consumption in China overtake that of the European Union (EU) in 2007, the US in 2010 and continental North America in 2013 [258]. The growth in electricity consumption in China since the economic reform is shown in *Figure 15*.

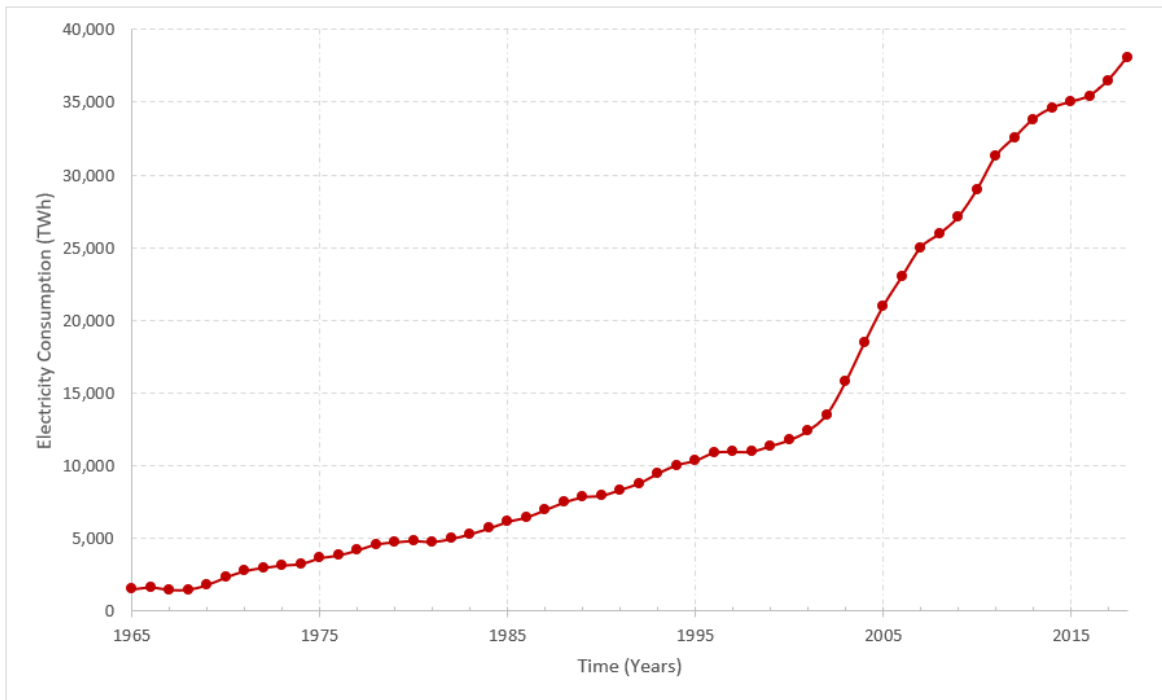


Figure 15 - Electricity Consumption in China (1965 - 2018) [274]

The increased consumption in China has seen the Asia Pacific become the highest regional consumer of electricity globally, as seen in *Figure 16*. Since 1965 the region has increased the percentage of consumption compared to the global total from 11.92% to 43.17%. In the same period, Africa, the Middle East and South and Central America have seen small increases, whilst the Commonwealth of Independent States (CIS), Europe and North America have all decreased their percentage of the global total as seen in *Table 6*.

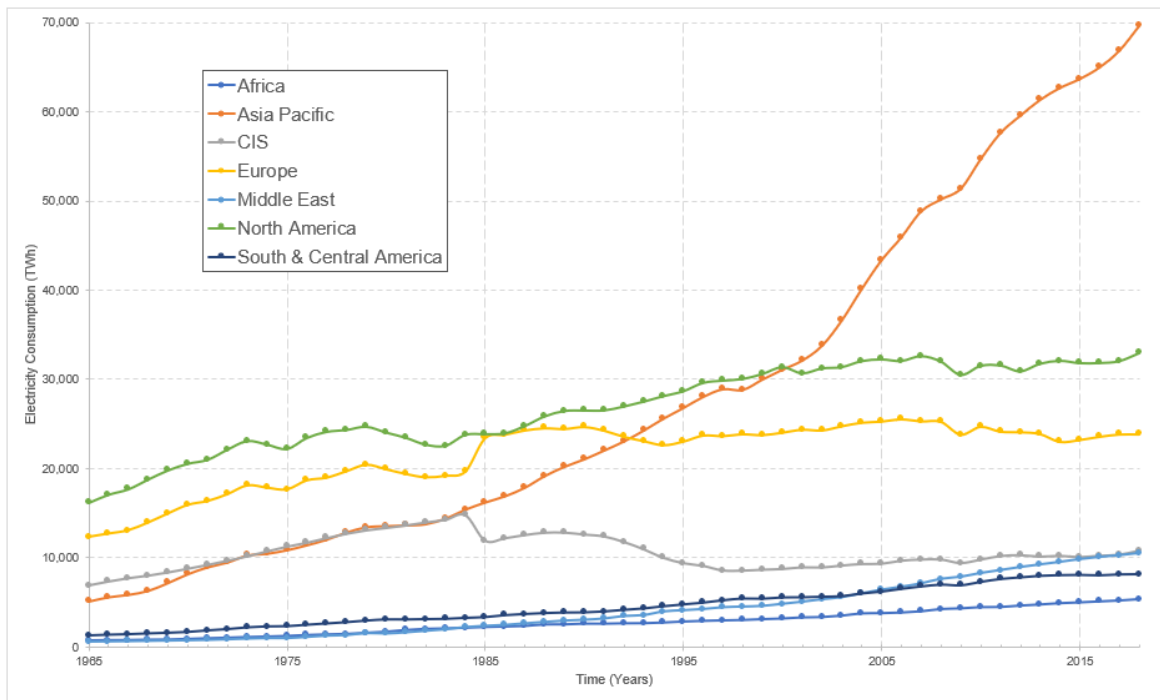


Figure 16 - Historical Global Electricity Consumption by Region [274]

Table 6 - Percentage of Global Electricity Consumption by Region [274]

Year	Region						
	Africa	Asia Pacific	CIS	Europe	Middle East	North America	South and Central America
1965	1.65	11.02	16.02	28.58	1.3	37.55	2.97
2000	2.92	28.59	8.04	22.1	4.41	28.83	5.1
2018	3.33	43.17	6.71	14.79	6.51	20.43	5.06

It has been shown that during the early stages of a country's economic development the focus is on production levels and that environmental quality deteriorates [260, 282]. This has clearly been seen in China due to the fast speed of its development [283].

China's development has been fuelled by vast amounts of fossil fuels [284]. Coal is particularly dominant in the country's fuel mix, meeting around 70% of consumers' electricity demand [267]. Whilst the land mass of China is just 2.2% of the world's total it consumes more than half of the world's coal [280].

The link between increased pollution and fossil fuels has been extensively documented in literature [267]. This link can clearly be seen in China, where increasing use of fossil fuels such as coal has resulted in severe air pollution [284], and seen the country become the largest emitter of particulate matter and greenhouse gases such as sulphur dioxide (SO₂) and nitrogen oxides [285].

Air pollution is not a problem faced solely by China but one which has become one of the largest global issues of the Anthropocene epoch [284]. Today approximately 92% of the world's population are exposed to air pollution levels in excess of the suggested limits of the World Health Organization (WHO) [283, 286]. Populations in Africa, Asia and the Middle East are particularly at risk [286]. The ever-increasing global demand for electricity is augmenting the air pollution problem and other issues such as global warming [285].

Air pollution in China at times causes heavy haze episodes when particulate matter levels spike [267]. During these periods the population is advised to stay indoors and close all windows and doors. The increase in indoor activities leads to an increase in electricity consumption through the use of appliances such as air conditioners and air purifiers [267]. These pollution mitigation activities have led to the hypothesis of the self-aggravation of air pollution [267].

It has been shown in [260, 282] that when economic growth reaches an inflection point, environmental protection awareness increases. This is true in China where over the past decade the public in the country have shown an increased awareness of the problem and its adverse health impacts [267]. The issue of air pollution levels has also been a major concern for the government in China since 2013 as it tries to find a trade-off between environmental protection and continuing economic growth [282, 283]. In September of that year, the Ministry of Ecology and Environment of China implemented strict energy conservation and emission reduction policies, "Atmosphere Ten Plans," to reduce pollution and increase public health and quality of life [282-283].

Another way in which China is trying to combat pollution and global warming is by changing the fuel mix in its electricity network. Since 2000 it has made rapid progress in developing renewable energy with an average annual growth rate over the last decade of 62.5% [285]. This growth has seen China become the global leader in renewable energy [285]. The

country's government have set several targets with regards to this shift, including 60% renewable energy and 86% renewable electricity by 2025 [285].

China's renewable energy production is currently dominated by hydropower. However, as 80% of this resource has already been explored, other options need to be examined [285]. Fortunately, China has vast resources of other renewable resources such as solar and wind, which has led to an annual increase in capacity of 100.3% and 58.2%, respectively, between 2006 and 2015 [285].

3.1.2. Association of Southeast Asian Nations (ASEAN)

Developing countries in Asia and around the globe have looked closely at the symbiotic relationship between electricity consumption and economic growth in China. They have also looked closely at the risks of the continued reliance on non-sustainable energy sources.

The Association of Southeast Asian Nations (ASEAN) is a regional intergovernmental organization in Southeast Asia which promotes inter-governmental co-operation on a range of policies [260-261]. ASEAN was created in 1967 when five countries; Indonesia, Philippines, Singapore and Thailand signed the ASEAN Declaration. The bloc now consists of 10 member countries after Brunei (1984), Vietnam (1995), Laos (1997), Myanmar (1997) and Cambodia (1997) joined the collation.

According to the United Nations the ASEAN region is home to nearly 650 million people [287]. There has been a rapid increase in urbanization levels in Southeast Asia in recent times with urban populations rising from 40% in 2000 to nearly 50% in 2018 [259]. Driven by rapid economic growth and population urbanization the region is increasingly influencing world energy trends with demand increasing by over 50% between 2000 and 2013 [261]. However, whilst millions of the region's inhabitants have gained access to electricity since 2000, there are still approximately 45 million without access today [259]. Access to electricity has been identified as essential to ASEANs economic growth programs [260].

Over recent years, several published studies have examined the current and near future energy demands of ASEAN member states by both the ASEAN Centre for Energy (ACE) and the International Energy Agency (IEA) [259–261]. The studies hypothesized that energy demand in the region could rise by about 80% up to 2040 and that some countries like

Malaysia would possibly double their consumption [261]. Other scenarios found that in order to meet economic growth targets, the regions energy consumption would rise by 2.7 times compared to 2013 levels [261].

Southeast Asia has large concentration of population and economic activities along its extensive coastlines and has a strong reliance on the region's natural resources such as agriculture and forestry [261]. Therefore, it is at high risk from the effects of climate change [261]. As a result of this, policymakers in the region are focused on finding a sustainable model that allows the region to meet the energy needs required to enable continued economic growth [259–261].

The region has relied heavily on fossil fuels for its energy demands in the past [260], and currently three-quarters of ASEAN's electricity demand is currently met by fossil fuels [259]. However, in lessons learnt from China, policymakers in the region have intensified efforts to create a sustainable energy solution for the future [259, 261]. Renewable energies are currently a significant component of the ASEAN energy fuel mix meeting around 25% of primary demand [261]. ACE and IEA both agree that they are likely to play an even larger role in the future as cost reductions in renewable energy (RE) technologies are taken advantage of [259–261]. The potential of both solar and wind have been identified as significant candidates in meeting the renewable energy aims of the region [260-261]. Several frameworks have now been put in place to better support investment in wind and solar [259].

3.2. Case Study Country—Myanmar

Due to the high costs of fossil fuels and environmental issues, countries in the global south are planning exploitation of their renewable energy potential for meeting their energy needs. In this work, Myanmar is chosen as a case study for which photovoltaic (PV) is seen as the preferred technology owing to its modular nature and Myanmar's tremendous PV potential. The aim is to assess the solar-PV potential for a selected location in Myanmar and to determine the impacts on current and future electricity demand profiles in order to aid system planning.

3.2.1. Background

Myanmar (officially the Republic of the Union of Myanmar) was the 9th country to join ASEAN and is the second largest country in Southeast Asia [268]. It is currently one of the

lowest consumers of electricity in the world. In 2011 it was ranked 191 [288], and in 2016 the average electricity consumed per capita was around 150–160 kWh [289]. This figure is far lower than the top 10 consumers (*Table 7*) [290], and much lower than the world average of 3000 kWh. It is even lower than the average of least developed countries figure of 174 kWh [288].

Table 7 – Top 10 Consumers of Electricity Per Capita [290, 291]

Rank	Country	2020 Population (Millions)	Energy Consumption (kWh Per Capita)
1	Iceland	0.34	53,832
2	Norway	5.42	23,000
3	Bahrain	1.7	19,597
4	Kuwait	4.27	15,591
5	Canada	37.74	15,588
6	Finland	5.54	15,250
7	Qatar	2.88	14,782
8	Luxembourg	0.63	13,915
9	Sweden	10.01	13,480
10	United States	330	12,994

The low per capita consumption rates of Myanmar are part of a large internal problem in the country: access to electricity [289]. Whilst in ASEAN the number of people without access to electricity has fallen by around two-thirds [261] in Myanmar the electrification rate is around 31%–34% [270, 289]. This figure is far lower than global average of 87% [292]. At present, there are around 2.3 m million residential connections in Myanmar [293]. This means that around 39.6–41.4 million people out of a population of nearly 60 million do not have access to electricity.

The national grid mainly caters to the urban areas; therefore, it is the country’s major cities that have the highest electrification rates. Yangon city’s electrification rate of 78% is the highest in the country. However, 66% of the population live in rural areas [264], which are poorly electrified with an average rate of less than 20% [268]. Rural communities rely on traditional biomass for their energy needs, particularly for cooking and lighting [288].

Even though Myanmar has one of the fastest growing economies in Asia [294], it is thought that the country’s current energy situation is significantly hindering economic growth as well

as human development [264]. To overcome these issues the government approved the National Electrification Plan (NEP) in September 2014 [288]. The NEP targets 100% electrification of households by 2030 [288-289, 293], with around 98% of new connections being grid-based [264]. The estimated capital cost of the project is somewhere between \$5.9 and \$10 billion, with financial help coming from the World Bank and the Japanese government [289, 293]. As well as assisting economic growth, it is believed that meeting the NEP targets will improve living standards in the country and enhance activities such as education [264].

The scale of the program is immense and will involve connecting more than 7.2 million households to the national grid. *Figure 17* shows the current and targeted annual electrification rate required to supply 100% of households by 2030. To achieve 100% electrification, household connections will need to increase from 189,000 per year currently to around 450,000 per year over the course of the program and even reach as high as over 517,000 in the latter stages [293]. It will also require around 2600 MW of additional generation to be commissioned [293].

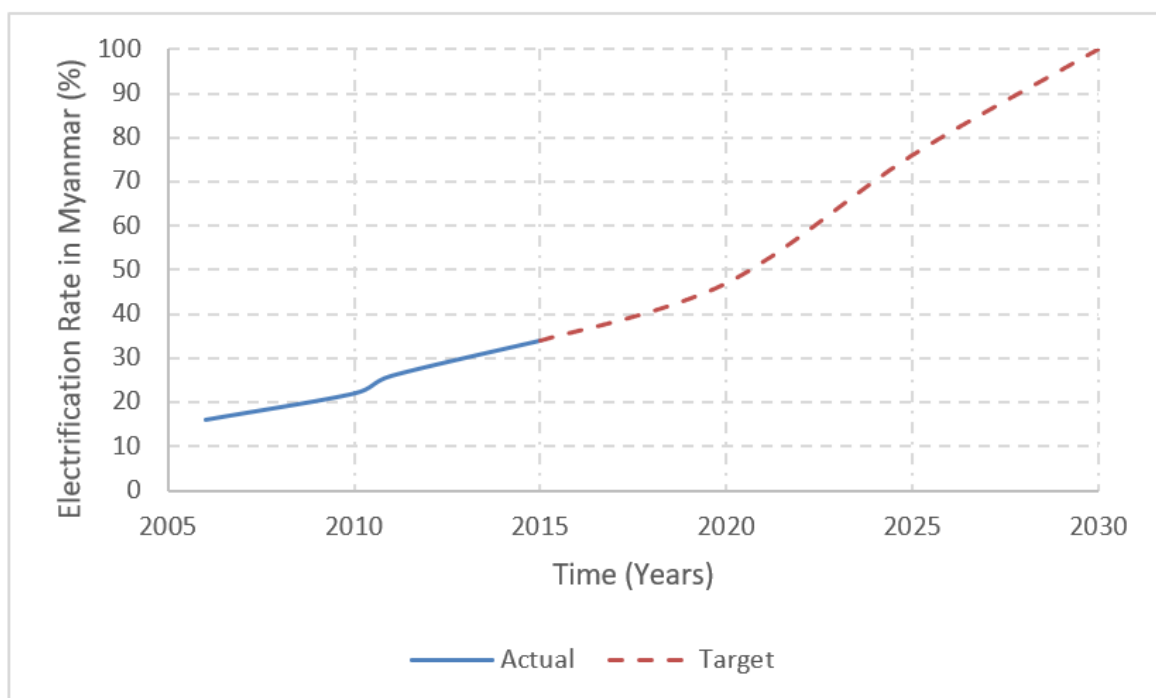


Figure 17 – Electrification Rate in Myanmar [293]

Whilst their main priority is electrifying the population, the government of Myanmar has also set goals for their future energy mix through policies such as the National Renewable

Energies Policy and Planning–Draft (NREPP). The NREPP has set the goal of achieving an energy mix, which includes 38% hydropower and 9% (2000MW) from other RES by 2030–2031 [260].

3.2.2. Climate Conditions in Myanmar

The Köppen–Geiger (KG) climate classification is a widely used system used to describe terrestrial conditions [294]. The KG classification is based on five major types, which are defined by temperature, precipitation and seasonal fluctuations. The latest KG world map shows that Myanmar has three distinct climatic regions; temperate in the mountainous north and west region, tropical wet central dry region, and tropical monsoon in southern and coastal delta regions. Myanmar has three seasons; Cool (November through February), Hot (March through May) and Rainy (June through October) [294].

3.2.3. Myanmar’s Electricity Fuel Mix

As of 2016 Myanmar had an installed capacity of around 4900 MW with a peak load of around 200 MW, it also had an off-grid capacity of about 135 MW [289]. Myanmar is considered to have an abundance of domestic energy resources such as gas and oil [295–296]. However, the majority of the gas extracted in the country (75%–80%) is exported to neighbours such as Thailand and China, whilst the indigenous coal has a low calorific value so the coal burned in electricity generation plants needs to be imported. Myanmar also has an abundant potential for hydropower resources and the country is currently highly dependent on hydropower to meet its electricity needs [268]. In 2015 65% of the electricity generated in Myanmar came from hydropower, with natural gas providing 33.4% and coal the other 1.6% [268]. The high dependency on hydropower in the current energy mix means that robust supply during the dry seasons (cool and hot) cannot be guaranteed [297]. As a result the country is vulnerable to power shortages for much of the year when rainfall is low which often results in blackouts [289, 297]. Therefore, the future viability of large-scale hydropower projects is uncertain [264]. Whilst the current reliance on fossil fuels for power generation is unsustainable both environmentally and economically [264].

3.2.4. Solar Photovoltaic (PV) Potential in Myanmar

Myanmar has tremendous potential for RE, and whilst it is currently in an early stage, solar-PV energy is one of the most promising RE candidates [268]. Sunlight in the country is abundant and Myanmar receives 4.5–5.5 kWh/m² of solar radiation per day [269]. 60% of

the country's land area was identified as suitable for PV installations and the PV generation potential is estimated to be around 40 TWh per year [288]. For Myanmar solar-PV also has the advantage of working complementarily with hydropower. Whilst solar-PV output will drop during the rainy season, it can compensate for the decline in hydropower output during the cool and hot seasons [288].

3.2.5. Future Energy Outlook

Previously several researchers have assessed the electricity outlook of the ASEAN region in the coming decades [260–262, 294–296]. They all concluded that electricity consumption in the area will grow rapidly over the next 20 years due to economic and population growth as well as government policies aimed at increasing access to electricity. They also point out that at the same time the ASEAN member countries have stated their aspirations to move towards a more sustainable energy mix and are, therefore, promoting the uptake of renewable technologies. Studies have shown that due to their climatic conditions, many Southeast Asian countries including Myanmar have high PV potential, and that many new PV projects are expected to be constructed in the near future to try to close the supply–demand gap in a sustainable manner [269, 295-296].

3.3. Methodology for Assessing Photovoltaic Energy Potential and its Impact on Electricity Demand Profiles

3.3.1. Case Study Location

Yangon City, Myanmar, is the region considered for PV generation forecasting and electricity demand forecasting. Formally known as Rangoon, Yangon City is the state capital of the Yangon Region of Myanmar and served as the capital city of the country until 2006. It is the largest city in Myanmar and home to over seven million people. As of 2015, the electrification rate in the city was 78% and it consumed 44% of the electricity in Myanmar (4.95 GWh out of a total of 11.25 GWh) [284]. Located in the heart of lower Myanmar, it has a KG classification of tropical monsoon climate, and experiences little variance in both temperature and sunlight hours throughout the year as shown in *Table 8*.

Table 8 – Climate Conditions in Yangon City

Season	Average Minimum Temperature(°C)	Average Maximum Temperature (°C)	Relative Humidity (%)	Daily Sunlight (Hours)
--------	---------------------------------	----------------------------------	-----------------------	------------------------

Cool	19.8	32	66	11.4
Hot	23.7	35	71	12.2
Rainy	24	29.8	85.8	12.5

3.3.2. PV Generation Modelling

PV generation modelling involved two stages: pre-sizing and detailed system simulation. PVGIS 5, which is a free-to-use Geographic Information System (GIS)-based online PV energy estimation tool, was used for pre-sizing. PVGIS 5 generates PV energy output data with hourly time resolution for 365 days of the year for both standalone and grid-connected systems. A typical grid-connected polycrystalline PV system on the outskirts of Yangon City was simulated using PVGIS. Based on the simulation, the size of the PV system needed to substantially supply the annual electricity demand of the Yangon City was estimated at approximately 1 MW. It should be noted that the 1MW load would not be connected to the network at a single point but at many points across the network.

Being a satellite-based GIS, PVGIS also serves as a source of weather data. Averaged monthly, seasonal and annual irradiance datasets were created using the daily solar irradiance data obtained from PVGIS 5. PVsyst is an industrial standard detailed PV system design software, which has an up-to-date library of PV modules and inverters. The average monthly datasets from PVGIS were imported into PVsyst in order to model the potential electricity generation of a 1 MW PV system on the outskirts of Yangon City with an assumed operational start time of 2020. The details of the PV installation modelled in PVsyst are shown in *Table 9*.

Table 9 – Photovoltaic Installation Details

Location	Latitude	16.8° N
	Longitude	96.1° E
	Altitude	4m
Summary	Module Type	Generic 250W 25V 60 cell Si-poly
	Number of Modules	4000
	Module Area	6508m ²
	Array Design	250 strings of 16 modules

	Inverter Type	generic 500kW 320-700V LF Tr 50 Hz
	No of Inverters	2
Optimisation	Plane Tilt	24°
	Azimuth	0°

3.3.3 PV Generation Forecasting

Polycrystalline PV modules have an expected lifespan of around 20 years. The output of these modules over their lifetime is dependent on their annual degradation rate. Degradation rates in modern crystalline silicon PV modules is between 0.2% and 0.5% [298]. In Mongolia and India, data has shown that the degradation rate of polycrystalline PV modules was about 0.4% per year over 4 years of operation [292]. In this study, the analysis is over a 10-year period, and therefore the upper future of 0.5% was chosen as the degradation rate used to generate future annual PV output profiles up to 2030.

3.3.4. Electricity Demand Forecasting

Actual load profiles for developing countries such as Myanmar are difficult to obtain [285]. The load profiles used in this work are based on a synthetic load scenario created in [264] and refers to the hourly, over the day, variation in the maximum demand of 100 residences over 365 days of a typical year. The scenario was developed based on data from the local energy use patterns in the neighbouring countries with climate and economic environments like Myanmar. The scenario used assumptions about the basic electricity demand of urban residences in developing countries in East Asia such as lighting, fans, televisions and other home appliances such as refrigerators and mobile phone chargers. It was also assumed in the scenario that the peak demand would occur during the daytime due to the use of fans to combat the perennial high temperatures of the region. The data from neighbouring countries and the assumptions about basic electricity needs were used together by the author to generate a typical daily synthetic load profile and seasonal variations reflective of the electricity demand of urban household consumers in Myanmar.

Using the typical daily profile and the maximum variations in the seasonal profile of [264], average daily profiles with an hourly resolution were created for the twelve months of a year. These monthly profiles were then used to generate aggregated annual and seasonal (cool, hot and rainy) load profiles for Yangon City. The data from the seasonal profile from [264]

showed very little variance in the projected demand over the course of a year. The average daily peak demand was 250 kW. The maximum averaged daily peak demand occurred in March when the peak was 261.49 kW, 4.6% above the yearly average. July had the lowest averaged daily peak demand at 240.09 kW, 3.9% below the yearly average. The aggregated seasonal figures showed an even smaller variance. The hot season had the highest average daily peak demand at 252.56 kW, 1% above the yearly average. The cool season had the lowest average daily peak demand at 247.78 kW, 0.9% below the yearly average.

The aggregated synthetic seasonal load profiles for urban Yangon City are shown in *Figure 18* where the rainy season profile (grey dotted line) can just be seen slightly below the profile for the cool season (blue solid line), highlighting the low variation in load over the seasons. The low variance in load is due to the climate in the region and the assumption that electricity demand is driven by basic needs such as cooling and lighting [264].

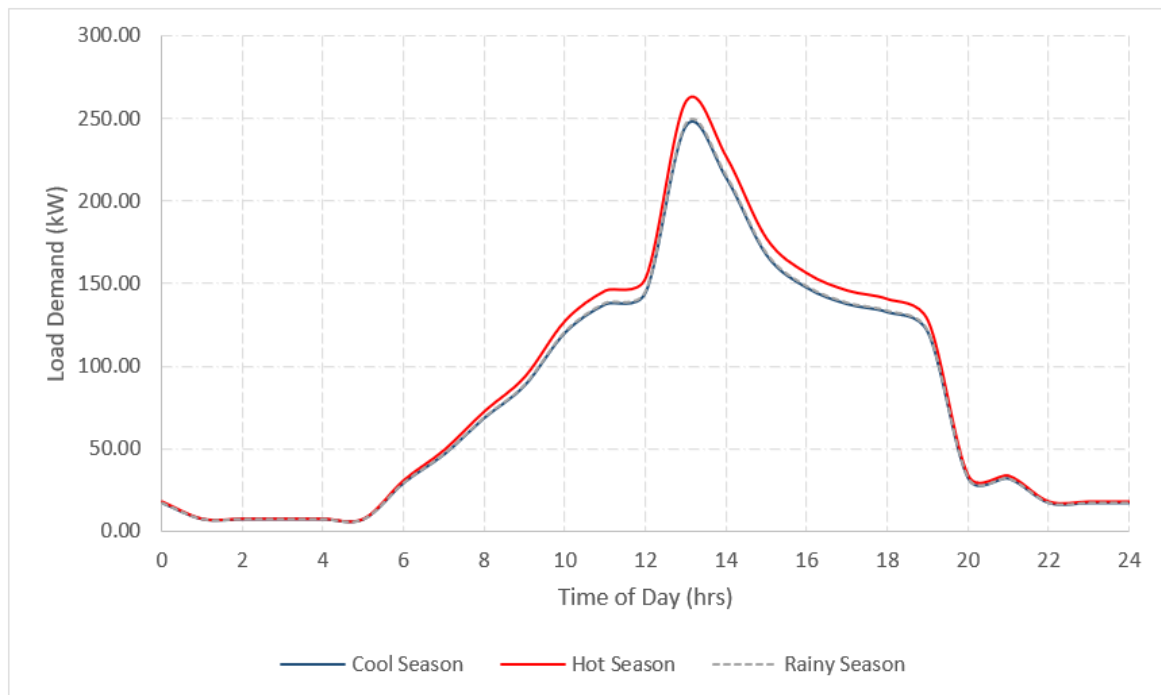


Figure 18 – Averaged Synthetic Daily Load Profiles for Residential Properties in Urban Yangon City

The ACE predict that load in Myanmar and other South-East Asia countries will increase 3.8% annually up to 2035 [260]. This figure was calculated considering electrification programs such as NEP as well as a GDP increase of 4.7% annually and a population growth of 0.9% annually in the region over the same time period. Using the predicted annual load increase figure from ACE, synthetic future annual load figures for urban Yangon City were generated up to 2030.

3.3.5. Load Matching

Solar supply rate is a measure of the percentage of load supplied by solar PV Systems, it is calculated by dividing the annual load by the annual supply of a solar PV system [299]. However, solar PV systems can only supply power during daylight hours and this is not taken into consideration with solar supply calculations [300].

Load matching is the correlation between generation and load and refers to the degree of matching between generation and load profiles at instantaneous points in time. It is commonly used in the study of Net Zero Energy Buildings to evaluate performance in terms of the amount of on-site energy produced that is locally consumed [301].

At any instant the level of load matching can be calculated as follows [302]:

Equation 1 – Load Matching

$$M(t) = \frac{\min((L(t), P(t)))}{L(t)}$$

where M is the load matching, L is the load, P is the electricity produced and t is an instantaneous point in time.

To study the load matching by the output of the solar PV installation described in *Table 9* to the load of urban Yangon City, normalized annual diurnal profiles for the year 2020 were created using feature scaling as follows:

Equation 2 – Normalisation

$$x(n) = \frac{x - \min(x)}{\max(x) - \min(x)}$$

where x is the original value and $x(n)$ is the normalized (per unit value) of PV output or electricity demand at the n th hour.

Normalizing the data gave peak points in both the PV output profiles and the load profiles a value of 1, with all other values scaled to the peak with values between 0 and 1. Normalization allows better visualization of the correlation between the two profiles as it absorbs the large differences in the absolute two profiles. Future profiles up to 2030 were then forecasted using the annual load increase rate of 3.8% and the PV degradation rate of 0.5% with the 2020 profiles as a baseline.

3.3.6 Scenarios Considered

To assess the solar-PV potential for Yangon City, two forecasted scenarios were created to examine the profile matching between the output of the PV system and the local load. The first scenario looks at figures from 2020, the assumed first year of operation for the PV installation. The second scenario looks at the figures from 2030 to determine the effects of electricity demand increase and PV system degradation.

3.4. PV Generation Potential Analysis

Analysis of the results obtained through the PVsyst simulation showed that in the first year of operation the PV installation described in *Table 9* would inject a total of 16,345,600 kWh into the local grid at an average of 4490 kWh/Day. With the highest average normalized output (the energy injected into the grid) occurring in the cool season of November to February (5502 kWh/day). During the hot season of March to April the average would be slightly less at 4882 kWh/day. During the rainy season of June to October the output would drop noticeably to 3434 kWh/day.

Table 10 shows the breakdown of the average energy injected into the grid by month. *Table 10* shows that the lowest average injection of energy would occur in June (*Figure 19*) with 2974 kWh/day, and the highest in February (*Figure 20*) with 5876 kWh/day.

Table 10 – Daily Average Energy Injected into Grid

Month	Season	Energy Injected into Grid (kWh/day)
January	Cool	5551
February	Cool	5876
March	Hot	5648
April	Hot	5352
May	Hot	3646
June	Rainy	2974
July	Rainy	3017
August	Rainy	3100
September	Rainy	3545
October	Rainy	4534
November	Cool	5207
December	Cool	5372

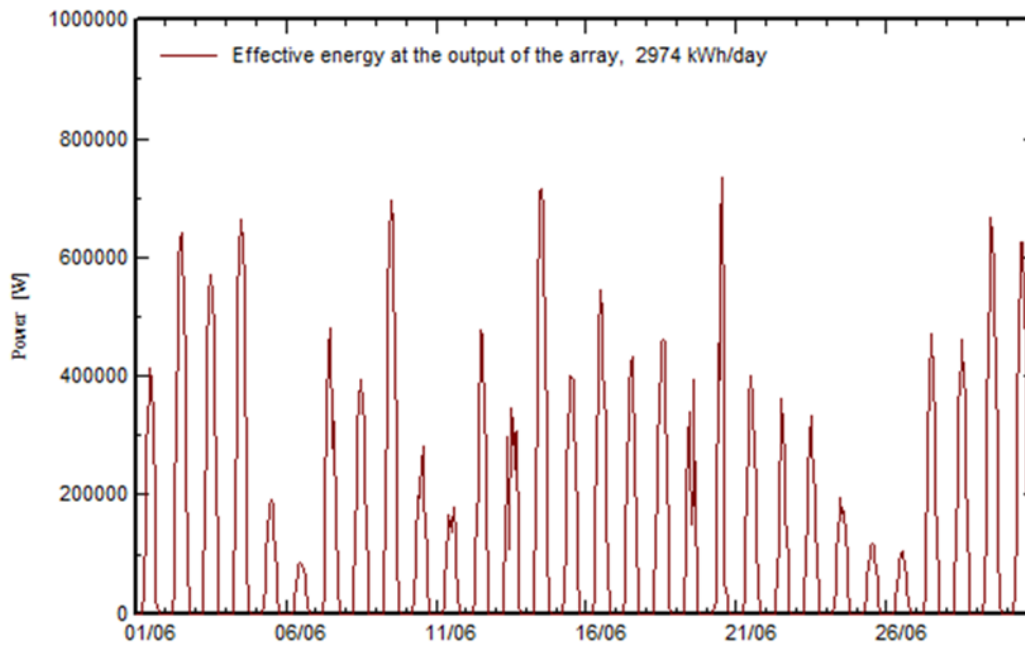


Figure 19 – Energy Injected into the Grid in the Month of June

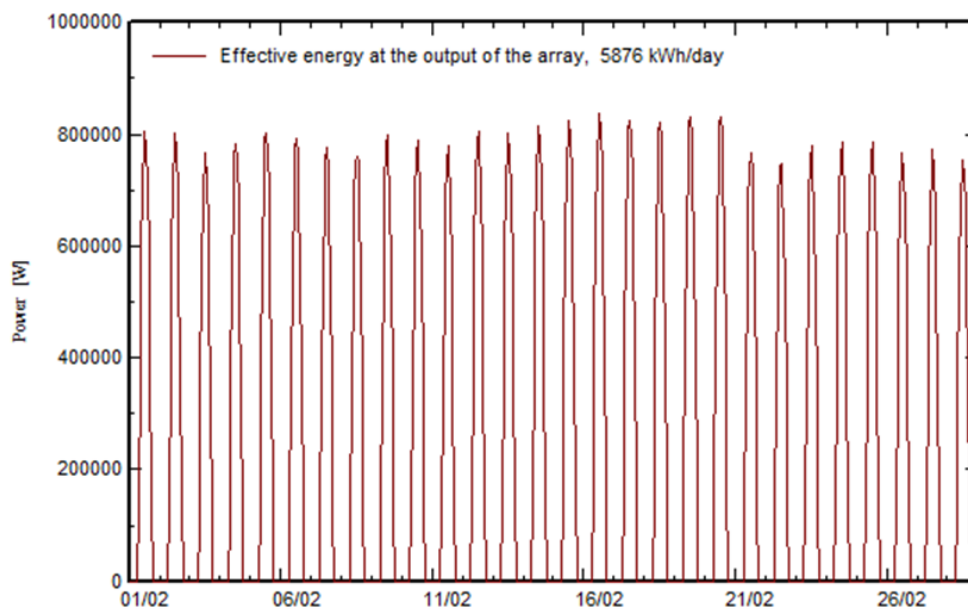


Figure 20 – Energy Injected into the Grid in the Month of February

From *Figure 20* it can be seen that there is little variation in the daily output of the PV system during the cool season. The average daily output for February was 5876kWh/day, whilst the lowest daily output was 5505kWh/day and the highest output was 6396kWh/day. The hot season also experienced little variation in daily output. For example during the month of April the average daily output was 5376kWh/day, whilst the lowest daily output was 4629kWh/day and the highest output was 6013kWh/day. However, from *Figure 19* it can clearly be seen that

the unpredictable weather of the rainy season caused a large variation in the daily output of the PV system. The lowest output during June was just 671kWh/day (6th June) whilst the highest was 5364kWh/day (14th June). This large variation in output meant that the average output over the month was 2974kWh/day, which is much lower than the typical output for months in both the cool and hot seasons.

The International Electrotechnical Commission (IEC) 61724 “Photovoltaic system performance” series of standards defines performance ratio (PR) as ‘the ratio of the effective energy produced by a PV system.’ For a grid connected PV system PR is calculated by [303]:

Equation 3 – Performance Ratio

$$PR = \frac{E_{Grid}}{G_{lobInc} \times P_{nomPv}}$$

where: EGrid is energy injected into the grid, G_{lobInc} is the global incident irradiance in the collection pane, P_{nomPv} is the standard test conditions power.

PR is used to evaluate the quality of the performance of a PV system [303]. The results of performance evaluation were typical of installations in global south countries with tropical weather conditions like those in the Yangon City, Myanmar region. The PR over a year of the proposed installation in Yangon city was 0.798. The PR was consistent throughout the year as can be seen in *Figure 21*. February was the poorest performing month (PR = 0.779) and August the best (0.824). During the rainy season the PR was 0.818, in the cool season it was 0.791, and in the hot season it was 0.790.

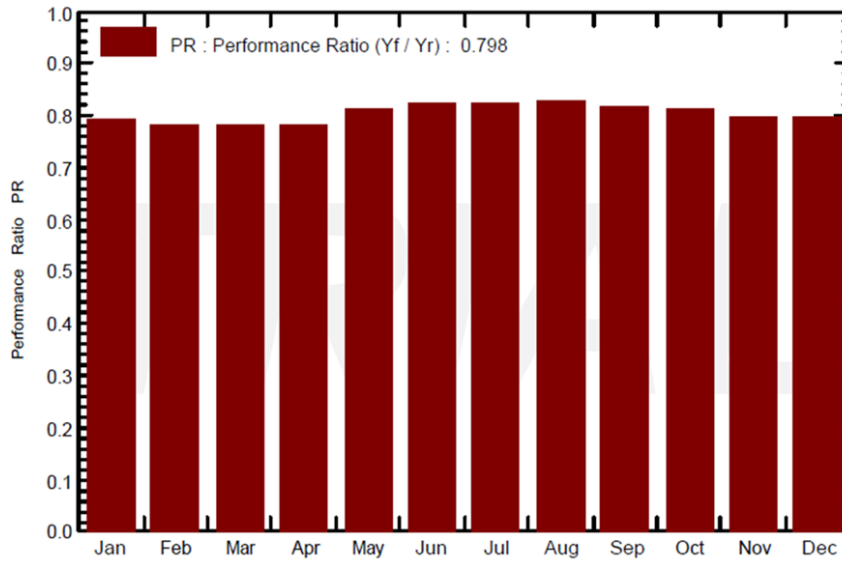


Figure 21 - Average Monthly Performance Ratio

The PR figures show that 79.8% of the energy collected by the installation was converted into useful energy and injected into the grid, meaning that the combined annual losses of the installation were 20.2%. Figure 22 shows a detailed breakdown of the annual losses of the system.

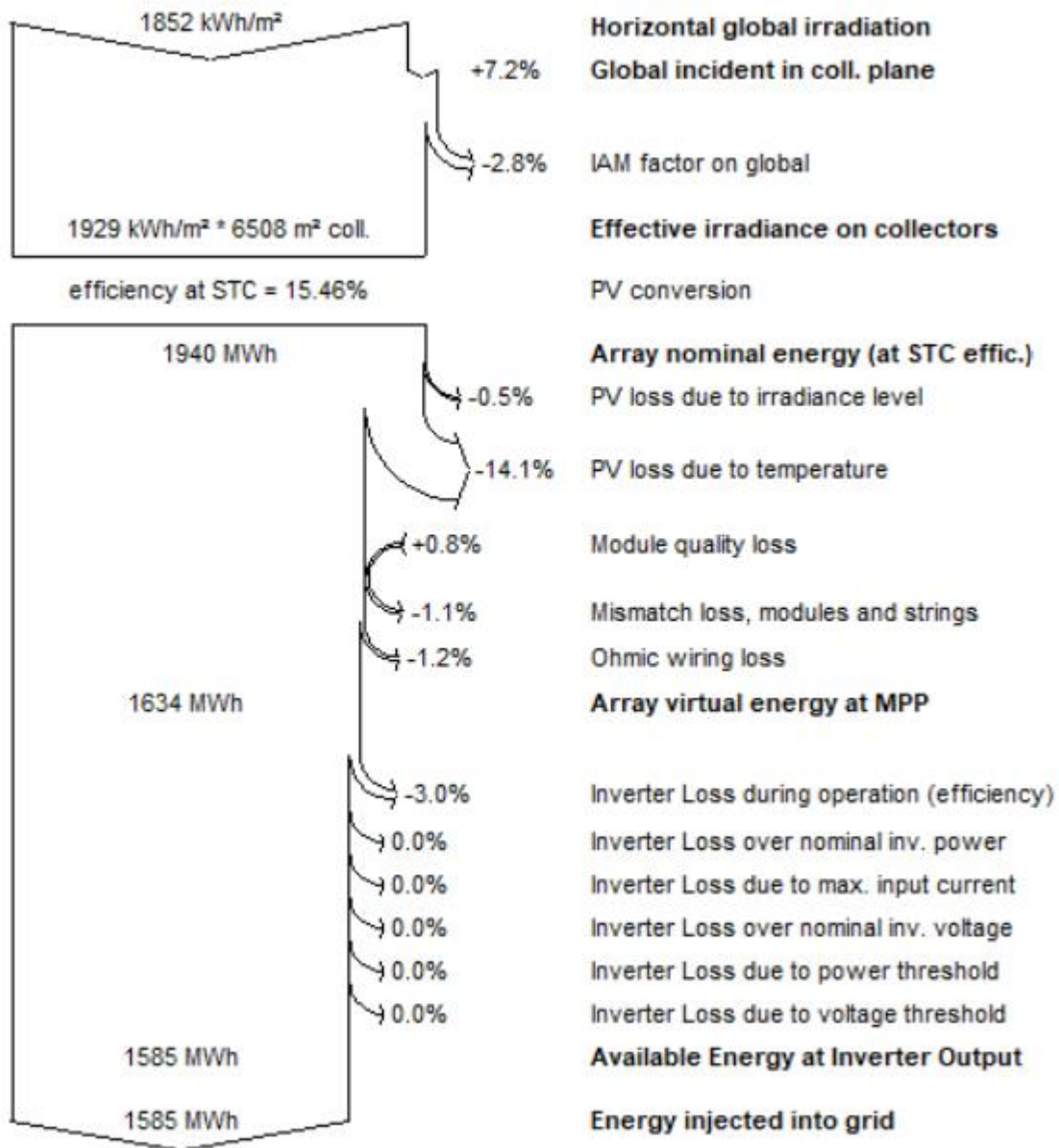


Figure 22 – System Loss Diagram of Simulated PV System in Yangon City

Some of the causes of losses in the system were due to inverter efficiency, ohmic wiring losses and PV module and string mismatch. The main cause of losses in the system was due to temperature and low irradiance (14.8%). This high figure helps to explain why PV output was lower in the hot season compared to the cool season. Figure 23 shows the normalized production of the installation over the first year of operation.

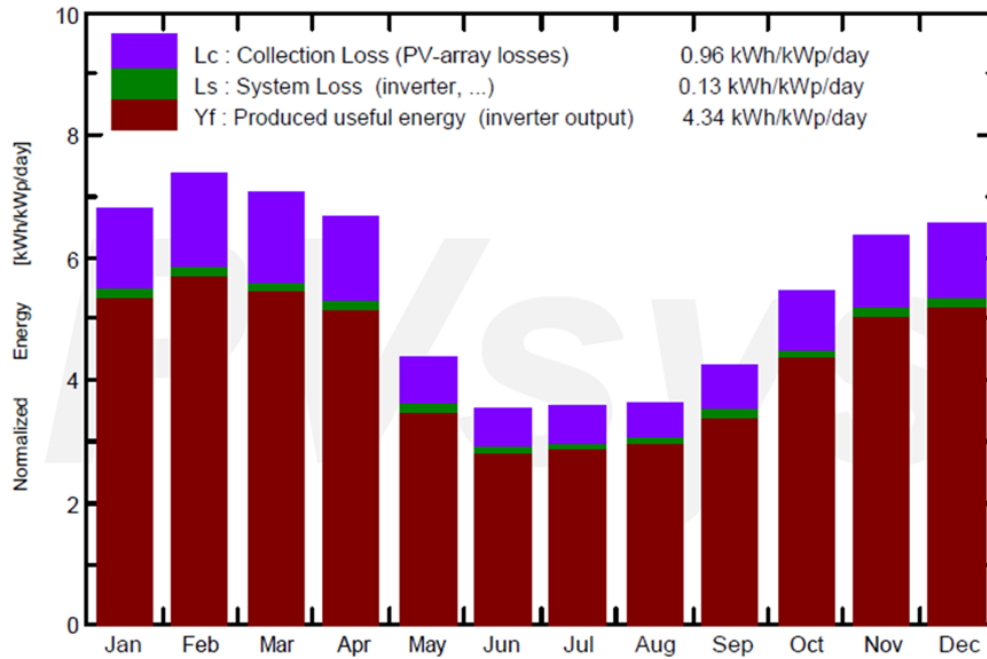


Figure 23 – Normalised Monthly Production

The data obtained from the PVsyst™ simulation were used to create average daily PV output profiles of the PV system described in Table 9 at the same hourly resolution as the synthetic seasonal load profiles created for urban Yangon City. As with the synthetic load profiles, aggregated monthly, seasonal (Figure 24) and annual output profiles were then generated from the monthly profiles.

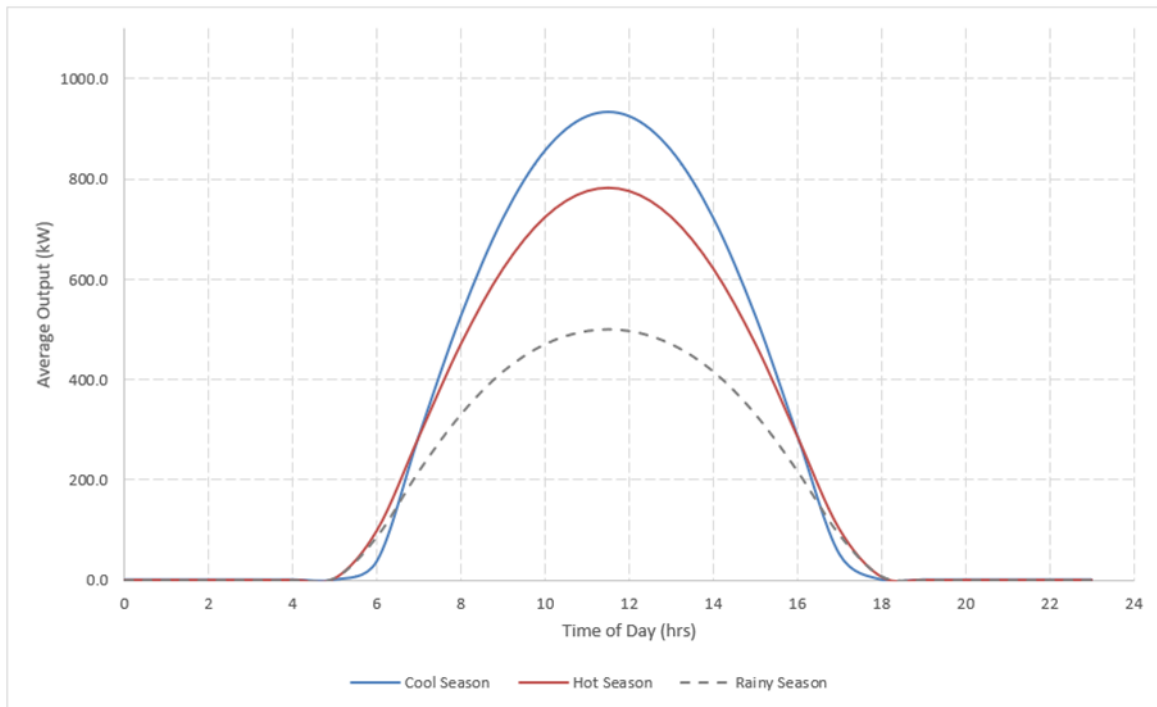


Figure 24 – Averaged Daily PV Output Profiles

Although the cool season had the fewest daylight hours, 12 as opposed to 14 for both the hot and rainy seasons, the average daily output was highest in this season. Output fell by 11.4% in the hot season and by 39.6% in the rainy season.

3.5. Solar Supply and Load Matching

The results obtained from this study found that in the first year of operation of the proposed PV installation (2020) the solar supply rate was 0.99, suggesting that there is a 99% match between energy needs and the output from the PV installation. However, as stated previously, the solar supply rate does not consider whether the output from the PV installation temporally coincides with load.

Figure 25 shows the normalized yearly profiles of both the PV installation and the local load, with the shaded area highlighting the degree of matching between the output of the PV system and the local load it is supplying.

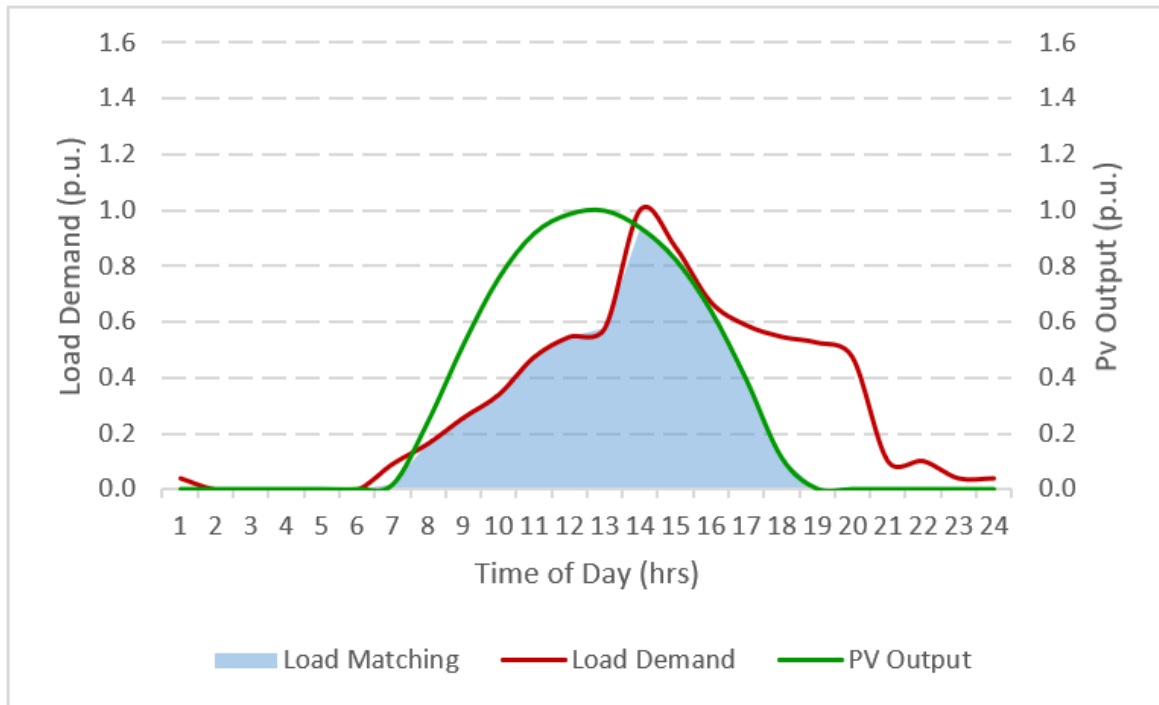


Figure 25 – Load Matching in 2020

The degree of load matching for the year would be 71%, and as seen in *Figure 25* there is a reasonable correlation between the output of PV installation and the load of an urban setting such as Yangon City. As stated previously this work assumes that the times of high peak demand in areas such as Yangon City would occur during the hottest parts of the day (early afternoon) as consumers use electric devices such as fans to combat the high temperatures. *Figure 25* also shows that these times coincide with the times of high PV output.

Analysis of the results also showed that, as expected due to the climatic conditions and basic energy needs of the region under study, there was little variance in both solar supply rate and load matching for the three seasons. The solar supply rate was lowest in the cool season at 0.98 and highest in the rainy season at 1.09 a difference of 0.12. In terms of load matching the maximum variation in seasons (6.6%) was again between the cool season (67.7%) and the rainy season (74.3%).

Figure 26 and *Figure 27* show the forecasted load profiles, forecasted PV output profiles and load matching in 2025 and 2030 respectively, assuming the expected regional annual load demand increase, and the degradation rate of the PV system discussed previously.

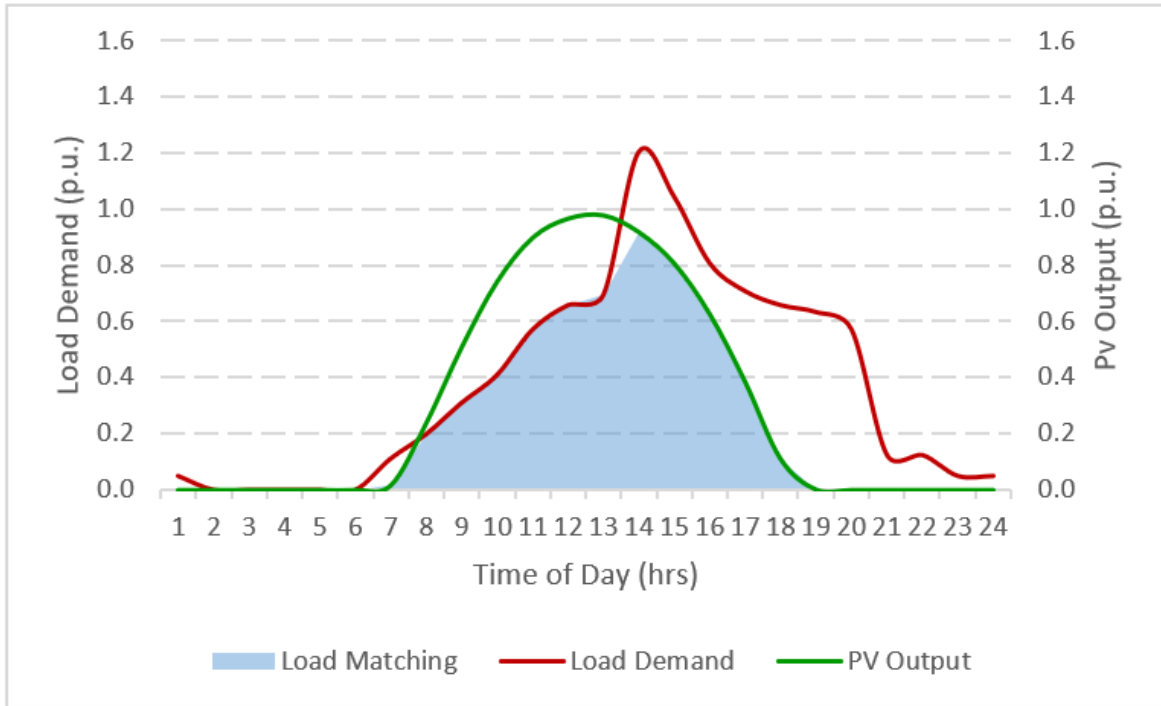


Figure 26 – Load Matching in 2025

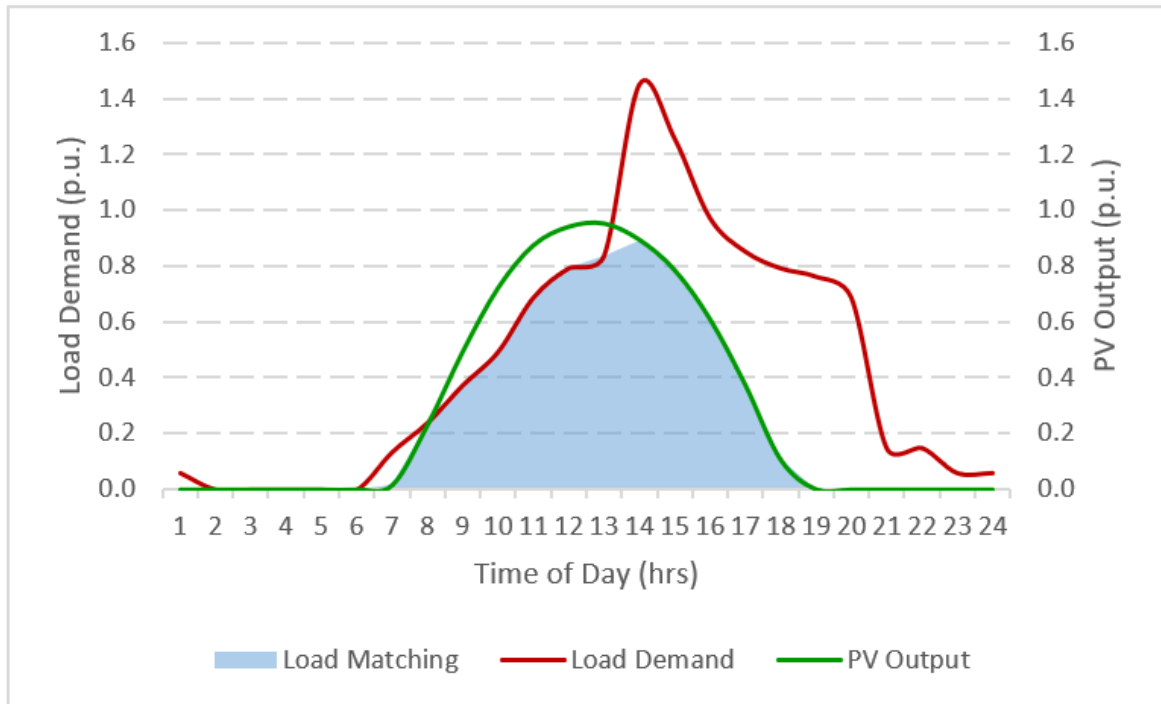


Figure 27 – Load Matching in 2030

The increase in load and degradation of the PV system output mean that by 2030 the solar supply rate would decrease to 0.65 and load matching would decrease to 57.3%. Figure 28

shows the decrease in solar supply factor and load matching of the PV system in the first 10 years of operation (2020–2030).

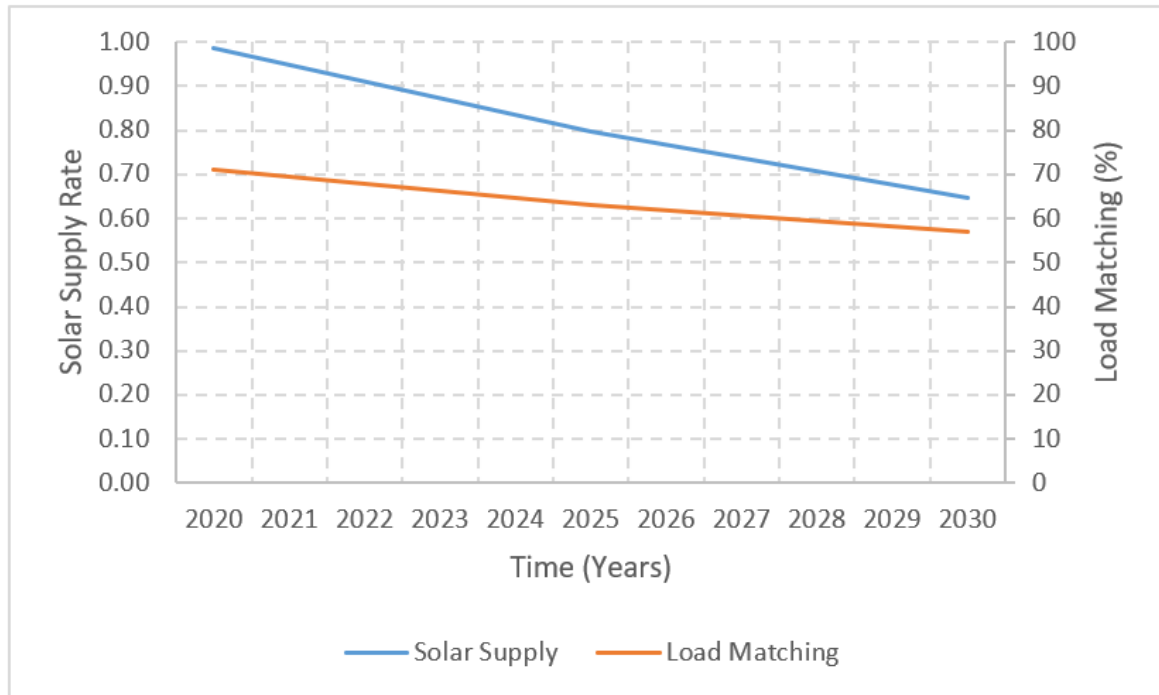


Figure 28 – Solar Supply Rate and Load Matching for First 10 Years of Operation

There has been a continued rise in the penetration levels of variable energy sources (VES) such as solar/PV over the previous few decades [304]. Due to the move towards a more sustainable energy future this rise is expected to continue [305]. One stumbling block to the continued integration of PV is thought to be the relationship between PV output and load demand. This is particularly true in Europe where the highest output levels coincide with periods of low demand.

3.6. Implications On Future Electricity Mix Planning

The results from this study have shown that for developing nations in the global south with economic and climate conditions similar to Myanmar that there is a good correlation between PV output and local load demand. During the first year of operation of the PV installation the majority of the electricity generated (approximately 75%) would coincide with local demand. This means that there will still be grid support needs from non-renewable generation technologies/ storage, although at a lower capacity that needs to be factored into the electricity generation planning. The results also show that if load demand in the region

continues as predicted, the correlation between PV output and local load demand will increase over time. It is evident in the case of Myanmar, it is a suitable candidate for meeting the country's ambitions of creating a sustainable network with significant levels of RE in the near future.

However, to create sustainable electrical power systems in countries like Myanmar, it becomes more important to study the effects of increasing renewable penetration levels on load (demand) profiles. The planning of their future energy mixes are reliant on the forecasting of future load profiles for which an ANN framework is proposed later in this work.

Chapter 4

Forecasting: An Important Tool for Electricity Planning

Future power networks are certain to have high penetrations of renewable distributed generation such as photovoltaics (PV). As energy flow becomes inevitably more complex with larger integration of renewable generation, electric vehicles and energy storage in modern power networks, power system planning methods are becoming more complicated compared to how they were with conventional, mostly thermal, generation. The restructuring of electricity networks means accurate load profiles are increasing important [219]. Traditional methods of creating load profiles that rely on historical data will not be suitable for modelling the increasingly complex electricity networks of the future. Hence it has become important to develop suitable new load profile generation methodologies that rely on publicly available data that can be used to aid different network related analyses by operators.

In this chapter a new computational approach for generating synthetic residential load profiles of the future which combines artificial intelligence and statistical probability is presented. The accuracy of the approach is assessed through the use of a case study of a typical distribution network containing varying levels of modern loads (EV charging) and customer side generation (PV).

4.1 Proposed Future Load Profile Generation (Forecasting) Framework

Load profiles represent the variation of After Diversity Maximum Demand (ADMD) of domestic consumers over a day. The standard method of constructing an hourly load profile is by recording the energy consumption, at feeder or substation level in an electricity distribution network, at regular intervals and dividing this by the number of customers on that feeder to produce the ADMD. The nature of customers is changing under de-carbonisation. Residential customers with generating technologies such as PV are prosumers as they produce and export electricity in addition to the typical consumer roles. In the smart grid context, historic forecasts of load profile will not be appropriate. Net load profiles at the residential customer level will need to be prosumption profiles, factoring in the drastic changes in load (for example, due to electric vehicles (EV), heat pumps etc.) and at-home generation technologies (PV, Micro-CHP etc.). Synthetically generated net load profiles are therefore important for scenario-based assessment studies.

Several studies have used artificial intelligence models for predicting energy demand of buildings [306]. Günay [307] modelled the gross electricity demand in Turkey using Artificial Neural Network (ANN) models with weather and socio-economic factors as inputs. Zameer et al. [308] used genetic programming based on an ensemble of neural networks to demonstrate the feasibility of wind energy prediction (in Europe) by using publicly available weather and energy data. With regard to the challenge of predictive modelling for uncertain penetration levels of future distributed resources, a number of researchers have recently had reasonable success by employing statistical probability distributions [309-311]. For example, Munkhammar et al. [311] demonstrated the use of the Bernoulli distribution for incorporating EV demand into load profiles. However, these statistical probability distributions fail to take into account the time varying behaviour in the energy consumption of distributed resources as they assume a constant load. Therefore, a framework for synthetic net residential load profile generation proposed combining artificial intelligence and statistical probability distributions, that can be used for scenario-based assessment studies, is proposed as shown in *Figure 29*. The framework summarises the author's and PhD supervisor's accumulated experience in using artificial intelligence methods and observations of literature.

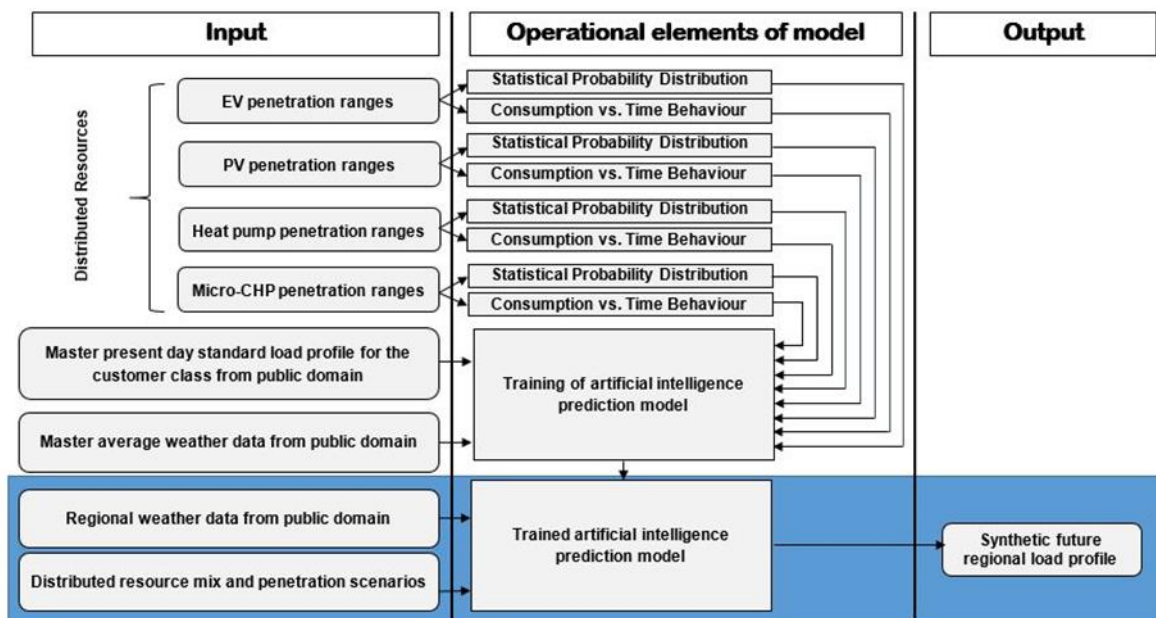


Figure 29 – Proposed Net Residential Load Profile Generation Framework

Please note that in the work discussed in this chapter that heat pumps and micro combined heat and power (CHP) generation were not investigated as inputs of the model.

The net residential load profile generation problem is inherently data centric. The choice of data, artificial intelligence methods and inclusion of operational elements of the framework such as statistical probability distribution is dictated by the data available. A method tailored for the data available and scenario under consideration, can be generated based on the framework.

4.2 Choice of Artificial Intelligence Model

Testing was carried out to determine a suitable AI model to use in this work. The AI models tested included 4 different linear regression models, 3 regression trees, 6 support vector machines, 2 regression tree ensembles and one artificial neural network. The same computer environment (Matlab) was used to create all the AI models to ensure validity of the comparison was maintained. All the models investigated were generated using the default Matlab settings and were trained using the same data set. 10 models of each AI technique were created (160 in total) and the average values of these 10 runs of coefficient of correlation (R Value), error (mean square error) and training time were then compared. The results of these tests are presented in Table 11.

Table 11 – Artificial Intelligence Model Testing Results

Artificial Intelligence Method	Coefficient of Correlation (R Value)	Error (MSE)	Training Time (Seconds)
Linear Regression Models			
Linear	0.79	0.048458	9.2
Interactions Linear	0.93	0.028354	8.0
Robust Linear	0.79	0.048901	10.7
Stepwise Linear	0.93	0.028361	20.9
<i>Average</i>	<i>0.86</i>	<i>0.038518</i>	<i>12.2</i>
Regression Trees			
Fine Tree	1.00	0.000401	12.5
Medium Tree	1.00	0.000951	11.5
Coarse Tree	0.99	0.004960	10.8
<i>Average</i>	<i>1.00</i>	<i>0.002104</i>	<i>11.6</i>
Support Vector Machines			
Linear SVM	0.78	0.049757	28.3
Quadratic SVM	0.95	0.022058	41.5
Cubic SVM	0.99	0.002573	146.8
Fine Gaussian SVM	0.99	0.001305	47.5

Medium Gaussian SVM	0.99	0.002073	39.2
Coarse Gaussian SVM	0.94	0.012596	50.4
<i>Average</i>	<i>0.94</i>	<i>0.015060</i>	<i>59.0</i>
Regression Tree Ensembles			
Boosted Trees	0.98	0.003462	46.3
Bagged Trees	0.99	0.001294	49.6
<i>Average</i>	<i>0.99</i>	<i>0.002378</i>	<i>48.0</i>
Artificial Neural Network			
Feed Forward Network	1.00	0.000266	6.0

The results of the testing of the different AI models clearly showed that artificial neural networks were the most suitable candidate to use in this work. Therefore, the decision was made to investigate further the viability of basic ANN models to synthesize future load profiles of networks with varying penetration levels of typical modern-day loads such as PV and electric vehicle charging was investigated first as described in the next section. Chapter 5 is dedicated to a detailed description of ANNs and their application for load forecasting using the MATLAB ANN toolbox.

4.3 Viability of Future Load Profile Generation Based on Public Data using ANN

The exact penetration levels of consumer-side technologies such as PVs and EVs in the future energy demand mix is presently uncertain. The charging profiles of different EV technologies is also evolving as EV technology is evolving. As there is a step change in load the objective is not to generate future load profiles based on historic datasets of load, but to use standardised load profiles and load/generation-weather relationships.

Previous literature reveals that a large proportion of the variability in electricity demand is dependent on weather variables such as air temperature, humidity, wind speed, cloud cover and irradiation [312-313]. It is also evident that the sensitivity of residential and commercial consumers electricity demand to meteorological variables is higher than that for industrial consumers [314]. Irradiance, air temperature, wind speed and air mass are weather features that affect PV power output [315]. Liu et al posit that there is no obvious correlation between wind speed and PV output power [316]. Aste et al find that performance ratio for crystalline silicon PV modules is fairly constant in the face of changes in air mass [317]. Seasonal variations in weather affect the PV output power from month to month. The existing literature

seems to agree that irradiance and air temperature are the two most important weather features that impact on the output power of a PV system. The charging profiles of EVs have no obvious correlation to weather [318]. They are dictated by consumer driving behaviour which in turn is correlated to the socio-economic factors of the region. As temperature and irradiance are influencing parameters common to load and PV generation, it makes sense to include these as inputs for generating future aggregate load profiles.

The feasibility of using publicly available weather and electrical vehicle charging data to generate future penetration level scenario based residential load profiles is investigated here.

4.3.1 Data Description

The UK Energy Research Centre (UKERC) has developed load profile models for all 4 seasons of a typical year [319]. The load data used in this study is for residential customers unrestricted by usage timings. The load profiles from UKERC have hourly time-resolution and are publicly available. As described in the previous section, temperature and irradiation are the main weather data to be considered. There are a number of weather databases which provide weather data for a typical year for different locations such as NREL (National Renewable Energy Laboratory) National Solar Radiation Data base, NASA Surface meteorology and Solar Energy, PVGIS (Photovoltaic Geographical Information System) climate-SAF etc. PVGIS climate-SAF was selected as the reference solar database for the UK as it provides up-to-date data in the public domain for Europe. The data is available with hourly time resolution for 365 days a year. A MATLAB program was written to create seasonal average hourly weather (temperature and global irradiation) datasets. The Low Carbon London (LCL) project conducted customer trials of new transport and heating loads on distribution networks in London. Residential EV charging profile data for this study was taken from the project [320].

4.3.2 PV Generation

Middlesbrough, UK is considered as the region where future load profiles are to be generated. At the time of this study in the UK, PV systems of 4 kWp rating were eligible for the highest feed-in tariff incentive. Hence this system size was considered. The crystalline silicon PV technology was selected as it is the most mature PV technology with the highest market share. Typical PV systems were modelled using PVGIS 5 online software which generates PV output data with hourly time resolution for 365 days a year. Seasonal average

typical PV generation datasets were created using a MATLAB program similar to that described for weather data. *Figure 30* shows the seasonal variation in PV generation. As expected, summer and spring months have higher power outputs for longer duration as compared to autumn and winter.

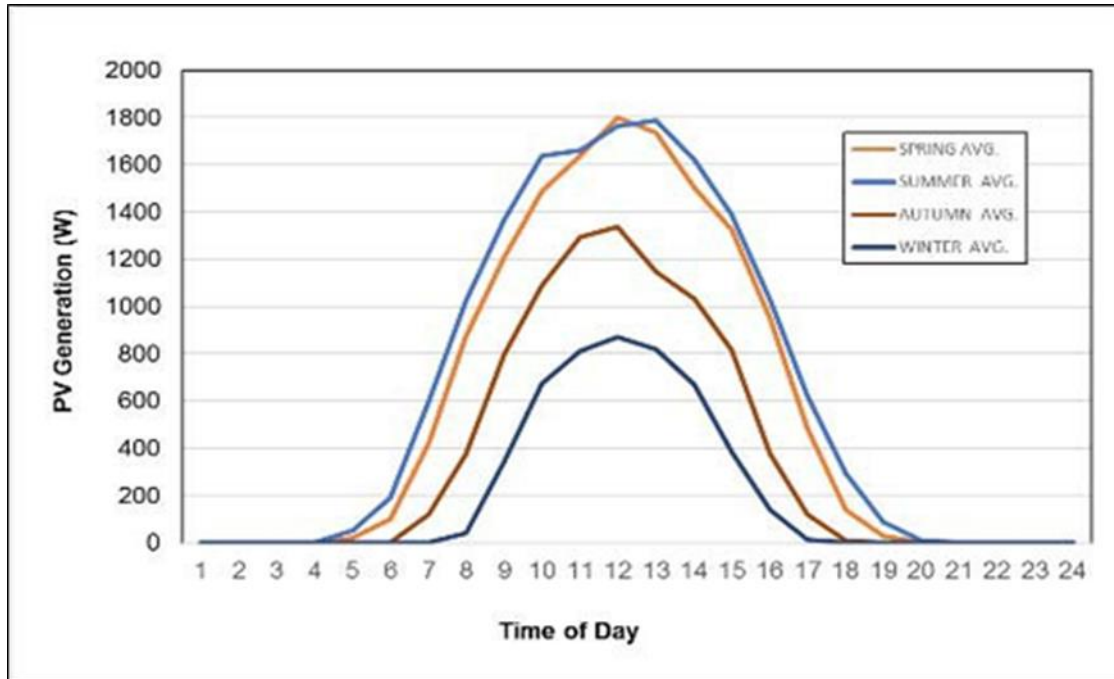


Figure 30 – Seasonal Variation in PV Output Profiles of the Typical PV system

4.3.3 PV and EV Penetration Scenarios

PV and EV penetration level in this work is defined as the ratio of the number of houses with a typical PV system or EV to the total number of houses in the distribution network for which the load profile is representative. In this work, PV penetration level was varied in steps of 10% from 0 to 100%, along with a similar variation in EV penetration level corresponding to PV penetration level.

4.3.4 Creation of Composite Future Load Profiles

Composite future load profiles are essential for testing the feasibility of the ANN based load profile generation methodology. After generating seasonal PV generation profiles, composite future load profiles, for the whole range of EV and PV penetration scenarios described in the previous section for all seasons of a typical year, were created. This was done by aggregating seasonal UKERC profile class 1 load profiles with penetration-level-weighted PV generation (negative demand) profiles and EV charging profiles from LCL. As future load

profiles for the penetration scenarios described are not yet available these composite load profiles were construed as close substitutes to the actual.

4.3.5 ANN Design and Training

In terms of computational structure, ANNs are composed of neurons, which at a very basic level mimic neurons in the human body in terms of learning and processing information. In this work, a feed forward neural network is used. In this ANN design, neurons are arranged in successive layers and information flows from the input layer to the hidden layer and then to output layer. The method used for ANN training is supervised learning where the training data includes both the input and the target outputs. Levenberg-Marquardt algorithm is used for ANN training owing to its training speed and ease of implementation using MATLAB neural network toolbox.

The input variables for the ANN model were time of day, global irradiation (W/m²), temperature (oC), PV penetration level (%) and EV penetration level (%). The output is load for the particular hour (kW). The ANN model was trained on input weather and target load data for spring, summer and winter for the range of penetration scenarios described in section II.C. As complexity increases the difficulty in training and the training time, it was aimed to keep the ANN structure as simple as possible. A single hidden layer was considered between the input and output layers. Initially the ANN was trained with 5 input nodes corresponding to the 5 input variable, 10 hidden nodes (default MATLAB architecture) and 1 output node corresponding to the load. The use of the default ANN architecture gave a Pearson correlation coefficient (R) value close to 1, between predicted outputs and targets outputs of the ANN. The ANN was re-trained after reducing the number of hidden nodes by one to see the decline in R-value. This iterative procedure continued until the optimum ANN architecture with 6 hidden nodes shown in *Figure 31* resulted. The feasibility of the proposed method for future load profile generation was investigated using the case study of different PV and EV penetrations for the autumn season for which the ANN does not have a priori knowledge from training.

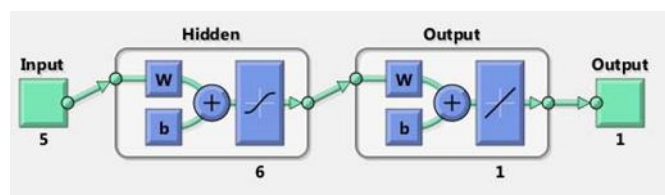


Figure 31 – ANN Architecture for Future Load Profile Prediction Model

4.3.6 Prediction Performance Metrics

The statistical metrics used for examining the prediction accuracy and comparing the performance of ANN to regression were the root mean square error (RMSE), the mean absolute error (MAE) and the mean absolute percentage error (MAPE). They are defined by the following statistical equations.

Equation 4 – Root Mean Square Error

$$RMSE = \sqrt{\frac{\sum_{i=1}^n (P_i - A_i)^2}{n}}$$

Equation 5 – Mean Absolute Error

$$MAE = \frac{\sum_{i=1}^n |P_i - A_i|}{n}$$

Equation 6 – Mean Absolute Percentage Error

$$MAPE = \frac{\sum_{i=1}^n \left| \frac{P_i - A_i}{A_i} \right|}{n} \times 100$$

Where P_i and A_i are the synthetic load profile data and actual load profile data at the i point respectively, and n is the total number of data points (i.e., 24 per load profile for hourly resolution).

4.3.7 Validation and Viability of ANN use

To validate the suitability of the proposed ANN for generating synthetic future residential load profiles, the performance of ANN model was compared to multiple linear regression (MLR) – a common prediction model. This section compares the training and prediction performance of both models.

Training

Both ANN and regression models were trained using the same input weather and target load data, and the whole range of penetration levels of PV and EV described in section II.C, with hourly resolution. The training data was for spring, summer and winter of the typical year. To analyse the fitness of the model the output of the ANN and regression models with the

training data was compared to the actual load profiles (targeted training outputs). Owing to the 112 (in-total) combinations of PV and EV penetration scenarios and 3 seasons, there were 336 twenty-four-hour load profiles (ANN, MLR and actual) to be compared. *Figure 32* and *Figure 33* show representative comparison obtained for 2 (out of the 300 scenarios) namely: 10% PV penetration and 10% EV penetration in spring and 50% PV penetration and 70% EV penetration in winter.

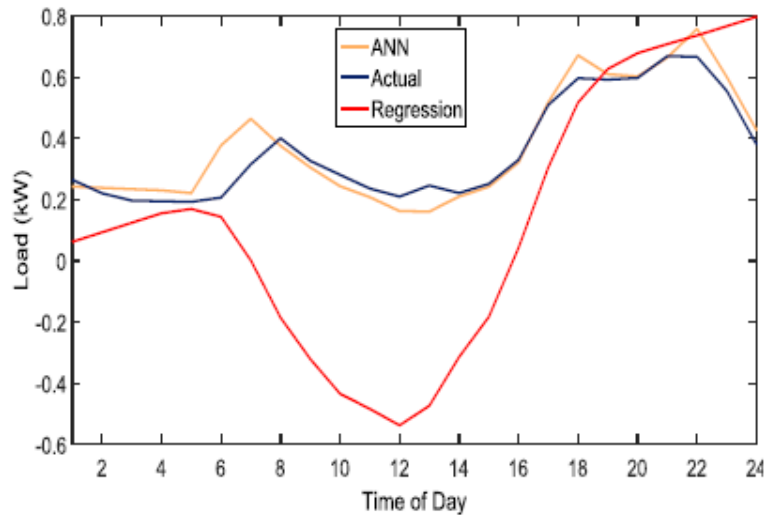


Figure 32 – Training Results for 10% PV and 10% EV Penetration in Spring

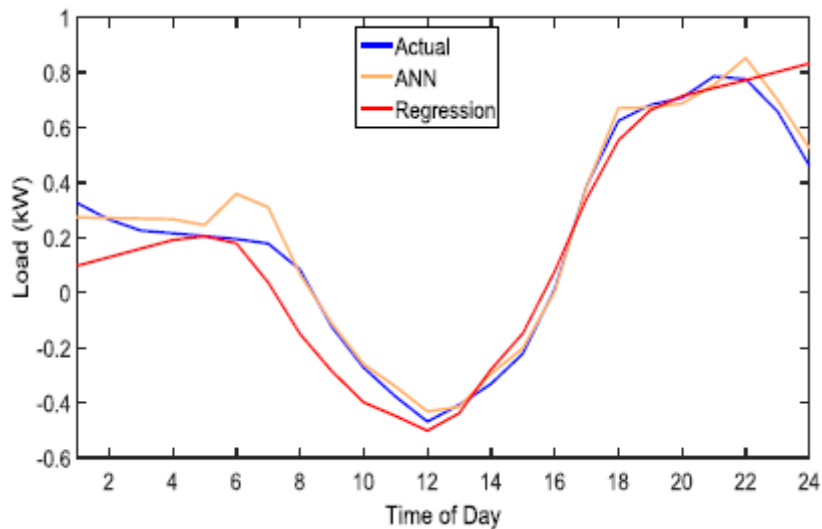


Figure 33 – Training Results for 50% PV and 70% EV Penetration in Winter

For a typical day in spring, with 10% PV penetration and 10% EV penetration, ANN shows a markedly better approximation to the actual load profile than MLR - as shown in *Figure 32*. In *Figure 33*, for the scenario of 50% PV penetration and 70% EV penetration on a typical winter,

the difference between the training performance of both models is not so apparent. However, because these two scenarios are only small portions of a large training dataset, a statistical description of training performance over the entire dataset is desirable and is described by the MAPE, MAE and RMSE values in *Table 12*.

Table 12 – Training Performance of ANN and MLR for All Four Seasons Combined and The Full Range of EV and PV Penetration Scenarios

Error	ANN	MLR
MAPE	7.29%	18.36%
MAE	0.0349	0.1959
RMSE	0.0492	0.2562

From *Table 12*, it is apparent that ANN has much better training accuracy than MLR. MAPE of 7.29% for ANN means that the ANN trains with about 93% accuracy as compared to about 82% for MLR. The MAE and RMSE values also support the fact that ANN trains better.

Validation

Input weather data, PV and EV penetration levels and composite load profiles for autumn season of the typical year (for which the ANN models have no a priori knowledge) was used to test both ANN and MLR prediction models. *Figure 34* compares the predicted load profile for a day in autumn with the actual load profile, for a scenario of 20% PV penetration and 30% EV penetration. The predicted load profile using ANN closely approximates the actual load profile. On the other hand, MLR prediction shows a marked divergence from the actual load profile. The superior prediction performance of ANN is statistically supported by *Table 2*, with MLR showing a prediction accuracy of just about 15% for the test season (autumn). The ANN model has been proved to be a viable model for generation of synthetic load profile in the face of increasing penetration of PV and EV resources. The complexity of the prediction process can be easily visualised from the comparison to the MLR model.

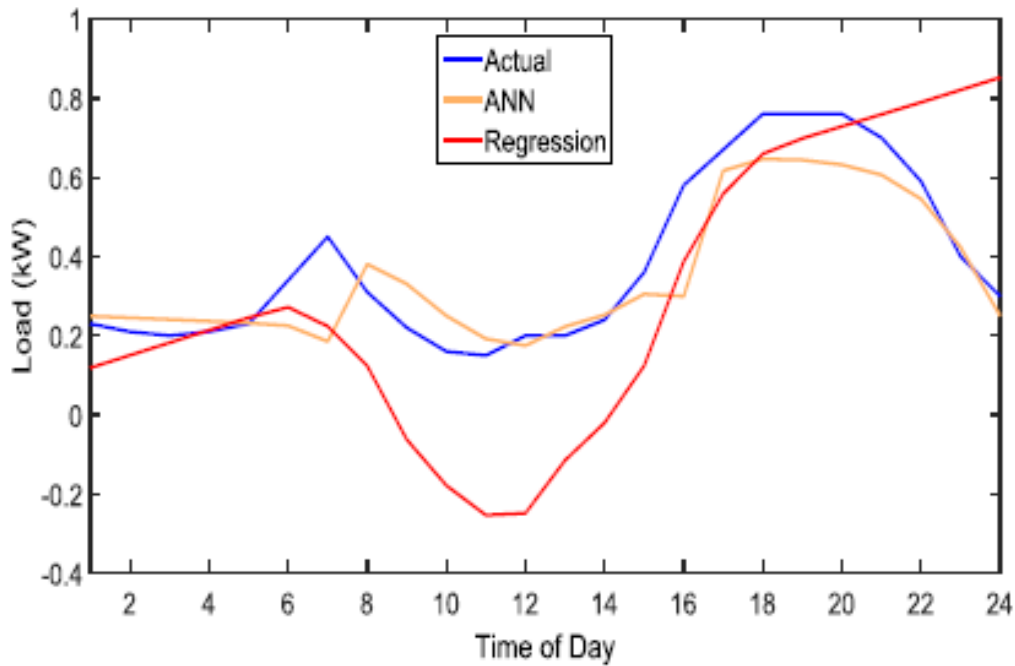


Figure 34- Testing Results for 20% PV and 30% EV Penetration in Autumn

Table 13– Testing Performance of ANN and MLR for 20% PV Penetration and 30% EV Penetration in Autumn

Error	ANN	MLR
MAPE	20.84%	74.83%
MAE	0.0765	0.1959
RMSE	0.1035	1.2481

In order to minimise training difficulty and time the structure of the ANN model was kept as simple as possible. The experimental results show that the ANN model has the ability to capture non-linear relationships even when trained with limited data from publicly available sources. The model was built using the Matlab Neural Network Toolbox with default settings, namely: a function fitting neural network, with 10 neurons in one hidden layer, hyperbolic tangent sigmoid transfer functions in the hidden layer, a linear transfer function in the output layer with the network trained using the Levenberg–Marquardt backpropagation (supervised) training algorithm. The results prove the feasibility of the proposed ANN based method for synthesising future residential load profiles under increasing levels of EV and PV penetration.

4.4 Knowledge gap in the design of ANN load forecasting methods

Over the years several authors have proposed different empirical rules which have been claimed as can be used in the design of ANN models in order to improve their performance

[251, 306]. For example, when designing an ANN model with one hidden layer different authors have proposed a variety of different formula to determine the number of hidden nodes: n , $2n$, $n/2$ and $2n + 1$, where n is the number of input nodes in the model as reported in [309]. In a model which has five inputs, use of these formulae would mean the hidden nodes used would be 5, 2.5, 10 or 11 depending on the formula employed. This translates to a high amount of effort in load forecasting using ANN applications due to the exploratory and iterative nature of the designing process. The hidden node ranges mentioned in the example also clearly shows why empirical rules do not work well for all applications [306], and why designing ANNs is often considered to be more of an art form rather than a science.

The next chapter provides a details of ANNs and their components, structures algorithms etc. and proceeds to develop a systematic approach that could be employed for designing ANN models for load forecasting by nations of the Global South or elsewhere.

Chapter 5

Development of a Systematic Artificial Neural Network (ANN) Design Approach for Load Forecasting using Matlab

The viability of basic ANN models to synthesize future load profiles of networks with varying penetration levels of typical modern-day loads such as PV and electric vehicle charging has been proven through a UK-based study in chapter 4. As outlined in section 4.7, ANN forecasting so far has been reliant on empirical rules which translated to a high amount of effort due to the exploratory and iterative nature of the designing process.

This chapter aims to address the knowledge gap and simplify the design process, through the development of a new systematic approach that could be employed in designing any ANN model for load forecasting by nations of the Global South or elsewhere.

The investigation was carried out using the neural network toolbox (NNTool-box) in Matlab. The NNTool-box supports the design, implementation and simulation of ANNs [321] whilst freeing the user from writing complex algorithms which allows them to speed up the design process and concentrate on trying to find the optimal model design [200].

The NNTool-Box has been used in several research papers in recent years in several fields of study including economics [322], medicine [323-324], science [325-327] and engineering [321, 328-337]. The toolbox has also been used in several load forecasting studies, although they have mostly been in the short-term horizon [226, 239, 241, 338] and medium-term [157, 200]. The popularity of the toolbox has also seen several papers use it to analyse different ANN design parameters [339-341].

5.1 Matlab Parameter Testing

In reviewing the literature on ANNs it was found that five parameters were commonly used by authors to try to improve the prediction capabilities of their models. These were training function, number of neurons, number of hidden layers, network architecture and transfer functions used in the hidden layer(s) and output layer. To determine the effects of each of these parameters on the prediction capabilities of ANN models used in load forecasting scenarios a number of tests were carried out. This section details those tests and presents the results.

5.1.1 Performance Indicators

When evaluating the results from any testing it is important to properly define some performance indicators [342]. In the testing discussed here performance was measured in terms of mean square error (MSE) and the coefficient of correlation, also known as the Pearson correlation coefficient or more simply as the (R) value. MSE is a metric commonly used to measure of the goodness of fit in the training, validation and testing sets of ANN models [343–346]. It is a measure of the average squared difference between targets and outputs of a network [344]. Therefore, the smaller the value of MSE the closer the fit is to the data and the better the performance of a network [343]. R values are a measure of the relationship between two variables. They are commonly used to show the prediction accuracy of ANN models by evaluating the relationship between predicted and actual values [343–347]. Where an R value near to 1 indicates a high degree of correlation between actual and predicted values (good prediction performance) and R values close to 0 indicate poor correlation between actual and predicted values (poor prediction performance) [348].

5.1.2 Default Matlab ANN Network Architecture Testing

Load forecasting using ANNs is essentially an input-output fitting problem. The recommended network architecture to use in input-output fitting problems is the function fitting network (Fitnet) and is the default network used in the Matlab NNtoolbox. A number of Fitnets were created to determine the effects the number of neurons, number of hidden layers and training function each had the prediction capabilities of ANNs.

Initial Testing

An initial test was carried out to determine which of the twenty training functions available in Matlab arena could be used in this study (see *Table 14*).

Table 14 - Matlab NNTool-Box Training Functions

Training Function	Matlab Syntax
<i>Backpropagation Training Functions that use Jacobian Derivatives (BTFJDs)</i>	
Levenberg-Marquardt Backpropagation	trainlm
Bayesian Regulation Backpropagation	trainbr
<i>Backpropagation Training Functions that use Gradient Derivatives (BTFGDs)</i>	
BFGS Quasi-Newton Backpropagation	trainbfg

Conjugate Gradient Backpropagation with Powell-Beale Restarts	traincgb
Conjugate Gradient Backpropagation with Fletcher-Reeves Updates	traincgf
Conjugate Gradient Backpropagation with Polak-Ribiere Updates	traincgp
Gradient Descent Backpropagation	traingd
Gradient Descent with Adaptive Learning Rules Backpropagation	traingda
Gradient Descent with Momentum	traingdm
Gradient Descent with Momentum & Adaptive Learning Rules Backpropagation	traingdx
One Step Secant Backpropagation	trainoss
RPROP Backpropagation	trainrp
Scaled Conjugate Gradient Backpropagation	trainscg
<i>Supervised Weight/Bias Training Functions (SWBTFs)</i>	
Batch Training with Weight & Bias Learning Rules	trainb
Cyclical Order Weight/Bias Training	trainc
Random Order Weight/Bias Training	trainr
Sequential order weight/bias training	trains
<i>Unsupervised Weight/Bias Training Functions (UsWBTFs)</i>	
Unsupervised Batch Training with Weight & Bias Learning Rules	trainbu
Unsupervised Batch Training with Weight & Bias Learning Rules	trainbuwb
Unsupervised Random Order Weight/Bias Training	trainru

The testing involved using the training dataset described in Section 4.3 to create an ANN with the default Matlab design of ten hidden neurons in one hidden layer in a function fitting network (Fitnet) using supervised learning. As expected, the Matlab ANN toolbox was unable to initialise training when employing any of the three unsupervised training functions (trainbu, trainbuwb and trainru). Sixteen of the supervised training functions when tested successfully converged to a solution in times from a few seconds to a little over 2 minutes when using Matlab R2017b Update 7 on a HP EliteDesk 800 G2 SFF PC with an Intel Core 3.2GH z 4 Core i5-6500 CPU and 8GB Physical / 11GB Virtual memory running Microsoft Windows 10.0.16299 Enterprise Operating System. However, the trainc function did not successfully converge to a solution when it was left to run for over 18 hours on several attempts. Due to these reasons the three unsupervised functions along with the trainc function were all deemed to be unsuitable candidates for the next phase of testing.

Training Functions and Neurons Testing

Tests were then carried out to examine the prediction capabilities of the 16 remaining supervised functions when using the standard Fitnet Matlab ANN architecture. These tests also studied the effects of altering the number of neurons in the hidden layer from one to twenty. In all 100 tests were carried out on each algorithm and 1,600 in total. *Figure 35 to*

Figure 37 show the average error between predicted values and actual values of each training function over the range of 1 to 20 neurons.

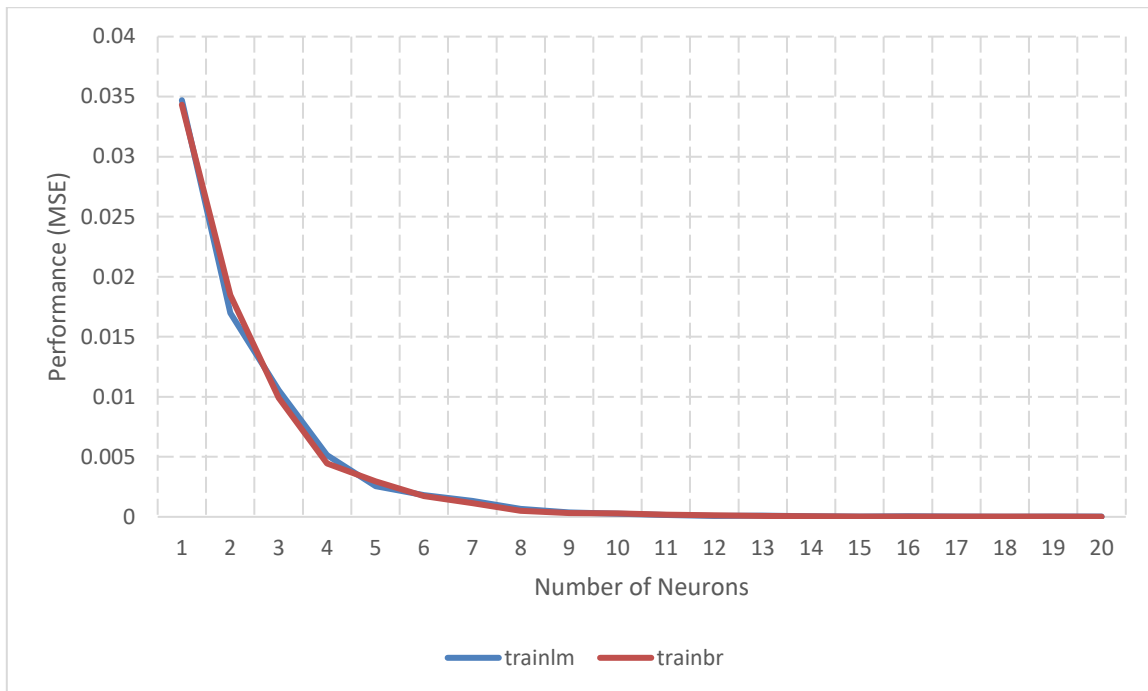


Figure 35 – Error of Backpropagation Training Functions that use Jacobian Derivatives in Neuron Testing

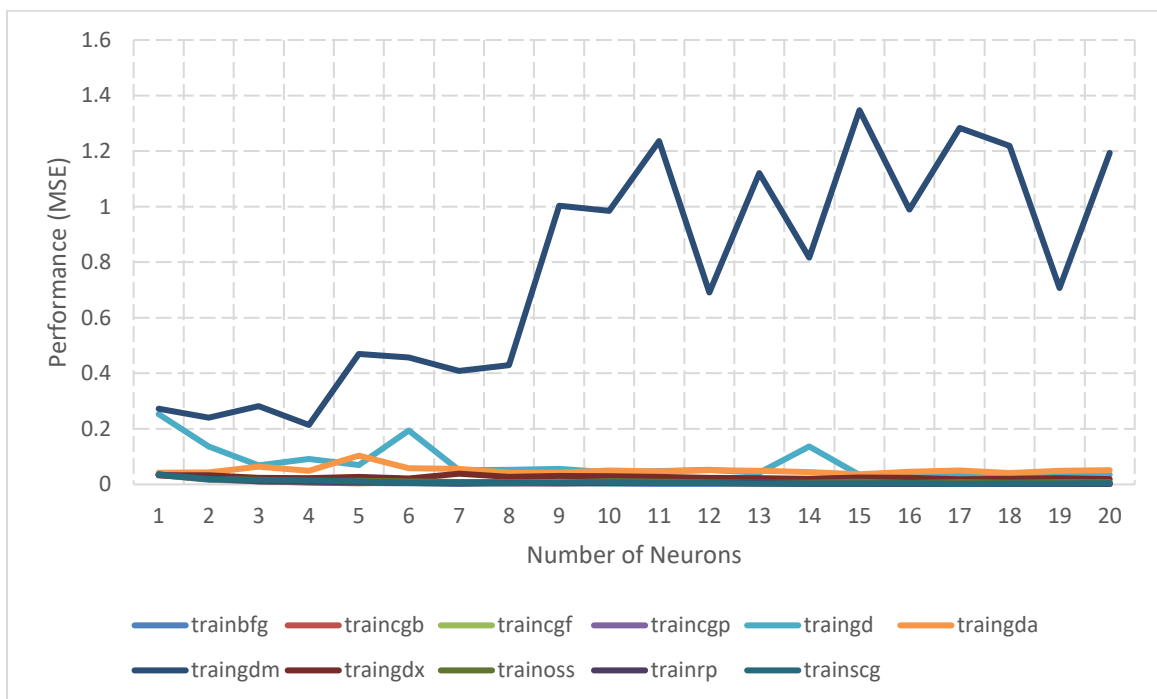


Figure 36 – Error of Backpropagation Training Functions that use Gradient Derivatives in Neuron Testing

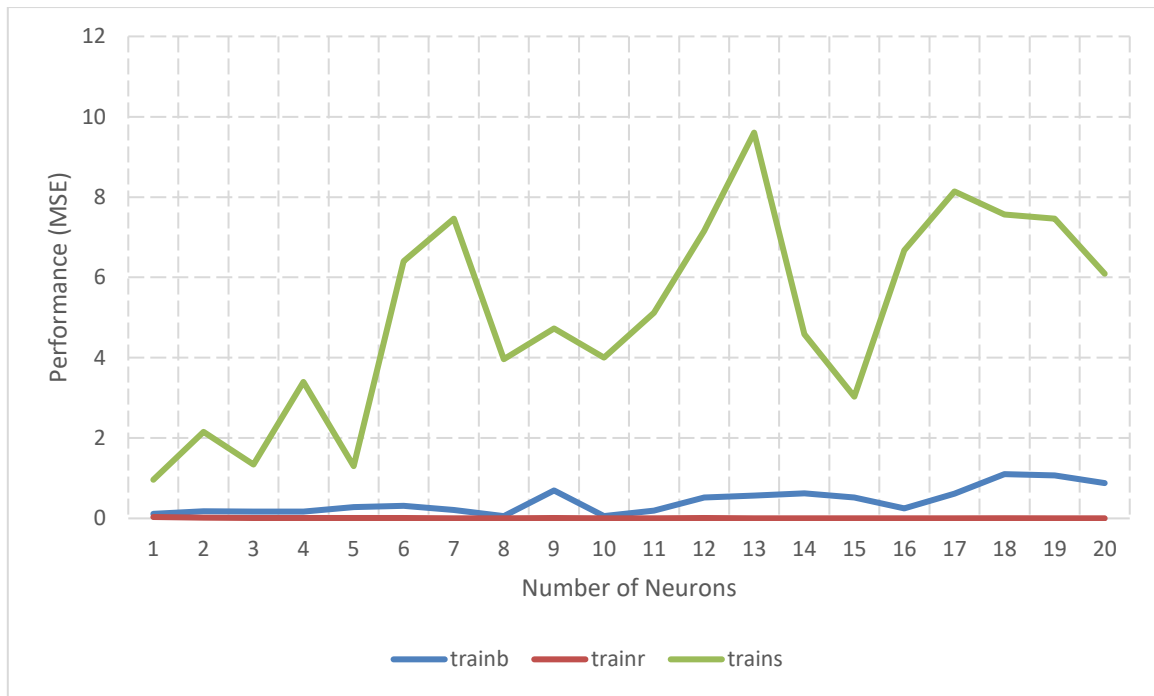


Figure 37 – Error of Supervised Weight/Bias Training Functions in Neuron Testing

From Figure 35 it can be seen that the error of both of the BTFJDs was similar. It can also be seen that as neurons are added to the network the performance of both functions increased with an almost exponential rate.

From Figure 36 it can be seen that the error of all the BTFGDs was not similar to each other. It can clearly be seen that the error of the *trqingdm* function was much worse than the other types of function that use gradient derivatives, and that the change in performance brought about by altering the number of neurons was not predictable as was seen with the *trainlm* and *trainbr* functions.

Results also showed that the error of the three SWBTFs were unlike to each other. From Figure 37 it can be seen that the *trains* function performed extremely poorly and erratically over the range of neurons. It can also be seen that whilst the *trainb* function performed better than *trains* it was still somewhat erratic and inferior to the performance of the *trainr* function.

Table 15 shows the average error of each training function in terms of mean square error over the full range of neurons tested (1 to 20). From these results it can again be seen that the error of the two backpropagation training functions that use Jacobian derivatives was similar. It can also be seen that the averaged error of the BTFJDs (0.00374) was substantially better

than the average error of the BTFGDs (0.08862) and the averaged error of the SWBTFs (1.83172).

The results in *Table 15* also show that whilst the averaged values of the three types of training function were considerably different the performance of individual functions in each of the three type categories was comparable. The coefficient of correlation (R value), also known as the Pearson correlation coefficient, figures shown in *Table 16* strengthen these findings. From these figures it can again be seen that the BTFJDs outperformed the other types of functions on average but some individual functions in each type had similar performances.

Table 15 – Error of Different Training Functions in a Single Layer Network

Function	Error (MSE)			
	Worst	Best	Variation	Average
Backpropagation Training Functions that use Jacobian Derivatives				
trainlm	0.0347038	0.0000121	0.0346917	0.0037461
trainbr	0.0343248	0.0000093	0.0343155	0.0037322
<i>Average</i>	<i>0.0345143</i>	<i>0.0000107</i>	<i>0.0345036</i>	<i>0.0037391</i>
Backpropagation Training Functions that use Gradient Derivatives				
trainbfg	0.0338772	0.0006297	0.0332475	0.0054425
traincgb	0.0337104	0.0017231	0.0319873	0.0068273
traincgf	0.0345752	0.0026901	0.0318851	0.0082406
traincgp	0.0344542	0.0028998	0.0315544	0.0083364
traingd	0.2529902	0.0341086	0.2188816	0.0758297
traingda	0.1036000	0.0364800	0.0671200	0.0507430
traingdm	1.3472420	0.2141410	1.1331010	0.7682005
traingdx	0.0386438	0.0185596	0.0200842	0.0254688
trainess	0.0355676	0.0057411	0.0298265	0.0110109
trainrp	0.0358002	0.0013701	0.0344301	0.0067734
trainsicg	0.0352436	0.0015827	0.0336609	0.0079448
<i>Average</i>	<i>0.1805186</i>	<i>0.0290842</i>	<i>0.1514344</i>	<i>0.0886198</i>
Supervised Weight/Bias Training Functions				
trainb	1.1022000	0.0565000	1.0457000	0.4292240
trainr	0.0345982	0.0037803	0.0308179	0.0082248
trains	9.6046200	0.9617960	8.6428240	5.0577011
<i>Average</i>	<i>3.5804727</i>	<i>0.3406921</i>	<i>3.2397806</i>	<i>1.8317166</i>

Table 16 – Coefficient of Correlation of Different Training Functions in a Single Layer Network

Function	Coefficient of Correlation (R Value)			
	Worst	Best	Variation	Average
Backpropagation Training Functions that use Jacobian Derivatives				
trainlm	0.9213	1.0000	0.0787	0.9915
trainbr	0.9212	1.0000	0.0788	0.9916
<i>Average</i>	<i>0.9213</i>	<i>1.0000</i>	<i>0.0787</i>	<i>0.9915</i>
Backpropagation Training Functions that use Gradient Derivatives				
trainbfg	0.9211	0.9982	0.0771	0.9872
traincgb	0.9204	0.9937	0.0733	0.9835
traincgf	0.9194	0.9914	0.0720	0.9816
traincgp	0.9197	0.9927	0.0730	0.9805
traingd	0.6336	0.9051	0.2715	0.8556
traingda	0.8434	0.9045	0.0611	0.8808
traingdm	0.2818	0.7465	0.4648	0.4257
traingdx	0.9178	0.9501	0.0322	0.9392
trainoss	0.9191	0.9857	0.0665	0.9746
trainrp	0.9156	0.9960	0.0804	0.9845
trainscg	0.9189	0.9950	0.0761	0.9815
<i>Average</i>	<i>0.8282</i>	<i>0.9508</i>	<i>0.1226</i>	<i>0.9068</i>
Supervised Weight/Bias Training Functions				
trainb	0.4188	0.8721	0.4533	0.6566
trainr	0.9179	0.9901	0.0722	0.9808
trains	0.5585	0.8964	0.3379	0.8282
<i>Average</i>	<i>0.6318</i>	<i>0.9195</i>	<i>0.2878</i>	<i>0.8219</i>

Training Functions and Hidden Layers Testing

The next stage of testing studied the effects of the number of layers on the prediction capabilities of the standard Fitnet network. These tests also studied the performance of the 16 training algorithms in different circumstances. Fitnet networks with one to six hidden layers each with 5, 10, 15 and 20 neurons in each were created and studied. In all 120 tests were carried out on each algorithm and 1,920 in total. *Figure 38 to Figure 40* show the average error of each training function over the range of 1 to 6 layers.

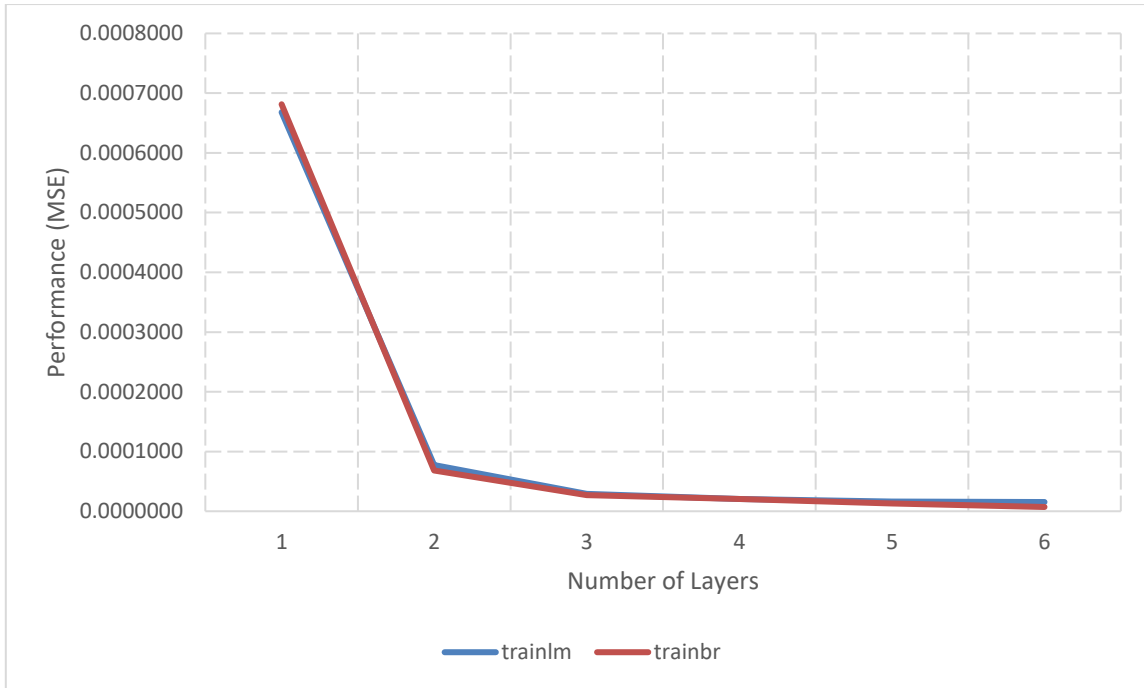


Figure 38 - Error of Backpropagation Training Functions that use Jacobian Derivatives in Layer Testing

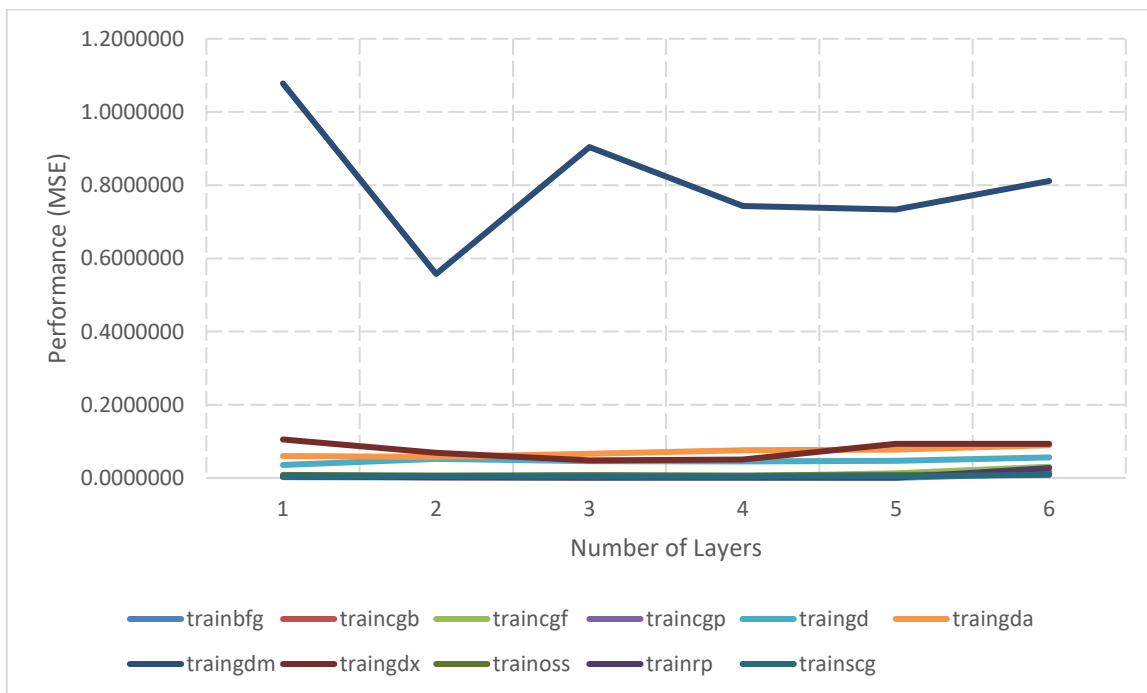


Figure 39 - Error of Backpropagation Training Functions that use Gradient Derivatives in Layer Testing

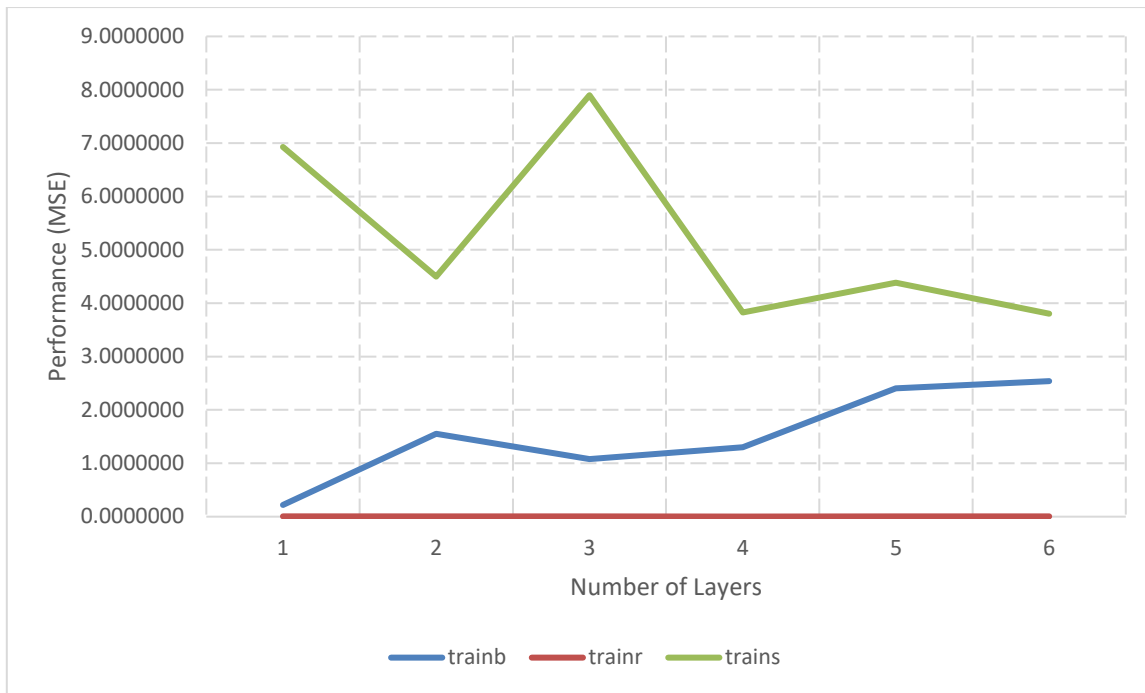


Figure 40 - Error of Supervised Weight/Bias Training Functions in Layer Testing

From Figure 35 it can be seen that as was the case with the neuron testing the error of both of the BTFJDs was similar. As layers were added to the ANN model the error of both functions decreased with an almost exponential rate. The biggest change in error was achieved by increasing the number of layers to 2 from 1 when the mean square error reduced by 88.42% for the trainlm function and 90.02% for the trainbr function as shown in Table 17. From it can be seen that the trainlm and trainbr functions behaved differently as more layers were added. With the trainlm function the rate of change in the improvement in error continually decreased as the number of layers increased. However, with the trainbr function the rate of change in error decreased up to 4 layers than increased again up to 6 layers.

Table 17 – Percentage Change in Error Brought About by Adding Layers to Backpropagation Training Functions that use Jacobian Derivatives

Function	Number of Layers				
	2	3	4	5	6
trainlm	-88.42	-62.57	-28.99	-20.69	-5.19
trainbr	-90.02	-60.55	-23.59	-36.26	-45.41

From Figure 39 it can be seen that the traingdm function again performed much more poorly and erratically than the other BTFGDs. Table 18 shows the average percentage change of the

mean square error brought about by increasing the number of layers in an ANN model trained using the eleven different BTFGDs. The results in *Table 18* show that the behaviour of the BTFGDs did not follow any pattern when the number of layers was increased.

Table 18 - Percentage Change in Error Brought About by Adding Layers to Backpropagation Training Functions that use Gradient Derivatives

Function	Number of Layers				
	2	3	4	5	6
trainbfg	-56.07	-20.90	-9.19	-41.97	2323.30
traincgb	-52.49	10.83	41.54	39.82	261.08
traincgf	-42.12	22.32	21.67	173.69	131.87
traincgp	-30.16	56.64	-22.38	1.92	110.69
traingd	45.53	-11.83	-1.46	4.25	19.74
traingda	-3.38	14.87	14.95	1.44	15.94
traingdm	-48.28	62.17	-17.81	-1.24	10.56
traingdx	-34.83	-29.84	5.34	84.85	-0.89
trainoss	-23.62	19.27	-11.68	16.19	32.18
trainrp	-45.30	-33.60	2.61	-8.48	1993.49
trainscg	8.26	-34.23	18.44	12.36	82.74

Results also showed that the error of the three supervised weight/bias training functions were again unlike to each other. From Figure 40 it can be seen that the trains function performed extremely poorly and erratically as layers were added. It can also be seen that whilst the trainb function performed better than trains the error increased as layers were added, and its performance was inferior to that of the trainr function.

Table 19 - Percentage Change in Error Brought About by Adding Layers to Supervised Weight/Bias Training Functions

Function	Number of Layers				
	2	3	4	5	6
trainb	606.02	-30.64	21.08	84.42	5.67
trainr	-31.91	-15.21	-26.25	11.78	-1.49
trains	-35.06	75.47	-51.58	14.73	-13.31

Table 20 - Error of Different Training Functions in Multiple Layer Networks

Function	Error (MSE)					
	Number of Layers					
	1	2	3	4	5	6
Backpropagation Training Functions that use Jacobian Derivatives						
trainlm	0.000668	0.000077	0.000029	0.000021	0.000016	0.000015
trainbr	0.000681	0.000068	0.000027	0.000021	0.000013	0.000007
<i>Average</i>	<i>0.000675</i>	<i>0.000073</i>	<i>0.000028</i>	<i>0.000021</i>	<i>0.000015</i>	<i>0.000011</i>
Backpropagation Training Functions that use Gradient Derivatives						
trainbfg	0.002757	0.001211	0.000958	0.000870	0.000505	0.012235
traincgb	0.004163	0.001978	0.002192	0.003102	0.004338	0.015663
traincgf	0.005645	0.003267	0.003997	0.004862	0.013308	0.030856
traincgp	0.006291	0.004393	0.006882	0.005342	0.005445	0.011471
traingd	0.035694	0.051945	0.045800	0.045130	0.047050	0.056340
traingda	0.059754	0.057737	0.066322	0.076238	0.077334	0.089665
traingdm	1.077980	0.557498	0.904099	0.743039	0.733859	0.811371
traingdx	0.105349	0.068657	0.048171	0.050742	0.093797	0.092962
trainoss	0.008873	0.006777	0.008083	0.007139	0.008295	0.010965
trainrp	0.003814	0.002086	0.001385	0.001421	0.001301	0.027235
trainscg	0.005008	0.005422	0.003566	0.004223	0.004745	0.008671
<i>Average</i>	<i>0.119575</i>	<i>0.069179</i>	<i>0.099223</i>	<i>0.085646</i>	<i>0.089998</i>	<i>0.106130</i>
Supervised Weight/Bias Training Functions						
trainb	0.219798	1.551808	1.076260	1.303185	2.403291	2.539527
trainr	0.005385	0.003667	0.003109	0.002293	0.002563	0.002525
trains	6.930749	4.500932	7.897890	3.824276	4.387539	3.803602
<i>Average</i>	<i>2.385310</i>	<i>2.018802</i>	<i>2.992420</i>	<i>1.709918</i>	<i>2.264464</i>	<i>2.115218</i>

Table 21 - Coefficient of Correlation of Different Training Functions in Multiple Layer Networks

Function	Coefficient of Correlation (R Value)					
	Number of Layers					
	1	2	3	4	5	6
Backpropagation Training Functions that use Jacobian Derivatives						
trainlm	0.99853	0.99983	0.99994	0.99996	0.99997	0.99997
trainbr	0.99850	0.99985	0.99994	0.99995	0.99997	0.99997
<i>Average</i>	<i>0.99851</i>	<i>0.99984</i>	<i>0.99994</i>	<i>0.99995</i>	<i>0.99997</i>	<i>0.99997</i>
Backpropagation Training Functions that use Gradient Derivatives						
trainbfg	0.99393	0.99734	0.99791	0.99806	0.99893	0.95259
traincgb	0.99070	0.99599	0.99514	0.99318	0.99047	0.94825
traincgf	0.98725	0.99277	0.99100	0.98912	0.97518	0.94984
traincgp	0.98591	0.99044	0.98464	0.98826	0.98818	0.97319
traingd	0.91175	0.87663	0.89186	0.89324	0.88629	0.85512
traingda	0.86656	0.87252	0.85013	0.81990	0.81572	0.75484
traingdm	0.49102	0.55768	0.33849	0.38663	0.36612	0.35350
traingdx	0.82244	0.89460	0.87627	0.85772	0.74955	0.73443
trainoss	0.98041	0.98487	0.98217	0.98471	0.98204	0.97585
trainrp	0.99168	0.99547	0.99697	0.99696	0.99715	0.97407
trainscg	0.98912	0.98777	0.99223	0.99050	0.99105	0.98414
<i>Average</i>	<i>0.91007</i>	<i>0.92237</i>	<i>0.89971</i>	<i>0.89984</i>	<i>0.88552</i>	<i>0.85962</i>
Supervised Weight/Bias Training Functions						
trainb	0.74999	0.38564	0.39385	0.27862	0.43612	0.39190
trainr	0.98845	0.99246	0.99335	0.99533	0.99493	0.99497
trains	0.84946	0.89486	0.86911	0.83968	0.84676	0.77220
<i>Average</i>	<i>0.86263</i>	<i>0.75765</i>	<i>0.75210</i>	<i>0.70454</i>	<i>0.75927</i>	<i>0.71969</i>

Analysis of Results

In analysing the results of the neuron and layers tests conducted on the function fitting network it was clear that there was a large difference in the performance of the different training functions.

In the neuron testing the average error of all 1600 tests was 0.4048. The average error of the 100 tests carried out using the trainbr algorithm was the lowest average at 0.0037. Whilst the average error of the trains function was 5.0577. The average R value of all 1600 tests

was 0.8219. The trainlm function had the best average R value at 0.9915, whilst the worst average R value was 0.4257 (traingdm).

Table 22 – Average Results of the Neuron Testing

Function	Error	R Value
BTFJDs		
trainlm	0.003746	0.9915
trainbr	0.003732	0.9916
<i>Average</i>	<i>0.003739</i>	<i>0.9915</i>
BTFGDs		
trainbfg	0.005443	0.9872
traincgb	0.006827	0.9835
traincgf	0.008241	0.9816
traincgp	0.008336	0.9805
traingd	0.075830	0.8556
traingda	0.050743	0.8808
traingdm	0.768200	0.4257
traingdx	0.025469	0.9392
trainoss	0.011011	0.9746
trainrp	0.006773	0.9845
trainscg	0.007945	0.9815
<i>Average</i>	<i>0.088620</i>	<i>0.9068</i>
SWBTFs		
trainb	0.429224	0.6566
trainr	0.008225	0.9808
trains	5.057701	0.8282
<i>Average</i>	<i>1.831717</i>	<i>0.8219</i>

The results of the layer testing showed a similar large range in performance of the sixteen functions. The average error of the 1920 layer tests was 0.4867 and the average R value was 0.8835. The trainbr algorithm again had the best average error in the layer testing at 0.000136. Whilst the average error of the 120 tests with the trains function was 5.2241. The average R value of the layer tests was 0.7593. the trainlm and trainbr functions had the best average R value of 0.9997, whilst the traingdm had the worst average R value of 0.4156.

Table 23 - Average Results of the Layer Testing

Function	Error	R Value
BTFJDs		
trainlm	0.000138	0.9997
trainbr	0.000136	0.9997
<i>Average</i>	<i>0.000137</i>	<i>0.9997</i>
BTFGDs		
trainbfg	0.003089	0.9898
traincgb	0.005239	0.9856
traincgf	0.010322	0.9809
traincgp	0.006637	0.9851
traingd	0.046993	0.8858
traingda	0.071175	0.8299
traingdm	0.804641	0.4156
traingdx	0.076613	0.8225
trainoss	0.008355	0.9817
trainrp	0.006207	0.9920
trainscg	0.005272	0.9891
<i>Average</i>	<i>0.094959</i>	<i>0.8962</i>
SWBTFs		
trainb	1.515645	0.4394
trainr	0.003257	0.9932
trains	5.224164	0.8453
<i>Average</i>	<i>2.247689</i>	<i>0.7593</i>

Due to the large range in performance of the different training functions in both the neuron and layer tests it was decided to discontinue testing of some functions. The time taken to train for the majority of the networks generated ranged from a few seconds to a few minutes. Even in the case of the most complicated architectures, 6 hidden layers with 20 neurons in each, the networks completed training in a little over one-hour. As it is intended that any model generated in the work would be used for long-term forecasting of load profiles it was felt that this was an acceptable time. Therefore, the decision was made not to use time as a metric for performance analysis. Instead, the error (MSE) values and the coefficient of correlation (R) values were used. *Table 24* shows the decision matrix that was used to rank the performance of each training function.

Table 24 – Training Function Matrix

Algorithm	Error			R Value			Overall	
	Best Run	Worst Run	Avg.	Best Run	Worst Run	Avg	Score	Rank
Trainlm	1	3	2	2	1	2	11	1
Trainbr	2	7	1	1	2	1	14	2
Trainbfg	3	2	3	3	3	3	17	3
Trainrp	6	1	4	4	11	4	30	4
Traincgb	8	4	6	6	4	5	33	5
Trainscg	7	5	5	5	8	7	37	6
Traincgf	13	12	8	8	6	6	53	7
Traincgp	12	13	7	7	5	9	53	8
Trainoss	11	11	10	10	7	10	59	9
Traingdx	10	9	11	11	10	11	62	10
Traingda	5	8	13	13	12	12	63	11
Traingd	4	10	12	12	13	13	64	12
Trainr	15	15	9	9	9	8	65	13
Trainb	9	6	15	15	15	15	75	14
Trains	14	14	14	14	14	14	84	15
Traingdm	9	16	16	16	16	16	89	16

When reviewing the results based on the training function ranking it was found that five of the functions outperformed the other eleven considerably in all tested scenarios in terms of MSE and R values. For example, in the neuron tests the average MSE of the top 5 algorithms was 0.00530 compared to 0.58645. In these tests the top 5 had an average R value of 0.988 compared to only 0.862 of the other 11 algorithms

Table 25 – Comparison of Results from Fitnet Testing

Metric	Test	Training Function		
		All	Top 5	Bottom 11
MSE	Neurons	0.404840	0.005304	0.586448
	Layers	0.486743	0.002962	0.706643
	Overall	0.445792	0.004133	0.646545
R Value	Neurons	0.901	0.988	0.862
	Layers	0.883	0.993	0.834
	Overall	0.892	0.991	0.848

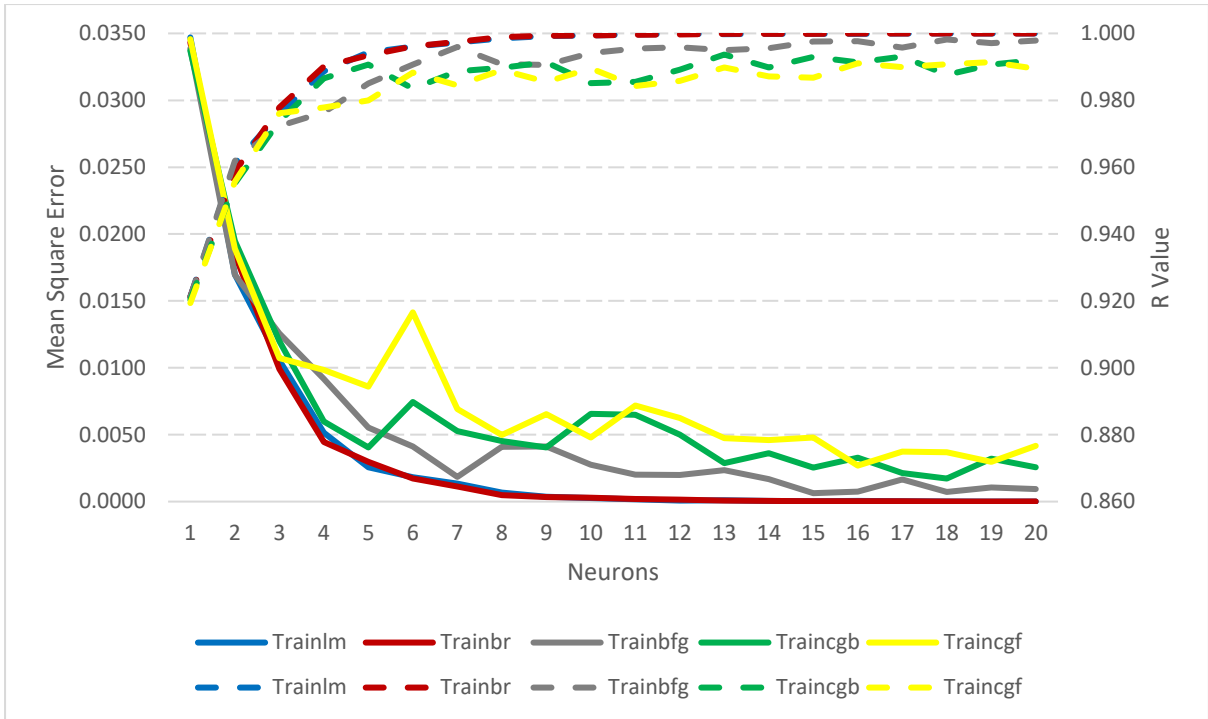


Figure 41 – Performance of Top 5 Training Functions During Neuron Testing of the Fitnet Network

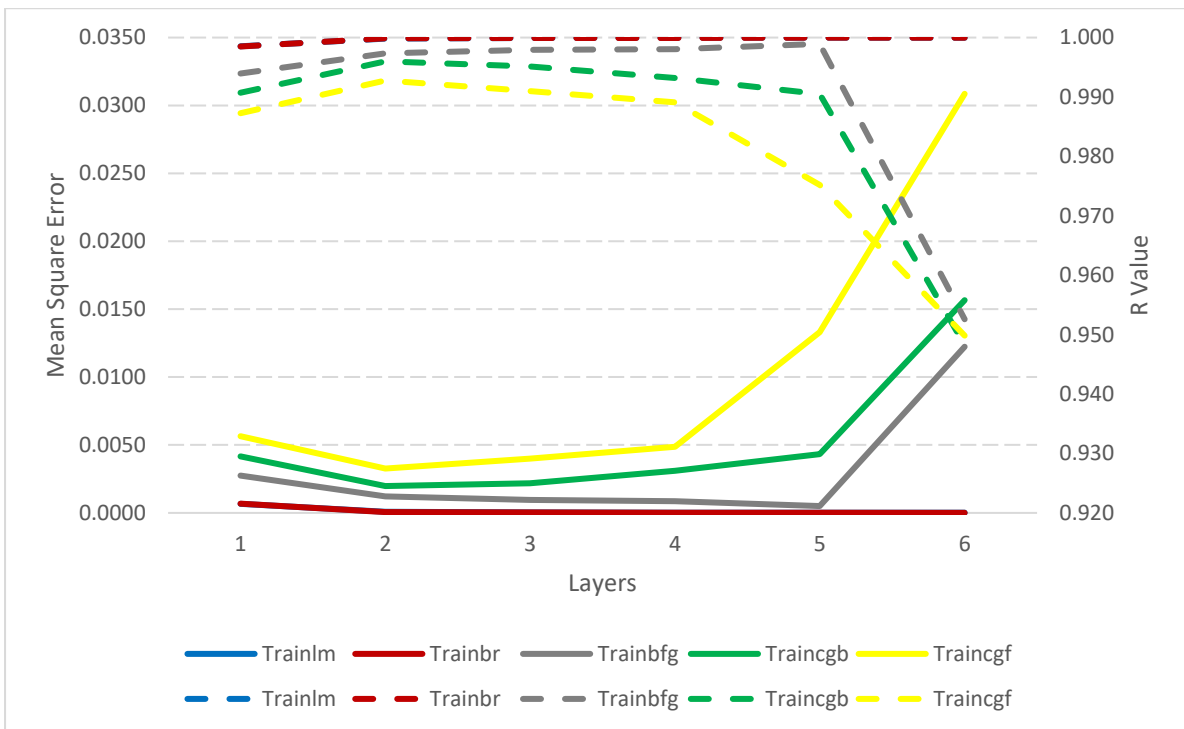


Figure 42 - Performance of Top 5 Training Functions During Layer Testing of the Fitnet Network

The best performing algorithms were:

- Levenberg-Marquardt backpropagation (trainlm),
- Bayesian Regulation backpropagation (trainbr),
- Broyden–Fletcher–Goldfarb–Shanno (BFGS) quasi-Newton backpropagation (trainbfg),
- Conjugate gradient backpropagation with Powell-Beale restarts (traincgb),
- Resilient (RPROP) backpropagation (trainrp).

Testing of the other eleven training functions was discontinued at this time.

5.1.3 Network Architecture Testing

Initial Testing

Research showed that there are twenty network architectures available in the Matlab NN-toolbox in addition to the recommended Feed Forward Neural Network (see Table 26).

Table 26 - Matlab Network Topologies

Network	Matlab Syntax
Historical Networks	
Elman Neural Network	elmannet
Hopfield Recurrent Network	newhop
Linear Layer	newlind
Perceptron	perceptron
Static Networks	
Cascade-Forward Neural Network	cascadeforwardnet
Exact Radial Basis Network	newrbe
Feed-Forward Neural Network	feedforwardnet
Function Fitting Neural Network	fitnet
Generalized Regression Neural Network	newgrnn
Learning Vector Quantization Neural Network	lvqnet
Pattern Recognition Neural Network	patternnet
Probabilistic Neural Network	newpnn
Radial Basis Network	newrb
Static Self-Organizing Networks	
Competitive Neural Layer	competlayer
Self-Organizing Map	selforgmap
Dynamic Networks	
Distributed Delay Neural Network	distdelaynet
Layered Recurrent Neural Network	layrecnet
Linear Neural Layer	linearlayer
Nonlinear Auto-Associative Time-Series Network	narxnet
Nonlinear Auto-Associative Time-Series Network with External Input	narxnet

An initial test was carried out to determine which of these twenty training functions could be used in this study. This involved using the training dataset described in Section 4.6 to create an ANN with the default Matlab design of ten hidden neurons in one hidden layer using supervised learning.

These tests identified three static and two dynamic network architectures that could be used, namely:

- Static networks
 - Cascade-forward neural network (`cascadeforwardnet`),
 - Feed-forward neural network (`feedforwardnet`),
 - Pattern recognition neural network (`paternnet`),
- Dynamic Networks
 - Nonlinear auto-associative time-series network (`narnet`),
 - Nonlinear auto-associative time-series network with external input (`narxnet`).

Next, 10 runs of each of these networks were carried out with all other settings and parameters left as standard. The results from these tests were compared to the results obtained from 10 runs of a `Fitnet` network with standard settings and parameters.

Analysis of Initial Testing Results

The results from the 60 runs of initial testing on network analysis were then studied. Again, it was found that there was little variation in the time taken to train the networks and so the same performance metrics used previously were again employed. From the results it was clear that the `paternet` performance was far inferior to the other networks tested as shown in *Figure 43*.

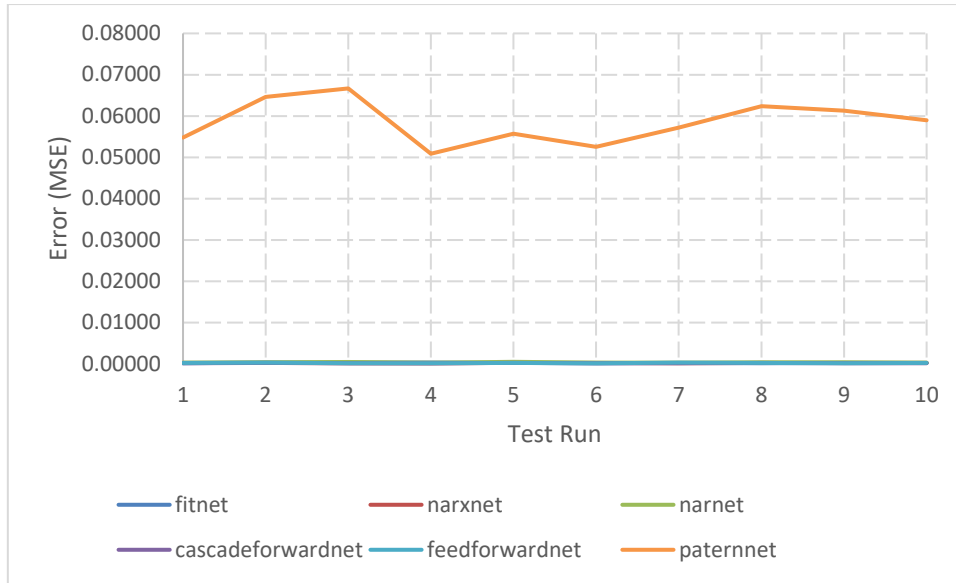


Figure 43 - Network Architecture Initial Testing

Further analysis showed that the average error of both the narxnet and cascadeforwardnet was lower than that of the default fitnet. It also showed that the average coefficient of correlation (R Value) of all three networks was alike. Therefore, the decision was made to use these networks in the next stage of testing.

Table 27 – Average Error of Top 3 In Network Architecture Initial Testing

Network Architecture	Error (MSE)		
	Worst Run	Best Run	Average
fitnet	0.000316	0.000141	0.000217
narxnet	0.000230	0.000103	0.000184
cascadeforwardnet	0.000226	0.000125	0.000167

Table 28 - Average R-Value of Top 3 In Network Architecture Initial Testing

Network Architecture	R Value		
	Worst Run	Best Run	Average
fitnet	0.9993	0.9997	0.9995
narxnet	0.9993	0.9997	0.9995
cascadeforwardnet	0.9995	0.9997	0.9996

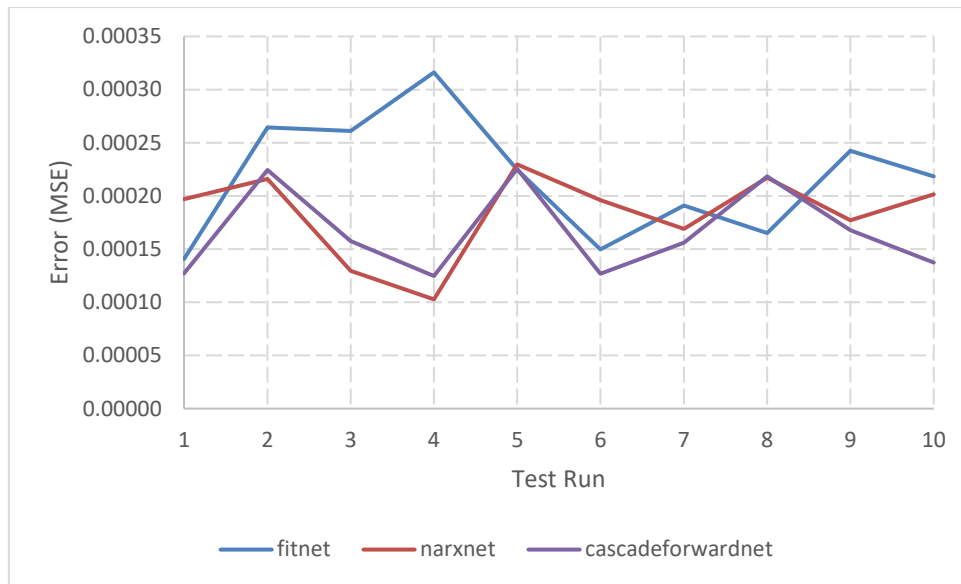


Figure 44 - Top 3 Network Architectures from Initial Testing

Neuron Testing

This stage of testing involves carrying out the same tests described for the neuron tests for the Fitnet network on the NARXnet and CFNN networks. The difference being that only the five best performing algorithms were used. The testing involved generating 200 networks each for the NARXnet and CFNN networks and an additional 100 Fitnet networks for each of the five training functions still under study. In all 2000 further networks were generated during this stage of testing and as with all the other networks generated in this work they were saved for further study.

COVID-19 Lockdown Measures

During this stage of testing the COVID-19 pandemic began and access to the university campus and computing facilities was suspended. In order to continue progress on the work the majority of the testing was completed on a personal laptop. The laptop being a HP Notebook with an AMD A6-7310 APU processor and 8GB (6.95GB usable) physical memory running Windows 10 Home 21H1 operating system and Matlab R2018b Update 7.

This was deemed acceptable as the same version of Matlab was used in all tests so would not affect the main metrics used in the study, error and coefficient of correlation. As stated previously due to the nature of forecasting scenario training time was not considered of great importance. However, it was still noted and when discussed here will refer to the average time taken to train a network when using the personal laptop detailed above.

Results

The average training time of the 1,000 tests carried out on each network architecture was very similar. The Fitnet was quickest at an average of 5.94 seconds over the range of 1 to 20 neurons using all five training functions. The average training time of CFNN was 6.56 seconds and NARXnet was slightly slower at 8.05 seconds.

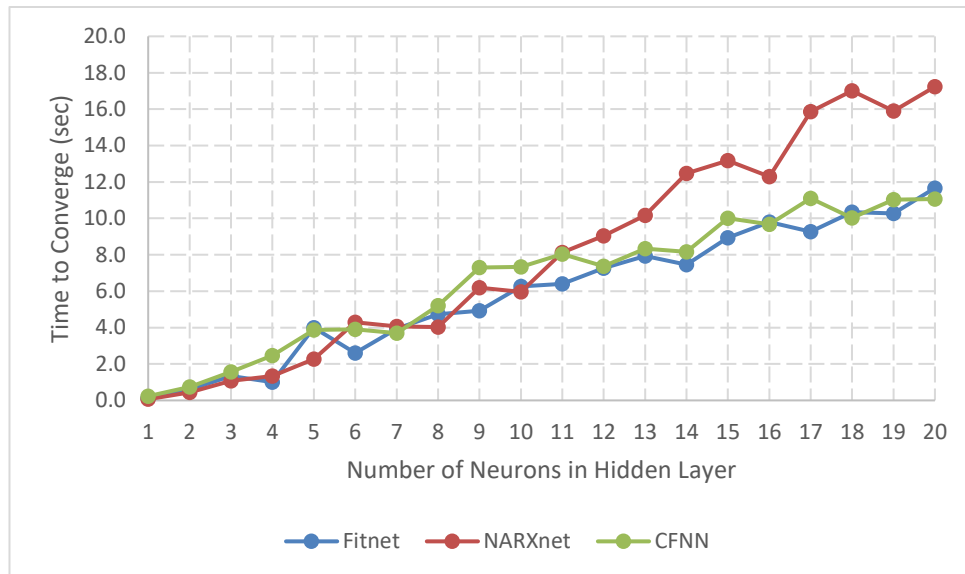


Figure 45 – Average Training Time of Network Architectures During Neuron Testing

The average performance of the three network architectures studied was alike in terms of error and R-values and showed similar patterns. With one and two neurons in the hidden layer the performance of NARXnet was noticeably superior to the other two architectures. As more neurons were added the performance of the three networks became more alike. They also all showed a similar pattern whereby adding more and more neurons resulted in a diminishing increase in performance. As would be expected the average R-values of the three networks followed the same pattern as the error results.

Overall, the NARXnet architectures performed the best with an average error of 0.001711 compared to the Fitnet average of 0.004283 and CFNN average of 0.003298. However, further analysis showed that as more neurons were added the performance of the Fitnet and CFNN architectures improved more than that of the NARXnet and outperformed it in the range of 10 to 20 neurons as can be seen in *Table 29*.

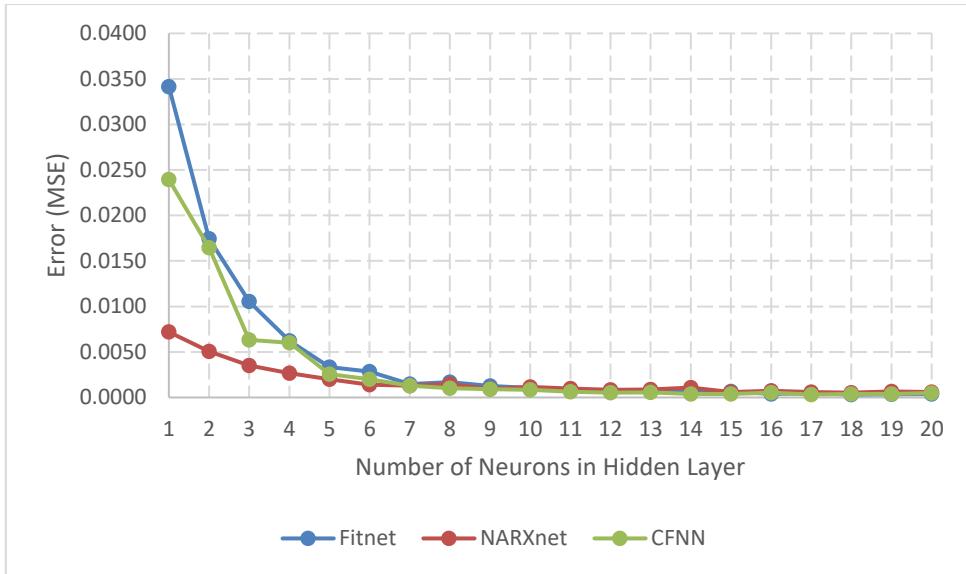


Figure 46 - Average Error of Network Architectures During Neuron Testing

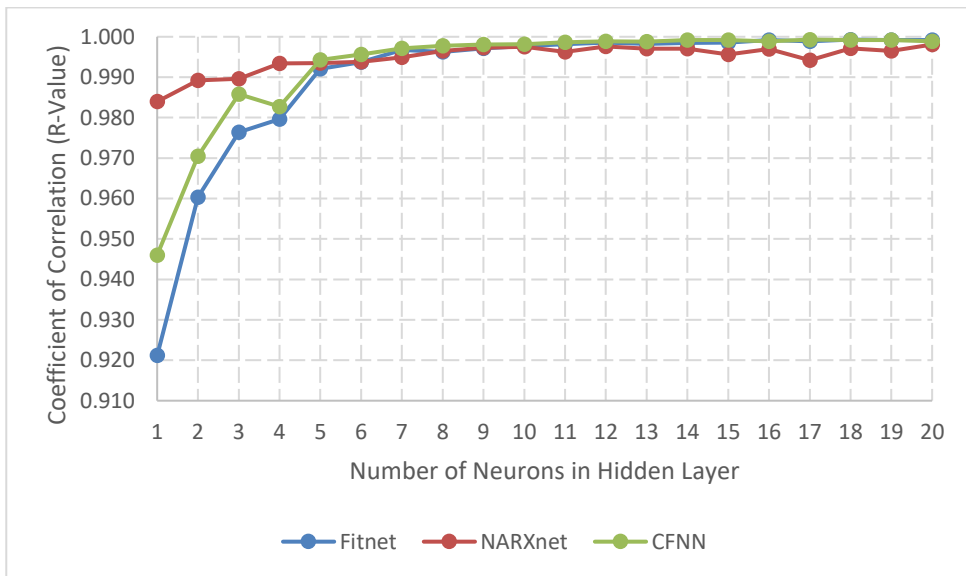


Figure 47 - Average R-Value of Network Architectures During Neuron Testing

Table 29 – Average Error of Network Architectures During Neuron Testing

Neurons	Network Architecture		
	Fitnet	NARXnet	CFNN
1	0.034164	0.007199	0.023949
2	0.017454	0.005048	0.016468
3	0.010537	0.003517	0.006344
4	0.006224	0.002656	0.006025
5	0.003345	0.001990	0.002580

6	0.002842	0.001407	0.001993
7	0.001480	0.001307	0.001294
8	0.001670	0.001487	0.001012
9	0.001273	0.000938	0.000900
10	0.001061	0.001153	0.000843
11	0.000829	0.000991	0.000629
12	0.000692	0.000836	0.000512
13	0.000822	0.000863	0.000546
14	0.000687	0.001082	0.000382
15	0.000658	0.000588	0.000373
16	0.000370	0.000752	0.000514
17	0.000504	0.000597	0.000325
18	0.000315	0.000528	0.000397
19	0.000357	0.000674	0.000368
20	0.000379	0.000611	0.000499
Overall	0.004283	0.001711	0.003298

Layer Testing

This stage of testing involved carrying out the same tests described for the hidden layer tests for the Fitnet network on the NARXnet and CFNN networks. Again, only the five best performing training algorithms were used. 1,200 tests were carried out on each network architecture and 3,600 in total.

Results

As stated a number of times previously training time was not considered of great importance in this study. However, the training time of the CFNN network architectures is worth noting. Due to the connections to preceding layers in the CFNN architecture training time increased dramatically as the number of hidden layers was increased. From 1 to 3 hidden layers training time of the CFNN architectures was similar to that of the Fitnet and NARXnet architectures. For 4 and 5 hidden layers the training time far exceeded that of the other two architectures. Tests on five layered CFNN architectures with high numbers of neurons (15 to 20 in each layer) could not be carried out on the personal laptop detailed earlier as it would shut down after around 14 to 16 hours of training due to overheating. So special permission was given to access the university campus in order to complete testing. Even when using PCs on campus with similar specifications to that of the desktop PC used in the Fitnet testing stage testing still took between 12 to 16 hours for the larger network configurations.

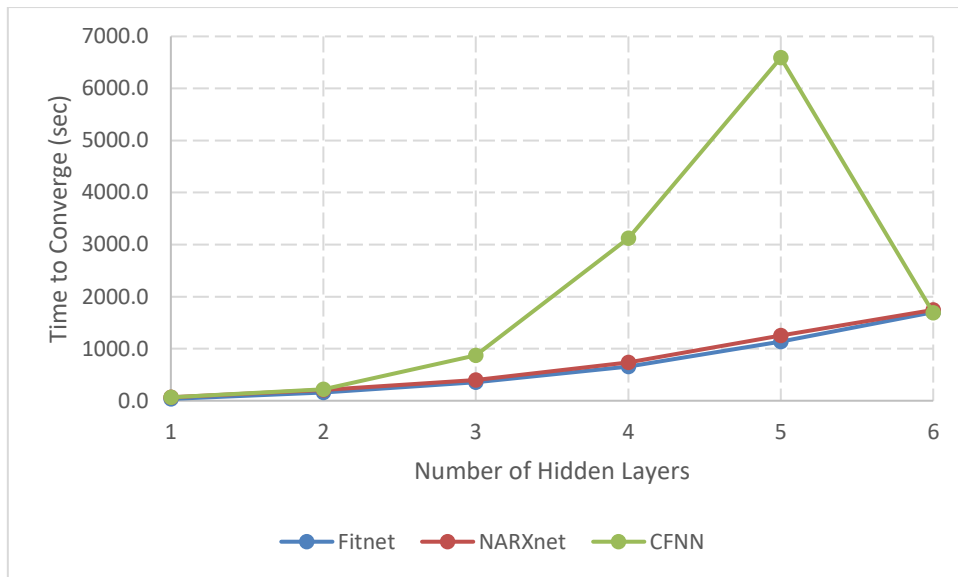


Figure 48 - Average Training Time of Network Architectures During Layer Testing

The average performance of the three network architectures studied was very similar. The average error across the range of 1 to 6 neurons of the Fitnet architectures was 0.00230282, the average of the NARxnet architectures was 0.0022204 and for CFNN it was 0.00240701. However, when looking at *Figure 49* and *Figure 50* it can be seen that the behaviour of each architecture differed over the range of hidden layers investigated.

The Fitnet architecture displayed a consistent behaviour. Increasing the hidden layers from one to three resulted in an increase in performance. Whilst increasing the hidden layers from 4 to 6 resulted in a decrease in performance as the networks became too large and overtrained and lost generalisation capability.

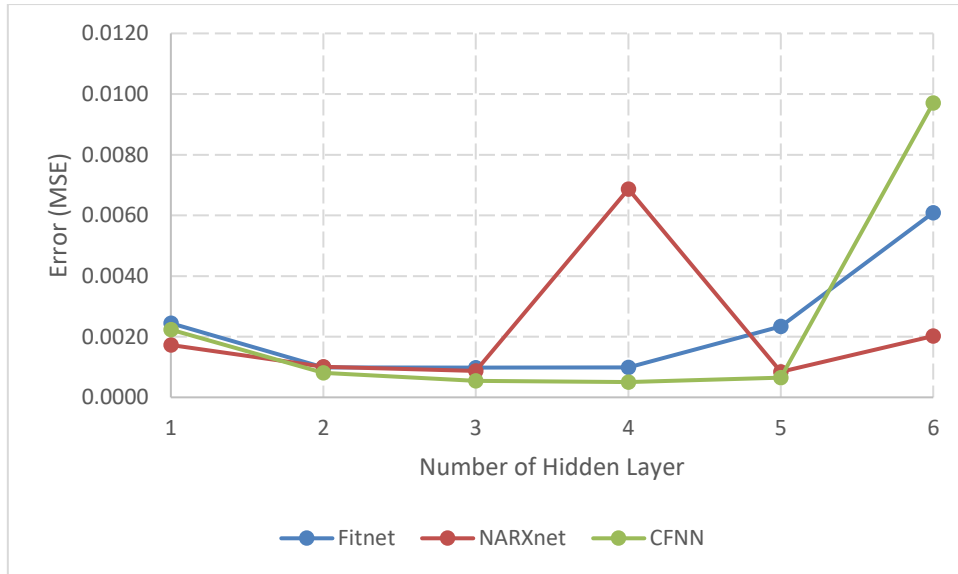


Figure 49 - Average Error of Network Architectures During Layer Testing

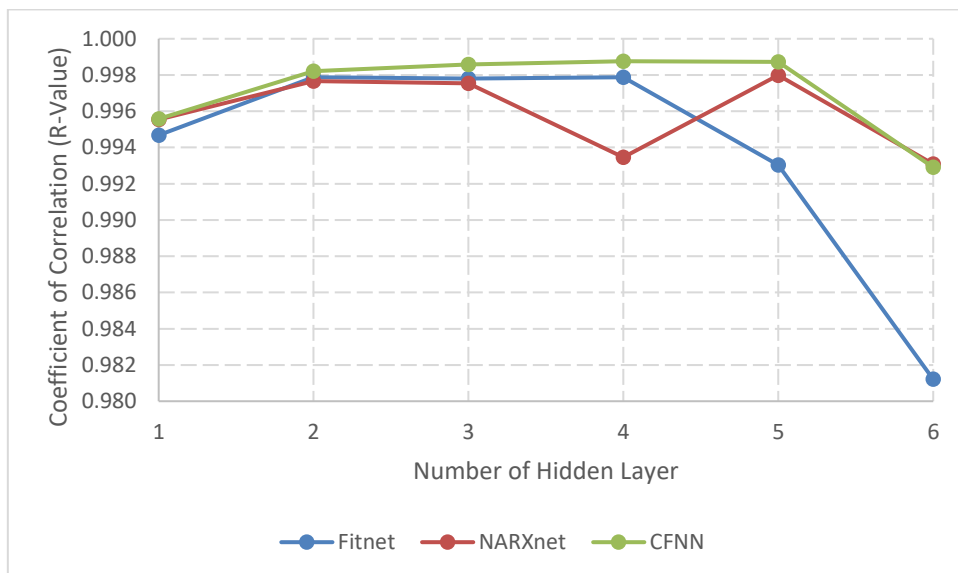


Figure 50 - Average R-Value of Network Architectures During Layer Testing

Table 30 - Average Error of Network Architectures During Layer Testing

Layers	Architecture		
	Fitnet	NARXnet	CFNN
1	0.0024394	0.00172179	0.00223488
2	0.0009898	0.00100409	0.00080985
3	0.00098101	0.00087005	0.00054297
4	0.00098475	0.0068672	0.00050414
5	0.00233327	0.00084155	0.00064428

6	0.00608868	0.00201774	0.00970597
Overall	0.00230282	0.0022204	0.00240701

Validation

The results from the testing described in this chapter was used to improve the accuracy of the synthetic load profiles that were generated by the ANN model described in Chapter 4 for a study of the efficacy of smart grid technologies to reduce PV curtailment as described in the next chapter. As stated previously all ANN models were trained using 3 seasons of data (Spring, Summer and Winter) with the Autumn data being used to validate results.

When validating the data from all of the hidden layer results an issue was found with the accuracy of results. When looking at the results it would appear that increasing the number of hidden layers from 1 to 3 increased the performance of each of the network architectures studied. However, during validation using the Autumn data it was found that increasing the number of hidden layers dramatically reduced predication capability when presented with data the ANN models had no a priori knowledge.

5.1.4 Transfer Function Testing

The default setup of all three network architectures under study use tansig functions in the hidden layer(s) and purlin functions in the output layer. The last round of testing studied the effects of changing the default transfer functions in both the hidden layer(s) and the output layer with the 14 other functions available in Matlab (see *Table 31*). The tests were carried on networks which contained 10 neurons in one hidden layer.

Table 31 - Matlab Neural Network Toolbox Transfer Functions

Transfer Function	Matlab Syntax
Positive Hard Limit Transfer Function	hardlim
Symmetric Hard Limit Transfer Function	hardlims
Linear Transfer Function	purelin
Positive Linear Transfer Function	poslin
Symmetric Saturating Linear Transfer Function	satlins
Positive Saturating Linear Transfer Function	satlin
Inverse Transfer Function	netinv

Logarithmic Sigmoid Transfer Function	logsig
Symmetric Sigmoid Transfer Function	tansig
Elliot Sigmoid Transfer Function	elliotsig
Radial Basis Transfer Function	radbas
Radial Basis Normalized Transfer Function	radbasn
Triangular Basis Transfer Function	tribas
Competitive Transfer Function	compet
Soft Max Transfer Function	softmax

Firstly 10 runs were carried out on each of the three network architectures with the default transfer function configuration. The results from these tests were used to compare the effects changing transfer functions made to prediction capability.

Next, 10 runs of each of the transfer function in the hidden layer was carried out on each of the three network architectures with all other settings and parameters left as standard. 350 tests were carried out to study the different transfer functions in the hidden layer. This process was then repeated on the output layer of the different networks with another 350 tests carried out. All tests were carried out using the personal laptop described in the network architecture section.

Transfer Functions in the Hidden Layer(s)

In the tests conducted on the Fitnet network none of the 14 transfer functions examined improved the error compared to the average results of the default function (tansig). The logsig function had the smallest increase in error compared to tansig at 12%, followed by radbas (33.7%) and softmax (41.9%).

In the NARXnet testing four transfer functions improved the error compared to the default function. The logsig function reduced the error by 39.8% followed by elliotsig (33.4%), radbasn (21.8%) and radbas 9.9%.

In the CFNN testing four functions again improved the error compared to the default function. However, in the CFNN tests softmax saw the largest reduction in error (66.9%), followed by logsig (59.6), radbas (59.4%), and radbasn (51.0%).

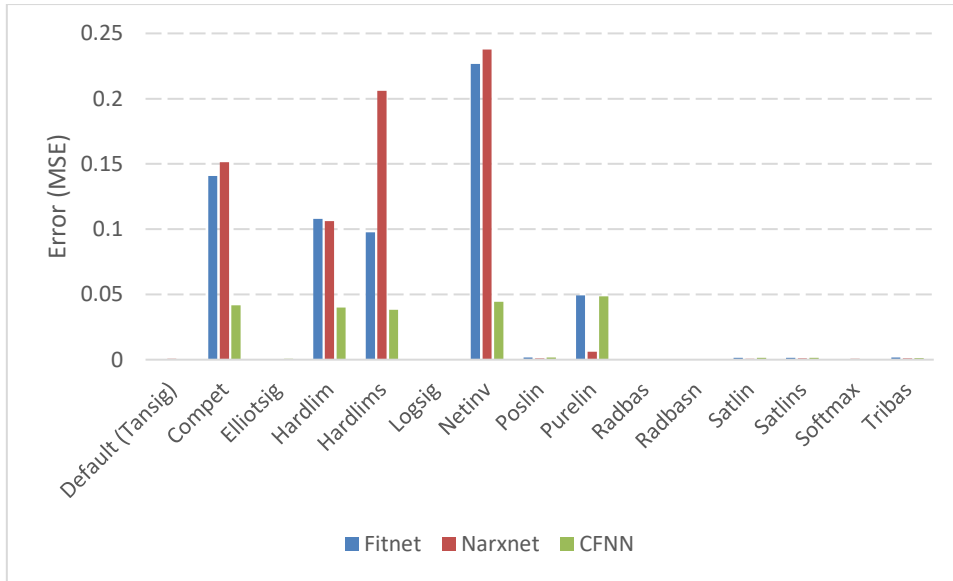


Figure 51- Average Error During Hidden Layer Transfer Function Testing

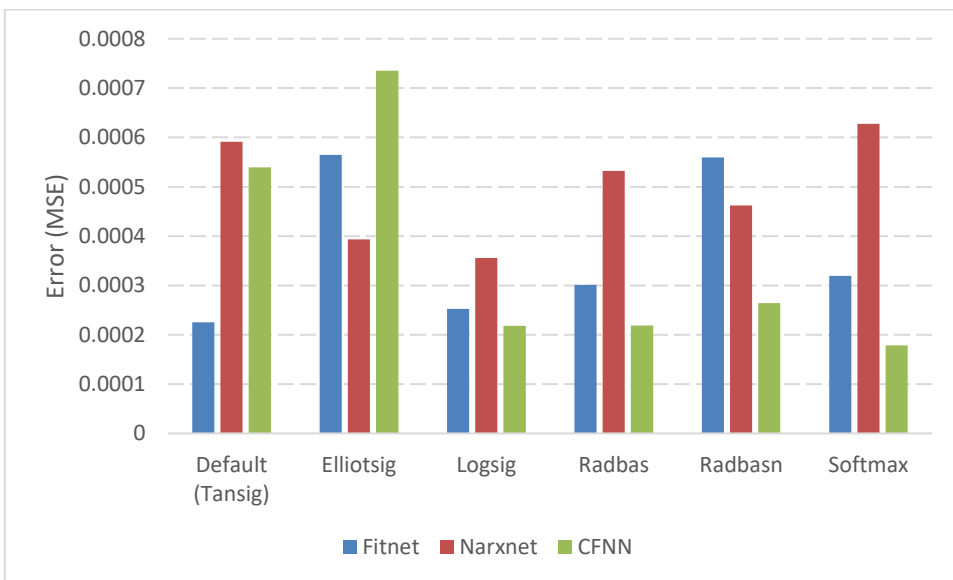


Figure 52 - Average of Top 5 During Hidden Layer Transfer Function Testing

Table 32 - Average Error During Hidden Layer Transfer Function Testing

Transfer Function	Architecture		
	Fitnet	Narxnet	CFNN
Default (Tansig)	0.0002252	0.0005910	0.0005393
Compet	0.1407252	0.1513460	0.0417539
Elliotsig	0.0005646	0.0003936	0.0007355
Hardlim	0.1078749	0.1062950	0.0400238
Hardlims	0.0975034	0.2060674	0.0382323
Logsig	0.0002522	0.0003556	0.0002180

Netinv	0.2267180	0.2376870	0.0444223
Poslin	0.0017922	0.0010157	0.0017342
Purelin	0.0492708	0.0060219	0.0486469
Radbas	0.0003011	0.0005323	0.0002188
Radbasn	0.0005591	0.0004618	0.0002642
Satlin	0.0015470	0.0007624	0.0013561
Satlins	0.0013784	0.0010444	0.0013469
Softmax	0.0003195	0.0006273	0.0001783
Tribas	0.0016934	0.0009248	0.0012524

Table 33 – Top 5 Functions in Hidden Layer Transfer Function Testing

Rank	Architecture		
	Fitnet	Narxnet	CFNN
1	<i>Default (Tansig)</i>	Logsig	Softmax
2	Logsig	ElliotSig	Logsig
3	Radbas	Radbasn	Radbas
4	Softmax	Radbas	Radbasn
5	ElliotSig	<i>Default (Tansig)</i>	<i>Default (Tansig)</i>

Transfer Functions in the Output Layer

In the tests conducted on the Fitnet network again none of the 14 transfer functions examined improved the error compared to the average results of the default function (purelin). The satlin function had the smallest increase in error compared to tansig at 8.1%, followed by elitotsig (67.5%) and softmax (139.0%). All of the other functions tested saw massive increases in error.

In the NARXnet testing only one function improved the error compared to the default function. This was the satlin function which reduced the error by 29.7%. There was an increase in the error of 49.0% for the softmax function and 91.6% for the eliotsig function. All the other functions examined saw massive increases in error.

In the CFNN testing only one function again improved the error compared to the default function. Again, it was the satlin function which reduced the error by 29.7%. There was an increase in the error of 5.9% for the softmax function and 206.7% for the eliotsig function. As with the other two network architectures all the other functions examined saw massive increases in error.

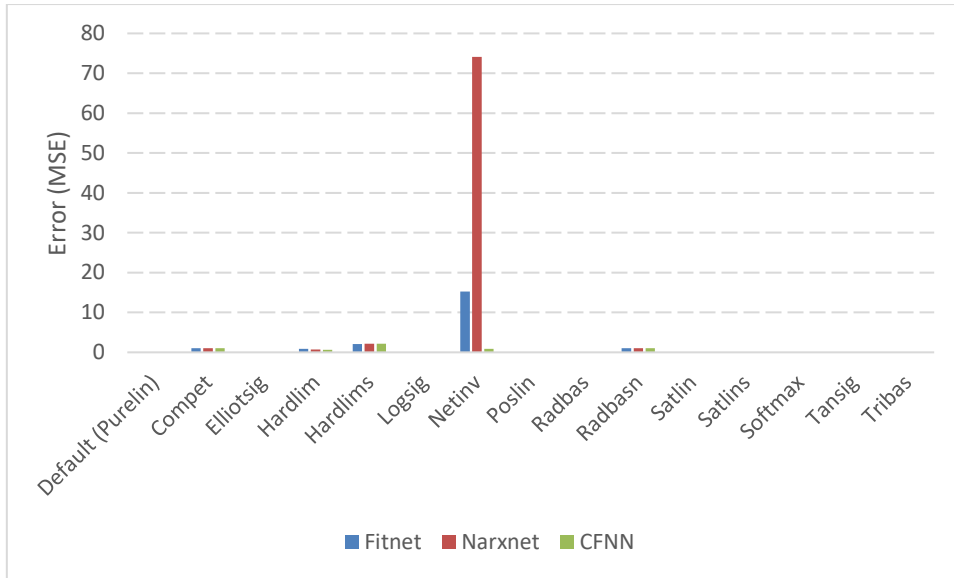


Figure 53 - Average Error During Output Layer Transfer Function Testing

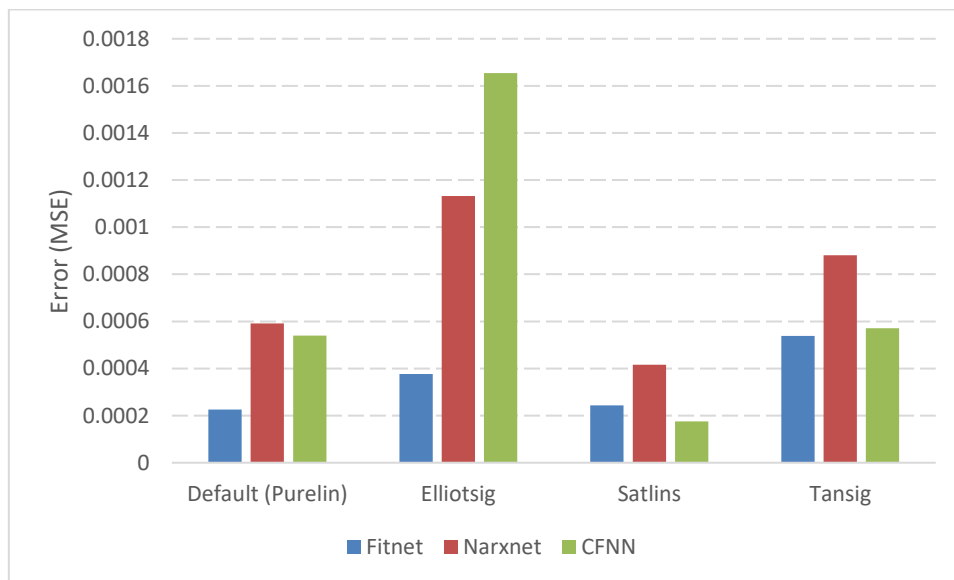


Figure 54 - Average of Top 3 During Output Layer Transfer Function Testing

Table 34 - Average Error During Output Layer Transfer Function Testing

Transfer Function	Architecture		
	Fitnet	Narxnet	CFNN
Default (Purelin)	0.0002252	0.0005910	0.0005393
Compet	1.0577900	1.0690400	1.0518700
Elliotsig	0.0003772	0.0011320	0.0016542
Hardlim	0.8977840	0.7416130	0.6027740
Hardlims	2.0808480	2.1365690	2.1702400
Logsig	0.0573367	0.0579057	0.0565279

Netinv	15.2879240	74.1040035	0.8389740
Poslin	0.0908633	0.0540987	0.0544663
Radbas	0.0756693	0.0671477	0.0735554
Radbasn	1.0428410	1.0485220	1.0727090
Satlin	0.0541939	0.0540243	0.0543952
Satlins	0.0002434	0.0004155	0.0001756
Softmax	0.0567700	0.0582796	0.0555794
Tansig	0.0005381	0.0008804	0.0005712
Tribas	0.0637493	0.0612549	0.0633131

Table 35 - Top 5 Functions in Output Layer Transfer Function Testing

Rank	Architecture		
	Fitnet	Narxnet	CFNN
1	<i>Default (Purelin)</i>	Satlin	Satlin
2	Satlin	<i>Default (Purelin)</i>	<i>Default (Purelin)</i>
3	ElliotSig	Softmax	Softmax
4	Softmax	ElliotSig	ElliotSig
5	Radbasn	Radbasn	Radbasn

5.1.5 Discussion of Results

The results from testing proved that training function, number of neurons, number of hidden layers, network architecture and transfer functions used in the hidden layer(s) and output layer can all improve the predictive capabilities of ANN models. However, validating the results using data that the models had no a priori knowledge of clearly demonstrated that the data obtained from the Matlab interface can be misleading. This was most clearly shown in the layer testing. In layer testing of the two backpropagation training functions that use Jacobian derivatives (trainlm and trainbr) the results obtained from Matlab indicated that there was a large increase in performance when the number of hidden layers was increased from one to two. The results also indicated that performance continued to increase as more hidden layers were added (see *Figure 38*). However, validation showed that increasing the number of hidden layers massively reduced the prediction capabilities of models as the larger the models became the less they were able to generalise, a common problem discussed in literature.

The results also showed the difficulty in predicting how the different free parameters in ANN models will behave. For example, when increasing the number of neurons in a network it

was seen that the training function used changed the behaviour. When using functions such as `trainlm` and `trainbr` performance increased with an almost exponential rate. However, when using function such as `traindgm` and `trains` there was no discernible pattern. With the `traingdm` function increasing the neurons from 8 to 9 resulted in a large increase in error, increasing neurons from 9 to 10 saw a small decrease in error, adding another neuron results in another increase in error yet adding another neuron to the network saw a large decrease in error. This unpredictable behaviour occurred over the full range of neurons tested (see *Figure 36*).

The results also indicated that it is not possible to predict how training functions will behave based on the type. The two backpropagation training functions that use Jacobian derivatives did display similar characteristics in testing. However, the eleven backpropagation training functions that use gradient derivatives displayed large characteristic differences to each other. As did the three supervised weight/bias training functions.

The network architecture testing also showed that behaviour of ANN models cannot be made based on network topology. Testing showed that the three best performing architectures were two of the nine static networks (`Fitnet` and `CFNN`) and one of the six dynamic networks (`NARXnet`).

The results from the transfer function testing clearly showed that the combination of parameters can massively affect overall performance. When looking at the results from the testing conducted on the hidden layer transfer functions it was seen that the network architecture used massively affected the results (see *Table 33*). When conducting tests using the `Fitnet` architecture none of the 14 transfer functions studied improved the error compared to the default setting of using the `tansig` function. However, when using both the `NARXnet` and `CFNN` architectures four functions were found to improve the performance compared to the default setting. Again, though there was a difference between these two architectures. With the `NARXnet` architecture the `logig` function gave the biggest improvement in performance but in the `CFNN` architecture it was `softmax` which wasn't even one of the top five functions tested on the `NARXnet` architecture. Testing on the transfer function in the output layer also showed how the combination of transfer function and network architecture can significantly affect performance.

As stated several times previously, training time of the ANN models generated in this work was not considered important. However, the work has shown that the process of improving the predictive capabilities of ANN models is a time consuming and complex endeavour when using the current facilities in Matlab. In all almost 10,000 networks were generated and analysed in this work, and to fully study the effects of the different combinations of parameters have on performance many more would need to be carried out. Even with tests that only took a few seconds to converge to a solution time was needed to record results and save files for future use. Then time was needed to validate results obtained from Matlab as especially in the case of layer testing the results were often misleading and inaccurate. Therefore, it is the conclusion from this testing that a new systematic approach is needed for designing ANN models in Matlab.

5.2 Systematic ANN Design Approach developed for load forecasting using MATLAB

Stage one of the proposed approach is data acquisition. It involves data collection, data pruning and pre-processing to remove abnormal data entries (see *Figure 55*).

The second stage of the process is network design and implementation. This starts with extensive and systematic testing of network parameters such as network type, number of neurons, training function and transfer function. In lessons learnt from the testing on ANN models described in this chapter the evaluation process in this stage would involve using data the models had no a priori knowledge of. The data from this stage is then used to create a final design network.

Lessons learnt from testing have also shown that this stage of the process needs to be automated. This involves the creation of a new graphics user interface (GUI) in Matlab. The Proposed GUI would test network type, number of neurons, training function and transfer function using multiple runs to overcome the issue of randomisation. Where the averaged indicate that changes to a network parameter setting resulted in an improvement in performance the results would be validated as described above. The results from this stage would be used to determine the optimal model design.

The final stage of the process is evaluating the performance of the optimal ANN model in predicting future load profiles. The first step of this stage is supervised learning. Next, the

model is tested again as part of supervised learning using data, but which the model has no a priori knowledge of. Finally, the model is validated for general load forecasting outside the training case using other datasets.

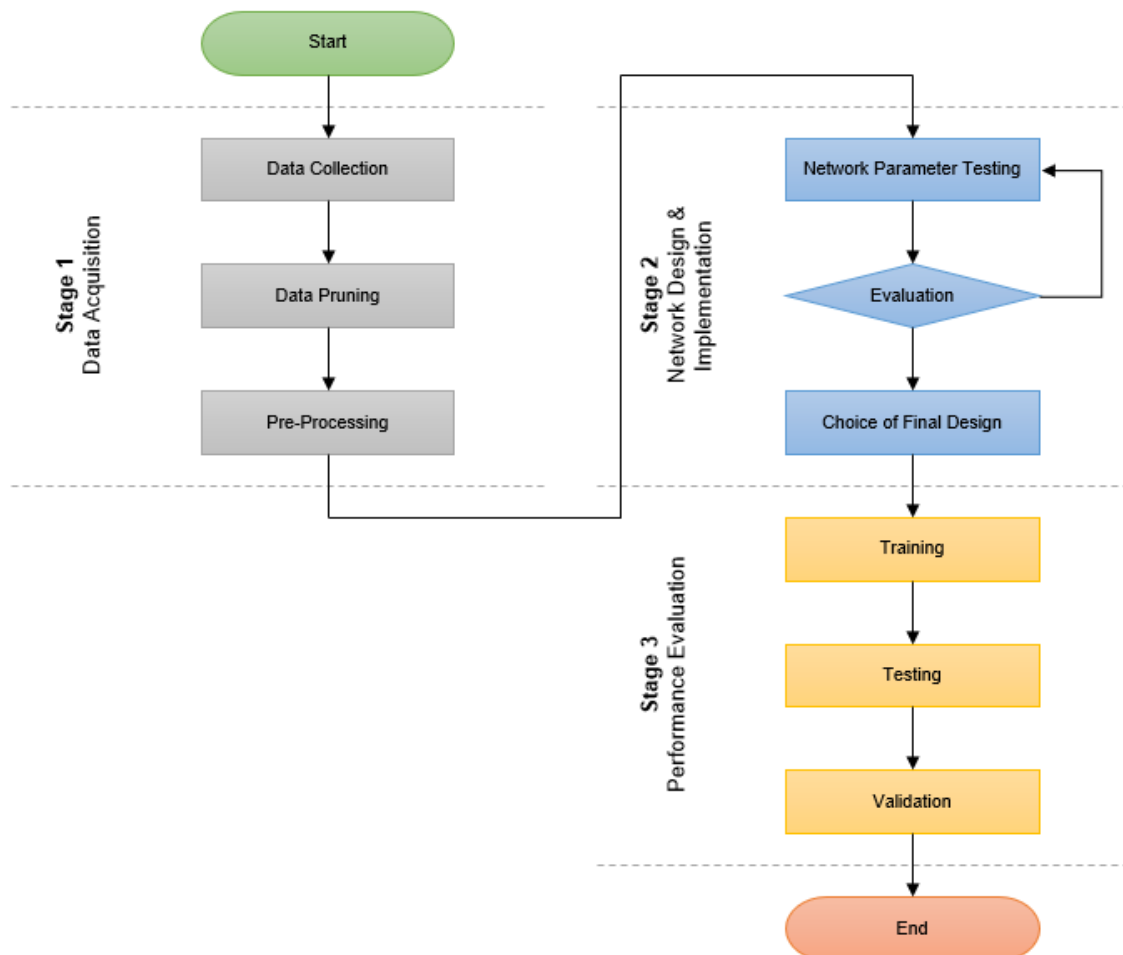


Figure 55 – Flowchart: Proposed Systematic Design Approach

5.2.1 Use of the Systematic Design Approach

This systematic design approach was used to improve the predication capability of the ANN model that had been created in the work described in Chapter 4. As stated previously during validation with data that the ANN model had no apriori knowledge of, the model synthetically generated composite load profiles with a combined Mean Absolute Percentage Error (MAPE) of 0.01365 and a root mean square error (RMSE) of 7.81 over a full range of PV and EV penetration scenarios from 0 to 100% for a low voltage network in Newcastle-Upon-Tyne, England.

Using the systematic approach, the optimal ANN model was found in terms of neurons, hidden layers and training function (at the time work on network architectures and transfer functions was still ongoing). The optimal network was found to have 13 neurons in one hidden layer which was trained using the Bayesian regularization backpropagation algorithm. This model was used to synthetically generate load profiles for the work discussed in the next chapter. Validation of this model using the same data used with the original model from Chapter 4 saw the MAPE lower to 0.00608 and the RMSE lower to 3.48.

This work highlighted the need to validate results in stage 2 using data that models have no a priori knowledge of as the results obtained through Matlab were misleading in terms of performance of networks with increasing numbers of hidden layers. It also showed the need to automate stage 2 of the process due to time and effort it took to complete.

Chapter 6

Investigating Energy Potential for Future Electricity Mix Planning

One of the main issues faced by network operators with regards to PV output is its temporal mismatch to load demand [100]. This is seen in many countries where PV output occurs at times of low demand where the PV output pushes the net load down further. This means that networks are less likely to be capable of absorbing PV output at peak output times [349]. This issue was highlighted in a report from the National Renewable Energy Laboratory (NREL) that stated that the most common reason for curtailment of wind and PV generators in the USA was due to oversupply, typically at low load periods [96].

As PV penetration levels continue to rise so does the risk of curtailment with one study suggesting it could be as high as 30 to 60% in the near future [99]. This represents a missed opportunity to meet decarbonisation targets by reducing CO₂ emissions of electricity networks [102] and reduces the economic viability of PV projects [96, 98-100, 103].

This chapter details works carried out to maximise the energy potential of PV in future energy mix by investigating the efficacy of two low-cost smart grid solutions: Demand Side Management (DSM) and Active Voltage Control (AVC), to maximise PV output yield by minimising curtailment whilst avoiding costs to distribution network operators. The work focuses on scenario-based impact assessments underpinned by a net prosumer load forecasting framework as part of power system planning to aid sustainable energy policymaking.

6.1 Background

The decarbonisation of the energy network has created higher demand for electricity over oil and coal. Some of the electrical power network assets such as transformers and switchgear assets were installed as early as the 1950s and are still in use today [1]. For example, the UK's National Infrastructure Delivery Plan 2016–2021 identifies that “much of the existing infrastructure which has served us well is now old” and that “major investment is required to accommodate new generation and replace ageing assets”. However, there is also a greater focus now on lowering the cost of delivering electricity. The performance-based electricity distribution model Revenue = Incentives + Innovation + Outputs (RIIO) of the UK which has been in operation from 2015 [2] is representative of this drive. In the continuing drive to

reduce cost, given the high cost of assets, especially at the transmission and sub-transmission voltage levels, it is safe to assume that even in the near- or medium-term, power networks will be mostly composed of present-day assets.

There will be high volumes of customer-side renewable generation due to the decarbonisation targets. However, the exact penetration levels, renewable generation type and their share in the demand mix is presently uncertain. Due to technological advances, PV (photovoltaic) system costs has been on a continuous decline and, by 2017, PV module were more than 80% cheaper compared to a decade ago [350]. PV systems also have a low maintenance cost due to their static nature. At the domestic residence level, PV systems are one of the most popular types of renewable generation. Currently, Germany has the highest PV installed capacity in Europe; with over 49 GW [351]. More than 98% of PV systems are connected to low voltage distribution networks [352]. Even though the present levels of PV penetration in most other countries are relatively low, given the ambitious targets (e.g., 175 GW by 2022 for India by the Ministry of New & Renewable Energy), scenarios similar to Germany with high PV penetration is not far away.

A decentralised power supply becomes problematic for the traditional operating mode of the electricity network where net load on the network is largely foreseeable, power supply is controlled and there is a uni-directional electricity flow from large generators to consumers [3]. Conventional power distribution networks have limited PV generation hosting capacity and 'high PV generation - low demand' conditions can result in network voltage limit violations [353]. Extensive research has recently been carried out on assessments of the impacts of distributed generation on the electricity distribution network [354-356]. Such impact analyses have been able to identify the detrimental effect of future load on network assets [357-359]. Accelerated aging of transformer oil and insulation [357], deterioration of functioning of aged circuit breakers and switchgear [358], and higher maintenance requirements of transformer tap changers [359] are a few of the identified detrimental effects that have a direct commercial significance. While there are schemes in place for prioritizing the grid injection of renewable energy [360], the detrimental effects identified as associated with increase in PV penetration levels have resulted in grid codes making active curtailment of PV generation becoming a mandatory requirement now in several countries [361]. For example, according to Engineering Recommendation G98, PV systems in the UK LV distribution networks are required to curtail generation when the voltage rise at the point of connection exceeds the mandated limit [362].

Incentives like feed-in tariffs offered by government bodies have driven the installation of PV systems, but, as customers have to invest a large capital on installing PV systems and are getting paid for the energy they generate. Curtailing PV generation reduces the PV energy yield and therefore the systems financial viability [96]. Maximizing the energy yield and penetration levels of PV systems is therefore important with respect to both climate change mitigation and energy economics.

Several approaches have been considered in the literature in order to improve the network hosting capacity of PV and other renewables and maximize the energy capture. These approaches include network reinforcement, network reconfiguration, static VAR control, energy storage [363] and smart grid solutions such as Demand Side Management (DSM) [364] and Active Voltage Control (AVC) [361, 365].

6.2 Case Study

6.2.1 Countries and Locations Considered

The United Nations (UN) classifies countries into one of three broad categories: developed economies, economies in transition and developing economies [366]. To fully study the efficacy of DSM and AVC in reducing PV curtailment one country from each of these three categories was chosen to study. The UK was chosen as an example of a developed country, as according to the UN it is one of the seven most developed economies in the world [366]. India was chosen as an example of an economy in transition as the United States Trade Representative removed it from the list of developing nations in February 2020 [367]. Myanmar was chosen as an example of a developing nation as the UN categorises it as one of the least developed countries in the world [366].

Newcastle upon Tyne was chosen as the location for investigation in the UK, whilst Mumbai was chosen to investigate India and Yangon City was chosen to investigate Myanmar.

6.2.2 Climate Conditions of Locations Under Investigation

The Köppen-Geiger (KG) classification system was first presented by the German scientist Wladimir Köppen in 1900 [368]. It was the first quantitative classification of the worlds climates and is still widely used today [369-370]. The KG system classifies climates into five main zones: the equatorial zone (A), the arid zone (B), the warm temperate zone (C), the

snow zone (D) and the polar zone (E) [368, 371]. It further classifies climates into 30 sub-types by using a second letter which differentiates climates with regards to precipitation and a third letter which differentiates according to temperature [228, 368].

According to the KG classification system Newcastle was a warm temperate fully humid (Cfb) climate [368]. KG classifies Mumbai as equatorial savannah with dry winter (Aw) [368]. The latest KG world map shows that Myanmar has three distinct climatic regions, and that Yangon is in the equatorial monsoon region of the country (Am) [368].

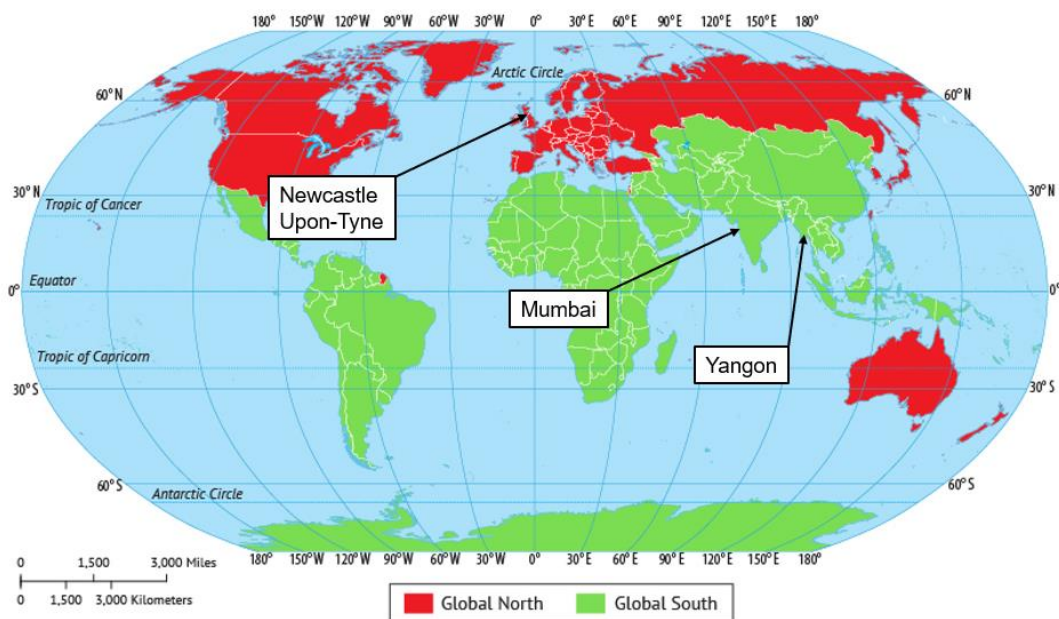


Figure 56 - Case Study Locations

6.2.2 Distribution Networks Considered

A typical UK distribution network model shown in *Figure 57* from [372] was used. The low voltage feeder shown in detail from the secondary distribution transformer has 384 houses. The total number of houses connected to an 11 kV feeder is 3072 (= 8 x 384) and to the 33/11 kV substation is 18,432 (= 6 x 3072) houses.

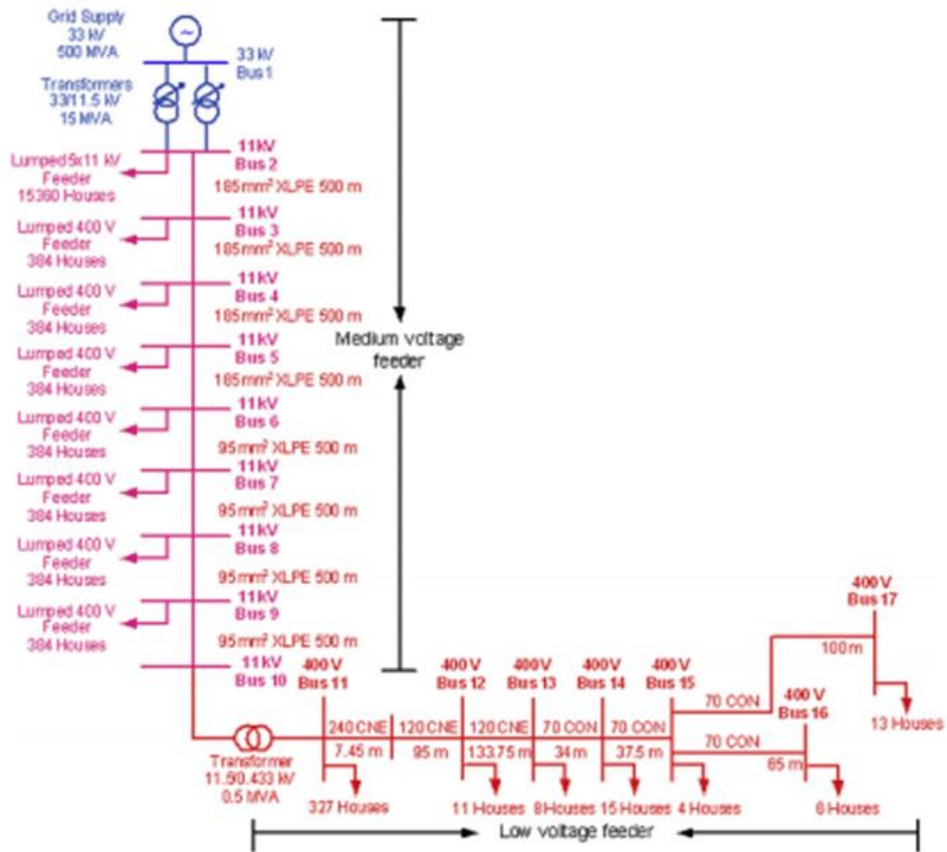


Figure 57 - Typical UK Distribution Network [372]

A typical South-East Asian distribution network was used to investigate both Mumbai and Yangon (Figure 58). The model consists of a 33/11 kV 15 MVA transformer substation with nine outgoing feeders (11 kV), supplying 14385 houses. A typical 415 V LV feeder (shown in red) supplying 385 houses was considered in detail, similar to Newcastle.

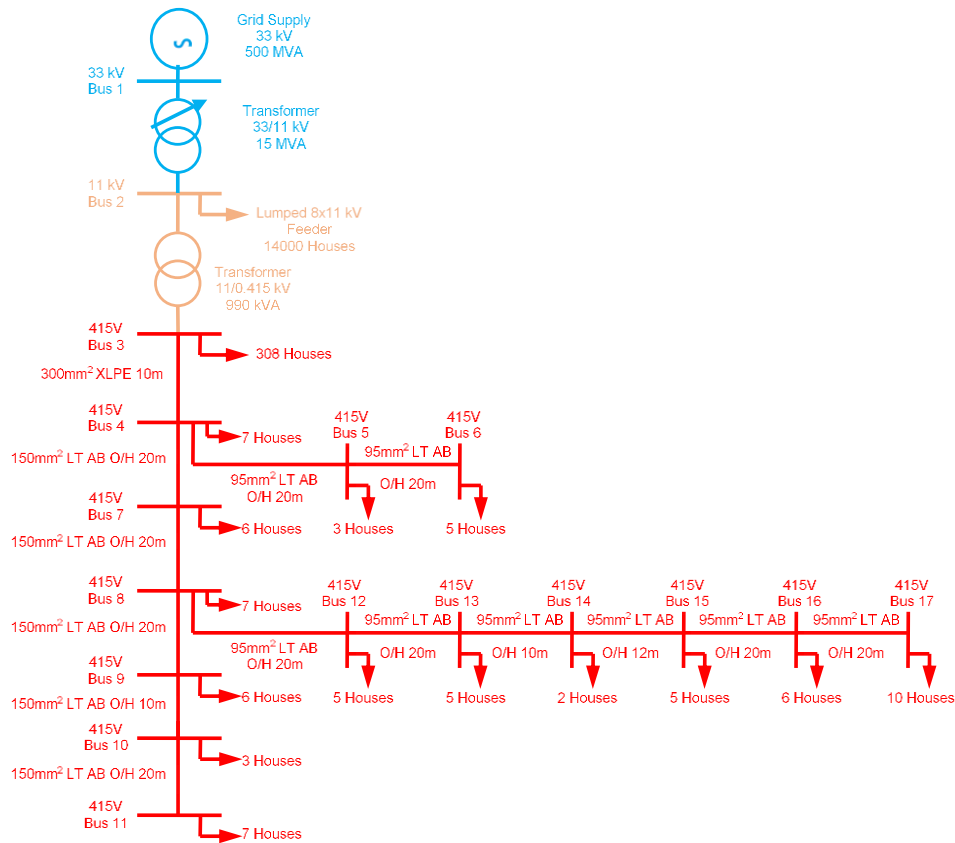


Figure 58 - Typical South-East Asian Distribution Network

6.2.3 PV Generation Simulation

A 3.6 kW polycrystalline rooftop residential grid-connected PV system was considered as typical for all three countries and was modelled as being connected to each house on the networks shown in *Figure 57* and *Figure 58*. PVGIS [373] was used as the solar resource database as well as PV generation simulation tool. Technical data of Sharp ND-R250A5 polycrystalline PV modules and SMA H5 inverter were used for simulation. Daily PV generation profiles for a typical year were generated for all locations. Systems were assumed to be stationary and at optimal tilt.

All three systems were modelled with typical system losses of 14%. The overall losses of the systems were higher for Mumbai (25.62%) and Yangon (25.95%) compared to Newcastle (18.24%). This was mostly due to higher losses associated with the working temperature of the systems (see *Table 36*).

Table 36 - PV System Loses

Losses (%)	Newcastle	Mumbai	Yangon
System	14	14	14
Temperature & Irradiance	3.7	11.1	12.26
Other	0.54	0.52	0.31
<i>Total</i>	<i>18.24</i>	<i>25.62</i>	<i>25.95</i>

The PV system’s annual energy yield was found to be 3280 kWh (equivalent to 911 kWh/kW) for Newcastle. For the system in Mumbai, the yield was around 80% more than that of Newcastle at 6017 kWh (equivalent to 1671 kWh/kW). The system in Yangon City was slightly lower than that of Mumbai at 5267 kWh (1463 kWh/kW) annual yield. *Figure 59* shows the average monthly output of the PV systems for the three case study locations.

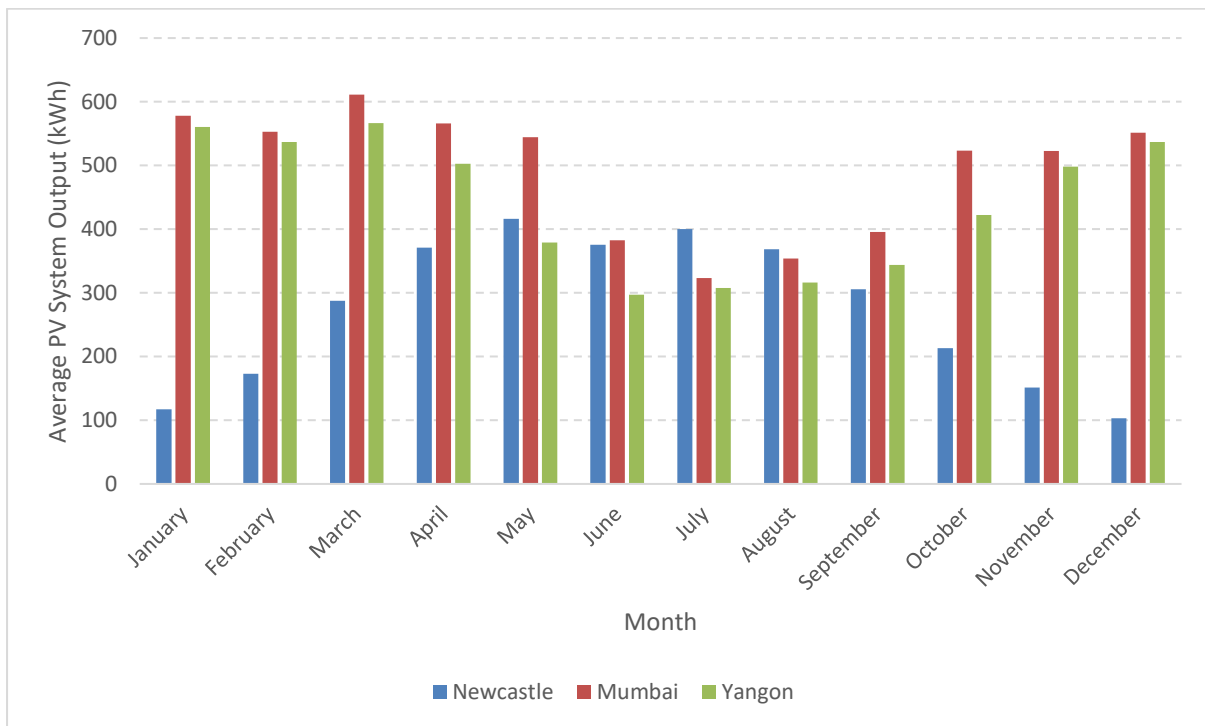


Figure 59 - Average Monthly Output of PV Systems

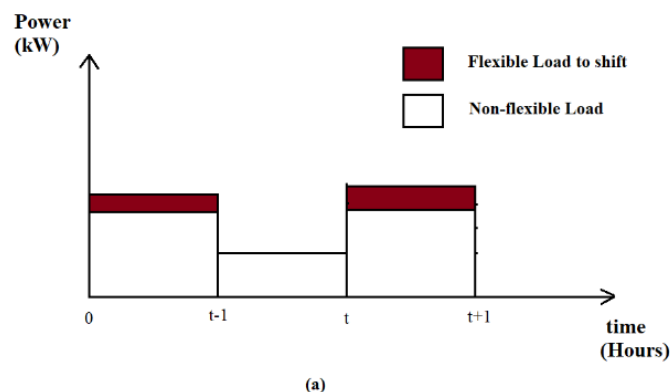
6.2.4 PV Penetration Scenarios for Assessment

In this study, PV penetration level was defined as the fraction of the number of houses in the distribution network considered having a typical PV system. 11 scenarios each, are studied for each location. PV penetration level is varied from 0 to 100% in steps of 10%, to create the 11 scenarios.

6.2.5 Smart Grid Solutions Investigated

Demand Side Management

DSM is the control of customer loads in order to achieve a better match between the available supply and the demand. Of the DSM strategies available, the load shifting strategy (Figure 60), which is the movement of operation of selected loads between times of the day, was chosen in this work. This strategy is most suited for maximising self-consumption of energy (and hence the economic value) from PV systems installed at customer premises. DSM can be either 'Active' or 'Passive'. 'Active' Demand Side Management (ADSM) is defined as the automated (intelligent) control of residential electricity demand to meet the needs of the power supply system [374]. This has become possible with the roll out of smart meters and the development of home automation technologies. 'Passive' DSM (PDSM) requires customers to be active participants, the control action of load shifting is realised by the customers based on inputs from network operator/electricity company. DSM implementations can be based on price signals such as time of use (ToU) tariffs and real-time pricing or based on incentive schemes e.g., buy-back programs [375]. *Figure 61* is representative of a plausible ADSM scheme and shows an ADSM controller incorporated into a smart grid architecture [376] in which maximisation of PV energy capture would be realised through direct load control by the ADSM controller. In PDSM a similar maximisation of PV energy could be realised, for example, through a mobile phone app that evokes customer load action [377].



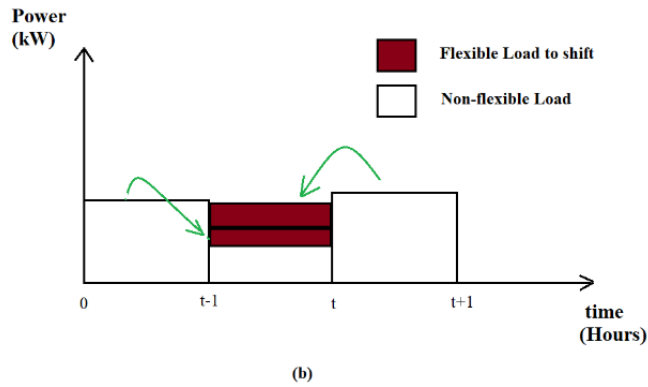


Figure 60 (a) Before Load Shifting and (b) After Load Scheduling

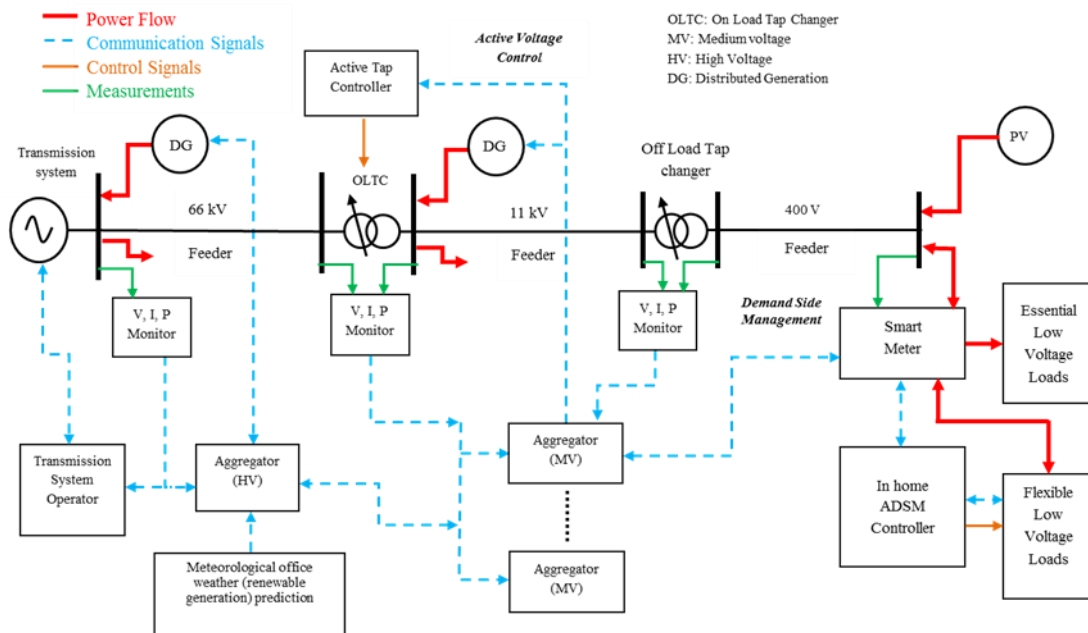


Figure 61 - Smart Grid Architecture (adapted from [374]) with an Indicative ADSM Controller

Load shifting can be expressed mathematical as [378-379]:

Equation 7 – Load Shifting

$$\text{Load Shifting} \rightarrow \text{Minimize } \sum_{t=1}^N (P_{load}(t) - (\text{Objective}(t)))^2$$

$$\text{Desired Consumption at time 't'} \rightarrow \text{Objective}(t)$$

$$\text{Actual Consumption at time 't'} \rightarrow P_{load}(t) = \text{Forecast}(t) + \text{Connect}(t) - \text{Disconnect}(t)$$

where, Forecast(t)=Forecasted consumption at time t, Connect(t)=Connected load amount at time t and Disconnect(t)=Disconnected load amount at time t.

Appliances chosen as flexible loads for DSM in this study are shown in Table 37. The table also shows the household share (percentage of household with the specific appliance), cycle duration and energy consumption/cycle considered for the chosen flexible loads based on information assimilated from [380-382]. While the share of Dishwashers was below 1% in India before 2020, manufacturers have witnessed a 400% surge in demand due to COVID lockdown and homeworking restrictions [383]. Mumbai and Yangon, being the commercial capitals of their countries, it is assumed that the increase in PV penetration will be coincidental with an increase in uptake of Dishwashers.

Table 37 - Details of Flexible Loads Chosen for DSM

Appliance	Household Share in UK (%)	Household Share in India (%)	Household Share in Myanmar (%)	Energy Consumption/ Cycle (kWh)
Washing Machine	95	43	43	1.8
Dishwasher	40	Below 1%	Below 1%	1.2
Electric Water Heating	10	45	45	3

Load profiles of these flexible loads chosen for DSM for a typical day were available from [384] for the UK. Owing to the lack of such appliance level consumption data in India and Myanmar, the same profiles were assumed for all cases. *Figure 62* shows the load profiles for the three categories of flexible loads.

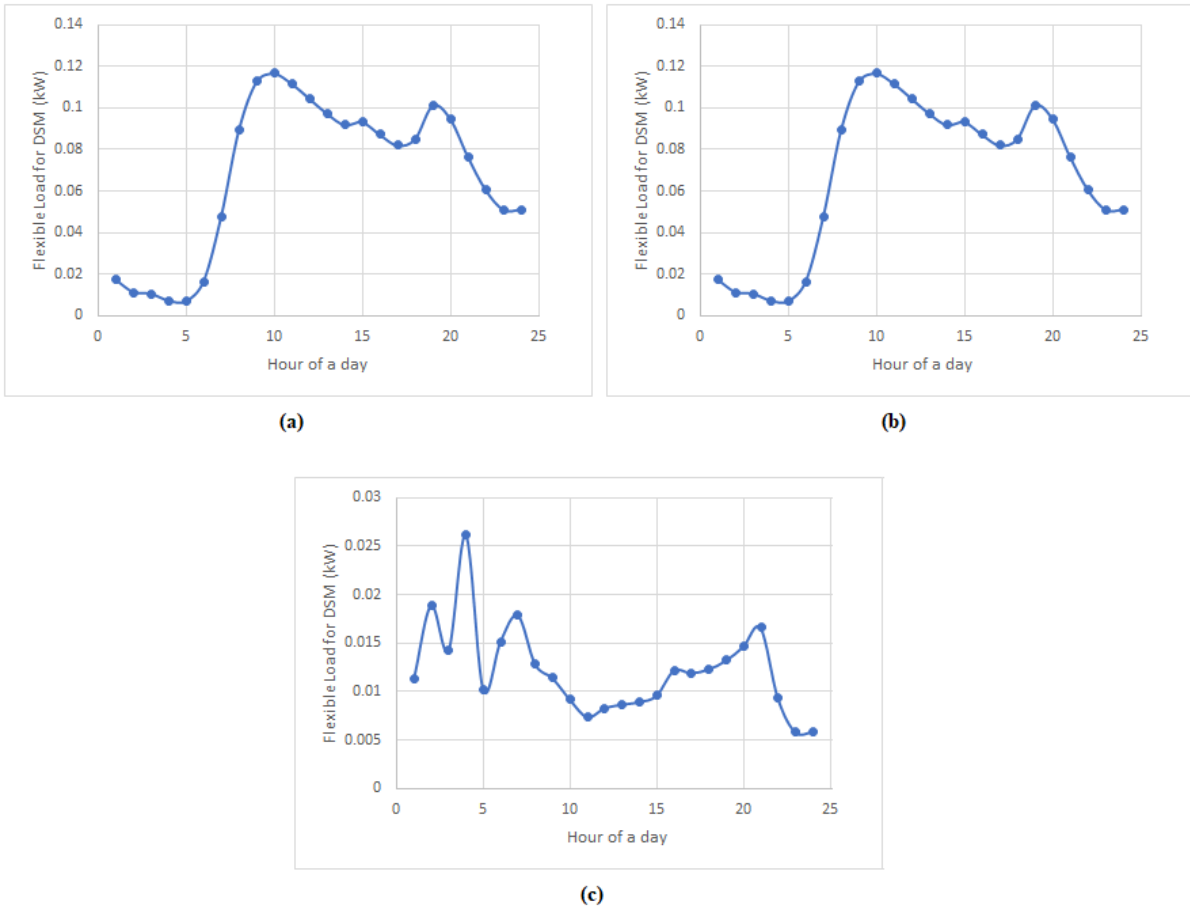


Figure 62 - Typical Load Profiles of Flexible Loads (a) Washing Machine, (b) Dishwasher and (c) Electric Water Heating for A Single Domestic Dwelling

With the use of appropriate control logic and knowledge of the network topology, the feeder level controller (Aggregator MV) shown in *Figure 61* would be able to make nodal voltage predictions. The in-home ADSM controller can receive these predictions via the smart meter and trigger load-shifting of the flexible loads according to the DSM program.

Active Voltage Control

Active Voltage Control (AVC) is a part of the active management of the network. Grid codes usually require that the voltage at the end customer terminal does not deviate from the nominal value by more than a few percent (e.g., within -6% to +10% for the LV network in Europe). To satisfy this requirement, the voltage of all nodes in the network should be kept close to their nominal value at the extremities of the distribution network operation. Transformer tap changers, voltage regulating transformers and reactive power compensation are some of the techniques that are used for achieving this control [385]. Amongst these, transformer tap changers are the most common and hence, in this study, AVC is considered by means of transformer tap changing, as shown in *Figure 63* for one

phase of a three-phase primary substation transformer. The on-load tap changer (OLTC) on the high voltage winding (winding 2) regulates the voltage by varying the transformer ratio V_2/V_1 . Tap position 0 corresponds to no voltage correction and tap position N_{Taps} yields the maximum voltage correction.

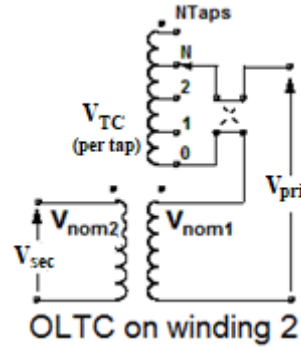


Figure 63 - One Phase of Primary Substation Transformer

Reversing the switch connects the regulation winding in opposite polarity and yields negative tap positions. Hence the tap range is $-N_{Taps} \leq N \leq +N_{Taps}$. Voltage regulation by the OLTC can be described by the equation:

Equation 8 – Voltage Regulation by OLTC

$$V_{sec} = \frac{V_{pri} V_{nom1}}{(1 + N \cdot V_{TC}) V_{nom2}}$$

where V_{nom1} and V_{nom2} are the nominal voltages of winding 1 and 2, N is the tap position, V_{sec} is the transformer output voltage after tap changing, V_{pri} is the source voltage incoming to the transformer primary part and V_{TC} is the voltage per tap.

Normally, control of OLTCs at primary substations is by means of an automatic voltage controller, which controls the tap changer on the high voltage side of the transformer, in order to keep the voltage on the low voltage side within limits. In contrast to conventional voltage regulation (which uses Scalar LDC), the automatic voltage controllers in this case deploys Vector Line Drop Compensation (LDC), which is intended to keep the voltage in the distribution feeder within limits by compensating for voltage drop along fictitious impedance and modifying the controller algorithm to keep the transformer terminal voltage equal to a reference value. As vector LDC also counts on changes in power factor, the results are more reliable and the mathematical expression is as follows [238],

Equation 9 – Reference Voltage

$$Reference\ Voltage \rightarrow V_{ref}(t) = |V_{sec}(t) - \sqrt{3}I(t) \cdot (R_{ref} + jX_{ref})|$$

Where $V_{sec}(t)$ = Secondary Voltage of Transformer, R_{ref} = Line Resistance, X_{ref} = Line Reactance and $I(t)$ = Line Current.

Tap-changer is operated by comparing the reference voltage with the deadband which is a small voltage range introduced in the transformer's design in order to avoid unnecessary switching around the target voltage.

Tap movements are usually made if $|V_m - V_{ref}| > \text{Deadband}/2$ for a certain time delay of t_{step} (which is 1-minute duration in this study) according to the following equation:

Equation 10 – Tap Changer Operation

$$Tap_{change}(t + t_{step}) = \begin{cases} -1, & \text{if } V_{max}(t) > V_{up}^{TC}, V_{min}(t) - V_{TC} \geq V_{low}^{TC} \\ 1, & \text{if } V_{min}(t) < V_{up}^{TC}, V_{max}(t) + V_{TC} \leq V_{low}^{TC} \\ 0, & \text{else} \end{cases}$$

where $V_{max} = 1.1\text{pu}$ -Voltage at current tap position, $V_{min} = \text{Voltage at current tap position} - 0.9\text{pu}$, $V_{TC} = \text{voltage per tap} = 0.125\text{pu}$, $V_{low}^{TC} = \text{minimum deadband voltage} = -2.5\%$ of V_{TC} and $V_{up}^{TC} = \text{maximum deadband voltage} = +2.5\%$ of V_{TC} .

6.3 Performance Assessment

High PV penetration levels can result in situations where the LV network voltage exceeds the statutory limits. Current grid codes (for example, G98 in the UK) require residential PV systems to turn-off and curtail generation during periods of voltage rise. The main aim of this work was to analyse the efficacy of smart grid solutions (DSM and AVC), between countries at different stages of economic development, in facilitating higher PV penetration in residential distribution networks, given grid code requirements using the 11 PV penetration scenarios for Newcastle, Mumbai and Yangon described in the previous sections. The LV distribution networks for all cases were designed for an ADMD of 2 kW per customer. However, in terms of PV, Mumbai's and Yangon's output were much higher compared to Newcastle for the same PV system size. As described in section 2.3.1 it is possible to realise a certain ADSM load action also through PDSM. PDSM as a holistic strategy without the need for smart appliances or direct load control would be preferable in the first instance for developing countries like India and Myanmar because of economic reasons. As such, DSM is chosen as the first preferred solution to prevent PV curtailment, followed by AVC. The two-stage approach is shown in Figure 64. The objective is to maximise the PV energy

capture by self-consumption and consequently to reduce the burden caused by the reverse power flow on electrical network assets to maintain the optimal assets' lives.

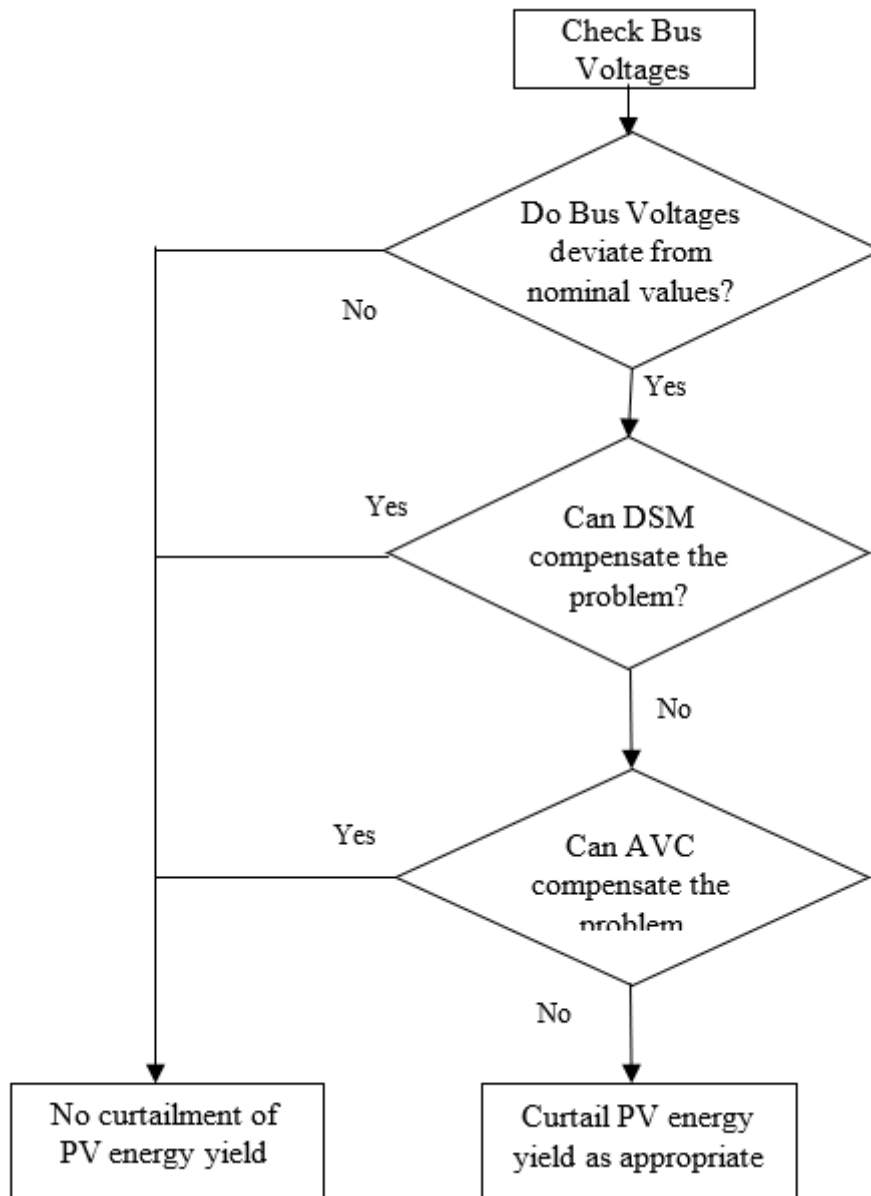


Figure 64 – Maximising PV Energy Capture by DSM and AVC

For load shifting, the scenario-based assessments considered a representative DSM logic outlined in *Figure 65* is applied to each flexible load category (washing machine, dishwasher and electric water heater). *Figure 66* outlines the AVC operation scheme considered for the study.

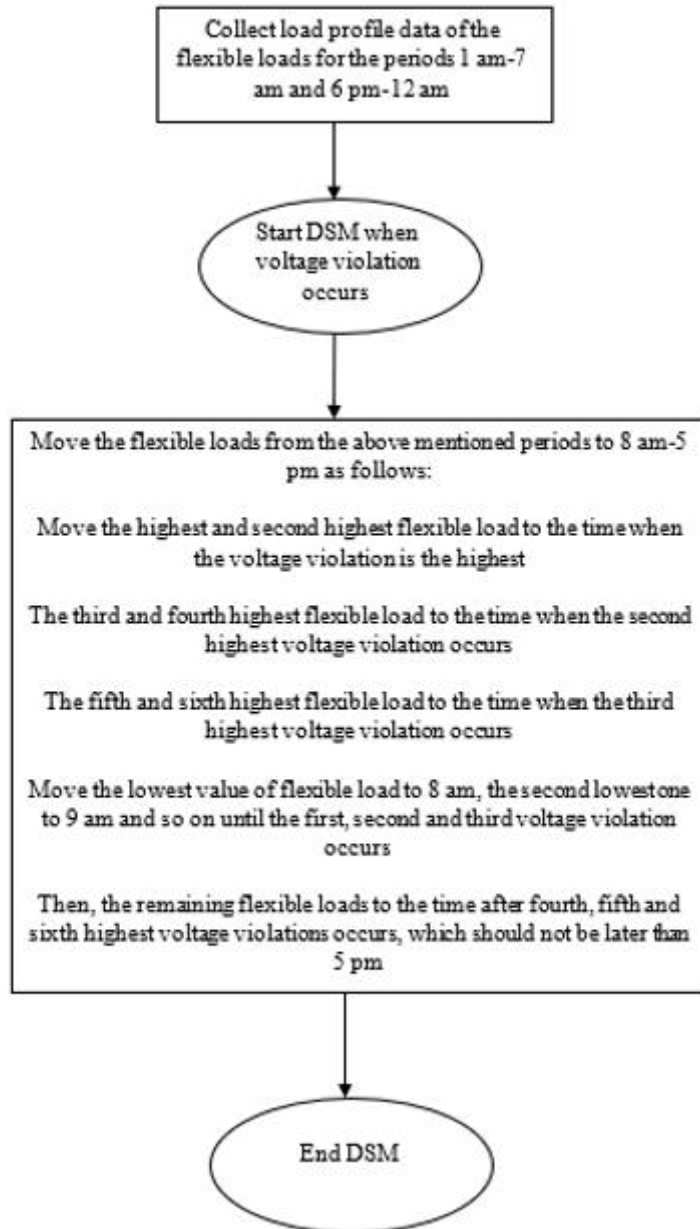


Figure 65 – Load Shifting DSM Scheme Considered

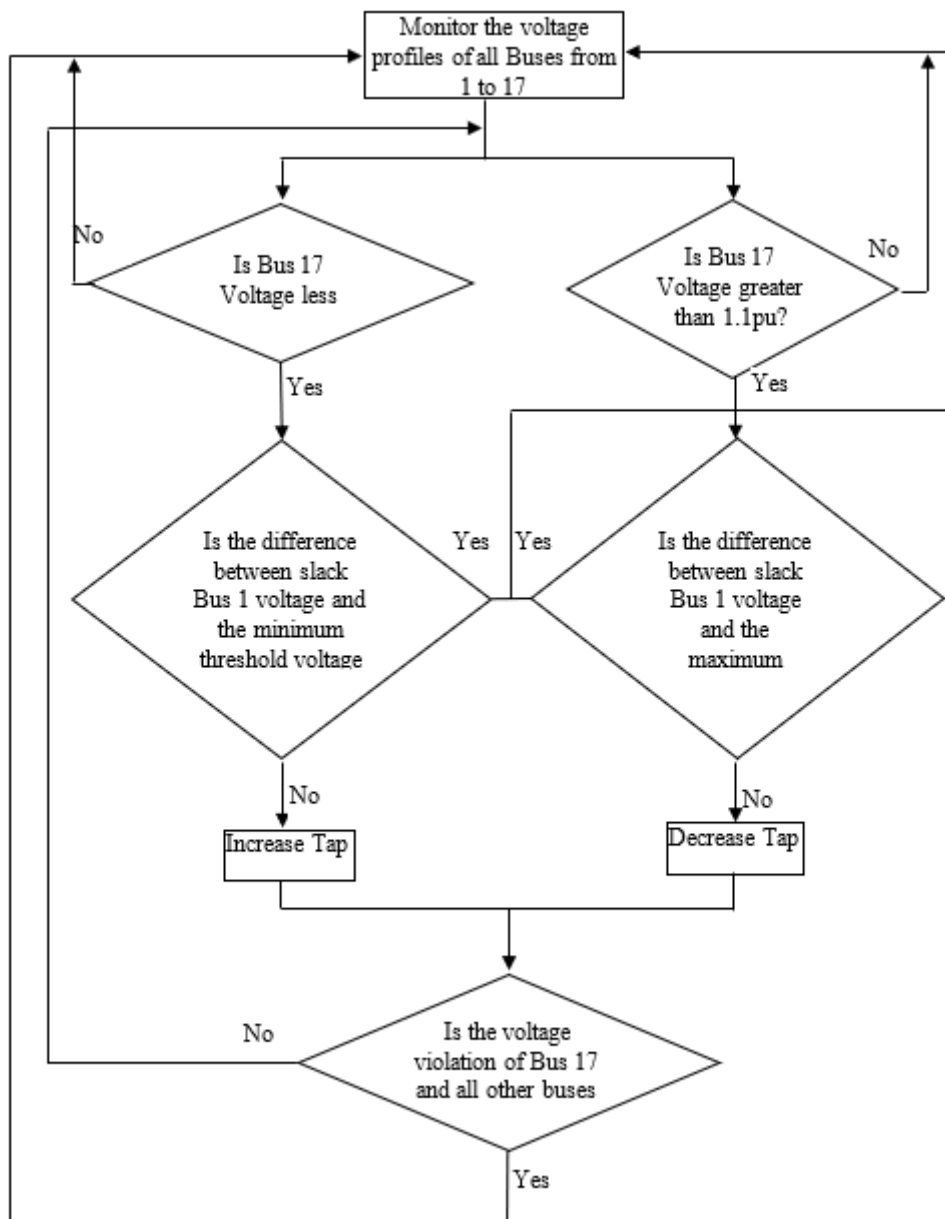


Figure 66 – AVC Operation Scheme Considered

6.4 Net Load Profiles

Residential load profiles represent the variation of After Diversity Maximum Demand (ADMD) of domestic consumers over a day. The standard method of constructing an hourly load profile is by recording the energy consumption, at feeder or substation level in an electricity distribution network, at regular intervals and dividing this by the number of customers on that feeder to produce the ADMD. The nature of customers is changing under de-carbonisation. Residential customers with generating technologies such as PV are prosumers as they produce and export electricity in addition to the typical consumer roles. In the smart grid context, historic forecasts of load profile will not be appropriate. Net load profiles at the

residential customer level will need to be prosumption profiles, factoring in the drastic changes in load (for example, due to electric vehicles (EV), heat pumps etc.) and at-home generation technologies (PV, Micro-CHP etc.). Synthetically generated net load profiles are therefore important for scenario-based assessment studies.

Several studies have used artificial intelligence models for predicting energy demand of buildings [306]. Günay [307] modelled the gross electricity demand in Turkey using Artificial Neural Network (ANN) models with weather and socio-economic factors as inputs. Zameer et al. [308] used genetic programming based on an ensemble of neural networks to demonstrate the feasibility of wind energy prediction (in Europe) by using publicly available weather and energy data. With regard to the challenge of predictive modelling for uncertain penetration levels of future distributed resources, a number of researchers have recently had reasonable success by employing statistical probability distributions [309-311]. For example, Munkhammar et al. [311] demonstrated the use of the Bernoulli distribution for incorporating EV demand into load profiles. However, these statistical probability distributions fail to take into account the time varying behaviour in the energy consumption of distributed resources as they assume a constant load. Therefore, a framework for synthetic net residential load profile generation proposed combining artificial intelligence and statistical probability distributions, that can be used for scenario-based assessment studies, is proposed as shown in *Figure 67*. The framework summarises authors' accumulated experience in using artificial intelligence methods and observations of literature.

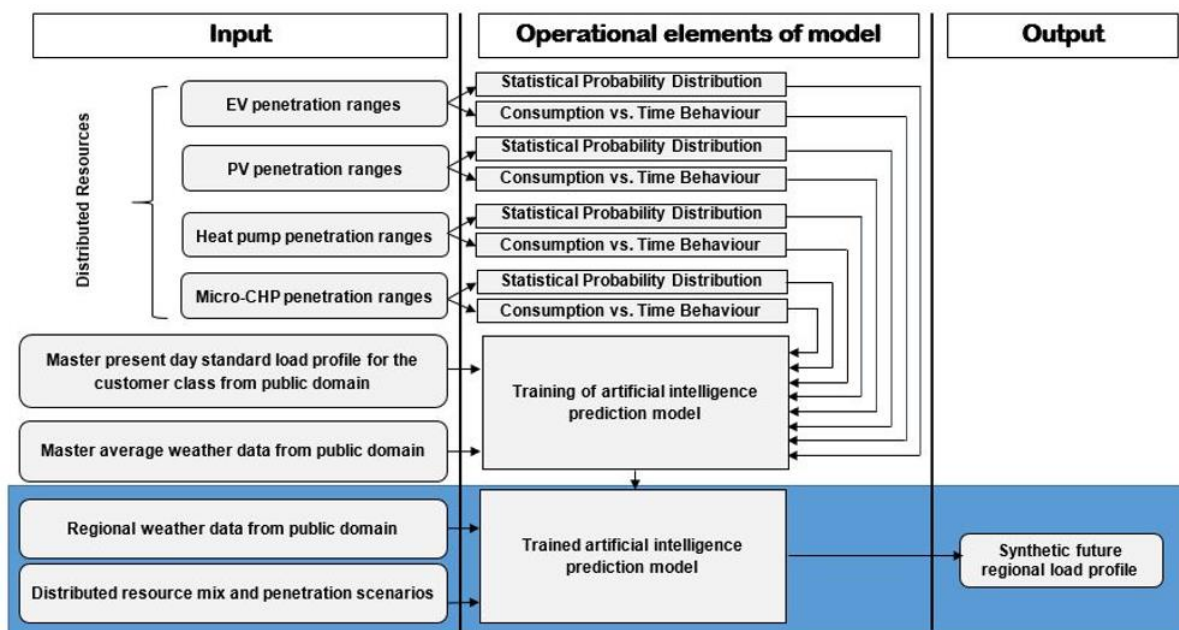


Figure 67 – Net Residential Load Profile Generation Framework

The net residential load profile generation problem is inherently data centric. The choice of data, artificial intelligence methods and inclusion of operational elements of the framework such as statistical probability distribution is dictated by the data available. A method tailored for the data available and scenario under consideration, can be generated based on the framework. Artificial Neural Networks (ANNs) are capable of mapping nonlinear relationships between inputs and outputs with a high level of accuracy [250, 386-387]. ANNs are used in a wide variety of tasks in different fields including finance, industry, science, and engineering [250-253]. ANNs is particularly suited for load forecasting where high levels of accuracy are required [252]. ANN based methods were developed for all three case scenario locations and net load profiles were generated for all 11 scenarios described previously.

6.4.1 Newcastle Case

The load profiles used in the Newcastle case scenario were generated using the ANN model developed previously in the project that generated net load profiles for UK residential customers under variable PV generation and electric vehicles (EV) charging penetration scenarios as presented in [388]. The model was generated using the Matlab Neural Network Toolbox and was trained using publicly available data. During validation with data that the ANN model had no apriori knowledge of, the model synthetically generated composite load profiles with a combined Mean Absolute Percentage Error (MAPE) of 0.01365 and a root mean square error (RMSE) of 7.81 over a full range of PV and EV penetration scenarios from 0 to 100%.

For the Newcastle case study, an improvement in the ANN model performance was focussed on. ANN architecture is highly problem dependent [389] where the choice of number of hidden neurons, hidden layers and training algorithm are all considered to be critical decisions in improving the performance of an ANN model [252, 390]. Therefore, testing was conducted to find the optimal design network by comparing the performance of 3520 networks created with different combinations of the 17 supervised training algorithms available in the Matlab environment, hidden layers from 1 to 6 and nodes in each layer from 1 to 20. The optimal network was found to have 13 neurons in one hidden layer which was trained using the Bayesian regularization backpropagation algorithm. Validation of this model using the same data used with the original model saw the MAPE lower to 0.00608 and the RMSE lower to 3.48.

Figure 68 summarises the training of the ANN model and its inputs for predicting net load profiles. UKERC [391] was the source of load data during training. PV generation data was based on PVsyst software simulations using public domain weather data from PVGIS. The net load profiles for different PV penetration scenarios studied in this work for Newcastle were created using five inputs, namely time of day (hour), PV penetration level (0 to 100% in steps of 10%), EV penetration level (set to 0) and temperature and irradiance values. Temperature and irradiance values were from the SARA solar radiation database accessible through the PVGIS website.

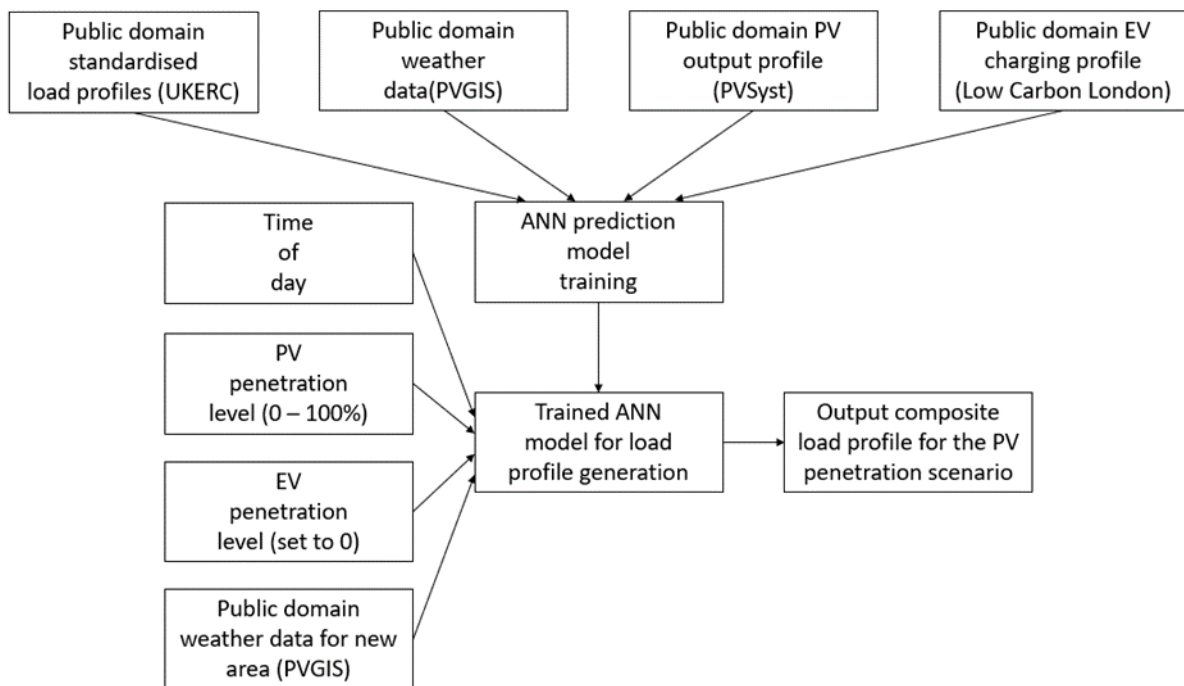


Figure 68 – ANN Based Net Load Profile Generation for Newcastle

6.4.2 Mumbai Case

The ANN model developed and validated by the authors in [392] was used to generate load profiles for Mumbai. Like many developing countries, owing to the lack of resources, there is a severe shortage of data in the public domain. In contrast to the PV data (resolution of 15 minutes for all days of a typical year), the load data set was extremely limited [48 data values in total, 24 hourly values each for summer and winter]. This made ANN training extremely challenging and was mitigated by means of Bayesian Regularisation [392]. Figure 69 shows the synthetic residential load profiles for Mumbai generated by the ANN model. However, optimising the ANN model for extremely limited data posed a challenge, the ANN model could only learn the load behaviour not the PV behaviour. For this reason, net load

profiles were based on summation of ANN predicted load profiles and PVGIS PV generation profiles

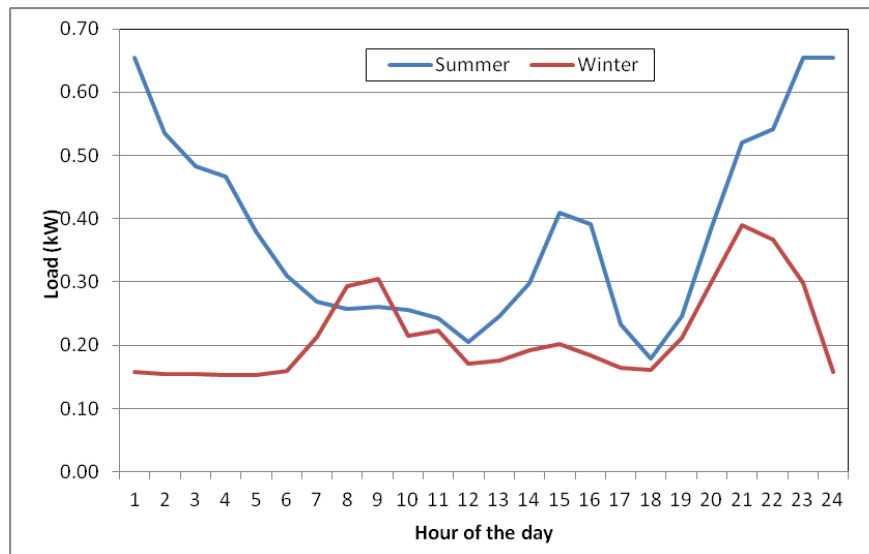


Figure 69 - ANN Generated Synthetic Residential Load Profiles for Mumbai

6.4.3 Yangon Case

Actual load profiles for developing countries such as Myanmar are difficult to obtain [351]. The load profiles used for the Yangon case scenario are based on those created earlier in the project to study the potential of PV in meeting the increasing load demand of developing countries in the global south such as Myanmar. The profiles were based on a synthetic load scenario created in [3] and refers to the hourly, over the day, variation in the maximum demand of 100 residences over 365 days of a typical year. The scenario was developed based on data from the local energy use patterns in the neighbouring countries with climate and economic environments similar to Myanmar. The scenario used assumptions about the basic electricity demand of urban residences in developing countries in East Asia such as lighting, fans, televisions and other home appliances such as refrigerators and mobile phone chargers. It was also assumed in the scenario that the peak demand would occur during the daytime due to the use of fans to combat the perennial high temperatures of the region. The data from neighbouring countries and the assumptions about basic electricity needs were used together by the author to generate a typical daily synthetic load profile and seasonal variations reflective of the electricity demand of urban household consumers in Myanmar.

Using the typical daily profile and the maximum variations in the seasonal profile of [3] average daily profiles with an hourly resolution were created for the twelve months of a year.

Aggregated seasonal and annual load profiles were then generated from the monthly profiles.

The data from the seasonal profile from [3] showed very little variance in the projected demand over the course of a year. The average daily peak demand was 250kW. The maximum averaged daily peak demand occurred in March when the peak was 261.49kW, 4.6% above the yearly average. July had the lowest averaged daily peak demand at 240.09kW, 3.9% below the yearly average. The aggregated seasonal figures showed an even smaller variance. The hot season had the highest average daily peak demand at 252.56kW, 1% above the yearly average. The cool season had the lowest average daily peak demand at 247.78kW, 0.9% below the yearly average.

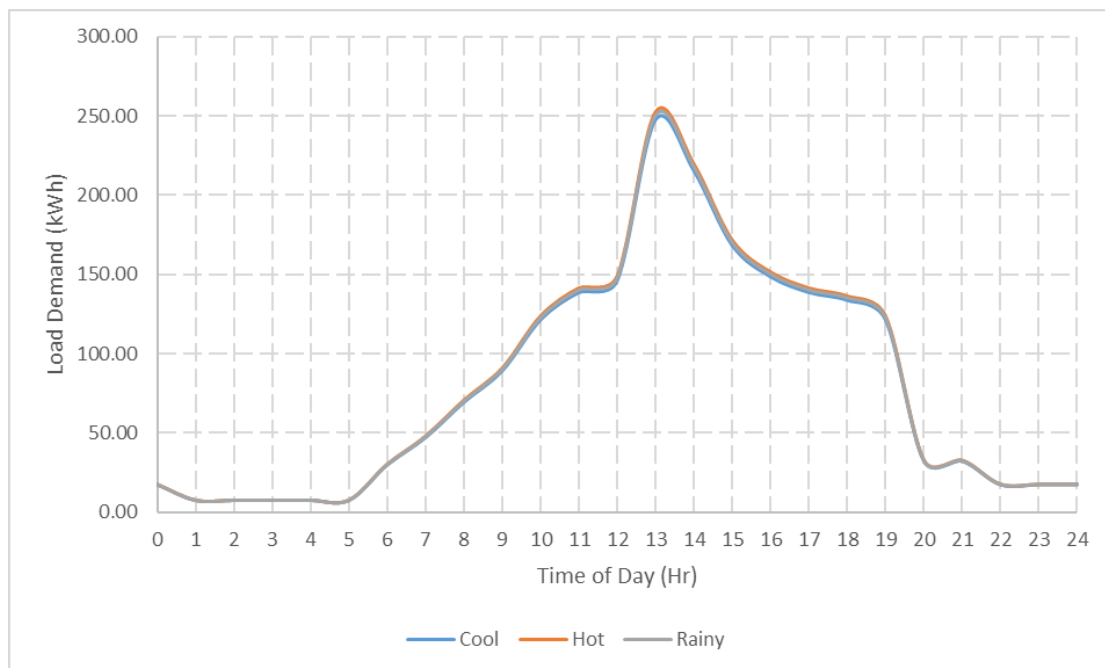


Figure 70 - Averaged Synthetic Daily Load Profiles for Urban Yangon City

The aggregated synthetic seasonal load profiles for urban Yangon City are shown in Figure 16 where the rainy season profile (grey dotted line) can just be seen slightly below the profile for the cool season (blue solid line), highlighting the low variation in load over the seasons. The low variance in load is due to the climate in the region and the assumption that electricity demand is driven by basic needs such as cooling and lighting [3].

6.5 PV Energy Yield Estimation Algorithms

At the low voltage distribution level (230/400 V UK, 240/415 V India, Myanmar) the grid codes of both the UK [64] and India [65,66] mandate an upper voltage limit of 1.1 p.u. For PV inverters connected to LV networks, G83, the UK's previous grid code required disconnection at the same voltage of 1.1 p.u. However, the new grid code G98 requires PV inverters to disconnect only at 1.14 p.u. It is understood that this is for reasons of stability as disconnection of large amount of renewable generation at the same instant can create instability. Therefore, there are two voltages which are of significance 1.1 p.u. and 1.14 p.u. Most PV inverters are now manufactured to comply with G98. India and Myanmar also use the same inverter technologies as the UK at the same frequency. It was assumed that with higher PV penetration India and Myanmar will follow the UK and the two voltages mentioned would be the ones of significance.

Economic analysis is central to energy policymaking. Most economic analysis considered PV energy yield (in kWh) for a period of one year. As such, the efficacy of DSM and AVC for maximising PV energy capture following the two-stage approach in *Figure 64* is also assessed for a one-year period for the scenarios considered.

The Post-Curtailment Energy Yield Estimation (PC-EYE) algorithms for the three cases part of the assessment process namely (i) Base case (without DSM or AVC), (ii) Case with DSM and (iii) Case with DSM and AVC, are shown below. These were not developed as part of the author's PhD. They were developed by the author's supervisor Dr Gobind Pillai as part of his doctoral thesis and then improved by his masters student Thet Paing Tun. The author has only used them as a tool for investigating different scenarios. Details of the algorithms are provided to aid the readers understanding of the analysis presented in subsequent sections.

MATLAB was used to code the algorithms. Bus voltages were calculated using Distflow (Distribution load flow) [393]. The DSM and AVC programs were based on the schemes presented earlier in *Figure 65* and *Figure 66*. 1.14 p.u. was the threshold voltage at which curtailment action was initiated. The grid voltage upper limit of 1.1 p.u. was set as the voltage for initiating DSM and AVC actions to maximise energy capture by preventing curtailment.

Algorithm: Post-Curtailment Energy Yield Estimation Algorithm (Base case)

- 1: Read the PV penetration scenario
 - 2: Read PV generation profile and net load profile for the day and location.
 - 3: In hourly time steps, run Distflow program $\{V_{n+1} = V_n - [(\frac{\sum_{k=1}^n P_k - jQ_k}{V_n}) \times Z_{(n+1)_n}]\}$ and record voltages at all Buses for all hours of the day.
 - 4: For all voltages greater than 1.14 p.u. from 3, turn all the PV systems at the relevant Buses off and record the value of PV energy curtailed at the bus. Aggregate the energy curtailed at each Bus over the day.
 5. Repeat 2-4 for all days of the year and aggregate the energy curtailed at each Bus over the year
-
-

Algorithm: Post-Curtailment Energy Yield Estimation Algorithm (DSM)

- 1: Read the PV penetration scenario
 - 2: Read PV generation profile and net load profile for the day and location.
 - 3: In hourly time steps, run Distflow program $\{V_{n+1} = V_n - [(\frac{\sum_{k=1}^n P_k - jQ_k}{V_n}) \times Z_{(n+1)_n}]\}$ and record voltages at all Buses for all hours of the day.
 - 4: For all Buses, check if voltage exceeds 1.1 p.u. at any step during the day. If yes activate the DSM program, run Distflow and record the newly resulted Bus voltages.
 - 5: For all voltages greater than 1.14 p.u. from 4, turn all the PV systems at the relevant Buses off and record the value of PV energy curtailed at the bus. Aggregate the energy curtailed at each Bus over the day.
 6. Repeat 2-5 for all days of the year and aggregate the energy curtailed at each Bus over the year
-
-

Algorithm: Post-Curtailment Energy Yield Estimation Algorithm (DSM and AVC)

- 1: Read the PV penetration scenario
 - 2: Read PV generation profile and net load profile for the day and location.
-

-
- 3: In hourly time steps, run Distflow program $\{V_{n+1} = V_n - [(\frac{\sum_{k=1}^n P_k - jQ_k}{V_n}) \times Z_{(n+1)_n}]\}$ and record voltages at all Buses for all hours of the day.
 - 4: For all Buses, check if voltage exceeds 1.1 p.u. at any step during the day. If yes activate the DSM program, run Distflow and record the newly resulted Bus voltages.
 - 5: For all Buses, check if voltage exceeds 1.1 p.u. at any step during the day. If yes activate the AVC program, run Distflow and record the newly resulted Bus voltages.
 - 6: For all voltages greater than 1.14 p.u. from 4, turn all the PV systems at the relevant Buses off and record the value of PV energy curtailed at the bus. Aggregate the energy curtailed at each Bus over the day.
 7. Repeat 2-6 for all days of the year and aggregate the energy curtailed at each Bus over the year
-

6.6 Results and Discussions

Simulations were run for the 11 scenarios of varying PV penetration (steps of 10%) described in section 2.2.1. Three different cases were considered: (i) Base case (without DSM or AVC), (ii) Case with DSM and (iii) Case with DSM and AVC. Time period considered in the simulations was one year. It was identified that for all locations under study, the mid-summer period is the period of highest irradiation in the year when voltage rise and consequently PV energy curtailment was most severe. The performance of the smart grid solutions considered for the worst-case scenario, the peak irradiation day in summer, is representative of the efficacy. Owing to this reason, some of the results discussed below only focus on the peak day in summer. The bus that is located the farthest from the main grid source (Bus 17) is the most severely affected by any reverse power flow from the domestic PV sources back to grid [394]. So, Bus 17 was chosen to visualise the effectiveness of DSM and AVC.

6.6.1 Base Case Scenario

Newcastle Case

Simulation results for the Newcastle case indicated that for the first 10 PV penetration scenarios, from 0% to 90% penetration level, there were no voltage limit (1.1 p.u.) violations at any Buses. *Figure 71* shows the Bus voltages at 90% penetration for the peak summer day. For the 100% PV penetration scenario, voltage limit violation was found to occur for Bus 13 to Bus 17. *Figure 72* shows Bus 17 voltage and duration of PV energy curtailment for this

scenario. The curtailment voltage threshold of 1.14 p.u. was never exceeded even for the 100% PV penetration scenario. Evidently, revision of the grid code from G83 to G98 and changing the disconnection threshold has had a positive impact on PV energy capture. Under G83's curtailment voltage threshold of 1.1 p.u., the aggregate annual energy curtailment between Bus 1 – Bus 17 would have been 15911 kWh.

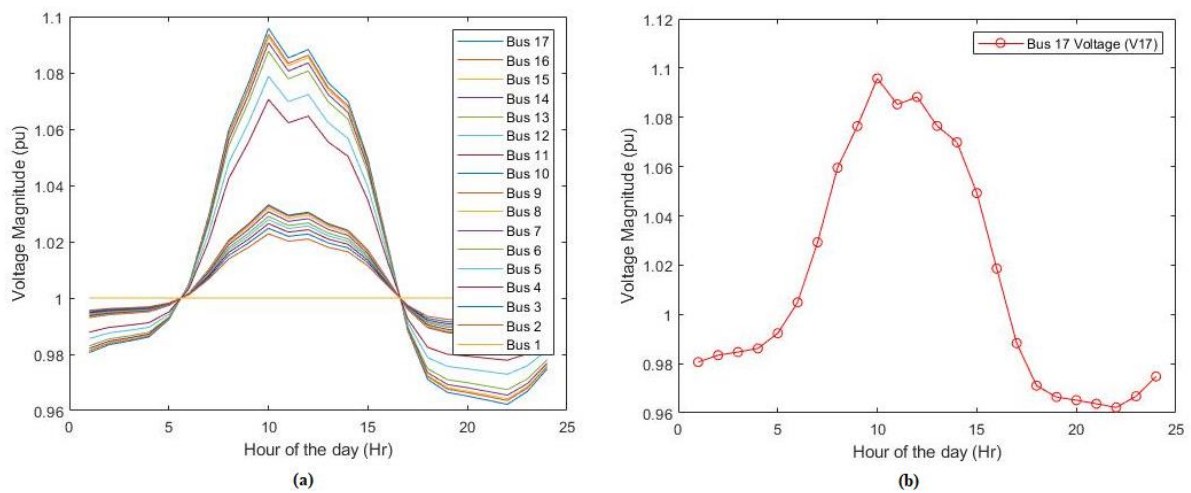


Figure 71 (a) Bus Voltages and (b) Bus 17 Voltage at 90% PV Penetration for the Newcastle Case During Peak Summer Day

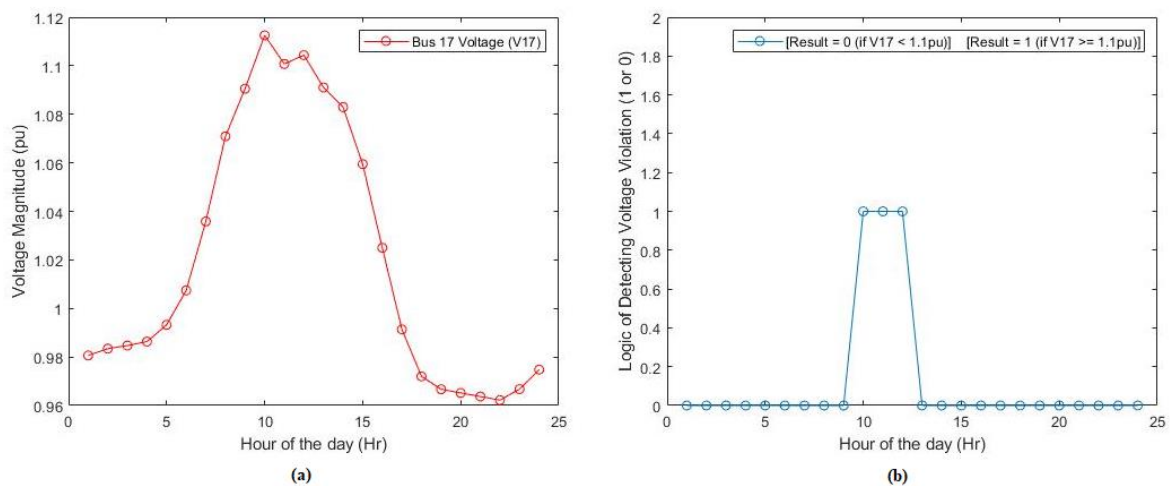


Figure 72 (a) Bus 17 Voltage and (b) Duration of Voltage Limit Violation at 100% PV Penetration for the Newcastle Case During Peak Summer Day

Mumbai Case

Simulation results for the Mumbai case indicated that for up to 40% PV penetration level there were no voltage limit violations at any Buses. Figure 73 shows the Bus voltages at 40% penetration for the peak summer day. Table 38 lists the Buses that were affected by voltage limit violations for each PV penetration scenario were violations occurred. Figure 74 shows the

voltages at all Buses for PV penetration levels from 50% to 100%. *Figure 75* and *Figure 76* shows Bus 17 voltage and duration voltage violation for the 50% and 100% PV penetration. The severity of voltage rise with increasing PV penetration is clearly evident. The threshold voltage of 1.14 p.u. was exceeded for scenarios with PV penetration level from 70% and above. *Figure 75* provides a summary of curtailment results.

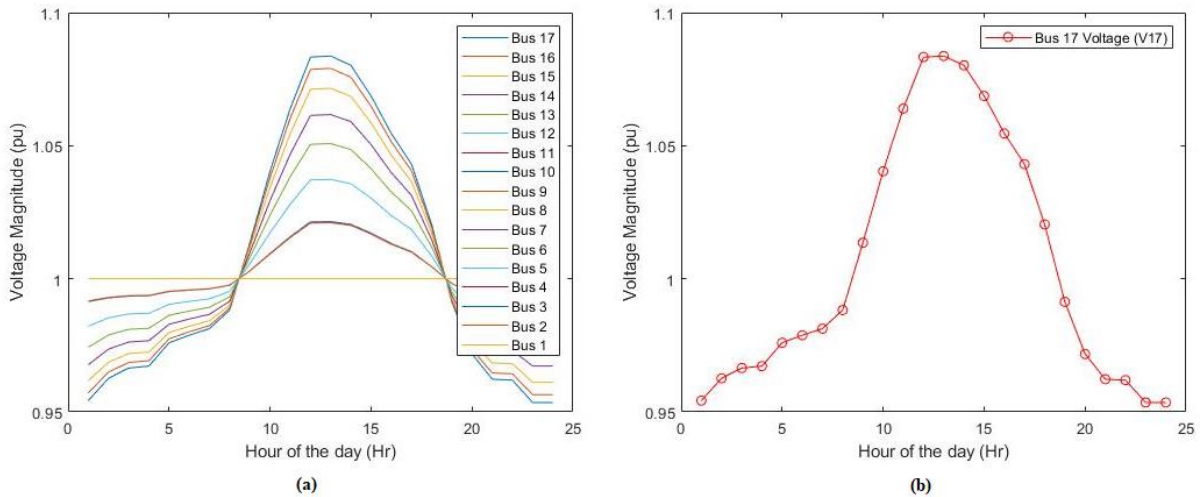


Figure 73 (a) Bus Voltages and (b) Bus 17 Voltage at 40% PV Penetration for The Mumbai Case During the Peak Summer Day

Table 38 – PV Penetration Level vs Buses with Voltage Limit Violation for The Mumbai Case During the Peak Summer Day

PV Penetration Level (%)	Buses with Voltage Violation (>1.1 p.u.)
50%	Bus 17
60%	Bus 15 to Bus 17
70%	Bus 14 to Bus 17
80%	Bus 13 to Bus 17
90%	Bus 13 to Bus 17
100%	Bus 12 to Bus 17

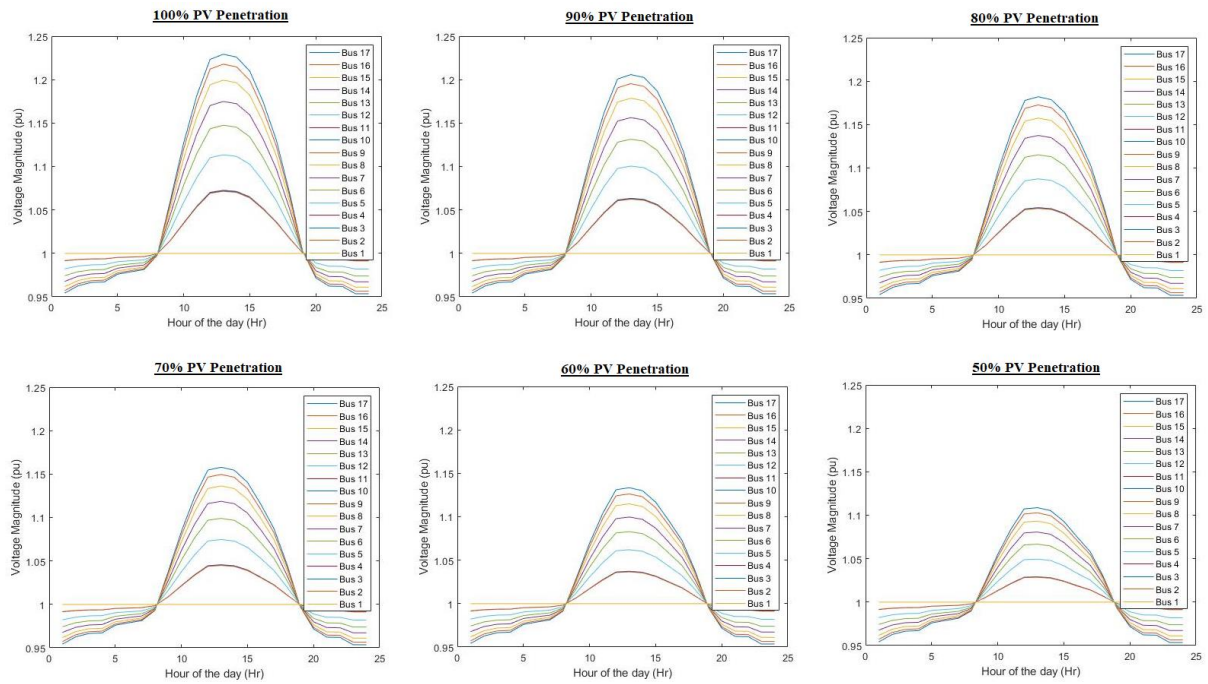


Figure 74 - All Bus Voltage for 50-100% PV Penetration Levels for the Mumbai Case During the Peak Summer Day

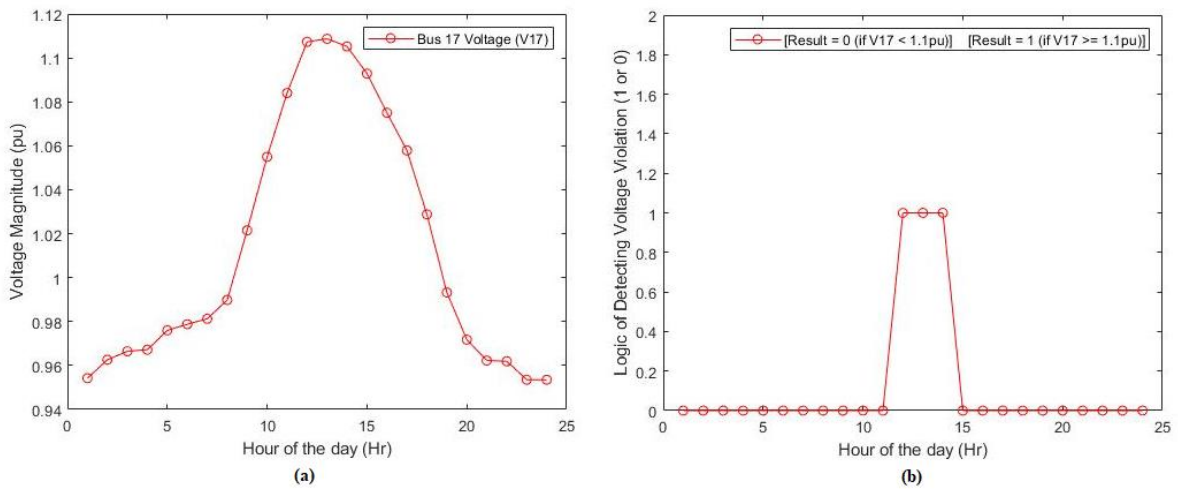


Figure 75 (a) Bus 17 Voltage and (b) Duration of Bus 17 Voltage Limit Violation at 50% PV Penetration for the Mumbai Case During the Peak Summer Day

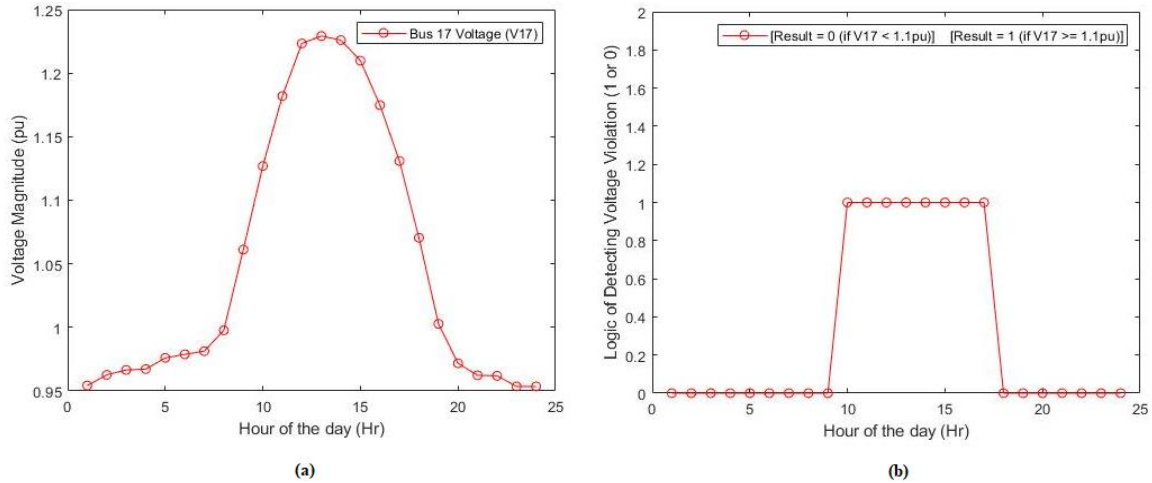


Figure 76 (a) Bus 17 Voltage and (b) Duration of Bus 17 Voltage Limit Violation at 100% PV Penetration for the Mumbai Case During the Peak Summer Day

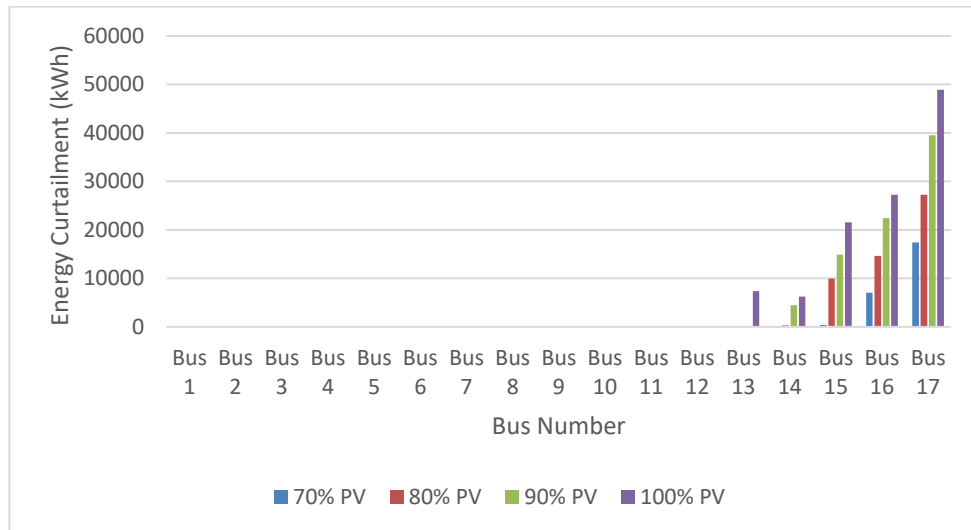


Figure 77 - Annual Energy Curtailment for the Base Case in Mumbai

For the typical meteorological year, the simulation results showed that Buses 15-17 were affected by PV energy curtailment when the PV penetration level exceeded 70%. Buses 14-17 were affected by PV energy curtailment when the PV penetration level exceeded 80%. And Buses 13-17 were affected by PV energy curtailment when the PV penetration level reached 100%. At 100% PV penetration the annual energy curtailment at Bus 17 is 48941 kWh which meant that 81% of the annual energy generation from the residential PV systems connected to the Bus will be curtailed. At 70% penetration, the respective curtailment value was 29% of the annual energy generation at the Bus. For PV systems connected to Bus 15, the curtailment was a mere 1% of the annual energy produced by the systems at 70% penetration. However, at 100% penetration the curtailment was 72% of the annual energy

produced by the PV systems connected to the Bus. For Bus 13, curtailment only happened for the 100% scenario. The aggregate energy curtailment at the Bus of 7381 kWh translated to approximately 24% of the annual energy yield of PV systems connected to the Bus being curtailed.

Yangon Case

Simulation results for the Yangon case indicated that for up to 30% PV penetration level there were no voltage limit violations at any Buses. At 40% PV penetration buses 16 and 17 were affected by voltage limit (1.1p.u.) violation. The violation at bus 17 lasted for 4 hours (11am to 2pm) peaking at 1.116 at 12pm. The violation at bus 16 lasted for 3 hours (12pm to 2pm) peaking at 1.11 then lowering to 1.105 at 1pm and lowering further to 1.101 at 2pm. The voltage limit violations at buses 16 and 17 at 40% PV penetration for the peak summer day are shown in Figure 78. Table 39 lists the Buses that were affected by voltage limit violations for each PV penetration scenario were violations occurred.

The first time the threshold voltage of 1.14 p.u. was exceeded was at 50% PV penetration when the threshold was exceeded at Buses 15, 16 and 17 and the peak voltage at Bus 17 was 1.177 p.u.. In the 100% PV penetration scenario all the buses from Bus 2 to Bu 17 exceeded the threshold voltage and were affected by PV curtailment. At 100% PV penetration the annual energy curtailment at Bus 17 is 136490 kWh.

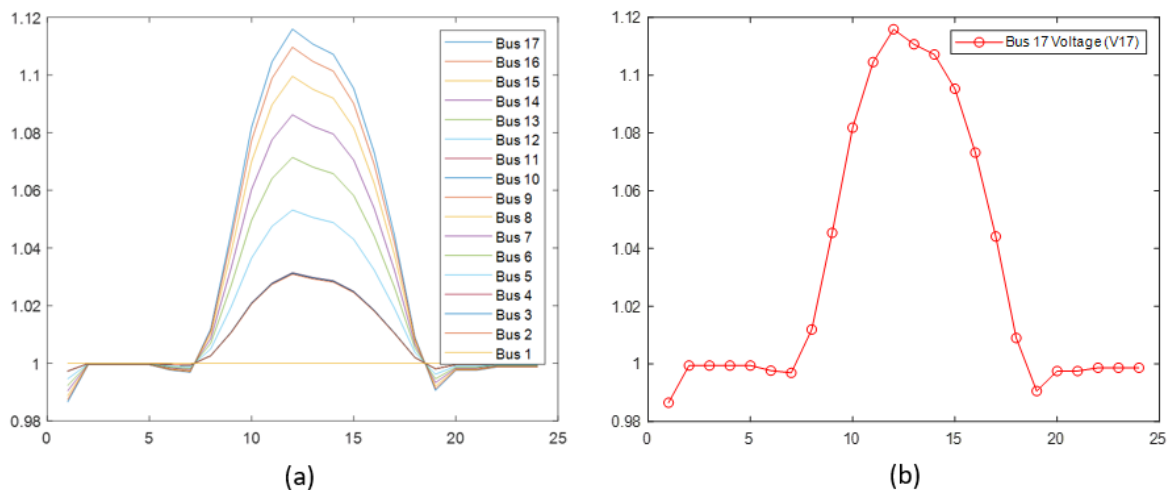


Figure 78 (a) Bus Voltage and (b) Bus 17 Voltage at 40% PV Penetration for The Yangon Case During Peak Summer Day

Table 39 - PV Penetration Level vs Buses with Voltages Greater Than 1.1 p.u. for The Yangon Case During the Peak Summer Day

PV Penetration Level (%)	Buses with Voltage Violation (>1.1 p.u.)
40%	Bus16 to Bus 17
50%	Bus 13 to Bus 17
60%	Bus 12 to Bus 17
70%	Bus 12 to Bus 17
80%	Bus11 to Bus 17
90%	Bus11 to Bus 17
100%	Bus9 to Bus 17

6.6.2 Case Scenario with Demand Side Management

Newcastle Case

Two DSM participation scenarios were considered. A high customer participation scenario considered 50% of the houses in the network participating in DSM. A lower customer participation scenario considered 15% of the houses in the network participating in DSM and is assumed to be a more accurate representation of current customer behaviour. PC-EYE (with DSM) algorithm was run with DSM program following the scheme in *Figure 65* for the flexible load categories Washing machine, Dishwasher and Electric water heating as described previously.

It can be seen from *Figure 78* that the voltage violation at the most sensitive Bus (Bus 17) was fully compensated by the DSM program when 50% of the houses in the network participated in DSM. However, 15% of houses participating in DSM was not able to fully compensate the voltage limit violation as can be seen from *Figure 79*. The duration of voltage violation, however, was shortened. Voltage violation at 11 AM was eliminated but those at 10AM and 12 noon remained.

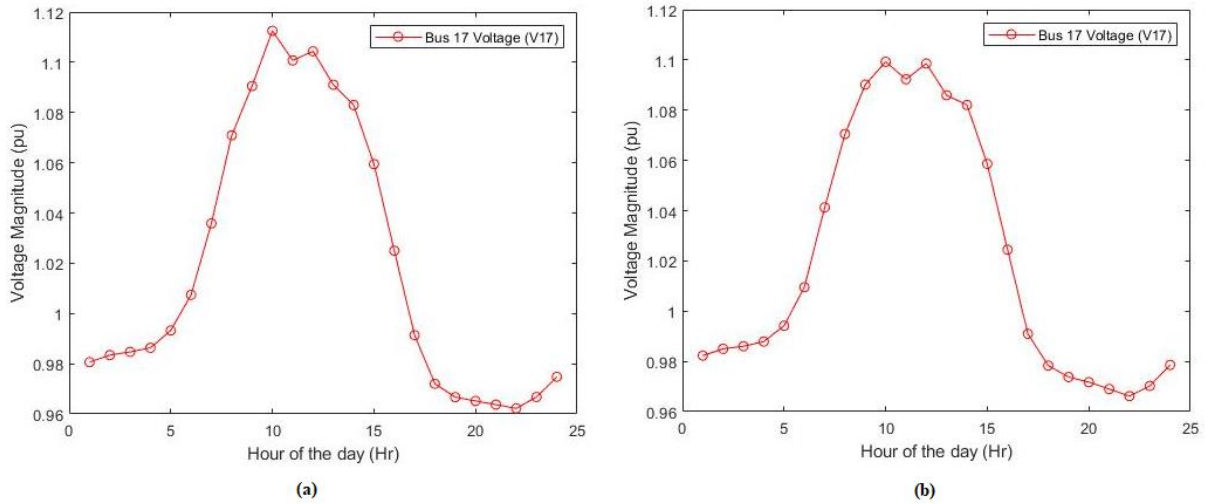


Figure 79 - Bus 17 Voltages for the Newcastle Case at 100% PV Penetration During Summer (a) Base Case and (b) With 50% Housing Participation in DSM Program

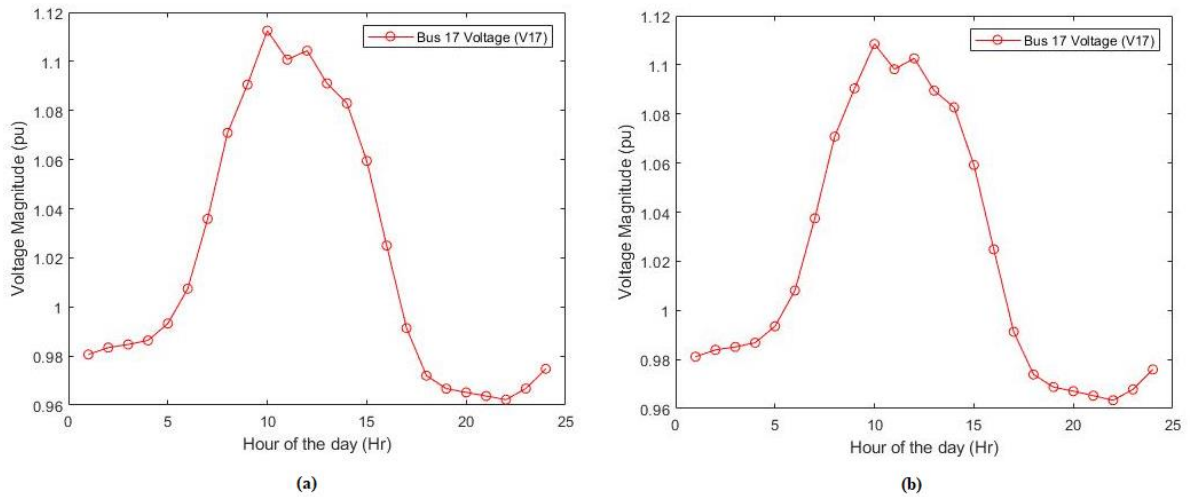


Figure 80 - Bus 17 Voltages for the Newcastle Case at 100% PV Penetration During Summer (a) Base Case and (b) With 50% Housing Participation in DSM Program

Mumbai Case

A high and a low DSM participation scenario were considered as in the case of Newcastle with 50% and 15% housing participation, respectively. Results showed that DSM had minimal impact for the Mumbai case. Figure 80 compares Bus 17 voltage with 50% DSM participation to the Base case for 70% PV penetration, which was the minimum penetration level to have energy curtailment in the Base case. There is no impact on voltage violation and PV energy curtailment was not compensated. Figure 81 and Figure 82 show the aggregate annual energy curtailment for all Buses with 15% and 50% DSM participation. There is very little improvement from the Base case curtailment shown previously in Figure 77. Despite being the comparatively easier to realise solution for India, DSM did not prove to be an effective solution for maximising PV energy capture. This is due to the high solar

resource of India. While the residential distribution network in Newcastle is based on copper cables, the system in Mumbai utilises aluminium overhead conductors. This difference in network topology, also means that Mumbai is more susceptible to voltage limit violations under high PV penetration.

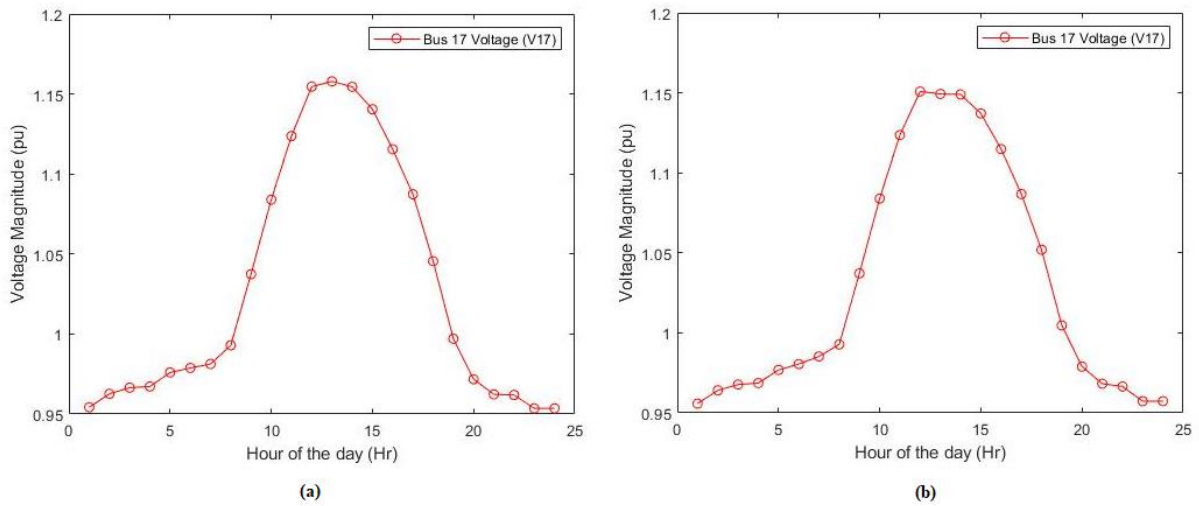


Figure 81 - Bus 17 Voltages for the Mumbai Case at 70% PV Penetration During Summer (a) Base Case and (b) With 50% of Housing Participation in DSM Program

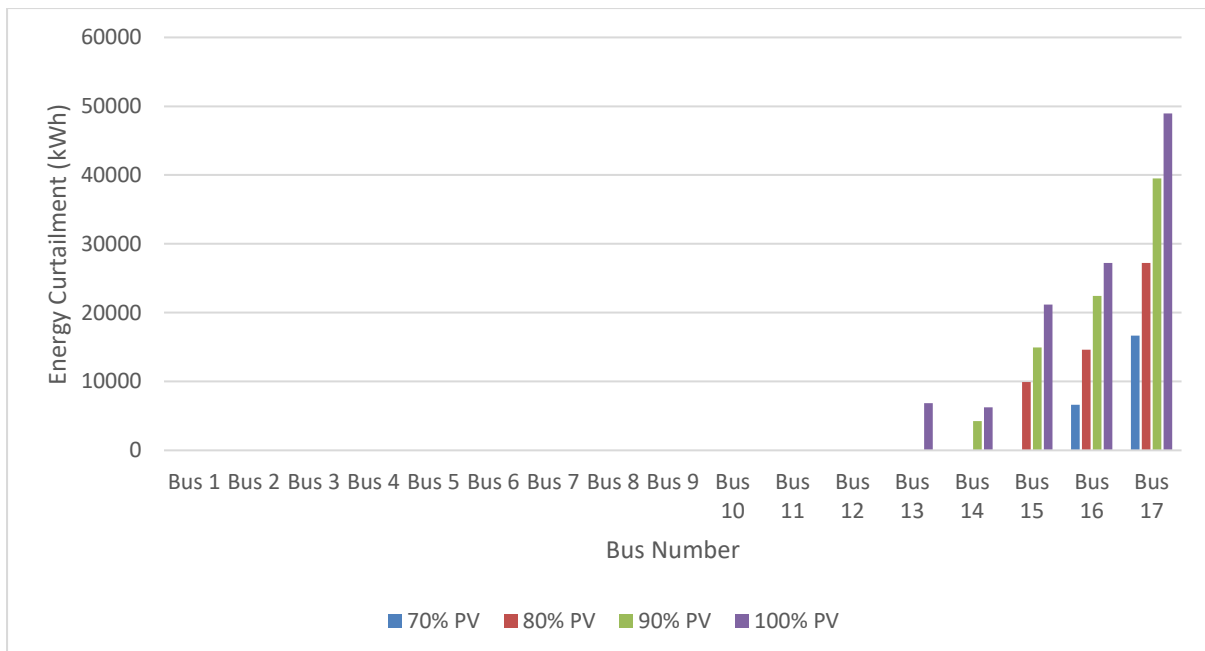


Figure 82 - Annual Energy Curtailment for the Mumbai Case with 15% Housing Participation in DSM

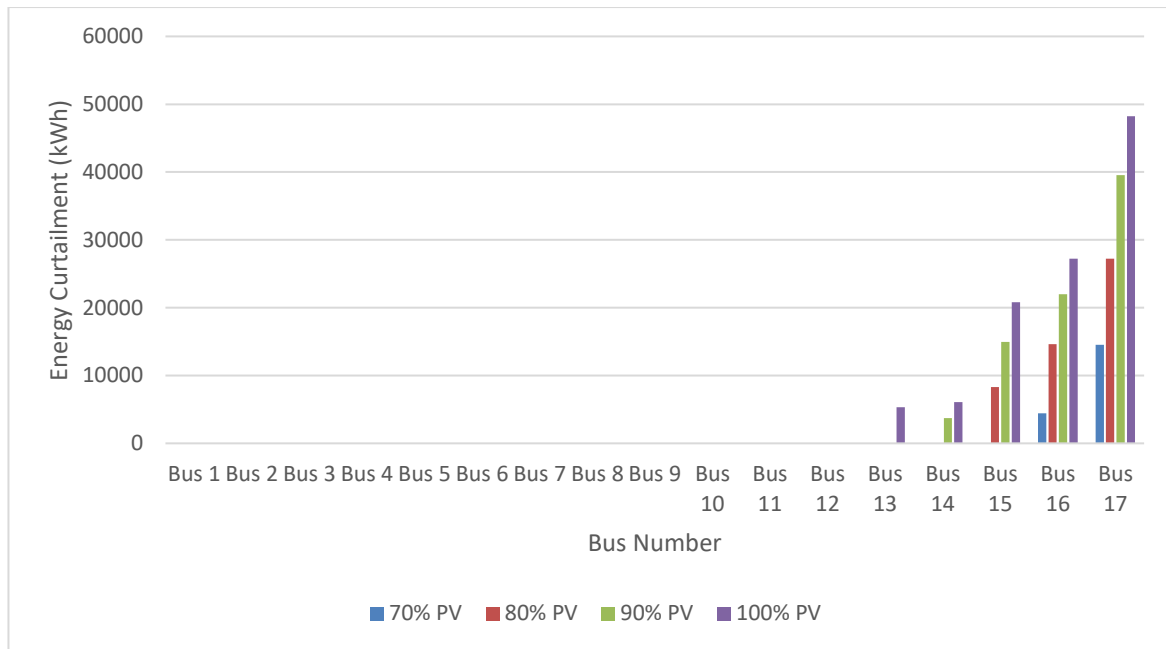


Figure 83 - Annual Energy Curtailment for the Mumbai Case with 50% Housing Participation in DSM

Yangon Case

For the Yangon case a high and a low DSM participation scenario of 15% and 50% was again considered. As with the Mumbai case results showed that DSM had minimal impact even for the high (50%) participation scenario. This can be seen in *Figure 84* which compares Bus 17 voltage for the base case to the 50% DSM participation for 40% PV penetration, which was the minimum penetration level where the voltage level surpassed 1.1 p.u. in the base case. The lack of impact of DSM can be clearly seen in *Table 5* which compares the voltage level at bus 17 when the level surpassed 1.1 p.u. in the base case when the PV penetration was set at 40%.

Even at the higher participation scenario of 50% DSM participation curtailment at bus 17% when the PV penetration was 100% was unchanged. At 100% PV penetration 50% DSM was only able to lower the curtailment over the whole network of 17 busses by 5.56%. This was because as with the Mumbai the network topology was more susceptible to voltage limit violations under high PV penetration than the Newcastle topology.

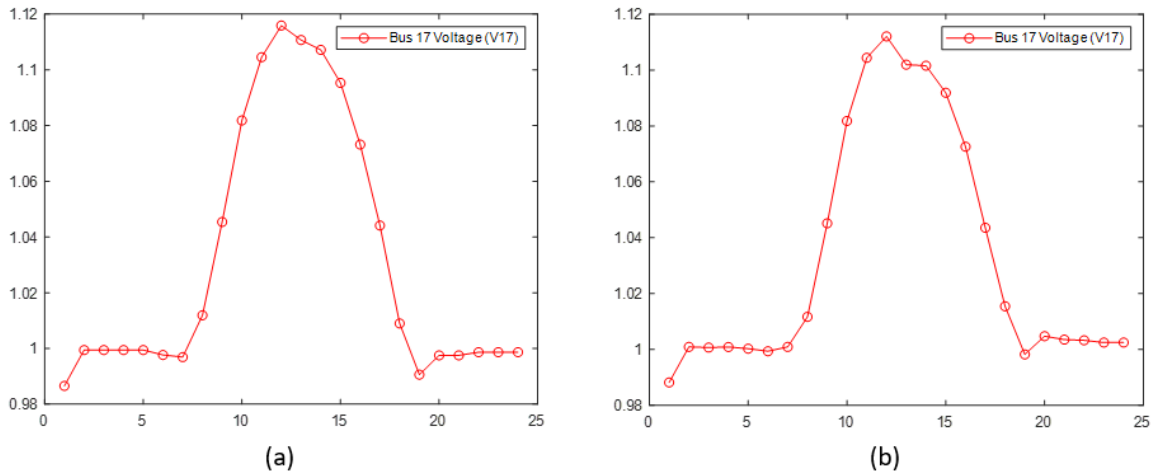


Figure 84 - Bus 17 Voltages for the Yangon Case at 40% PV Penetration During Summer (a) Base Case and (b) With 50% of Housing Participation in DSM Program

Table 40 - Comparison of Voltage Levels for Bus 17 in the Yangon Network When PV Penetration was 40%

Time	Voltage Level (p.u.)		
	Base Case	15% DSM Case	50% DSM Case
11am	1.105	1.105	1.104
12pm	1.116	1.115	1.112
1pm	1.111	1.108	1.102
2pm	1.107	1.106	1.102

6.6.3 Case with Demand Side Management and Active Voltage Control

Newcastle Case

Results from running the PC-EYE algorithm with DSM and AVC with 15% housing participation in DSM not only shortened the duration of voltage violation, but also fully compensated it. Figure 83 shows all Bus voltages. Bus 17, where there was voltage limit violation even with DSM, showed no violation when AVC was combined with DSM. The combination of AVC and DSM is found to be efficient in fully eliminating voltage violations for the Newcastle network for the worst-case high PV penetration scenario.

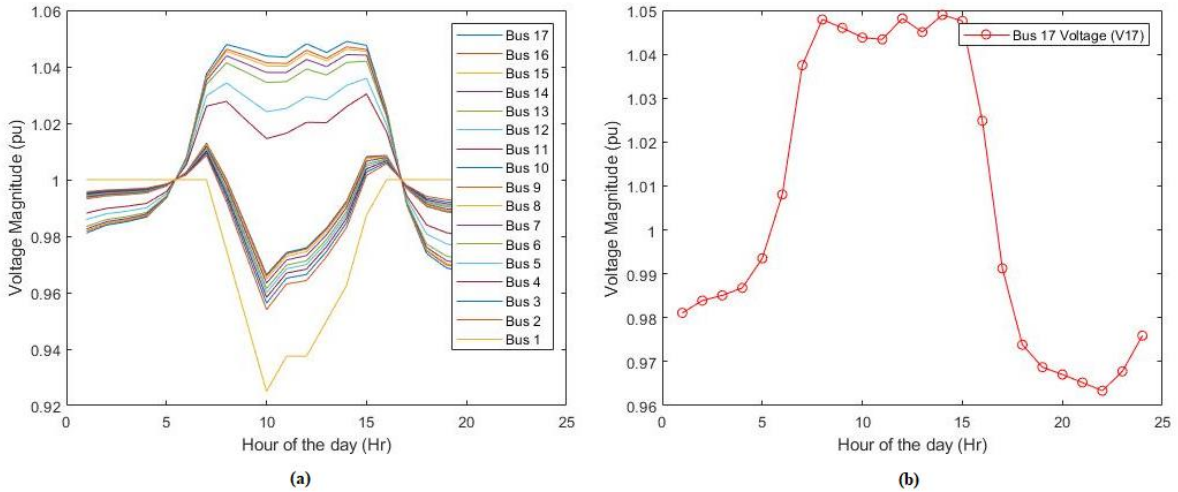


Figure 85 (a) Bus Voltages and (b) Bus 17 Voltage at 100% PV Penetration for the Newcastle Case During Peak Summer with 15% Housing Participation in DSM and AVC

Mumbai Case

Results from running the PC-EYE algorithm with DSM and AVC with 15% housing participation in DSM for 70% - 100% PV penetration is shown in Figure 86 - Figure 90. The OLTC tap change action by the AVC program and its impact on voltage profiles is evident from the figures. It was identified from earlier simulations that DSM had minimal impact on clearing voltage violation and reducing PV curtailment for Mumbai. Figure 86 and Figure 87 shows that up to 80% PV penetration can be accommodated in the Mumbai case study network without voltage limit violation or PV energy curtailment, by combining AVC with DSM.

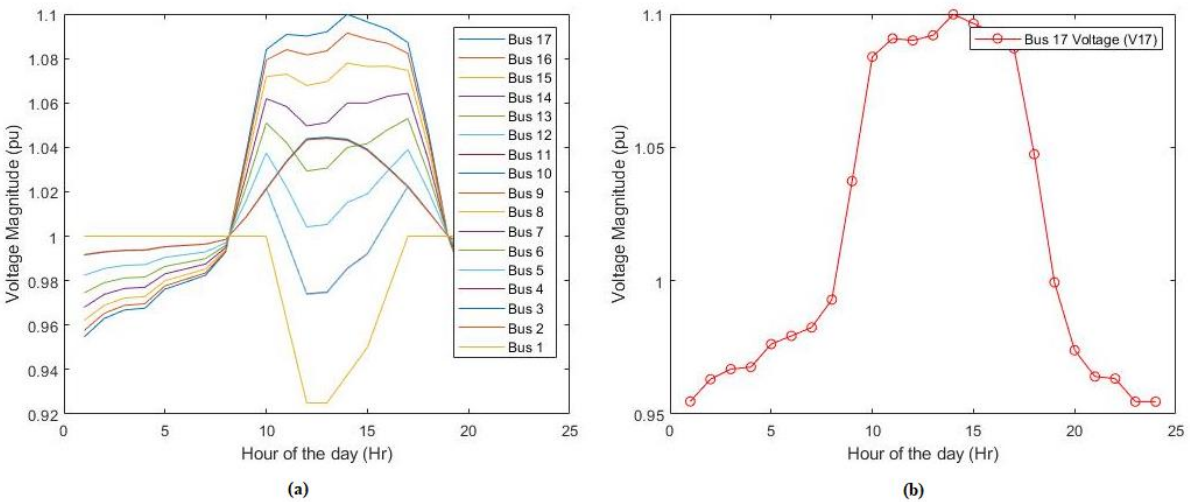


Figure 86 (a) Bus Voltages and (b) Bus 17 Voltage at 70% PV Penetration for the Mumbai Case During Peak Summer with 15% Housing Participation DSM and AVC

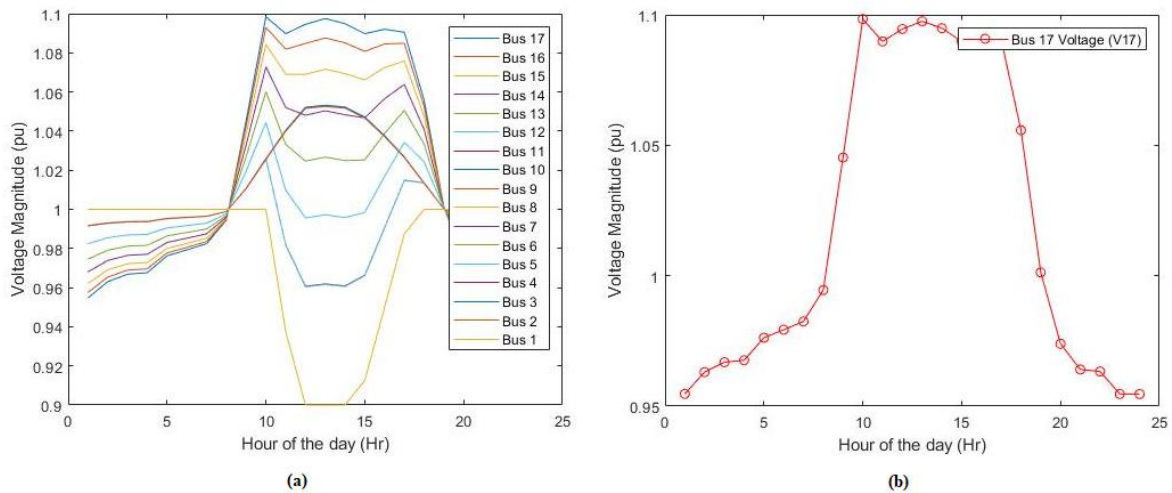


Figure 87 (a) Bus Voltages and (b) Bus 17 Voltage at 80% PV Penetration for the Mumbai Case During Peak Summer with 15% Housing Participation DSM and AVC

It can be seen from Figure 88 that when the PV penetration is 90% in Mumbai network voltage violation still existed at Bus 16 and 17 for which voltages were greater than 1.1 p.u. However, the duration of voltage violation was shortened. All Bus voltages were less than curtailment threshold voltage of 1.14 p.u. Consequently, combining DSM with AVC was able to eliminate PV energy curtailment in the network completely even at 90% penetration. This can only be the impact of AVC, as it was evident from simulations in the previous section that DSM alone had minimal impact for the Mumbai case.

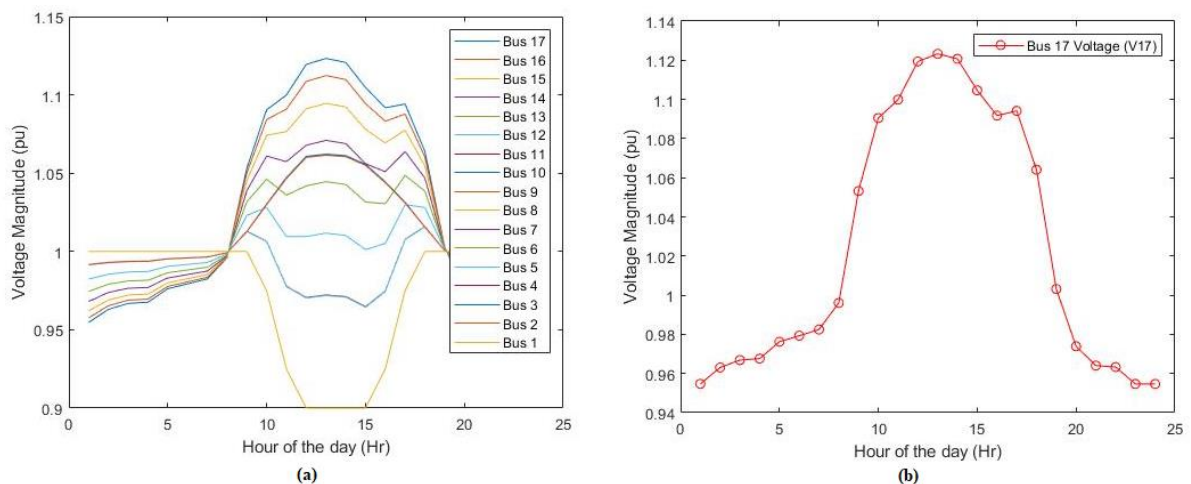


Figure 88 (a) Bus Voltages and (b) Bus 17 Voltage at 90% PV Penetration for the Mumbai Case During Peak Summer with 15% Housing Participation DSM and AVC

In contrast to the results at 90% PV penetration, voltage limit violation and PV energy curtailment remained when PV penetration was at 100%. As seen in Figure 86, Buses 15-17 were affected by voltage limit violation even with AVC and DSM. Only Bus 16 and 17 voltages were above the curtailment threshold. It can be seen from Figure 87 that the duration

of voltage limit violation was considerably reduced when AVC was applied with DSM. Impact of OLTC hitting tap limits during AVC is evident from voltages of Buses close to OLTC in Figure 84.

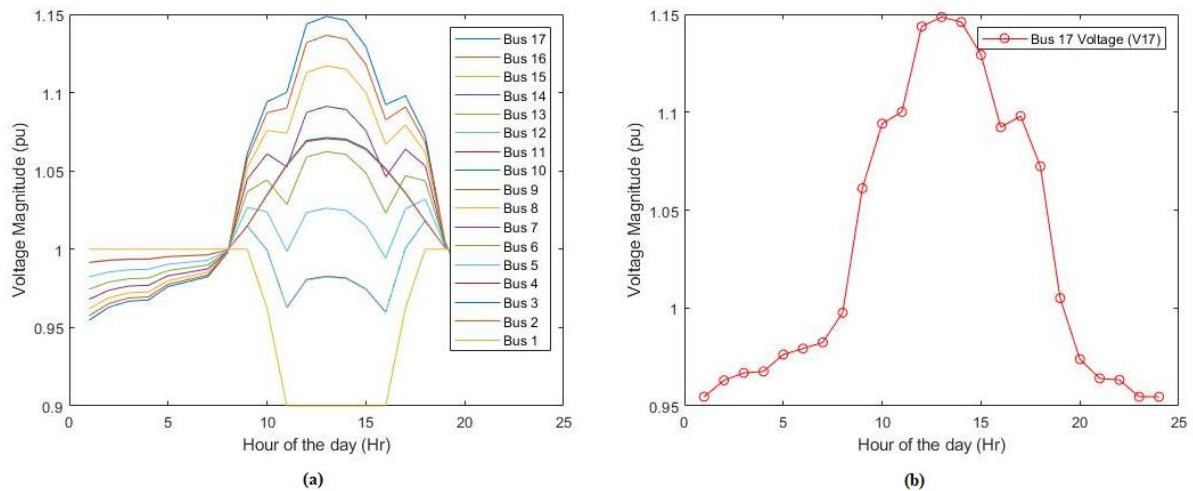


Figure 89 (a) Bus Voltages and (b) Bus 17 Voltage at 100% PV Penetration for the Mumbai Case During Peak Summer with 15% Housing Participation DSM and AVC

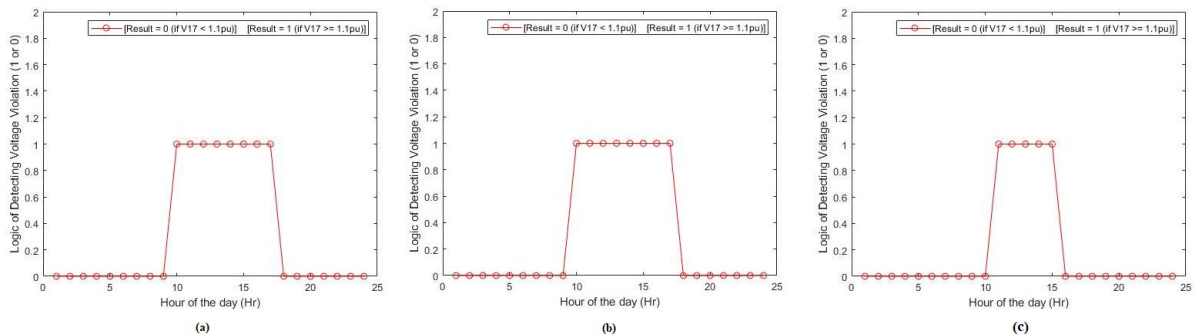


Figure 90 - Duration of Bus 17 Voltage Violation for the Mumbai case at 100% PV Penetration During Peak Summer (a) Base, Case, (b) 15% Housing Participation DSM and (c) 15% Housing Participation DSM and AVC

As shown in Figure 89 there is a significant reduction in the amount of PV energy curtailed in a year when AVC was applied in combination with DSM. DSM in this case was with 15% housing participation. The curtailment that still existed at 100% PV penetration with 15% DSM and AVC was only at Buses 16 and 17. Annual energy curtailed was 1,208.4 kWh at Bus 16 while it was 13,706.8 kWh at Bus 17. For a typical PV system connected to Bus 17, curtailment was around 23% of its annual energy yield, whereas the value was at 80% for the Base case without DSM and AVC. The base case (refer to Figure 77) also had curtailment from Bus 13 onwards. At 100% PV penetration, the aggregate annual energy curtailment in the LV network with 15%DSM and AVC was 110470.6 kWh. When the higher participation scenario, with 50% houses participating in DSM was considered along with

AVC, the reduction in aggregate annual energy curtailed in the LV network from PV systems at 100% penetration was a mere 2.5%. This is indicative of AVC being more effective than DSM for the Indian network and solar resource conditions. *Table 41* summarises the aggregate annual PV energy curtailment in the LV network for the Mumbai case for all scenarios where curtailment occurred.

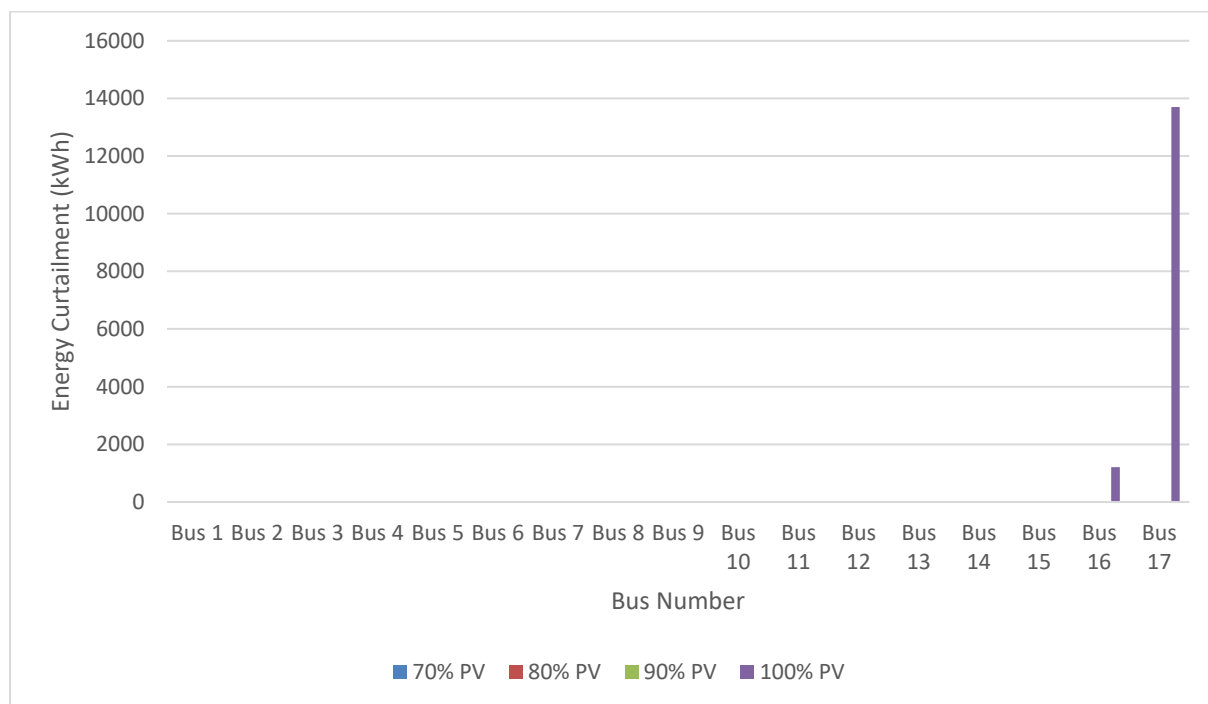


Figure 91 - Annual Energy Curtailment for the Mumbai Case with 15% Housing Participation DSM and AVC

Table 41 - Summary of Aggregate Annual PV Energy Curtailment in the LV Network for the Mumbai Case

Scenario	Total PV Energy Curtailment in Base Case (kWh)	Total PV Energy Curtailment with 15% DSM (kWh)	Total PV Energy Curtailment with 50% DSM (kWh)	Total PV Energy Curtailment with 15% DSM + AVC (kWh)
70% PV Penetration	24802.9	23270.3	18945.6	0
80% PV Penetration	52129.6	51808.9	50161.2	0
90% PV Penetration	81338	81159.7	80179.7	0
100% PV Penetration	111380.2	110470.6	107690.5	14915.2

It is clear that the houses connected to buses which are far away from the main grid source may not harvest as much energy from their own PV systems because of the shut-down time

of their PV inverters when the voltage exceeds a certain limit of 1.14pu. DSM and AVC aids maximisation of energy capture because of the reduction in curtailment. The average amount of financial loss prevented because of the reduction in curtailment can be calculated as [395]:

$$\text{Equation 11 – Prevented Annual Financial Loss}$$

$$\text{Prevented Financial Loss (per year)} = \text{Amount of curtailment reduced} \times \text{Electricity Unit Price}$$

The reduction in curtailed energy means more power is consumed from the PV system rather than from the grid source. Prevented financial loss is therefore because of the reduction in grid import. Cost of a kWh of electricity in India on average is INR 6.034 [396]. Table 42 summarises the prevented financial loss at different PV penetration levels for the Mumbai case when 15% DSM is used in combination with AVC.

Table 42 - Prevented Financial Loss at Different PV Penetration Levels for the Mumbai Case

Bus	Prevented Financial Loss per Year in INR			
	70% PV	80% PV	90% PV	100% PV
13	-	-	-	8907.13
14	-	968.99	13426.28	18838.27
15	427.37	12004.53	18017.37	26044.37
16	7083.39	14725.33	22557.68	26171.31
17	10502.38	16426.36	23852.5	21258.64

Given the economic situation and consumer purchase power index in India, the financial savings to customers with DSM and AVC is significant. As voltage limit violations and reverse power flow are reduced and consequently the negative impact on network assets are limited, networks would be able to manage operations with the aging assets. Increasingly, electricity utilities are penalised for carbon emission and are given long term carbon emission reduction targets. Hence, there is also significant potential for avoided costs from the side of utility if renewable generation such as PV are maximised by means of these smart grid solutions. However, the actual value of avoided costs will depend on the nation's energy policies.

Yangon Case

Results from running the PC-EYE algorithm with DSM and AVC with 15% housing participation in DSM for 50% - 60% PV penetration are shown in Figure 92 and Figure 93. The OLTC tap change action by the AVC program and its impact on voltage profiles is

evident from the figures. Previous simulations showed that DSM alone had minimal impact on preventing voltage violations and PV curtailment in the Yangon case study. However, it can be seen in *Figure 92* that AVC successfully prevent any PV curtailment at 50% penetration by stopping the voltage limit violations that had occurred at Buses 15 to 17 that had occurred in the base case scenario.

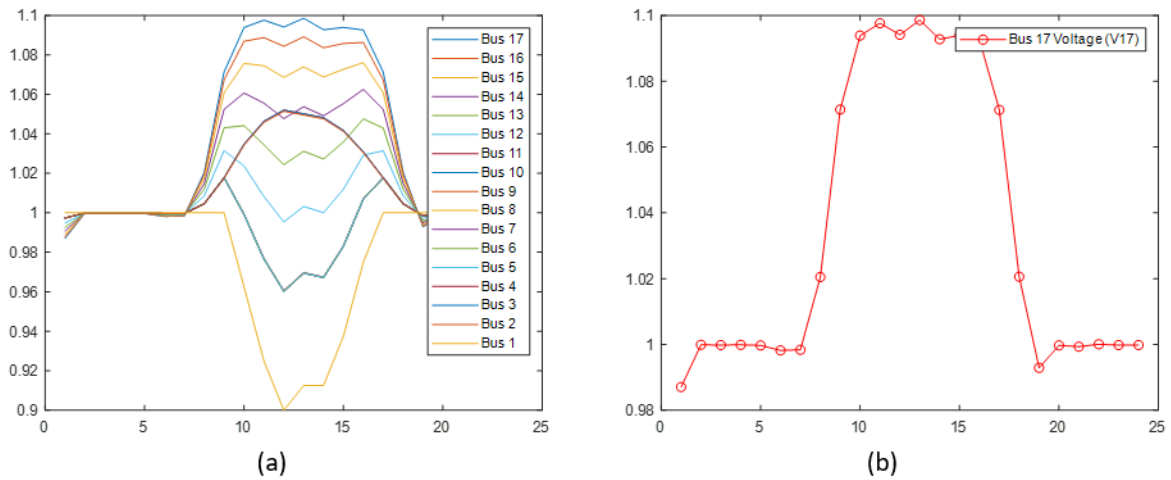


Figure 92 (a) Bus Voltages and (b) Bus 17 Voltage at 50% PV Penetration for the Yangon Case During Peak Summer with 15% Housing Participation DSM and AVC

From *Figure 93* it can be seen that at 60% PV penetration in the Yangon case study AVC was not successful in preventing PV curtailment at the buses in the network. However, AVC did reduce the number of buses that had to curtail PV output. In the base case scenario curtailment occurred at buses 13 to 17. AVC reduced this to buses 16 to 17.

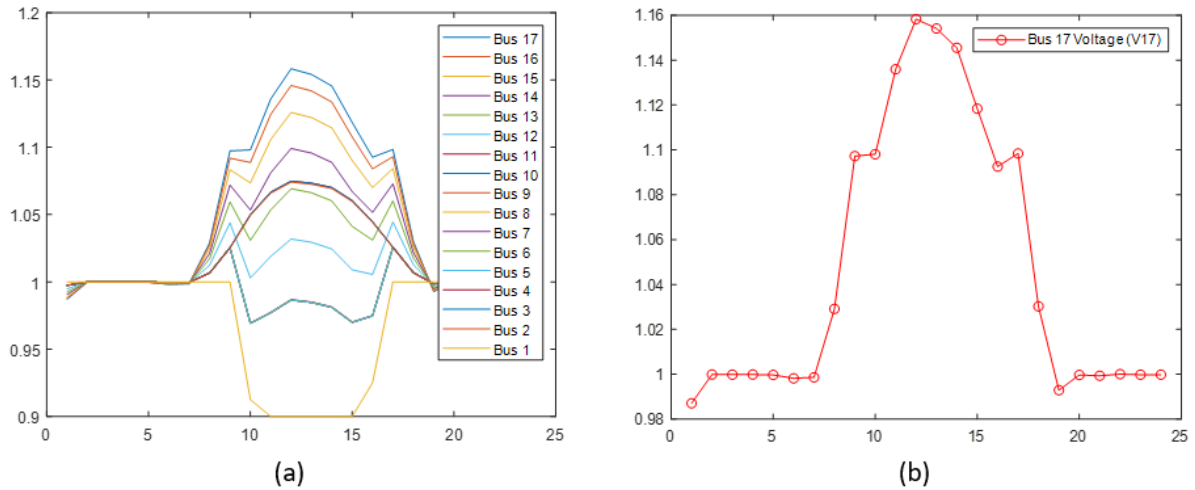


Figure 93 (a) Bus Voltages and (b) Bus 17 Voltage at 60% PV Penetration for the Yangon Case During Peak Summer with 15% Housing Participation DSM and AVC

Table 43 compares the busses that exceeded the threshold voltage of 1.14 and where therefore subject to PV curtailment in the base case scenario and the case scenario of 15% DSM and AVC for all the penetration levels that suffered from PV curtailment in the base case of Yangon city. From Table 8 it can clearly be seen that AVC reduced the number of buses that would be subjected to PV curtailment in all the PV penetration scenarios where curtailment occurred in the base case of Yangon.

Table 43 - Comparison of Threshold Voltage Violations for the Base Case and AVC Scenarios of Yangon for Penetration Levels of 50 – 100%

PV Penetration Level (%)	Buses That Exceed Threshold Voltage (>1.14 p.u.)	
	Base Case	AVC Case
50	Bus15 to Bus 17	none
60	Bus 13 to Bus 17	Bus 16 to Bus 17
70	Bus 12 to Bus 17	Bus 14 to Bus 17
80	Bus 12 to Bus 17	Bus 13 to Bus 17
90	Bus2 to Bus 17	Bus6 to Bus 17
100	Bus2 to Bus 17	Bus4 to Bus 17

The Yangon case study used the same model of a typical South-East Asian distribution network used in the Mumbai case study. Due to their geographic locations Yangon and Mumbai have similar climatic conditions. This meant that the output of the PV systems modelled in the two case locations was similar in terms of their annual output and daily and monthly profiles. However, in the Yangon case study AVC was not as successful in preventing PV curtailment compared to the Mumbai scenario. This was because the PV

system used in the scenarios was oversized for the lower load demands of Yangon causing the voltage violation to be more severe and therefore more difficult to prevent.

The findings of the case studies highlighted the importance of accurate information in technical studies and the impact of load profiles on the results of such studies.

6.7 Conclusions

The results of this work showed that the recent upgraded policies and grid codes implemented by the UK had facilitated higher energy capture from renewable like PV. The increase in the voltage-based curtailment threshold brought about the move from grid code G83 to G98 prevented the need for any PV energy curtailment in the UK based study even without any smart-grid solutions in place. They also showed that whilst DSM could be a preferred smart-grid solution for preventing PV curtailment because of its potential for holistic deployment via demand response schemes for many countries in the global south, technically the combination of the weaker LV networks in the region with significantly higher solar resources meant that it is not effective in preventing PV energy curtailment. The results indicated that the combination of DSM and AVC could be deployed to extend the PV penetration level before curtailment occurred for locations in the global south. They also showed that whilst the combination of DSM and AVC could not completely prevent PV curtailment at the highest PV penetration levels the combination could still reduce the amount of curtailment at all PV penetration levels leading to greater financial profitability of future PV projects.

Chapter 7

Conclusions

As mentioned in the Introduction chapter, the main aim of this work is to support scenario-based impact assessments for power system planning by means of ANN and thus aid sustainable energy policymaking, especially for developing countries. The main conclusions drawn from the PhD work and suggestions for future work are described below.

7.1 Transition to a Sustainable Energy Future

Energy has played a fundamental role throughout history in human development [16]. Today it affects all aspects of human life. Electricity is the most important form of energy in the modern world [47], and it is a widely held belief that electricity consumption is the engine of modern economic growth, especially in developing countries. The validity of this belief has been demonstrated by China's rapid economic growth since the 1970s. It has also been shown that there is a symbiotic relationship between economic growth and energy consumption. Whilst energy is a vital component in the early stages of economic growth, economic growth leads to ever greater energy consumption. This symbiotic relationship can clearly be seen in the global south where electricity demand is increasing exponentially as many governments in the region follow the Chinese model for economic development and try to increase low levels of access to electricity. The importance of electricity to social and economic development means that demand is predicted to continue to grow by 45% between 2015 and 2030 and by over 300% by the end of the century [18].

Meeting the predicted increase in demand for electricity is one of the most important global issues today [23]. Fossil fuels have been the dominant energy source in the electricity generation sector since the industrial revolution and are still heavily relied upon today. Whilst energy consumption from fossil fuels leads to economic and social growth it also leads to environmental degradation most notably in the form of significantly increased greenhouse gas emissions (most notably CO₂) which leads to climate change [47, 124]. Therefore, organisations such as the IEA have stated that current trends in fossil fuel demand are patently economically, environmentally and socially unsustainable [53].

Today the international community are collectively working towards limiting the use of fossil fuels with the aim of transitioning to a sustainable decarbonised future [50]. Indeed, the

global sustainable energy agenda has become the primary challenge for many developed and developing countries [19]. Policy makers and energy experts around the world all agree that renewable energy sources and smart grid technologies are the best candidates to facilitate the transition to a sustainable energy paradigm [149, 201].

The transport sector is the second largest CO₂ emitter in the world, behind electricity generation [120]. It is also the only major sector where global GHG emissions are continually rising year on year in developed regions such as the EU [176-177]. Therefore, current research points to the importance of the role the transport sector also needs to play in mitigating climate change [177]. Electrification is regarded as the best strategy for decarbonising the transport sector [179]. As road vehicles are the main cause of GHG emissions in the sector policy makers around the globe such as the EU have focused their attention in recent times on electrifying road transport, in particular PLGs [145]. To fully utilise the environmental benefits of the electrification of the transport sector replacing fossil fuels with low-carbon energy sources such as renewable energy sources in the electricity fuel mix has been identified as essential [90, 207].

Increasing demand due to economic development programs and the transfer of the energy needs of the transport sector poses a major challenge for network operators and their aging and overworked systems [37, 179]. The proliferation of electric vehicle charging and renewable energy applications such as rooftop PV systems will also lead to dramatic changes to the behaviour and peaking characteristics of load (electrical demand) profiles particularly at the distribution level [397]. This change in behaviour brings new regulatory, economic and technical challenges to network operators and other stakeholders [397-400].

To overcome the challenges faced by network operators caused by the transition of the electricity sector accurate information is essential to allow proper allocation of funds and resources [160]. Accurate predictions of the future energy demand and its patterns are one of the most vital components of this information [16]. Normally these predictions would be made using historical data and trends [16]. However, renewable energy sources and electric vehicles are relatively new to the area and therefore there is insufficient historical data available to predict how they will influence future energy demand patterns. Therefore, it was clear from the review of literature undertaken that new techniques for predicting future energy use need to be investigated and refined to provide the accurate information required to support the energy transition. Accurate information on future energy demand profiles is

critical to network operators and other industries such as PV manufactures who require the information to evaluate and improve integration of their systems on to networks [247-248]. Accurate profiles are also needed to allow 'intelligent' vehicle charging to occur [37].

7.2 Load Forecasting

Load profiles are indispensable in the decision-making process of power transmission and distribution companies. The energy flow of electricity networks will inevitably become significantly more complex in the near future as the integration of modern-day technologies such as consumer-side renewable generation and electric vehicle charging gathers pace. The restructuring of electricity networks means accurate load profiles are increasing important [219]. Traditional methods of creating load profiles that rely on historical data will not be suitable for modelling the increasingly complex electricity networks of the future. Hence it has become important to develop suitable new load profile generation methodologies that rely on publicly available data that can be used to aid different network related analyses by operators.

The exact penetration levels of consumer-side technologies such as PVs and EVs in the future energy demand mix is presently uncertain. The charging profiles of different EV technologies is also evolving as EV technology is evolving. Hence it is important to have a scalable method that can generate future load profiles under different PV and EV penetration levels. As there is a step change in load the objective should not be to generate future load profiles based on historic datasets of load, but to use standardised load profiles and load/generation-weather relationships.

As a feasibility study, a computational method that is suitable for modelling the increasingly complex power networks of the future and could replace traditional load forecasting methods was presented to the 5th International Conference on Renewable Energy: Generation and Applications (ICREGA) in February 2018 (publication #1). The computational method chosen was the artificial intelligence technique artificial neural network (ANN). ANN was chosen as they have a proven ability to learn the complex nonlinear function mapping without the need of explicit mathematical formulation [157, 200, 237, 239, 249]. They have also displayed a high level of accuracy in forecasting scenarios in previous research [227, 237, 245-246].

The performance of the ANN model presented at the 5th ICREGA was compared to multiple linear regression (MLR) – a common prediction model. A comparison of results from the

ANN model against those using MLR demonstrated the superior performance of the ANN through the use of a case study for a targeted region in the UK. After training using publicly available data the ANN was able to synthetically generate load profiles with a mean absolute error (MAE) of 0.0349 when presented with data it had no a priori knowledge of over a full range of EV and PV penetration scenarios. This compared to the MLR models MAE of 0.1959. The experimental results of this study also showed that the ANN model performed with an accuracy of approximately 79% compared to the MLR model accuracy of approximately 15%. The experimental results show that the ANN model had the ability to capture non-linear relationships even when trained with limited data from publicly available sources. They also proved the feasibility of ANN models to synthesis future load profiles under increasing levels of PV generation and EV charging on distribution networks.

7.3 Renewable Energy Potential

China has experienced rapid economic growth and development with an average GDP growth rate of 9.8% since the Chinese Economic Reform (CER) in 1978, a rate far higher than the rest of the world [258]. The CER moved China away from a centrally planned (mostly agricultural) socialist system to a market-orientated system [277-278]. The move to a market-oriented system triggered the economic development of China which was supported by an increase in electricity consumption [258]. Due to the symbiotic relationship between economic growth and energy consumption electricity demand in China has continued to grow in the decades since the CER [265, 281]. The electricity that has powered China's economic development has been fuelled by vast amounts of fossil fuels [284].

Developing nations in the global south have looked closely at the symbiotic relationship between electricity consumption and economic growth in China. However, in lessons learnt from the Chinese case study governments are exploring other energy sources which have the potential to facilitate economic development in a more sustainable way to fossil fuels. Renewable technologies allow the three core dimensions of energy sustainability to be met, and many global south countries have large indigenous renewable resources such as PV. Due to these reasons countries in the global south are planning to exploit their renewable energy potential to meet their energy needs to facilitate ambitious economic development programs.

Yangon City, Myanmar was used as a case study to investigate the suitability of PV to meet the increasing electricity needs of developing countries in the global south. The case study

was also used to determine the impacts on current and future electricity demand profiles to aid system planning.

The case study used free to use software to generate accurate PV output profiles and publicly available data was used to generate realistic electricity load profiles for the case study location. This data was used to examine the diurnal variation in PV output and the effects of this variable output on local load demand profiles over the course of a year. The study also covered the first 10 years operation of the PV system to allow the effects of system degradation and annual load demand increases to be investigated.

The results showed that there was high correlation between the PV output and load demand. In the first year of the PV systems operation there was a 71% match between load and output. This was because the load profiles used in the study assumed that the majority of electricity demand in Yangon city would be used for basic needs such as cooling, the demand for which would coincide with high levels of PV output. The results also showed that due to the basic energy needs and the regional climatic conditions there would be little variation in load matching over the course of a year. Degradation of the PV system and projected electricity demand increase meant that the load matching would lower to 57.3% after 10 years of operation.

One stumbling block to the continued integration of PV into the global electricity generation mix is the perceived relationship between PV output and load demand. This is particularly true in Europe where the highest output levels coincide with periods of low demand both daily and seasonally. However, the results from this case study demonstrated that there is a much better correlation between PV output and electricity demand of countries in the global south due to their tropical climates and basic electricity requirements.

The strong correlation between PV output and local load demand demonstrated in this case study means that there would be little grid support needed from non-renewable generation and storage technologies to accommodate increasing PV levels. This proves that PV is a suitable candidate to add to the energy mix of global south countries in significant levels and can be used to meet projected increasing demand in the region.

While the results of this work demonstrate that PV is a suitable energy source for countries like Myanmar which boast high indigenous untapped resources, they also point to the

importance of including annual load increase rate and PV output degradation rate in system planning. They also demonstrate the importance of load profiles that can accurately model modern-day technologies that increasing significantly alter the nature of the load characteristics of networks in planning activities.

7.4 Systematic ANN Design Approach

There is a critical requirement for accuracy in load forecasting for the many different stakeholders in the electricity sector [235, 401-402]. Underestimated forecasts can cause poor quality of service and even blackouts because of under-generation [402]. Whereas overestimated forecasts can result in financial losses due to over-generation and unneeded reinforcement programs [402]. The restructuring of the electricity industry is increasing the importance of the accuracy of load forecasting [219, 401]. The accuracy of long-term forecasting is of particular importance as it is vital to ensure that correct decision-making in planning and management operations occurs [220].

Increasing demand and the changing pattern of electricity flow caused by new technologies is drastically changing the pattern of load profiles and making accurate load forecasting more difficult [230, 234, 241]. The penetration levels of new technologies vary from network to network around the world, as does the projected increase of these technologies. This means that there is no one forecasting model that can perform with a desired level of accuracy for all situations [230, 235]. Therefore, research is needed to develop a systematic approach that can be used to ensure that a suitable forecasting model can be found for any given set of unique conditions [230, 401-403]. Doing this will ensure that new technologies such as renewable energy generation sources can be cost-effectively utilised [158, 225, 240, 244].

As stated in Section 7.2 an ANN model generated using Matlab was presented at the 5th ICREGA which was proven to be able to forecast loads of the increasingly complex power networks of the future. Further work was carried out to investigate the different design parameters of the model that could be altered to increase prediction capabilities. The work proved that the five design parameters investigated could all significantly alter the prediction capabilities of ANN models used in load forecasting. However, validating the results using data that the models had no a priori knowledge of clearly demonstrated that the data obtained from the Matlab interface can be extremely misleading. The results also showed

the behaviour of the different design parameters could not be predicted by type and that the different combinations of design parameters tested greatly altered performance.

Using the results from these tests an ANN model was generated which was able to forecast loads for a case study location in the UK with higher predictive accuracy than the original ANN model presented at ICREGA. The improved model was later used to try to model load profiles for two countries in the global south (India and Myanmar) in a further case study. However, the ANN was unable to adequately model these profiles due to the different nature of the patterns, proving that no one forecasting model can perform with a desired level of accuracy for all situations.

Therefore, a three-stage systematic approach was proposed which could be used to simplify the process of designing ANN models that can be used for any unique load forecasting scenario with an acceptable level of accuracy. The amount of time needed to complete parameter testing highlighted the need to design and create a new graphical user interface to automate the second stage of the proposed approach (network design & implementation). The results also indicated the need to validate any results obtained through Matlab using a priori knowledge data to ensure that an optimal performance model is identified.

7.5 Maximising PV Energy Output Potential

Future power networks are certain to have high penetrations of PV distributed generation as operators and policy makers try to decarbonise their networks and promote economic growth [92]. Whilst PV is pivotal in meeting decarbonisation targets increasing penetration levels also pose significant challenges to network operators [92-94]. This is particularly true at the low voltage distribution level where the existing infrastructure is ill suited to high penetration levels of renewables such as PV [95]. With high penetration levels of microgeneration, curtailment of PV output according to grid code mandates during peak generation and low demand period is anticipated unless appropriate control means are put in place.

Power networks are currently moving into the smart-grid paradigm. The inherent cost attached to smart grids technologies means that the global economic inequality will be reflected in their deployment. Developing and transitioning nations with lower economic reserves to spare are often constrained in terms of the level and nature of changes they could make to their power networks.

Work was carried out that increments the state of the art by supporting power system planning by means of scenario-based impact assessments that can be used in aiding sustainable energy policymaking for developing countries. The work analysed the efficacy of low-cost smart grid solutions in maximising PV energy yield and therefore revenue returns for prosumers and avoided costs for distribution networks in a developing country (Myanmar), a transitioning country (India) and a developed country (UK).

The results showed that the recent upgraded policies and grid codes implemented by the UK had facilitated higher energy capture from renewable like PV. The increase in the voltage-based curtailment threshold brought about the move from grid code G83 to G98 prevented the need for any PV energy curtailment in the UK based study even without any smart-grid solutions in place.

The case studies that examined India and Myanmar showed that whilst demand side management (DSM) could be a preferred smart-grid solution for preventing PV curtailment because of its potential for holistic deployment via demand response schemes for many countries in the global south, technically the combination of the weaker LV networks in the region with significantly higher solar resources meant that it is not effective in preventing PV energy curtailment. Results from these two case studies showed that the combination of DSM with the other smart-grid solution investigated, active voltage control (AVC), could be deployed to extend the PV penetration level before curtailment occurred. They also showed that whilst the combination of DSM and AVC could not completely prevent PV curtailment at the highest PV penetration levels the combination could still reduce the amount of curtailment at all PV penetration levels.

Comparison of the results of the three case studies demonstrated that, while smart grid solutions are capable of enabling PV generation maximization and improving penetration levels, the extent of such benefits are location specific and are affected by the distribution network structure. The locations chosen for the case study of India (Mumbai) and Myanmar (Yangon) have similar climatic conditions resulting in similar PV daily and annual output profiles and seasonal variation load demand. The two case studies also used the same model of a typical South-East Asian distribution network. However, the efficacy of DSM and AVC in the two studies was noticeably different. The one difference between these case

studies was the magnitude and pattern of load demand profiles used, highlighting the need for accurate PV output and load demand profiles in any planning activities.

7.6 Recommendations for Future Work

The above sections detail how scenario-based impact assessments for power system planning can be supported by means of ANN load forecasting and its systematic design, and thus aid sustainable energy policymaking, especially for developing countries.

All of the ANN models generated in this work were trained with limited publicly available data sets. ANN models trained using limited data can suffer from low accuracy as there is often insufficient data to allow the model to properly learn the underlying relationship between inputs and outputs [245]. Limited data sets also increase the risk of models overtraining and losing generalisation capabilities. One of the original aims of this work was to examine methods that could be used to increase the performance of ANNs trained with limited data sets. However, lockdown measures put in place to combat the COVID-19 pandemic meant that the resources required to test methods that had been identified as having the potential to combat the issue of limited data were unavailable. The identified methods of dealing with the issues caused by limited data merits further study.

Testing of the design parameters of ANN models generated in Matlab highlighted the inaccuracy of results obtained through the current GUI and the amount of man-hours required to find an optimal performance model. A three-stage systematic approach was proposed which could be used to simplify the process of designing ANN models that could be used for any unique load forecasting scenario with an acceptable level of accuracy. The design of a new GUI is recommended to automate stage two of the approach to reduce man-hours and to ensure the optimal model is identified.

It is recommended that, in preparation of grid codes, further scenario-based assessments are carried out on other smart-grid solutions that can maximise renewable energy output. These assessments should have a focus on load profiles as well as the locational renewable resource conditions as demonstrated in this work. This future work could also explore the methods to compensate the energy loss and power quality problems in potential scenarios of increasing housing demand and PV penetration coming into existing distribution networks.

Levelised Cost of Electricity (LCoE) is used to calculate the cost of each unit of electricity generated by power plants with different power generation and costing structures. [58, 83]. The UK Department for Business, Energy & Industrial Strategy defines LCoE as the “Cost of Electricity Generation is the discounted lifetime cost of ownership and use of a generation asset, converted into an equivalent unit of cost of generation in £/MWh” [404]. Policy makers today used LCoE studies to determine the fuel mix of their electricity generation sectors. LCoE is well established but lacks in future risks involved in cost and yield, and therefore almost always prioritises expense-intensive traditional fossil-fired generators over capital-intensive renewables such as PV [405]. The systematic design approach of ANN models could be used to accurately model the uncertainties associated with PV generation and allow more representative LCoE studies to be carried out.

References

1. "Strategic Asset Management of Power Networks", IEC Basecamp, September 2019. [Online] Available at: <https://basecamp.iec.ch/download/iec-white-paper-strategic-asset-management-of-power-networks/>
2. "Regulating Energy Networks", Ofgem, 2020. [Online]. Available: www.ofgem.gov.uk/network-regulation-riio-model#block-views-publications-and-updates-block. [Accessed 21 October 2020]
3. Snape, J.R. Spatial and temporal characteristics of PV adoption in the UK and their implications for the smart grid. *Energies* 2016, 9(3), 210. Doi: <https://doi.org/10.3390/en9030210>
4. R. K. Vishnoi and L. P. Joshi, "Challenges in Reliable Power System Planning and Management with Large Scale Infusion of Renewable Sources in India," 2019 IEEE PES GTD Grand International Conference and Exposition Asia (GTD Asia), Bangkok, Thailand, 2019, pp. 63-67, doi: 10.1109/GTDAsia.2019.8715851.
5. A.Trpovski and T. Hamacher, "A Comparative Analysis of Transmission System Planning for Overhead and Underground Power Systems using AC and DC Power Flow," 2019 IEEE PES Innovative Smart Grid Technologies Europe (ISGT-Europe), Bucharest, Romania, 2019, pp. 1-5, doi: <https://doi.org/10.1109/ISGTEurope.2019.8905510>.
6. V. B. Venkateswaran, D. K. Saini and M. Sharma, "Environmental Constrained Optimal Hybrid Energy Storage System Planning for an Indian Distribution Network," in *IEEE Access*, vol. 8, pp. 97793-97808, 2020, doi: <https://doi.org/10.1109/ACCESS.2020.2997338>.
7. Y.Fu a, G.Huang, Y. Xie, R. Liao and J. Yin, "Planning electric power system under carbon-price mechanism considering multiple uncertainties – A case study of Tianjin", *Journal of Environmental Management*, vol. 269, pp. 1-16, September 2020, doi: <https://doi.org/10.1016/j.jenvman.2020.110721>
8. O. M. Babatunde, J. L. Munda and Y. Hamam, "Operations and planning of integrated renewable energy system: a survey," 2020 5th International Conference on Renewable Energies for Developing Countries (REDEC), Marrakech, Morocco, Morocco, 2020, pp. 1-6, doi: 10.1109/REDEC49234.2020.9163857.
9. B. Sun, B. Zou, J. Yan, X. Wang, Y. Yang and Y. Huang, "A Transmission System Planning Method Considering Demand-side Response and Capability for Accommodating Wind Power", *IOP Conf. Series: Materials Science and Engineering*, vol. 685, pp. 1-6, 2019. Doi: <https://doi.org/10.1088/1757-899X/685/1/012022>

10. "National Household Travel Survey". U.S. Department of Transportation: Federal Travel Administration, December 2019. [Online]. Available at: <http://nhts.ornl.gov/>. [Accessed: 25 September 2020].
11. Q. Hou, N. Zhanga, E. Dua, M. Miaob, F. Pengc and C. Kanga, "Probabilistic duck curve in high PV penetration power system: Concept, modeling, and empirical analysis in China", Elsevier: Applied Energy, vol. 242, pp. 205-215, 2019. Doi: <https://doi.org/10.1016/j.apenergy.2019.03.067>
12. J.H. Moon, H.N. Gwon, G.Y. Jo, W.Y. Choi and K.S. Kook, "Stochastic Modeling Method of Plug-in Electric Vehicle Charging Demand for Korean Transmission System Planning", MDPI: Energies, vol. 13, no. 4404, pp. 1-14, 2020. Doi: <https://doi.org/10.3390/en13174404>
13. S. Merkli and R. S. Smith, "Power System Upgrade Planning with On-load Tap-changing Transformers, Switchable Topology and Operating Policies," 2019 18th European Control Conference (ECC), Naples, Italy, 2019, pp. 1424-1430, doi: <https://doi.org/10.23919/ECC.2019.8795955>.
14. A.Akrami, M.Doostizadeh and F.Aminifar, "Power system flexibility: an overview of emergence to evolution," in Journal of Modern Power Systems and Clean Energy, vol. 7, no. 5, pp. 987-1007, September 2019, doi: <https://doi.org/10.1007/s40565-019-0527-4>.
15. J. O. Dada and A. Moser, "REPLAN: Multi-Region Power System Planning Approach for Nigeria," 2019 IEEE PES/IAS PowerAfrica, Abuja, Nigeria, 2019, pp. 87-92, doi: <https://doi.org/10.1109/PowerAfrica.2019.8928896>.
16. Bilgen, S., 2014. Structure and environmental impact of global energy consumption. Renewable and Sustainable Energy Reviews, 38, pp.890-902.
17. Li, R., 2021. The overview of the development of future energy. IOP Conference Series: Earth and Environmental Science, 651(2), p.022044.
18. Chalvatzis, K. J., & Ioannidis, A. (2017). Energy supply security in the EU: Benchmarking diversity and dependence of primary energy. Applied Energy, 207, 465-476.
19. Ahmad, T., & Zhang, D. (2020). A critical review of comparative global historical energy consumption and future demand: The story told so far. Energy Reports, 6, 1973-1991.
20. Cîrstea, S. D., Moldovan-Teselios, C., Cîrstea, A., Turcu, A. C., & Darab, C. P. (2018). Evaluating renewable energy sustainability by composite index. Sustainability, 10(3), 811.

21. Lowe, P., Abdelhak Chibani, M., Barseghyan, H., Kolodziejczyk, B., Oyewole, O., Diendorfer, C., ... & Smon, I. World Energy Trilemma Index 2020. Report+ Summary.
22. Arachchi, J. I., & Managi, S. (2021). Preferences for energy sustainability: Different effects of gender on knowledge and importance. *Renewable and Sustainable Energy Reviews*, 141, 110767.
23. Šprajc, P., Bjegović, M., & Vasić, B. (2019). Energy security in decision making and governance-Methodological analysis of energy trilemma index. *Renewable and Sustainable Energy Reviews*, 114, 109341.
24. Grigoryev, L. M., & Medzhidova, D. D. (2020). Global energy trilemma. *Russian Journal of Economics*, 6, 437.
25. Solomon, B. D., & Krishna, K. (2011). The coming sustainable energy transition: History, strategies and outlook. *Energy Policy*, 39(11), 7422–7431. <https://doi.org/10.1016/j.enpol.2011.09.009>
26. Ritchie, H. and Roser, M., 2022. Energy. [online] Our World in Data. Available at: <<https://ourworldindata.org/energy>> [Accessed 5 February 2021].
27. Makarov, A. A., & Makarov, A. A. (2010). Laws of power industry development: Elusory essence. *Thermal Engineering*, 57(13), 1085–1092. <https://doi.org/10.1134/S004060151013001X>
28. "Melsted, O., & Pallua, I. (2018). The historical transition from coal to hydrocarbons: Previous explanations and the need for an integrative perspective. *Canadian Journal of History*, 53(3), 395–422. <https://doi.org/10.3138/cjh.ach.53.3.03>"
29. Speight, J. G. (2016). *Deep shale oil and gas*. Gulf Professional Publishing.
30. Makarov, A. A., Mitrova, T. A., & Kulagin, V. A. (Eds.) (2019). *Global and Russian energy outlook 2019*. Moscow: ERI RAS and Moscow School of Management SKOLKOVO.
31. Stern, J. (2020). The role of gases in the European energy transition. *Russian Journal of Economics*, 6(4), 390–405. <https://doi.org/10.32609/j.ruje.6.55105>
32. Yanık, S., Sürer, Ö., & Öztayşi, B. (2016). Designing sustainable energy regions using genetic algorithms and location-allocation approach. *Energy*, 97, 161-172.
33. Agyekum, E. B., Velkin, V. I., & Hossain, I. (2020). Sustainable energy: Is it nuclear or solar for African Countries? Case study on Ghana. *Sustainable Energy Technologies and Assessments*, 37, 100630.
34. Asaad, M., Ahmad, F., Alam, M. S., & Sarfraz, M. (2021). Smart grid and Indian experience: A review. *Resources Policy*, 74, 101499.

35. Bigerna, S., D'Errico, M. C., & Polinori, P. (2021). Energy security and RES penetration in a growing decarbonized economy in the era of the 4th industrial revolution. *Technological Forecasting and Social Change*, 166, 120648.
36. Shahbaz, M., Raghutla, C., Chittedi, K. R., Jiao, Z., & Vo, X. V. (2020). The effect of renewable energy consumption on economic growth: Evidence from the renewable energy country attractive index. *Energy*, 207, 118162.
37. Järventausta, P., Repo, S., Rautiainen, A., & Partanen, J. (2010). Smart grid power system control in distributed generation environment. *Annual Reviews in Control*, 34(2), 277-286.
38. Doluweera, G., Hahn, F., Bergerson, J., & Pruckner, M. (2020). A scenario-based study on the impacts of electric vehicles on energy consumption and sustainability in Alberta. *Applied Energy*, 268, 114961.
39. Awerbuch, S., & Yang, S. (2007). Efficient electricity generating portfolios for Europe: maximising energy security and climate change mitigation. *EIB papers*, 12(2), 8-37.
40. Kong, D., Xia, Q., Xue, Y., & Zhao, X. (2020). Effects of multi policies on electric vehicle diffusion under subsidy policy abolishment in China: A multi-actor perspective. *Applied Energy*, 266, 114887.
41. Antoniou, A., Storkey, A., & Edwards, H. (2017). Data augmentation generative adversarial networks. *arXiv preprint arXiv:1711.04340*.
42. Sachan, S., Deb, S., & Singh, S. N. (2020). Different charging infrastructures along with smart charging strategies for electric vehicles. *Sustainable Cities and Society*, 60, 102238.
43. Ferreira G, editor. *Alternative energies: updates on progress*. Berlin, Germany: Springer-Verlag ;2013.
44. Haque, M. and Wolfs, P., 2016. A review of high PV penetrations in LV distribution networks: Present status, impacts and mitigation measures. *Renewable and Sustainable Energy Reviews*, 62, pp.1195-1208
45. Nyambuu, U., & Semmler, W. (2020). Climate change and the transition to a low carbon economy—Carbon targets and the carbon budget. *Economic Modelling*, 84, 367-376.
46. Gandhi, O., Kumar, D. S., Rodríguez-Gallegos, C. D., & Srinivasan, D. (2020). Review of power system impacts at high PV penetration Part I: Factors limiting PV penetration. *Solar Energy*, 210, 181-201.
47. Mangla, S. K., Luthra, S., Jakhar, S., Gandhi, S., Muduli, K., & Kumar, A. (2020). A step to clean energy-Sustainability in energy system management in an emerging economy context. *Journal of Cleaner Production*, 242, 118462.

48. Safarian, S., Unnþórsson, R., & Richter, C. (2019). A review of biomass gasification modelling. *Renewable and Sustainable Energy Reviews*, 110, 378-391.
49. Destek, M. A., & Sarkodie, S. A. (2020). Are fluctuations in coal, oil and natural gas consumption permanent or transitory? Evidence from OECD countries. *Heliyon*, 6(2), e03391.
50. Chen, C., Pinar, M., & Stengos, T. (2020). Renewable energy consumption and economic growth nexus: Evidence from a threshold model. *Energy Policy*, 139, 111295.
51. Sarkodie, S. A., & Strezov, V. (2018). Empirical study of the environmental Kuznets curve and environmental sustainability curve hypothesis for Australia, China, Ghana and USA. *Journal of cleaner production*, 201, 98-110.
52. Jackson, R. B., Le Quéré, C., Andrew, R. M., Canadell, J. G., Korsbakken, J. I., Liu, Z., ... & Zheng, B. (2018). Global energy growth is outpacing decarbonization. *Environmental Research Letters*, 13(12), 120401.
53. Oliver, J., & Sovacool, B. (2017). The energy trilemma and the smart grid: implications beyond the United States. *Asia & the Pacific Policy Studies*, 4(1), 70-84.
54. Bebbington, J., Schneider, T., Stevenson, L., & Fox, A. (2020). Fossil fuel reserves and resources reporting and unburnable carbon: Investigating conflicting accounts. *Critical Perspectives on Accounting*, 66, 102083.
55. BP. (2019). *Statistical Review of World Energy, 2019—68th Edition*.
56. Miller, B. G. (2010). *Clean coal engineering technology*. Elsevier.
57. BP. (2020). *Statistical Review of World Energy, 2020—69th Edition*.
58. Tran, T. T., & Smith, A. D. (2018). Incorporating performance-based global sensitivity and uncertainty analysis into LCOE calculations for emerging renewable energy technologies. *Applied energy*, 216, 157-171.
59. Saint Akadiri, S., Alola, A. A., Olasehinde-Williams, G., & Etokakpan, M. U. (2020). The role of electricity consumption, globalization and economic growth in carbon dioxide emissions and its implications for environmental sustainability targets. *Science of The Total Environment*, 708, 134653.
60. Pan, X., Wang, L., Dai, J., Zhang, Q., Peng, T., & Chen, W. (2020). Analysis of China's oil and gas consumption under different scenarios toward 2050: An integrated modeling. *Energy*, 195, 116991.
61. "Zhang, F., 2019. In the Dark: How Much Do Power Sector Distortions Cost South Asia? South Asia Development Forum. World Bank, Washington, DC, <http://dx.doi.org/10.1596/978-1-4648-1154-8>"

62. Hasanov, F. J., Mahmudlu, C., Deb, K., Abilov, S., & Hasanov, O. (2020). The role of Azeri natural gas in meeting European Union energy security needs. *Energy Strategy Reviews*, 28, 100464.
63. Saidi, K., & Omri, A. (2020). Reducing CO₂ emissions in OECD countries: Do renewable and nuclear energy matter?. *Progress in Nuclear Energy*, 126, 103425.
64. Sarkodie, S. A., & Adams, S. (2018). Renewable energy, nuclear energy, and environmental pollution: accounting for political institutional quality in South Africa. *Science of the total environment*, 643, 1590-1601.
65. EDF. 2021. What is nuclear energy?. [online] Available at: <<https://www.edfenergy.com/about/nuclear/what-is-nuclear-energy>> [Accessed 22 April 2021].
66. World Nuclear Association 2021. Facts and Figures [online] Available at: <<https://www.world-nuclear.org/information-library/>> [Accessed 23 April 2021].
67. NEI 2021. What is Nuclear energy?. [online] Available at: <<https://www.nei.org/fundamentals/what-is-nuclear-energy>> [Accessed 22 April 2021].
68. AKYÜZ, E. (2017). Advantages and disadvantages of nuclear energy in Turkey: Public perception. *Eurasian Journal of Environmental Research*, 1(1), 1-11.
69. US Energy Information Agency 2021. Today In Energy. [online] Available at: <<https://www.eia.gov/>> [Accessed 23 April 2021]
70. EESI 2021. BioEnergy. [online]. Available at: <<https://www.eesi.org/topics/bioenergy-biofuels-biomass/description>> [Accessed 24 April 2021].
71. Office of EERE 2021. How do we get energy from water?. [online]. Available at: <<https://www.energy.gov/eere/water/how-hydropower-works>> [Accessed 25 February 2021].
72. EIA 2021. Hydropower Explained. [online]. Available at: <<https://www.eia.gov/energyexplained/hydropower/>> [Accessed 25 February 2021].
73. Li, X. Z., Chen, Z. J., Fan, X. C., & Cheng, Z. J. (2018). Hydropower development situation and prospects in China. *Renewable and Sustainable Energy Reviews*, 82, 232-239.
74. Kougias, I., Aggidis, G., Avellan, F., Deniz, S., Lundin, U., Moro, A., ... & Theodossiou, N. (2019). Analysis of emerging technologies in the hydropower sector. *Renewable and Sustainable Energy Reviews*, 113, 109257.
75. The Renewable Energy Hub UK 2021. A Brief History of Hydropower. [online]. Available at: <<https://www.renewableenergyhub.co.uk/main/hydroelectricity-information/history-of-hydroelectricity/>> [Accessed 24 April 2021].

76. Moran, E. F., Lopez, M. C., Moore, N., Müller, N., & Hyndman, D. W. (2018). Sustainable hydropower in the 21st century. *Proceedings of the National Academy of Sciences*, 115(47), 11891-11898.
77. Moreno, R., Ferreira, R., Barroso, L., Rudnick van de Wyngard, H., & Pereira, E. (2017). Facilitating the integration of renewables in Latin America: the role of hydropower generation and other energy storage technologies.
78. Hunt, J. D., Byers, E., Wada, Y., Parkinson, S., Gernaat, D. E., Langan, S., ... & Riahi, K. (2020). Global resource potential of seasonal pumped hydropower storage for energy and water storage. *Nature communications*, 11(1), 1-8.
79. Psiloglou, B. E., Kambezidis, H. D., Kaskaoutis, D. G., Karagiannis, D., & Polo, J. M. (2020). Comparison between MRM simulations, CAMS and PVGIS databases with measured solar radiation components at the Methoni station, Greece. *Renewable energy*, 146, 1372-1391.
80. Moslehi, K., & Kumar, R. (2010). A reliability perspective of the smart grid. *IEEE transactions on smart grid*, 1(1), 57-64.
81. Prakesh, S., Sherine, S., & Bist, B. (2017). Forecasting methodologies of solar resource and PV power for smart grid energy management. *International Journal of Pure and Applied Mathematics*, 116(18), 313-318.
82. Dondariya, C., Porwal, D., Awasthi, A., Shukla, A. K., Sudhakar, K., SR, M. M., & Bhimte, A. (2018). Performance simulation of grid-connected rooftop solar PV system for small households: A case study of Ujjain, India. *Energy Reports*, 4, 546-553.
83. Stolzenberger, C. H., & Then, O. (2015). Levelised cost of electricity 2015. *VGB PowerTech*, 95(12), 94-96.
84. Veers, P., Dykes, K., Lantz, E., Barth, S., Bottasso, C. L., Carlson, O., ... & Wiser, R. (2019). Grand challenges in the science of wind energy. *Science*, 366(6464), eaau2027.
85. Cirés, E., Marcos, J., de la Parra, I., García, M., & Marroyo, L. (2019). The potential of forecasting in reducing the LCOE in PV plants under ramp-rate restrictions. *Energy*, 188, 116053.
86. Chiaroni, D., Chiesa, V., Colasanti, L., Cucchiella, F., D'Adamo, I., & Frattini, F. (2014). Evaluating solar energy profitability: A focus on the role of self-consumption. *Energy Conversion and Management*, 88, 317-331.
87. A. Soualmia, R. Chenni, Rachid. Modeling and Simulation of 15MW Grid - Connected Photovoltaic System using PVsyst Software. 2016. In proceedings 2016 International renewable and sustainable energy conference (IRSEC). pp 702-705.

88. Ding, H., Zhou, D. Q., Liu, G. Q., & Zhou, P. (2020). Cost reduction or electricity penetration: Government R&D-induced PV development and future policy schemes. *Renewable and Sustainable Energy Reviews*, 124, 109752.
89. Jäger-Waldau, A. (2019). PV status report 2019. Publications Office of the European Union: Luxembourg.
90. D'Adamo, I., Gastaldi, M., & Morone, P. (2020). The post COVID-19 green recovery in practice: Assessing the profitability of a policy proposal on residential photovoltaic plants. *Energy Policy*, 147, 111910.
91. Al-Dousari, A., Al-Nassar, W., Al-Hemoud, A., Alsaleh, A., Ramadan, A., Al-Dousari, N., & Ahmed, M. (2019). Solar and wind energy: challenges and solutions in desert regions. *Energy*, 176, 184-194.
92. Sevilla, F. R. S., Parra, D., Wyrsh, N., Patel, M. K., Kienzle, F., & Korba, P. (2018). Techno-economic analysis of battery storage and curtailment in a distribution grid with high PV penetration. *Journal of Energy Storage*, 17, 73-83.
93. "M. Kabir, Y. Mishra, G. Ledwich, Z. Y. Dong, and K. P. Wong, "Coordinated control of grid-connected photovoltaic reactive power and battery energy storage systems to improve the voltage profile of a residential distribution feeder," *IEEE Trans. Ind. Inform.*, vol. 10, no. 2, pp. 967–977, May 2014."
94. Sharma, V., Haque, M. H., Aziz, S. M., & Kauschke, T. (2020, December). Reduction of PV Curtailment through Optimally Sized Residential Battery Storage. In *2020 IEEE International Conference on Power Electronics, Drives and Energy Systems (PEDES)* (pp. 1-6). IEEE.
95. Liu, M. Z., Procopiou, A. T., Petrou, K., Ochoa, L. F., Langstaff, T., Harding, J., & Theunissen, J. (2020). On the fairness of PV curtailment schemes in residential distribution networks. *IEEE Transactions on Smart Grid*, 11(5), 4502-4512.
96. Bird, L., Cochran, J., & Wang, X. (2014). Wind and solar energy curtailment: Experience and practices in the United States (No. NREL/TP-6A20-60983). National Renewable Energy Lab.(NREL), Golden, CO (United States).
97. Kikusato, H., Fujimoto, Y., Hanada, S. I., Isogawa, D., Yoshizawa, S., Ohashi, H., & Hayashi, Y. (2019). Electric vehicle charging management using auction mechanism for reducing PV curtailment in distribution systems. *IEEE Transactions on Sustainable Energy*, 11(3), 1394-1403.
98. Nelson, J., Kasina, S., Stevens, J., Moore, J., Olson, A., Morjaria, M., Smolenski, J., Aponte, J., 2018. Investigating the economic value of flexible solar power plant operation. *Energy + Environ. Econ.*
99. O'Shaughnessy, E., Cruce, J., & Xu, K. (2021). Rethinking solar PV contracts in a world of increasing curtailment risk. *Energy Economics*, 98, 105264.

100. O'Shaughnessy, E., Cruce, J. R., & Xu, K. (2020). Too much of a good thing? Global trends in the curtailment of solar PV. *Solar Energy*, 208, 1068-1077.
101. Perez, M., Perez, R., Rábago, K. R., & Putnam, M. (2019). Overbuilding & curtailment: The cost-effective enablers of firm PV generation. *Solar Energy*, 180, 412-422.
102. Golden, R., Paulos, B., 2015. Curtailment of renewable energy in California and Beyond. *Electricity J.* 28 (6), 36–50.
103. Sterling, J., Stearn, C., Davidovich, T., Quinlan, P., Pang, J., Vlahoplus, C., 2017. Proactive Solutions to Curtailment Risk: Identifying New Contract Structures for Utility-Scale Renewables. Smart Electric Power Alliance.
104. Solomon, A.A., Bogdanov, D., Breyer, C., 2019. Curtailment-storage-penetration nexus in the energy transition. *Appl. Energy* 235, 1351–1368.
105. "Candelise, C., Westacott, P., 2017. Can integration of PV within UK electricity network be improved? A GIS-based assessment of storage. *Energy Policy* 109, 604–703."
106. Manwell, J. F., McGowan, J. G., & Rogers, A. L. (2010). *Wind energy explained: theory, design and application*. John Wiley & Sons.
107. Herbert, G. J., Iniyar, S., Sreevalsan, E., & Rajapandian, S. (2007). A review of wind energy technologies. *Renewable and sustainable energy Reviews*, 11(6), 1117-1145.
108. Menezes, Eduardo José Novaes, Alex Maurício Araújo, and Nadège Sophie Bouchonneau Da Silva. "A review on wind turbine control and its associated methods." *Journal of cleaner production* 174 (2018): 945-953.
109. Johnson, G. L. (1985). *Wind energy systems* (pp. 147-149). Englewood Cliffs, NJ: Prentice-Hall.
110. Sahu, B. K. (2018). Wind energy developments and policies in China: A short review. *Renewable and Sustainable energy reviews*, 81, 1393-1405.
111. Esteban, M. D., Diez, J. J., López, J. S., & Negro, V. (2011). Why offshore wind energy?. *Renewable energy*, 36(2), 444-450.
112. Johnson, G. L. (1985). *Wind energy systems* (pp. 147-149). Englewood Cliffs, NJ: Prentice-Hall.
113. Hevia-Koch, P., & Jacobsen, H. K. (2019). Comparing offshore and onshore wind development considering acceptance costs. *Energy Policy*, 125, 9-19.
114. DeCastro, M., Salvador, S., Gómez-Gesteira, M., Costoya, X., Carvalho, D., Sanz-Larruga, F. J., & Gimeno, L. (2019). Europe, China and the United States: Three different approaches to the development of offshore wind energy. *Renewable and Sustainable Energy Reviews*, 109, 55-70.

115. Council, G. W. E. (2021). GWEC| global wind report 2021. Global Wind Energy Council: Brussels, Belgium.
116. Das, A., Jani, H. K., Nagababu, G., & Kachhwaha, S. S. (2020). A comprehensive review of wind–solar hybrid energy policies in India: Barriers and Recommendations. *Renewable Energy Focus*, 35, 108-121.
117. Murshed, M. (2021). Can regional trade integration facilitate renewable energy transition to ensure energy sustainability in South Asia?. *Energy Reports*, 7, 808-821.
118. "Chiu, C.L., Chang, T.H., 2009. What proportion of renewable energy supplies is needed to initially mitigate CO2 emissions in OEC Dmember countries? *Renew. Sust. Energ. Rev.*13 (6–7), 1669–1674."
119. Curto, D., Favuzza, S., Franzitta, V., Musca, R., Navia, M. A. N., & Zizzo, G. (2020). Evaluation of the optimal renewable electricity mix for Lampedusa island: The adoption of a technical and economical methodology. *Journal of Cleaner Production*, 263, 121404.
120. Affenzeller, J., Beaumel, L., Bergstein, M., Coppin, O., Faye, I., Hildermeier, J., ... & Thulin, N. (2017). *Electrification of the transport system: studies and reports*. European Commission.
121. REN21. *Renewables 2017 Global Status Report*; REN21 Secretariat: Paris, France, 2017.
122. Pérez-García, J., & Moral-Carcedo, J. (2016). Analysis and long term forecasting of electricity demand through a decomposition model: A case study for Spain. *Energy*, 97, 127-143.
123. Heffron, R. J., McCauley, D., & de Rubens, G. Z. (2018). Balancing the energy trilemma through the Energy Justice Metric. *Applied energy*, 229, 1191-1201.
124. Ozcan, B., Tzeremes, P. G., & Tzeremes, N. G. (2020). Energy consumption, economic growth and environmental degradation in OECD countries. *Economic Modelling*, 84, 203-213.
125. Aslan, A., Apergis, N., & Yildirim, S. (2014). Causality between energy consumption and GDP in the US: evidence from wavelet analysis. *Frontiers in Energy*, 8(1), 1-8.
126. Rafindadi, A. A., & Ozturk, I. (2017). Impacts of renewable energy consumption on the German economic growth: Evidence from combined cointegration test. *Renewable and Sustainable Energy Reviews*, 75, 1130-1141.
127. Cheng, B. S. (1999). Causality between energy consumption and economic growth in India: an application of cointegration and error-correction modeling. *Indian Economic Review*, 39-49.

128. Jafari, Y., Othman, J., & Nor, A. H. S. M. (2012). Energy consumption, economic growth and environmental pollutants in Indonesia. *Journal of Policy Modeling*, 34(6), 879-889.
129. Masih, A. M., & Masih, R. (1996). Energy consumption, real income and temporal causality: results from a multi-country study based on cointegration and error-correction modelling techniques. *Energy economics*, 18(3), 165-183.
130. Nasreen, S., & Anwar, S. (2014). Causal relationship between trade openness, economic growth and energy consumption: A panel data analysis of Asian countries. *Energy Policy*, 69, 82-91.
131. Fang, Z., & Chang, Y. (2016). Energy, human capital and economic growth in Asia Pacific countries—Evidence from a panel cointegration and causality analysis. *Energy Economics*, 56, 177-184.
132. Dogan, E. (2014). Energy consumption and economic growth: Evidence from low-income countries in sub-Saharan Africa. *International Journal of Energy Economics and Policy*, 4(2), 154-162.
133. Ouedraogo, N. S. (2013). Energy consumption and economic growth: Evidence from the economic community of West African States (ECOWAS). *Energy economics*, 36, 637-647.
134. Wolde-Rufael, Y. (2009). Energy consumption and economic growth: the experience of African countries revisited. *Energy Economics*, 31(2), 217-224.
135. Śmiech, S., & Papież, M. (2014). Energy consumption and economic growth in the light of meeting the targets of energy policy in the EU: The bootstrap panel Granger causality approach. *Energy Policy*, 71, 118-129.
136. Kasman, A., & Duman, Y. S. (2015). CO2 emissions, economic growth, energy consumption, trade and urbanization in new EU member and candidate countries: a panel data analysis. *Economic modelling*, 44, 97-103.
137. Apergis, N., & Payne, J. E. (2009). Energy consumption and economic growth: evidence from the Commonwealth of Independent States. *Energy Economics*, 31(5), 641-647.
138. Belke, A., Dobnik, F., & Dreger, C. (2011). Energy consumption and economic growth: New insights into the cointegration relationship. *Energy Economics*, 33(5), 782-789.
139. Bozoklu, S., & Yilanci, V. (2013). Energy consumption and economic growth for selected OECD countries: Further evidence from the Granger causality test in the frequency domain. *Energy Policy*, 63, 877-881.
140. Kahouli, B. (2019). Does static and dynamic relationship between economic growth and energy consumption exist in OECD countries?. *Energy Reports*, 5, 104-116.

141. Ozturk, I., Aslan, A., & Kalyoncu, H. (2010). Energy consumption and economic growth relationship: Evidence from panel data for low and middle income countries. *Energy Policy*, 38(8), 4422-4428.
142. US Energy Information Agency 2021. Energy Facts Explained. [online] Available at: <<https://www.eia.gov/energyexplained/us-energy-facts/>> [Accessed 26 April 2021]
143. Introduction to Modern Climate Change. Andrew E. Dessler: Cambridge University Press, 2011, 252 pp, ISBN-10: 0521173159
144. Zheng, S., Huang, G., Zhou, X., & Zhu, X. (2020). Climate-change impacts on electricity demands at a metropolitan scale: A case study of Guangzhou, China. *Applied Energy*, 261, 114295.
145. European Commission. (2018). A Clean Planet for all. A European long-term strategic vision for a prosperous, modern, competitive and climate neutral economy. depth analysis in support of the commission; Communication COM (2018), 773, 2018.
146. Solomon, S., Plattner, G. K., Knutti, R., & Friedlingstein, P. (2009). Irreversible climate change due to carbon dioxide emissions. *Proceedings of the national academy of sciences*, 106(6), 1704-1709.
147. Huy, P. D., Ramachandaramurthy, V. K., Yong, J. Y., Tan, K. M., & Ekanayake, J. B. (2020). Optimal placement, sizing and power factor of distributed generation: A comprehensive study spanning from the planning stage to the operation stage. *Energy*, 195, 117011.
148. NRDC 2021. Global Warming 101. [online] Available at: <<https://www.nrdc.org/stories/global-warming-101#causes>> [Accessed 6 March 2021]
149. Castellini, M., Menoncin, F., Moretto, M., & Vergalli, S. (2021). Photovoltaic Smart Grids in the prosumers investment decisions: a real option model. *Journal of Economic Dynamics and Control*, 126, 103988.
150. United Nations 2021. What Is The Kyoto Protocol?. [online] Available at: <https://unfccc.int/kyoto_protocol> [Accessed 6 March 2021]
151. Nasir, M. A., Huynh, T. L. D., & Tram, H. T. X. (2019). Role of financial development, economic growth & foreign direct investment in driving climate change: A case of emerging ASEAN. *Journal of environmental management*, 242, 131-141.
152. Stern, D. I. (2004). The rise and fall of the environmental Kuznets curve. *World development*, 32(8), 1419-1439.
153. Beckerman, W. (1992). Economic growth and the environment: Whose growth? Whose environment? *World Development*, 20, 481–496.

154. Lorente, D.B., Alvarez-Herranz, A., 2016. Economic growth and energy regulation in the environmental Kuznets curve. *Environ. Sci. Pollut. Control Ser.* 23, 16478e16494. <https://doi.org/10.1007/s11356-016-6773-3>.
155. Nassani, A.A., Aldakhil, A.M., Abro, M.M.Q., Zaman, K., 2017. Environmental Kuznets curve among BRICS countries: spot lightening finance, transport, energy and growth factors. *J. Clean. Prod.* 154, 474e487. <https://doi.org/10.1016/j.jclepro.2017.04.025>.
156. Zaman, K., Moemen, M.A.-e., 2017. Energy consumption, carbon dioxide emissions and economic development: evaluating alternative and plausible environmental hypothesis for sustainable growth. *Renew. Sustain. Energy Rev.* 74,1119e1130. <https://doi.org/10.1016/j.rser.2017.02.072>.
157. Yalcinoz, T., & Eminoglu, U. (2005). Short term and medium term power distribution load forecasting by neural networks. *Energy Conversion and Management*, 46(9-10), 1393-1405.
158. Aly, H. H. (2020). A proposed intelligent short-term load forecasting hybrid models of ANN, WNN and KF based on clustering techniques for smart grid. *Electric Power Systems Research*, 182, 106191.
159. Yap, J. T., Gabriola, A. J. P., & Herrera, C. F. (2021). Managing the energy trilemma in the Philippines. *Energy, Sustainability and Society*, 11(1), 1-17.
160. Khan, I., Hou, F., Irfan, M., Zakari, A., & Le, H. P. (2021). Does energy trilemma a driver of economic growth? The roles of energy use, population growth, and financial development. *Renewable and Sustainable Energy Reviews*, 146, 111157.
161. Gunningham, N. (2013). Managing the energy trilemma: The case of Indonesia. *Energy Policy*, 54, 184-193.
162. Akrofi, M. M. (2021). An analysis of energy diversification and transition trends in Africa. *International Journal of Energy and Water Resources*, 5(1), 1-12.
163. Monarca, U., Cassetta, E., Pozzi, C., & Dileo, I. (2018). Tariff revisions and the impact of variability of solar irradiation on PV policy support: The case of Italy. *Energy Policy*, 119, 307-316.
164. Shah, S. A. A., Longsheng, C., Solangi, Y. A., Ahmad, M., & Ali, S. (2021). Energy trilemma based prioritization of waste-to-energy technologies: implications for post-COVID-19 green economic recovery in Pakistan. *Journal of cleaner production*, 284, 124729.
165. International Energy Agency. *Southeast Asia Energy Outlook*; Springer: Berlin, Germany, 2019.
166. IEA. *Southeast Asia Energy Outlook*; Springer: Berlin, Germany, 2015.

167. IEA 2021. Energy Security. [online]. Available at: <<https://www.iea.org/topics/energy-security>> [Accessed 23 April 2021].
168. Rodríguez-Fernández, L., Carvajal, A. B. F., & Ruiz-Gómez, L. M. (2020). Evolution of European Union's energy security in gas supply during Russia–Ukraine gas crises (2006–2009). *Energy Strategy Reviews*, 30, 100518.
169. Novikau, A. (2021). What does energy security mean for energy-exporting countries? A closer look at the Russian energy security strategy. *Journal of Energy & Natural Resources Law*, 39(1), 105-123.
170. Ranjan, A., & Hughes, L. (2014). Energy security and the diversity of energy flows in an energy system. *Energy*, 73, 137-144.
171. Augutis, J., Krikštolaitis, R., Martišauskas, L., Urbonienė, S., Urbonas, R., & Ušpurienė, A. B. (2020). Analysis of energy security level in the Baltic States based on indicator approach. *Energy*, 199, 117427.
172. Lombardi, P., & Gruenig, M. (Eds.). (2016). *Low-carbon energy security from a European perspective*. Academic Press.
173. Huusom, J. K., & Gani, R. (2016). 12th International Symposium on Process Systems Engineering & 25th European Symposium of Computer Aided Process Engineering (PSE-2015/ESCAPE-25), 31 May-4 June 2015, Copenhagen, Denmark Preface. *Computers & Chemical Engineering*, 91, 1-2.
174. OECD.org 2021. In Focus. [online]. Available at: <<http://www.oecd.org/>> [Accessed 18 April 2021].
175. Energy Education 2021. Energy Diversification. [online]. Available at: <https://energyeducation.ca/encyclopedia/Energy_diversification> [Accessed 23 April 2021].
176. Georgatzi, V. V., Stamboulis, Y., & Vetsikas, A. (2020). Examining the determinants of CO2 emissions caused by the transport sector: empirical evidence from 12 European countries. *Economic Analysis and Policy*, 65, 11-20.
177. Zhang, R., & Fujimori, S. (2020). The role of transport electrification in global climate change mitigation scenarios. *Environmental Research Letters*, 15(3), 034019.
178. Islas-Samperio, J. M., Manzini, F., & Grande-Acosta, G. K. (2020). Toward a low-carbon transport sector in Mexico. *Energies*, 13(1), 84.
179. Dyke, K. J., Schofield, N., & Barnes, M. (2010). The impact of transport electrification on electrical networks. *IEEE Transactions on Industrial Electronics*, 57(12), 3917-3926.

180. Jian, L., Yongqiang, Z., Larsen, G. N., & Snartum, A. (2020). Implications of road transport electrification: A long-term scenario-dependent analysis in China. *ETransportation*, 6, 100072.
181. Kazemzadeh, M. R., Amjadian, A., & Amraee, T. (2020). A hybrid data mining driven algorithm for long term electric peak load and energy demand forecasting. *Energy*, 204, 117948.
182. de Andrade, J. V. B., Rodrigues, B. N., dos Santos, I. F. S., Haddad, J., & Tiago Filho, G. L. (2020). Constitutional aspects of distributed generation policies for promoting Brazilian economic development. *Energy Policy*, 143, 111555.
183. Akdemir, B., & Çetinkaya, N. (2012). Long-term load forecasting based on adaptive neural fuzzy inference system using real energy data. *Energy Procedia*, 14, 794-799.
184. Asian Development Bank, "MYANMAR Energy Sector Assessment, Strategy, and Road Map," 2016.
185. Wang, C. H., Grozev, G., & Seo, S. (2012). Decomposition and statistical analysis for regional electricity demand forecasting. *Energy*, 41(1), 313-325.
186. Lu, W. C. (2017). Greenhouse gas emissions, energy consumption and economic growth: a panel cointegration analysis for 16 Asian countries. *International journal of environmental research and public health*, 14(11), 1436.
187. C. Zhanga, K. Zhoua, S Yanga, Z Shaoa, 2017. On electricity consumption and economic growth in China. *Renewable and Sustainable Energy Reviews* 76 (2017) 353–368
188. "Tang Lei, Wang Xifan, Wang Xiuli, Shao Chengcheng, Liu Shiyu, Tian Shijun. Long-term electricity consumption forecasting based on expert prediction and fuzzy Bayesian theory. *Energy* 2019;167:1144e54."
189. Farhangi, H. (2009). The path of the smart grid. *IEEE power and energy magazine*, 8(1), 18-28.
190. "Wulf WM (2000) Great Achievements and Grand Challenges, The Bridge, Volume 30 Numbers 3&4, Fall/Winter, National Academy of Engineering, p. 5, viewed October 2016 <<https://www.nae.edu/Publications/Bridge/EngineeringAchievements/GreatAchievementsandGrandChallenges.aspx>>"
191. Fang, X., Misra, S., Xue, G., & Yang, D. (2011). Smart grid—The new and improved power grid: A survey. *IEEE communications surveys & tutorials*, 14(4), 944-980.
192. "Barbosa Filho, W.P., Azevedo, A.C.S., Belem, Para, 2013. Distributed generation: advantages and disadvantages. In: *Symposium of Studies and Research in Environmental Sciences in the Amazon*. Available at:

- https://paginas.uepa.br/pcambientais/simposio/anais_artigos_vol_2_simposio_2013.pdf."
193. Zeynali, S., Rostami, N., & Feyzi, M. R. (2020). Multi-objective optimal short-term planning of renewable distributed generations and capacitor banks in power system considering different uncertainties including plug-in electric vehicles. *International Journal of Electrical Power & Energy Systems*, 119, 105885.
 194. "Rakibuzzaman S, Mithulananthan N, Bansal RC, Ramachandaramurthy VK. A review of key power system stability challenges for large-scale PV integration. *Renew Sustain Energy Rev* 2015;41:1423e36."
 195. "I. K. Maharjan, Demand Side Management: Load Management, Load Profiling, Load Shifting, Residential and Industrial Consumer, Energy Audit, Reliability, Urban, Semi-Urban and Rural Setting. Saarbrücken, Germany: LAP (Lambert Acad. Publ.), 2010."
 196. Logenthiran, T., Srinivasan, D., & Shun, T. Z. (2012). Demand side management in smart grid using heuristic optimization. *IEEE transactions on smart grid*, 3(3), 1244-1252.
 197. Kutscher, C.F.; Milford, J.B.; Kreith, F. (2019). *Principles of Sustainable Energy Systems*. Mechanical and Aerospace Engineering Series (Third ed.).
 198. Wagner, J., Weibelzahl, M., Heffron, R. J., Körner, M. F., & Fridgen, G. (2021). How Different Electricity Pricing Systems Affect the Energy Trilemma: Assessing Indonesia's Electricity Market Transition.
 199. Georgitsioti, Tatiani (2015) Photovoltaic potential and performance evaluation studies in India and the UK. Doctoral thesis, Northumbria University.
 200. Ren, L., Liu, Y., Rui, Z., Li, H., & Feng, R. (2009, July). Application of Elman neural network and MATLAB to load forecasting. In 2009 International Conference on Information Technology and Computer Science (Vol. 1, pp. 55-59). IEEE.
 201. Kiss, B., Kácsor, E., & Szalay, Z. (2020). Environmental assessment of future electricity mix—Linking an hourly economic model with LCA. *Journal of Cleaner Production*, 264, 121536.
 202. Zhao, Y., Cao, Y., Shi, X., Li, H., Shi, Q., & Zhang, Z. (2020). How China's electricity generation sector can achieve its carbon intensity reduction targets?. *Science of the Total Environment*, 706, 135689.
 203. Alonso, A. (Ed.). (2012). *Infrastructure and methodologies for the justification of nuclear power programmes*. Elsevier.
 204. Kosai, S., & Unesaki, H. (2020). Short-term vs long-term reliance: Development of a novel approach for diversity of fuels for electricity in energy security. *Applied Energy*, 262, 114520.

205. Huld, T., Müller, R., & Gambardella, A. (2012). A new solar radiation database for estimating PV performance in Europe and Africa. *Solar Energy*, 86(6), 1803-1815.
206. Georgitsioti, T., Pearsall, N., Forbes, I., & Pillai, G. (2019). A combined model for PV system lifetime energy prediction and annual energy assessment. *Solar Energy*, 183, 738-744.
207. Tietjen, O., Pahle, M., & Fuss, S. (2016). Investment risks in power generation: A comparison of fossil fuel and renewable energy dominated markets. *Energy Economics*, 58, 174-185.
208. Cantarero, M. M. V. (2020). Of renewable energy, energy democracy, and sustainable development: A roadmap to accelerate the energy transition in developing countries. *Energy Research & Social Science*, 70, 101716.
209. Aldersey-Williams, J., & Rubert, T. (2019). Levelised cost of energy—A theoretical justification and critical assessment. *Energy policy*, 124, 169-179.
210. IEA, U. (2020). Global energy review 2020. Ukraine.[Online] [https://www. iea. org/countries/ukraine](https://www.iea.org/countries/ukraine) [Accessed: 2020-09-10].
211. Simpson, J., Loth, E., & Dykes, K. (2020). Cost of Valued Energy for design of renewable energy systems. *Renewable Energy*, 153, 290-300.
212. Obi, M., Jensen, S. M., Ferris, J. B., & Bass, R. B. (2017). Calculation of levelized costs of electricity for various electrical energy storage systems. *Renewable and Sustainable Energy Reviews*, 67, 908-920.
213. Hernández-Moro, J., & Martínez-Duart, J. M. (2013). Analytical model for solar PV and CSP electricity costs: Present LCOE values and their future evolution. *Renewable and Sustainable Energy Reviews*, 20, 119-132.
214. Papageorgiou, Asterios, et al. "Climate change impact of integrating a solar microgrid system into the Swedish electricity grid." *Applied energy* 268 (2020): 114981.
215. Pawel, I. (2014). The cost of storage—how to calculate the levelized cost of stored energy (LCOE) and applications to renewable energy generation. *Energy Procedia*, 46, 68-77.
216. "Frankfurt School-UNEP Centre/BNEF, Global Trends in Renewable Energy Investment, 2020."
217. COVID, G. A., & Post-Acute Care Study Group. (2020). Post-COVID-19 global health strategies: the need for an interdisciplinary approach. *Aging clinical and experimental research*, 1.
218. Pragholapati, A. (2020). COVID-19 impact on students.

219. Anwar, T.; Sharma, B.;Chakraborty, K.; Sirohia, H. Introduction To Load Forecasting. *International Journal of Pure and Applied Mathematics*, Volume 119 No. 15 2018, 1527-1538
220. Chow, J. H., Wu, F. F., & Momoh, J. A. (2005). Applied mathematics for restructured electric power systems. In *Applied mathematics for restructured electric power systems* (pp. 1-9). Springer, Boston, MA.
221. S. Fan, L. Chen, and W. J. Lee, "Short-term load forecasting using comprehensive combination based on multi-meteorological information," in *Proc. IEEE Ind. Commercial Power Syst. Tech. Conf.*, May 4–8, 2008, pp. 1–7.
222. A. Ahmad, N. Javaid, M. Guizani, N. Alrajeh and Z. A. Khan, "An Accurate and Fast Converging Short-Term Load Forecasting Model for Industrial Applications in a Smart Grid," in *IEEE Transactions on Industrial Informatics*, vol. 13, no. 5, pp. 2587-2596, Oct. 2017.
223. B. V. M. Vasudevarao, M. Stifter and P. Zehetbauer, "Methodology for creating composite standard load profiles based on real load profile analysis," 2016 IEEE PES Innovative Smart Grid Technologies Conference Europe (ISGT-Europe), Ljubljana, 2016, pp. 1-6.
224. A. Rahman and S. I. Chowdhury Arnob, "Developing load profile for domestic customers of Dhaka city through statistical prediction," 2016 3rd International Conference on Electrical Engineering and Information Communication Technology (ICEEICT), Dhaka, 2016, pp. 1-6.
225. Talaat, M., Farahat, M. A., Mansour, N., & Hatata, A. Y. (2020). Load forecasting based on grasshopper optimization and a multilayer feed-forward neural network using regressive approach. *Energy*, 196, 117087.
226. Hafeez, G., Alimgeer, K. S., & Khan, I. (2020). Electric load forecasting based on deep learning and optimized by heuristic algorithm in smart grid. *Applied Energy*, 269, 114915.
227. Ding, J., Wang, M., Ping, Z., Fu, D., & Vassiliadis, V. S. (2020). An integrated method based on relevance vector machine for short-term load forecasting. *European Journal of Operational Research*, 287(2), 497-510.
228. Park, D. C., El-Sharkawi, M. A., Marks, R. J., Atlas, L. E., & Damborg, M. J. (1991). Electric load forecasting using an artificial neural network. *IEEE transactions on Power Systems*, 6(2), 442-449.
229. Thatcher, M. J. (2007). Modelling changes to electricity demand load duration curves as a consequence of predicted climate change for Australia. *Energy*, 32(9), 1647-1659.

230. Almeshaie, E., & Soltan, H. (2011). A methodology for electric power load forecasting. *Alexandria Engineering Journal*, 50(2), 137-144.
231. Wang, Chi-hsiang, George Grozev, and Seongwon Seo. "Decomposition and statistical analysis for regional electricity demand forecasting." *Energy* 41.1 (2012): 313-325.
232. Mubarak, H., & Sapanta, M. D. (2018, September). Electrical load forecasting study using artificial neural network method for minimizing blackout. In 2018 5th International Conference on Information Technology, Computer, and Electrical Engineering (ICITACEE) (pp. 256-259). IEEE.
233. Elexon BSC 2021. What is a Load Profile?. [online]. Available at: <<https://www.elexon.co.uk/knowledgebase/what-is-a-load-profile/>> [Accessed 16/1/21].
234. Hammad, M. A., Jereb, B., Rosi, B., & Dragan, D. (2020). Methods and models for electric load forecasting: a comprehensive review. *Logist. Sustain. Transp*, 11(1), 51-76.
235. Abu-Shikhah, N., & Elkarmi, F. (2011). Medium-term electric load forecasting using singular value decomposition. *Energy*, 36(7), 4259-4271.
236. Sepasi, S., Reihani, E., Howlader, A. M., Roose, L. R., & Matsuura, M. M. (2017). Very short term load forecasting of a distribution system with high PV penetration. *Renewable energy*, 106, 142-148.
237. Xu, L., Wang, S., & Tang, R. (2019). Probabilistic load forecasting for buildings considering weather forecasting uncertainty and uncertain peak load. *Applied energy*, 237, 180-195.
238. S. A. Aleem, S.A. ; S. M. S. Hussain, T. S. Ustun, "A Review of Strategies to Increase PV Penetration Level in Smart Grids", *Energies*, vol. 13, no. 636, pp. 1-28, 2020.
239. Rafati, A., Joorabian, M., & Mashhour, E. (2020). An efficient hour-ahead electrical load forecasting method based on innovative features. *Energy*, 201, 117511.
240. Li, C. (2020). Designing a short-term load forecasting model in the urban smart grid system. *Applied Energy*, 266, 114850.
241. Tayab, U. B., Zia, A., Yang, F., Lu, J., & Kashif, M. (2020). Short-term load forecasting for microgrid energy management system using hybrid HHO-FNN model with best-basis stationary wavelet packet transform. *Energy*, 203, 117857.
242. Dagdougui, H., Bagheri, F., Le, H., & Dessaint, L. (2019). Neural network model for short-term and very-short-term load forecasting in district buildings. *Energy and Buildings*, 203, 109408.

243. Andersen, F. M., Larsen, H. V., & Gaardestrup, R. B. (2013). Long term forecasting of hourly electricity consumption in local areas in Denmark. *Applied energy*, 110, 147-162.
244. Zhao, E., Zhang, Z., & Bohlooli, N. (2020). Cost and load forecasting by an integrated algorithm in intelligent electricity supply network. *Sustainable Cities and Society*, 60, 102243.
245. Zhang, G., Patuwo, B. E., & Hu, M. Y. (1998). Forecasting with artificial neural networks:: The state of the art. *International journal of forecasting*, 14(1), 35-62.
246. Nespoli, A., Ogliari, E., Dolara, A., Grimaccia, F., Leva, S., & Mussetta, M. (2018, July). Validation of ANN training approaches for day-ahead photovoltaic forecasts. In *2018 International Joint Conference on Neural Networks (IJCNN)* (pp. 1-6). IEEE.
247. Georgitsioti, T., Pillai, G., Pearsall, N., Putrus, G., Forbes, I., & Anand, R. (2015). Short-term performance variations of different photovoltaic system technologies under the humid subtropical climate of Kanpur in India. *IET Renewable Power Generation*, 9(5), 438-445.
248. Pillai, G., Putrus, G., Pearsall, N., & Georgitsioti, T. (2017). The effect of distribution network on the annual energy yield and economic performance of residential PV systems under high penetration. *Renewable Energy*, 108, 144-155.
249. Chan, Z. S., Ngan, H. W., Rad, A. B., David, A. K., & Kasabov, N. (2006). Short-term ANN load forecasting from limited data using generalization learning strategies. *Neurocomputing*, 70(1-3), 409-419.
250. X. Wu and J. Liu, "A New Early Stopping Algorithm for Improving Neural Network Generalization," 2009 Second International Conference on Intelligent Computation Technology and Automation, Changsha, Hunan, 2009, pp. 15-18, doi: 10.1109/ICICTA.2009.11.
251. D. Hunter, H. Yu, M. S. Pukish, III, J. Kolbusz and B. M. Wilamowski, "Selection of Proper Neural Network Sizes and Architectures—A Comparative Study," in *IEEE Transactions on Industrial Informatics*, vol. 8, no. 2, pp. 228-240, May 2012, doi: 10.1109/TII.2012.2187914.
252. G. Zhang, B. E. Patuwo and M. Y. Hu, "Forecasting with artificial neural networks: The state of the art," *Int. J. Forecast.*, vol. 14, no. 1, pp. 35-62, 1998. doi: [https://doi.org/10.1016/S0169-2070\(97\)00044-7](https://doi.org/10.1016/S0169-2070(97)00044-7)
253. M. H. Al Shamisi, A. H. Assi and H. A. Hejase, "Using MATLAB to develop artificial neural network models for predicting global solar radiation in al ain City–UAE," in *Engineering Education and Research using MATLAB Anonymous Citeseer*, 2011.

254. "Xia, C.; Wang, J.; Mckenemy, K. Short, medium and long term load forecasting model and virtual load forecaster based on radial basis function neural networks. *Int. J. Electr. Power Energy Syst.* 2010, 32, 743–750."
255. Notton, G., Voyant, C., Fouilloy, A., Duchaud, J. L., & Nivet, M. L. (2019). Some applications of ANN to solar radiation estimation and forecasting for energy applications. *Applied Sciences*, 9(1), 209.
256. Cong Shuang. *Application and Theories of Neural Network Based on MATLAB NNTools[M]*. Hefei: University of Science and Technology of China Press, 1998
257. Wang, C.-H.; Grozev, G.; Seo, S. Decomposition and statistical analysis for regional electricity demand forecasting. *Energy* 2012, 41, 313–325, doi:10.1016/j.energy.2012.03.011.
258. Zhang, C.; Zhou, K.; Yang, S.; Shao, Z. On electricity consumption and economic growth in China. *Renew. Sustain. Energy Rev.* 2017, 76, 353–368, doi:10.1016/j.rser.2017.03.071.
259. International Energy Agency. *Southeast Asia Energy Outlook*; Springer: Berlin, Germany , 2019.
260. ASEAN Centre for Energy. *The 5th ASEAN Energy Outlook 2015–2040*; ACE: Oak Brook, IL, USA, 2017 .
261. IEA. *Southeast Asia Energy Outlook*; Springer: Berlin, Germany 2015.
262. ASEAN Centre for Energy. *The 4th ASEAN Energy Outlook 2013–2035*; International Energy Agency: Paris, France, 2015.
263. Soualmia, A.; Chenni, R. Modeling and simulation of 15MW grid-connected photovoltaic system using PVsyst software. In *Proceedings of the 2016 International Renewable and Sustainable Energy Conference (IRSEC)*, Los Alamitos, CA, USA , 2016; pp. 702–705.
264. Kim, H.; Jung, T.Y. Independent solar photovoltaic with Energy Storage Systems (ESS) for rural electrification in Myanmar. *Renew. Sustain. Energy Rev.* 2018, 82, 1187–1194, doi:10.1016/j.rser.2017.09.037.
265. Lin, B.; Zhu, J. Chinese electricity demand and electricity consumption efficiency: Do the structural changes matter? *Appl. Energy* 2020, 262, 114505, doi:10.1016/j.apenergy.2020.114505.
266. Al-Saeed, Y.W.; Ahmed, A. Evaluating Design Strategies for Nearly Zero Energy Buildings in the Middle East and North Africa Regions. *Designs* 2018, 2, 35, doi:10.3390/designs2040035.
267. Yi, F.; Ye, H.; Wu, X.; Zhang, Y.Y.; Jiang, F. Self-aggravation effect of air pollution: Evidence from residential electricity consumption in China. *Energy Econ.* 2020, 86, 104684, doi:10.1016/j.eneco.2020.104684.

268. Allison, M.; Pillai, G. Photovoltaic Energy Potential and its Impact on Electricity Demand Profiles. In International Conference on Science and Technology for Sustainable Development; Yangon, Myanmar , 2018.
269. Ismail, A.M.; Ramirez-Iniguez, R.; Asif, M.; Munir, A.B.; Muhammad-Sukki, F. Progress of solar photovoltaic in ASEAN countries: A review. *Renew. Sustain. Energy Rev.* 2015, 48, 399–412, doi:10.1016/j.rser.2015.04.010.
270. Myanmar, ADB. MYANMAR Energy Sector Assessment, Strategy, and Road Map; Asian Development Bank: Mandaluyong, Philippines , 2016.
271. Haque, M.; Wolfs, P.J. A review of high PV penetrations in LV distribution networks: Present status, impacts and mitigation measures. *Renew. Sustain. Energy Rev.* 2016, 62, 1195–1208, doi:10.1016/j.rser.2016.04.025.
272. Liu, C.; Xu, W.; Li, A.; Sun, D.; Huo, H. Analysis and optimization of load matching in photovoltaic systems for zero energy buildings in different climate zones of China. *J. Clean. Prod.* 2019, 238, 117914, doi:10.1016/j.jclepro.2019.117914.
273. Kandasamy, C.; Prabu, P.; Niruba, K. Solar potential assessment using PVSYST software. In Proceedings of the 2013 International Conference on Green Computing, Communication and Conservation of Energy (ICGCE), Los Alamitos, CA, USA , 2013 ; pp. 667–672.
274. Ritchie, H.; Roser, M. Energy. Available online: <https://ourworldindata.org/energy> (accessed on 21 May 2020).
275. Kraft, J.; Kraft, A. Relationship between energy and GNP. *J. Energy Dev.* 1978, 3, 2.
276. Salahuddin, M.; Alam, K.; Ozturk, I.; Sohag, K. The effects of electricity consumption, economic growth, financial development and foreign direct investment on CO2 emissions in Kuwait. *Renew. Sustain. Energy Rev.* 2018, 81, 2002–2010, doi:10.1016/j.rser.2017.06.009.
277. Knight, J.; Yueh, L. Job mobility of residents and migrants in urban China. *J. Comp. Econ.* 2004, 32, 637–660, doi:10.1016/j.jce.2004.07.004.
278. Iyer, L.; Meng, X.; Qian, N.; Zhao, X. Economic Transition and Private-Sector Labor Demand: Evidence from Urban China. *SSRN Electron. J.* 2013, doi:10.2139/ssrn.2365524.
279. Rong, S.; Liu, K.; Huang, S.; Zhang, Q. FDI, labor market flexibility and employment in China. *China Econ. Rev.* 2020, 61, 101449, doi:10.1016/j.chieco.2020.101449.
280. Xu, X.; Li, D.D.; Zhao, M. “Made in China” matters: Integration of the global labor market and the global labor share decline. *China Econ. Rev.* 2018, 52, 16–29, doi:10.1016/j.chieco.2018.05.008.

281. Slideshare.Net. 2020. BP Statistical Review of World Energy 2014: Presentation. Available online: https://www.slideshare.net/BP_plc/bp-statistical-review-of-world-energy-2014-presentation (accessed on 24 May 2020).
282. Li, Z.; Song, Y.; Zhou, A.; Liu, J.; Pang, J.; Zhang, M. Study on the pollution emission efficiency of China's provincial regions: The perspective of Environmental Kuznets curve. *J. Clean. Prod.* 2020, 263, 121497.
283. Zou, B.; Li, S.; Lin, Y.; Wang, B.; Cao, S.; Zhao, X.; Peng, F.; Qin, N.; Guo, Q.; Feng, H.; et al. Efforts in reducing air pollution exposure risk in China: State versus individuals. *Environ. Int.* 2020, 137, 105504, doi:10.1016/j.envint.2020.105504.
284. Zhu, Y.; Wang, Z.; Yang, J.; Zhu, L. Does renewable energy technological innovation control China's air pollution? A spatial analysis. *J. Clean. Prod.* 2020, 250, 119515, doi:10.1016/j.jclepro.2019.119515.
285. Yang, X.; Hu, H.; Tan, T. and Li, J. China's renewable energy goals by 2050. *Environ. Dev.* 2016, 20, 83-90.
286. Li, P.; Lu, Y. and Wang, J. The effects of fuel standards on air pollution: Evidence from China. *J. Dev. Econ.* 2020, 146, 102488.
287. World Population Prospects-Population Division-United Nations. Available online: <https://population.un.org/wpp/Download/Standard/Population/> (accessed on 29 May 2020).
288. Myanmar, ADB. MYANMAR Energy Sector Assessment, Strategy, and Road Map; Asian Development Bank: Mandaluyong, Philippines , 2016.
289. Dobermann, T. Energy in Myanmar; International Growth Centre (IGC): Tokyo, Japan, 2016.
290. International Energy Agency (IEA) via data.worldbank.org. 2020. World Development Indicators (WDI) | Data Catalog . Available online: <http://data.worldbank.org/data-catalog/world-development-indicators> (accessed on 29 May 2020).
291. CIA, The World Factbook. Available online: <https://www.cia.gov/library/publications/the-world-factbook/geos/bm.html> (accessed on 22 May 2020).
292. Bhagavathy, S.M.; Pillai, G.G. PV Microgrid Design for Rural Electrification. *Designs* 2018, 2, 33. doi:10.3390/designs2030033.
293. Castalia Strategic Advisors. Myanmar National Electrification Program (NEP) Roadmap and Investment Prospectus; 2014 .
294. Siala, K.; Stich, J. Estimation of the PV potential in ASEAN with a high spatial and temporal resolution. *Renew. Energy* 2016, 88, 445–456. doi:10.1016/j.renene.2015.11.061.

295. Ang, B.; Goh, T. Carbon intensity of electricity in ASEAN: Drivers, performance and outlook. *Energy Policy* 2016, 98, 170–179. doi:10.1016/j.enpol.2016.08.027.
296. Shi, X. The future of ASEAN energy mix: A SWOT analysis. *Renew. Sustain. Energy Rev.* 2016, 53, 672–680. doi:10.1016/j.rser.2015.09.010.
297. del Barrio Alvarez, Daniel, and Masahiro Sugiyama. "A SWOT analysis of utility-scale solar in Myanmar." *Energies* 13.4 (2020): 884.
298. Tévar, G.; Gómez-Expósito, A.; Arcos-Vargas, A.; Rodríguez-Montañés, M. Influence of rooftop PV generation on net demand, losses and network congestions: A case study. *Int. J. Electr. Power Energy Syst.* 2019, 106, 68–86. doi:10.1016/j.ijepes.2018.09.013.
299. Pillai, G.G.; Naser, H.A.Y. Techno-economic potential of largescale photovoltaics in Bahrain. *Sustain. Energy Technol. Assess.* 2018, 27, 40–45. doi:10.1016/j.seta.2018.03.003.
300. Molin, A.; Schneider, S.; Rohdin, P.; Moshfegh, B. Assessing a regional building applied PV potential – Spatial and dynamic analysis of supply and load matching. *Renew. Energy* 2016, 91, 261–274. doi:10.1016/j.renene.2016.01.084.
301. Sørnes, K.; Fredriksen, E.; Tunheim, K.; Sartori, I. Analysis of the impact resolution has on load matching in the Norwegian context. *Energy Procedia* 2017, 132, 610–615. doi:10.1016/j.egypro.2017.09.683.
302. Lopes, R.A.; Martins, J.; Aelenei, D.; Lima, C.P. A cooperative net zero energy community to improve load matching. *Renew. Energy* 2016, 93, 1–13. doi:10.1016/j.renene.2016.02.044.
303. Michael, G. Update on Edition 2 of IEC 61724: PV System Performance Monitoring. Available online: (accessed on 20 May 2020).
304. Mararakanye, N.; Bekker, B. Renewable energy integration impacts within the context of generator type, penetration level and grid characteristics. *Renew. Sustain. Energy Rev.* 2019, 108, 441–451. doi:10.1016/j.rser.2019.03.045.
305. Graabak, I.; Korpås, M.; Jaehnert, S.; Belsnes, M. Balancing future variable wind and solar power production in Central-West Europe with Norwegian hydropower. *Energy* 2019, 168, 870–882. doi:10.1016/j.energy.2018.11.068.
306. Z. Wang and R. Srinivasan, "A review of artificial intelligence based building energy use prediction: Contrasting the capabilities of single and ensemble prediction model", *Renewable and Sustainable Energy Reviews*, vol. 75, pp. 796-808, August 2017, doi: <https://doi.org/10.1016/j.rser.2016.10.079>
307. M. Günay, "Forecasting annual gross electricity demand by artificial neural networks using predicted values of socio-economic indicators and climatic

- conditions: Case of Turkey”, *Energy Policy*, vol. 90, pp. 92-101, March 2016, doi: <https://doi.org/10.1016/j.enpol.2015.12.019>
308. A. Zameer, J. Arshad, A. Khan and M. Raja, “Intelligent and robust prediction of short term wind power using genetic programming based ensemble of neural networks”, *Energy Conversion And Management*, vol. 134, pp. 361-372, February 2017, doi: <https://doi.org/10.1016/j.enconman.2016.12.032>
309. N. Daina, A. Sivakumar and J. Polak, “Modelling electric vehicles use: a survey on the methods”, *Renewable and Sustainable Energy Reviews*, vol. 68, pp. 447-460, February 2017, doi: <https://doi.org/10.1016/j.rser.2016.10.005>
310. S. Shojaabadi, S. Abapour, M. Abapour and A. Nahavandi, “Simultaneous planning of plug-in hybrid electric vehicle charging stations and wind power generation in distribution networks considering uncertainties”, *Renewable Energy*, vol. 99, pp. 237-252, December 2016, doi: <https://doi.org/10.1016/j.renene.2016.06.032>
311. Munkhammar, J. Widén and J. Rydén, “On a probability distribution model combining household powerconsumption, electric vehicle home-charging and photovoltaic powerproduction”, *Applied Energy*, vol. 142, pp. 135-143, March 2015, doi: <https://doi.org/10.1016/j.apenergy.2014.12.031>
312. C. Wang, G. Grozev and S. Seo, "Decomposition and statistical analysis for regional electricity demand forecasting", *Energy*, vol. 41, no. 1, pp. 313-325, 2012.
313. M. Thatcher, "Modelling changes to electricity demand load duration curves as a consequence of predicted climate change for Australia", *Energy*, vol. 32, no. 9, pp. 1647-1659, 2007
314. F. Apadula, A. Bassini, A. Elli and S. Scapin, "Relationships between meteorological variables and monthly electricity demand", *Applied Energy*, vol. 98, pp. 346-356, 2012.
315. T. Huld and A. Amillo, "Estimating PV Module Performance over Large Geographical Regions: The Role of Irradiance, Air Temperature, Wind Speed and Solar Spectrum", *Energies*, vol. 8, pp. 5159-5181, 2015
316. F. Liu, R. Li, Y. Li, R. Yan and T. Saha, "Takagi–Sugeno fuzzy modelbased approach considering multiple weather factors for the photovoltaic power short-term forecasting", *IET Renewable Power Generation*, vol. 11, no. 10, pp. 1281-1287, 2017.
317. N. Aste, C. Del Pero and F. Leonforte, "PV technologies performance comparison in temperate climates", *Solar Energy*, vol. 109, 2014.
318. J. Brady and M. O’Mahony, "Modelling charging profiles of electric vehicles based on real-world electric vehicle charging data", *Sustainable Cities and Society*, vol. 26, pp. 203-216, 2016.

319. "UKERC Energy Data Centre", Data.ukedc.rl.ac.uk. [Online]. Available: http://data.ukedc.rl.ac.uk/cgi-bin/dataset_catalogue/view.cgi.py?id=6. [Accessed: 05- Nov- 2017].
320. "Impact of Electric Vehicle and Heat Pump loads on network demand profiles", UK Power Networks, 2014.
321. Al Shamisi, M. H., Assi, A. H., & Hejase, H. A. (2011). Using MATLAB to develop artificial neural network models for predicting global solar radiation in Al Ain City–UAE. IntechOpen.
322. Sahi, G. (2018, April). Performance evaluation of artificial neural network for usability assessment of E-commerce websites. In 2018 3rd International Conference for Convergence in Technology (I2CT) (pp. 1-6). IEEE.
323. Garg, V. K., & Bansal, R. K. (2015, March). Comparison of neural network back propagation algorithms for early detection of sleep disorders. In 2015 International Conference on Advances in Computer Engineering and Applications (pp. 71-75). IEEE.
324. Khong, L. M., Gale, T. J., Jiang, D., Olivier, J. C., & Ortiz-Catalan, M. (2013, October). Multi-layer perceptron training algorithms for pattern recognition of myoelectric signals. In The 6th 2013 Biomedical Engineering International Conference (pp. 1-5). IEEE.
325. Ruslan, F. A., & Adnan, R. (2018, March). 4 Hours NNARX flood prediction model using "traingd" and "trainoss" training function: A comparative study. In 2018 IEEE 14th International Colloquium on Signal Processing & Its Applications (CSPA) (pp. 77-81). IEEE.
326. Azarmdel, H., Jahanbakhshi, A., Mohtasebi, S. S., & Muñoz, A. R. (2020). Evaluation of image processing technique as an expert system in mulberry fruit grading based on ripeness level using artificial neural networks (ANNs) and support vector machine (SVM). *Postharvest Biology and Technology*, 166, 111201.
327. Kumar, Y., Singh, L., Sharanagat, V. S., & Tarafdar, A. (2021). Artificial neural network (ANNs) and mathematical modelling of hydration of green chickpea. *Information Processing in Agriculture*, 8(1), 75-86.
328. Mondol, J. A. M., Panigrahi, S., & Gupta, M. M. (2011, August). Neural networks approach to biocomposites processing. In *Proceedings of 2011 IEEE Pacific Rim Conference on Communications, Computers and Signal Processing* (pp. 742-746). IEEE.
329. Abbas, G., Farooq, U., & Asad, M. U. (2011, October). Application of neural network based model predictive controller to power switching converters. In *The*

- 2011 International Conference and Workshop on Current Trends in Information Technology (CTIT 11) (pp. 132-136). IEEE.
330. Tran, V. L., Thai, D. K., & Kim, S. E. (2019). Application of ANN in predicting ACC of SCFST column. *Composite Structures*, 228, 111332.
331. Motahar, S. (2020). Experimental study and ANN-based prediction of melting heat transfer in a uniform heat flux PCM enclosure. *Journal of Energy Storage*, 30, 101535.
332. Souza, P. R., Dotto, G. L., & Salau, N. P. G. (2018). Artificial neural network (ANN) and adaptive neuro-fuzzy interference system (ANFIS) modelling for nickel adsorption onto agro-wastes and commercial activated carbon. *Journal of environmental chemical engineering*, 6(6), 7152-7160.
333. Heidari, E., Daeichian, A., Sobati, M. A., & Movahedirad, S. (2020). Prediction of the droplet spreading dynamics on a solid substrate at irregular sampling intervals: Nonlinear Auto-Regressive exogenous Artificial Neural Network approach (NARX-ANN). *Chemical Engineering Research and Design*, 156, 263-272.
334. Afram, Abdul, et al. "Artificial neural network (ANN) based model predictive control (MPC) and optimization of HVAC systems: A state of the art review and case study of a residential HVAC system." *Energy and Buildings* 141 (2017): 96-113.
335. Li, F., Wang, W., Xu, J., Yi, J., & Wang, Q. (2019). Comparative study on vulnerability assessment for urban buried gas pipeline network based on SVM and ANN methods. *Process Safety and Environmental Protection*, 122, 23-32.
336. Menke, J. H., Bornhorst, N., & Braun, M. (2019). Distribution system monitoring for smart power grids with distributed generation using artificial neural networks. *International Journal of Electrical Power & Energy Systems*, 113, 472-480.
337. Fischer, S., Frey, P., & Drück, H. (2012). A comparison between state-of-the-art and neural network modelling of solar collectors. *Solar energy*, 86(11), 3268-3277.
338. Walker, S., Khan, W., Katic, K., Maassen, W., & Zeiler, W. (2020). Accuracy of different machine learning algorithms and added-value of predicting aggregated-level energy performance of commercial buildings. *Energy and Buildings*, 209, 109705.
339. Wu, X. X., & Liu, J. G. (2009, October). A new early stopping algorithm for improving neural network generalization. In *2009 Second International Conference on Intelligent Computation Technology and Automation (Vol. 1, pp. 15-18)*. IEEE.
340. Liu, H. (2010, August). On the Levenberg-Marquardt training method for feed-forward neural networks. In *2010 sixth international conference on natural computation (Vol. 1, pp. 456-460)*. IEEE.

341. Novokhodko, A., & Valentine, S. (2001, July). A parallel implementation of the batch backpropagation training of neural networks. In IJCNN'01. International Joint Conference on Neural Networks. Proceedings (Cat. No. 01CH37222) (Vol. 3, pp. 1783-1786). IEEE.
342. Nespoli, A.; Ogliari, E.; Dolara, A.; Grimaccia, F.; Leva, S.; Mussetta, M. Validation of ANN Training Approaches for Day-Ahead Photovoltaic Forecasts. In Proceedings of the 2018 International Joint Conference on Neural Networks (IJCNN), Los Alamitos, CA, USA, 8–13 July 2018; pp. 1–6.
343. Toghraie, D.; Sina, N.; Jolfaei, N.A.; Hajian, M.; Afrand, M. Designing an Artificial Neural Network (ANN) to predict the viscosity of Silver/Ethylene glycol nanofluid at different temperatures and volume fraction of nanoparticles. *Phys. A Stat. Mech. Its Appl.* 2019, 534, 122142. doi:10.1016/j.physa.2019.122142.
344. Tran, V.-L.; Thai, D.-K.; Kim, S.-E. Application of ANN in predicting ACC of SCFST column. *Compos. Struct.* 2019, 228, 111332. doi:10.1016/j.compstruct.2019.111332.
345. Li, F.; Wang, W.; Xu, J.; Yi, J.; Wang, Q. Comparative study on vulnerability assessment for urban buried gas pipeline network based on SVM and ANN methods. *Process. Saf. Environ. Prot.* 2019, 122, 23–32. doi:10.1016/j.psep.2018.11.014.
346. Souza, P.; Dotto, G.L.; Salau, N.P.G. Artificial neural network (ANN) and adaptive neuro-fuzzy interference system (ANFIS) modelling for nickel adsorption onto agro-wastes and commercial activated carbon. *J. Environ. Chem. Eng.* 2018, 6, 7152–7160. doi:10.1016/j.jece.2018.11.013.
347. Motahar, S. Experimental study and ANN-based prediction of melting heat transfer in a uniform heat flux PCM enclosure. *J. Energy Storage* 2020, 30, 101535.
348. Notton, G.; Voyant, C.; Fouilloy, A.; Duchaud, J.L.; Nivet, M.L. Some Applications of ANN to Solar Radiation Estimation and Forecasting for Energy Applications. *Appl. Sci.* 2019, 9, 209. doi:10.3390/app9010209.
349. Denholm, P., O'Connell, M., Brinkman, G., Jorgenson, J., 2015. Overgeneration from Solar Energy in California: A Field Guide to the Duck Chart. National Renewable Energy Laboratory, Golden, CO
350. International Renewable Energy Agency. Renewable Power Generation Costs in 2017; Abu Dhabi, 2018.
351. N. Sönnichsen, "Cumulative solar photovoltaic capacity in Germany from 2013 to 2019", Statista, 2020. [Online] Available at: <https://www.statista.com/statistics/497448/connected-and-cumulated-photovoltaic-capacity-in-germany/>. [Accessed 7 September 2020]

352. Fraunhofer Institute for Solar Energy Systems, Germany. Recent Facts about Photovoltaics in Germany, 2018.
353. I. Konstantelos, S. Giannelos, G. Strbac, "Strategic Valuation of Smart Grid Technology Options in Distribution Networks.", IEEE Transactions on Power Systems 2017, vol. 32, pp. 1293-1303, 2017. Doi: <https://doi.org/10.1109/TPWRS.2016.2587999>
354. S. Eftekharnjad, V. Vittal, G. T. Heydt, B. Keel and J. Loehr, "Impact of increased penetration of photovoltaic generation on power systems," IEEE Transactions on Power Systems, vol. 28, no. 2, pp. 893-901, May 2013, doi: <https://doi.org/10.1109/TPWRS.2012.2216294>.
355. J. de Hoog, T. Alpcan, M. Brazil, D. A. Thomas and I. Mareels, "A Market Mechanism for Electric Vehicle Charging Under Network Constraints," IEEE Transactions on Smart Grid, vol. 7, no. 2, pp. 827-836, March 2016, doi: <https://doi.org/10.1109/TSG.2015.2495181>.
356. J. Allison, A. Cowie, S. Galloway et al., Simulation, implementation and monitoring of heat pump load shifting using a predictive controller, in Energy Conversion And Management, vol. 150, pp. 890-903, October 2017, doi: <https://doi.org/10.1016/j.enconman.2017.04.093>.
357. J. A. Jardini, H. P. Schmidt, C. M. V. Tahan, C. C. B. De Oliveira and S. U. Ahn, "Distribution transformer loss of life evaluation: a novel approach based on daily load profiles," IEEE Transactions on Power Delivery, vol. 15, no. 1, pp. 361-366, Jan. 2000, doi: <https://doi.org/10.1109/61.847274>.
358. V. Aravinthan and W. Jewell, "Controlled Electric Vehicle Charging for Mitigating Impacts on Distribution Assets," IEEE Transactions on Smart Grid, vol. 6, no. 2, pp. 999-1009, March 2015, doi: [10.1109/TSG.2015.2389875](https://doi.org/10.1109/TSG.2015.2389875).
359. R. Yan, B. Marais and T. Saha, "Impacts of residential photovoltaic power fluctuation on on-load tapchanger operation and a solution using DSTATCOM", Electric Power Systems Research, vol. 111, pp. 185-193, June 2014, doi: <https://doi.org/10.1016/j.epsr.2014.02.020>
360. Snape, J.R. Spatial and temporal characteristics of PV adoption in the UK and their implications for the smart grid. Energies 2016, 9(3), 210. Doi: <https://doi.org/10.3390/en9030210>
361. C. Mateo, P. Frías, R. Cossent, P. Sonvilla, B. Barth, "Overcoming the barriers that hamper a large-scale integration of solar photovoltaic power generation in European distribution grids.", Solar Energy, vol. 153, pp. 574-583, 2017. Doi: <https://doi.org/10.1016/j.solener.2017.06.008>

362. Energy Network Association, UK. Engineering Recommendation G98: Requirements for the connection of Fully Type Tested Micro-generators (up to and including 16A per phase) in parallel with public Low Voltage Distribution Networks on or after 27April2019, 2019.
363. S. H. Nengroo, M. U. Ali, A. Zafar, S. Hussain, T. Murtaza, T.; M. J. Alvi, K. V. G. Raghavendra, H. J. Kim, " Optimized Methodology for a Hybrid Photo-Voltaic and Energy Storage System Connected to a Low-Voltage Grid.", *Electronics* 2019, vol. 8, no. 2, 2019. Doi: <https://doi.org/10.3390/electronics8020176>
364. G. G. Pillai, G. A. Putrus and N. M. Pearsall, "The potential of demand side management to facilitate PV penetration," 2013 IEEE Innovative Smart Grid Technologies-Asia (ISGT Asia), Bangalore, 2013, pp. 1-5, doi: 10.1109/ISGT-Asia.2013.6698719
365. L. H. Macedo, J. F. Franco, R. Romero, M. A. Ortega-Vazquez and M. J. Rider, "Increasing the hosting capacity for renewable energy in distribution networks," 2017 IEEE Power & Energy Society Innovative Smart Grid Technologies Conference (ISGT), Washington, DC, 2017, pp. 1-5, doi: 10.1109/ISGT.2017.8086006.
366. UNITED NATIONS DEPARTMENT FOR ECONOMIC AND SOCIAL AFFAIRS. (2020). World economic situation and prospects 2020. UN.
367. USTR takes India off developing country list, Sriram Lakshman <https://www.thehindu.com/business/ustr-takes-india-off-developing-country-list/article30813126.ece>
368. Kotték, M., Grieser, J., Beck, C., Rudolf, B., & Rubel, F. (2006). World map of the Köppen-Geiger climate classification updated.
369. K. Siala and J. Stich, "Estimation of the PV potential in ASEAN with a high spatial and temporal resolution," *Renewable Energy*, vol. 88, pp. 445-456, 2016.
370. Peel, M. C., Finlayson, B. L., & McMahon, T. A. (2007). Updated world map of the Köppen-Geiger climate classification. *Hydrology and earth system sciences*, 11(5), 1633-1644.
371. Beck, H. E., Zimmermann, N. E., McVicar, T. R., Vergopolan, N., Berg, A., & Wood, E. F. (2018). Present and future Köppen-Geiger climate classification maps at 1-km resolution. *Scientific data*, 5(1), 1-12.
372. G. Pillai, G. Putrus, N. Pearsall, T. Georgitsioti, "The effect of distribution network on the annual energy yield and economic performance of residential PV systems under high penetration.", *Renewable Energy*, vol. 108, pp. 144-155, 2017. Doi: <https://doi.org/10.1016/j.renene.2017.02.047>

373. "Photovoltaic Geographical Information System", PVGIS, 2019. [Online] Available at: https://re.jrc.ec.europa.eu/pvg_tools/en/ [Accessed: 12 September 2020].
374. K. D. Santo, S. D. Santo, R. Monaro, M. Saidel, "Active demand side management for households in smart grids using optimization and artificial intelligence.", *Measurement*, vol. 115, pp. 152-161, 2018. Doi: <https://doi.org/10.1016/j.measurement.2017.10.010>
375. J. Ekanayake, N. Jenkins, K. Liyanage, J. Wu, and A. Yokoyama, *Smart grid: technology and applications*, UK: John Wiley & Sons, Ltd, 2012.
376. G. Putrus, E. Bentley, R. Binns, T. Jiang and D. Johnston, "Smart grids: energising the future", *International Journal of Environmental Studies*, vol. 70, pp. 691-701, 2013. Doi: <https://doi.org/10.1080/00207233.2013.798500>
377. U. Ramani, S. S. kumar, T. Santhoshkumar and M. Thilagaraj, "IoT Based Energy Management for Smart Home," 2019 2nd International Conference on Power and Embedded Drive Control (ICPEDC), Chennai, India, 2019, pp. 533-536, doi: <https://doi.org/10.1109/ICPEDC47771.2019.9036546>
378. P. Balakumar and S. Sathiya, "Demand side management in smart grid using load shifting technique," 2017 IEEE International Conference on Electrical, Instrumentation and Communication Engineering (ICEICE), Karur, 2017, pp. 1-6, doi: [10.1109/ICEICE.2017.8191856](https://doi.org/10.1109/ICEICE.2017.8191856).
379. K. Swathi, K. Balasubramanian, M. Veluchamy, "Residential Load Management Optimization in Smart Grid", *International Journal for Trends in Engineering & Technology*, vol. 13, no. 1, pp. 48-53, 2016.
380. Dept. of Energy and Climate Change, UK. *Energy Consumption in the UK Domestic data tables 2012 Update*, 2012.
381. S. Gottwalt, W. Ketter, C. Block, J. Collins and C. Weinhardt, "Demand side management—A simulation of household behavior under variable prices", *Energy Policy*, vol. 39, pp. 8163-8174, 2011. Doi: <https://doi.org/10.1016/j.enpol.2011.10.016>
382. I. Mansouri, M. Newborough, D. Probert, "Energy consumption in UK households: Impact of domestic electrical appliances.", *Applied Energy*, vol. 54, pp. 211-285, 1996. Doi: [https://doi.org/10.1016/0306-2619\(96\)00001-3](https://doi.org/10.1016/0306-2619(96)00001-3)
383. "Dishwasher sales suddenly shoot up in India", *The News Minute*, May 2020. [Online] Available at: <https://www.thenewsminute.com/article/dishwasher-sales-suddenly-shoot-india-125497> [Accessed: 3 November 2020]
384. J. Palmer and I. Cooper "United Kingdom Housing Energy Fact File", Department of Energy & Climate Change, United Kingdom, 2013.

385. Momoh, J. A. *Electric Power Distribution, Automation, Protection and Control*, USA: Taylor & Francis Group, 2008.
386. M. Firdaus, S. E. Pratiwi, D. Kowanda and A. Kowanda, "Literature review on Artificial Neural Networks Techniques Application for Stock Market Prediction and as Decision Support Tools," 2018 Third International Conference on Informatics and Computing (ICIC), Palembang, Indonesia, 2018, pp. 1-4, doi: 10.1109/IAC.2018.8780437.
387. K. G. Sheela and S. N. Deepa, "Review on methods to fix number of hidden neurons in neural networks", *Mathematical Problems in Engineering*, vol. 2013, 2013. doi: <http://dx.doi.org/10.1155/2013/425740>
388. M. Allison, E. Akakabota and G. Pillai, "Future load profiles under scenarios of increasing renewable generation and electric transport," 2018 5th International Conference on Renewable Energy: Generation and Applications (ICREGA), Al Ain, 2018, pp. 296-300, doi: 10.1109/ICREGA.2018.8337614.
389. A. P. Dedecker et al, "Optimization of Artificial Neural Network (ANN) model design for prediction of macroinvertebrates in the Zwalm river basin (Flanders, Belgium)," *Ecol. Model.*, vol. 174, (1-2), pp. 161-173, 2004. doi: <https://doi.org/10.1016/j.ecolmodel.2004.01.003>
390. G. Sahi, "Performance Evaluation of Artificial Neural Network for Usability Assessment of E-Commerce Websites," 2018 3rd International Conference for Convergence in Technology (I2CT), Pune, 2018, pp. 1-6, doi: 10.1109/I2CT.2018.8529613.
391. "UKERC Energy Data Centre", UK Energy Research Centre (UKERC), September 2020. [Online] Available at: https://ukerc.rl.ac.uk/DC/cgi-bin/edc_search.pl?GoButton=Detail&WantComp=42&WantResult=LD&&BROWSE=1 [Accessed: 18 October 2020]
392. G. Pillai, G. Putrus, N. Pearsall, "Generation of synthetic benchmark electrical load profiles using publicly available load and weather data.", *International Journal of Electrical Power & Energy Systems*, vol. 61, pp. 1-10, 2014. Doi: <http://dx.doi.org/10.1016/j.ijepes.2014.03.005>
393. J. Du, J. Tian, Z. Wu, A. Li, G. Abbas and Q. Sun, "An Interval Power Flow Method based on Linearized DistFlow Equations for Radial Distribution Systems," 2020 12th IEEE PES Asia-Pacific Power and Energy Engineering Conference (APPEEC), Nanjing, China, 2020, pp. 1-5, doi: <https://doi.org/10.1109/APPEEC48164.2020.9220372>.

394. G. G. Pillai, G. A. Putrus and N. M. Pearsall, "Impact of distribution network voltage rise on PV system energy yield," 2013 Annual IEEE India Conference (INDICON), Mumbai, 2013, pp. 1-5, doi: 10.1109/INDCON.2013.6725971.
395. S. L. Koh and Y. S. Lim, "Evaluating the economic benefits of peak load shifting for building owners and grid operator," 2015 International Conference on Smart Grid and Clean Energy Technologies (ICSGCE), Offenburg, 2015, pp. 30-34, doi: 10.1109/ICSGCE.2015.7454265.
396. "India Electricity Prices", Global Petrol Prices, 2020. [Online] Available at: https://www.globalpetrolprices.com/India/electricity_prices/ [Accessed 18 November 2020]
397. Tina, G.M.; Garozzo, D.; Siano, P. Scheduling of PV inverter reactive power set-point and battery charge/discharge profile for voltage regulation in low voltage networks. *Int. J. Electr. Power Energy Syst.* 2019, 107, 131–139. doi:10.1016/j.ijepes.2018.11.009.
398. Wu, D.; Aldaoudeyeh, A.M.; Javadi, M.; Ma, F.; Tan, J.; Jiang, J.N. A method to identify weak points of interconnection of renewable energy resources. *Int. J. Electr. Power Energy Syst.* 2019, 110, 72–82. doi:10.1016/j.ijepes.2019.03.003.
399. Monteiro, V.; Pinto, J.G.; Afonso, J.L. Improved vehicle-for-grid (iV4G) mode: Novel operation mode for EVs battery chargers in smart grids. *Int. J. Electr. Power Energy Syst.* 2019, 110, 579–587. doi:10.1016/j.ijepes.2019.03.049.
400. Foster, J.; Liu, X.; McLoone, S. Load forecasting techniques for power systems with high levels of unmetered renewable generation: A comparative study. *IFAC Pap.* 2018, 51, 109–114. doi:10.1016/j.ifacol.2018.06.245.
401. Feinberg E.A., Genethliou D. (2005) Load Forecasting. In: Chow J.H., Wu F.F., Momoh J. (eds) *Applied Mathematics for Restructured Electric Power Systems. Power Electronics and Power Systems.* Springer, Boston, MA. https://doi.org/10.1007/0-387-23471-3_12
402. Sallam, Abdelhay A., and Om P. Malik. *Electric distribution systems.* John Wiley & Sons, 2018.
403. (2000) BOX-JENKINS METHODOLOGY. In: Swamidass P.M. (eds) *Encyclopedia of Production and Manufacturing Management.* Springer, Boston, MA . https://doi.org/10.1007/1-4020-0612-8_98
404. Department for Business, Energy & Industrial Strategy, 2016. *ELECTRICITY GENERATION COSTS.* London: The Crown.
405. Awerbuch, Shimon. "Investing in photovoltaics: risk, accounting and the value of new technology." *Energy Policy* 28.14 (2000): 1023-1035.